Sedimentology and Organic Geochemistry of Potential Source and Reservoir Rocks of the Central Punjab, part of the Indus Basin

Dissertation

Rahmat Ali Gakkhar

Eingereicht am

Department für Angewandte Geowissenschaften und Geophysik
Lehrstuhl Prospektion und Angewandte Sedimentologie
Montanuniversität Leoben

Leoben, März 2010

Affidavit:

I declare in lieu of oath, that I wrote this thesis and performed the associated research myself, using only literature cited in this volume.

Rahmat Ali Gakkhar

Acknowledgement

All praise and gratitude are due to Almighty Allah alone Who created man in His own image and enjoined upon him to travel on the earth and enter into a profound and analytical study of the universe for spiritual appreciation of Allah and His attributes as well as for harnessing the material manifestations of the world to the mankind's profitable utilization. In the first place, therefore, I express my utmost thanks to Allah, the Omnipotent and Omniscient Creator, who has endorsed me with brain and body to partake of His knowledge and accomplish my work in the form of this thesis.

I do not possess the words to paint the exact of thankfulness formed in the deepest recess of my heart for my honorable supervisor Prof. Dr. Walter Vortisch, who took great pains, extending every possible facility in the office and in the laboratory and vast splendid research experience to solve various problems relating to the research work. His courteous behavior will be never forgotten.

I would like to pay my heartiest tribute to Prof. Dr. Reinhard Gratzer and Prof. Dr. Achim Bechtel for their help to carry out the work for organic geochemistry. Prof. Reinhard Gratzer spent his valuable time in helping me to format this thesis. My heartiest gratitude is for Prof. Dr. Hans-Jürgen Gawlick for his guidance in carbonate microfacies analysis. Dr. Eva Wegerer help is also gratefully acknowledged.

I want to pay my heartiest gratitude to Dipl.-Ing. L.E.A. Scheucher (PhD Student University of Leoben) for his help to identify minerals and their evaluation in X-Ray Diffractograms. Dipl.-Ing. O. Krische (PhD Student University of Leoben) my grateful acknowledgment for his support by the preparation of thin sections for carbonates microfacies analysis.

I am also thankful to Ursula Schmid (Secretary) and Franz Seidl (Technician) for their cooperation and help.

The role of the Oil and Gas Development Company (Pakistan) for providing the samples and additional Rock-Eval data, the financial support by Higher Education Commission of Pakistan and cooperation of Austrian Agency for International Cooperation in Education and Research (OeAD-GmbH) to me is gratefully acknowledged. May God bless all those, who helped me in the completion of my educational career.

Dedicated

To

My Family

Abstract

Biostratigraphy, sedimentology and hydrocarbon potential of Jurassic and Cretaceous strata of the Punjab Platform were studied, in order to enhance the success rate of hydrocarbon discovery. Two wells were investigated (Ali Sahib and Amir Wali), both drilled to 2050 m depth.

The oldest stratigraphic unit in both wells is the Jurassic Datta Formation (mainly sandstone, shale, claystone), followed by the Jurassic Samana Suk Formation. Main lithologies of this formation in Ali Sahib Well: limestone, shale, claystone, sandstone; in Amir Wali Well: limestone.

Intensive tropical weathering conditions (seasonal climate) in the provenance area is suggested for the (probably continental) sediments of the Datta Formation, which are comprised mainly by kaolinite-rich shales (occurrence of boehmite), and a minor portion of mature quartz arenite at the top. A fluvio-deltaic sedimentary environment is indicated by the clastic sediments of the Samana Suk Formation.

The carbonate sediments of the Samana Suk Formation and the Chichali Formation were deposited in outer deeper shelf region of a carbonate ramp setting, as documented by the mixing of shallow marine carbonate clasts and deep water organisms.

The Chichali Formation, which is mainly clastic in the Punjab Platform, was considered as early Cretaceous. However, *Saccocoma* and *Nautiloculina oolithica* proved late Jurassic Age of its lower part (limestone).

The Cretaceous Lumshiwal Formation is represented by mixed carbonatic-siliciclastic sediments in the Ali Sahib Well, indicating shallowing upward. Goethite in the clastic sediments of this formation (Amir Wali Well) indicates weathering in the provenance area under permanently humid conditions. Deeper marine depositional environment is suggested for the (?) Paleocene Ranikot Formation.

Source rock characterization was carried out by organic geochemistry, including biomarkers. Organic matter is mostly represented by Type-III kerogen, immature to marginal mature. The Chichali Formation (kerogen of algal/microbial origin) and the Datta Formation (mixed algal/bacterial and land plant origin) show in few samples relatively fair generative potential for hydrocarbons. For the Cretaceous Lumshiwal Formation and the Jurassic Samana Suk Formation, a kerogen origin is suggested as for the Datta Formation (s. above).

During Cretaceous age (the Chichali Formation and the Lumshiwal Formation), the depositional environment was anoxic/reducing marine. The present data indicate an oxic to dysoxic depositional environment of the Jurassic Datta Formation and Samana Suk Formation.

Content

1. INTRODUCTION AND LOCATIONS OF THE STUDIED WELLS

Punjab Province is located in the east of Pakistan and has a population about 80 million persons (estimated July 2009). According to population, Punjab is the greatest province of Pakistan. From north to south the surface of Punjab Province consists of Plateau (Potwar), the hill system between River Jhelum and River Indus, and plains, called Punjab Plains. The hill system is also called the Salt Range. The Potwar Plateau, the Salt Range and the Punjab Plains are the parts of Upper and Middle Indus Basin. The Salt Range has been well studied and its name is derived from the large salt deposits in the Salt Range Formation (Kazmi & Jan, 1997).

The stratigraphy of the Salt Range area has been incorporated in Kohat-Potwar Plateau as well as in the wells drilled in Punjab Plains. The stratigraphy varies increasingly with the distance from the Salt Range becomes greater and greater to southwards, so that the stratigraphy in Lower Indus Basin has greatly changed (Yasin & Janjua, 1994).

The Ali Sahib Well (Latitude: 30° 29′ 05.503″ N, Longitude: 72° 00′ 12.117″ E) in Khanewal District of the Punjab province; and the Amir Wali Well (Latitude: 30° 45′ 55.239″ N, Longitude: 71° 54′ 03.873″ E); in Jhang District of the Punjab Province, were drilled for the exploration of hydrocarbons up to target depth (TD) 2050 m (from Recent to Jurassic strata), by Oil and Gas Development Company in 2005, in the Punjab Platform (cf., Ch.1, Figs. 1.1-1.3). Both of the wells were dry and declared abandoned. The locations of our studied wells are in the south of the Salt Range (more than 200 km). The Ali Sahib Well is located to the northern end of Khanewal district and to the south of the Ravi River. The nearest gas fields in this area are Panjpir and Nandpur. Nandpur Well # 02 is the closest well to this location. The Nandpur Gas Plant is located approximately 10 km to the northwest of the Ali Sahib Well. The Amir Wali Well is located in the Jhang District, on the eastern bank of Chenab River. Natural gas has been discovered in this area from the Bahu Well 01 which is located approximately 5-7 km to the north of the Amir Wali Well (Figs. 1.2 & 1.3). Amir Wali Well is located approximately 35 km to the northwest of the Ali Sahib Well (Figs. 1.3 & 1.4). Both districts have well developed infrastructure and are connected by well developed roads and railway tracks. To link roads, the wells are connected by tracks drivable for jeeps.

Due to the low topography, there is no hindrance to the transport of heavy drilling machinery, except during the monsoon season of July and August.

The Jhang District is one of the oldest districts of subcontinent, it was formerly known as Riasat Jhagi Sial. Some people believe that Alexander the Great was defeated here by the Sial tribe. The Khanewal was established by the British Empire around 1900, now it is known for the second largest railway station in Pakistan.

1.1 CLIMATE

The region characterized by hot and dry summers and cold and dry winters. The temperature in the area may rise up to 50° C in the summer and falls as low as zero degree in the winter. The ground water is potable and suitable for all domestic and industrial requirements.

1.2 CULTURE

It is thought that pure and oldest dialect of Punjabi language which is known as "Jhangochi" or "Jhangi" have roots in this region (Sandal Bar). The Sandal Bar is a region between the rivers Chenab and Ravi in the Punjab Province. It spreads over almost 80 km in length (north to south) and 40 km in width (west to east). "Bar", in the local language, means a forested area where there are no resources for cultivation, like water (www.wikipedia.org). But now the most of the Bar is cultivable through well developed irrigation system of canals and from tube wells. Saandal was the name of a freedom fighter against great Mughal Empire and he had been living in this forest area.

Jhummer and Sammi are Punjabi folk dances which have the roots in Sandal Bar. Sammi is the name of dance for women and Jhummer is danced by men. The folk music of the area is called `Dhola` or `Jhang da Dhola`. The old women wear ´Kaghra´ which has some resemblance with modern skirt, and old men wear Dhudder. Tent pegging (naiza bazi) and Kabaddi are famous traditional sports in the regions. Teeyan and Trinjin were some important activities for women for weaving cloths using spinning wheels. But now the things are changing. The young women and young boys are getting education up to university level. Young men are also taking interest in

cricket and football. Pakistan´s only noble laureate Dr. Abdul Salam was also from district Jhang.

Khanewal is the part of the region which is famous for Pakistan's 'Cotton Belt' - an area covering Khanewal, Multan and Bahawalnagar. It is known to produce the finest cotton in the World. Wheat, sugar cane, corn and grams are other important crops of the region. A lot of vegetables and green fodder for cattle are also cultivated.

1.3 FAUNA AND FLORA

Camels, buffaloes, cows, sheep and goats have been raised by the local community to fulfill their requirements of meat and dairy products. Donkeys, horses and camels are still in use for the transportation of goods.

Figure 1.1: Map showing the position of Pakistan in World and the studied wells (from http://www.worldatlas.com/webimage/countrys/asia/pk.htm)

The forested areas are comprised of trees of numerous species, such as: Jand (*Prosopis spicigera*), Karir (*Capparis aphylla*), Beri (*Zizyphus jujuba*), Van (*Salvodora oleoids*), Kikar (*Acacia nilotica*), and Shesham (*Dalbergia sissoo*). (The botanical names of the trees are from www.wikipedia.org). At places mango trees have been cultivated in the region. Some herbs are found nearby river courses.

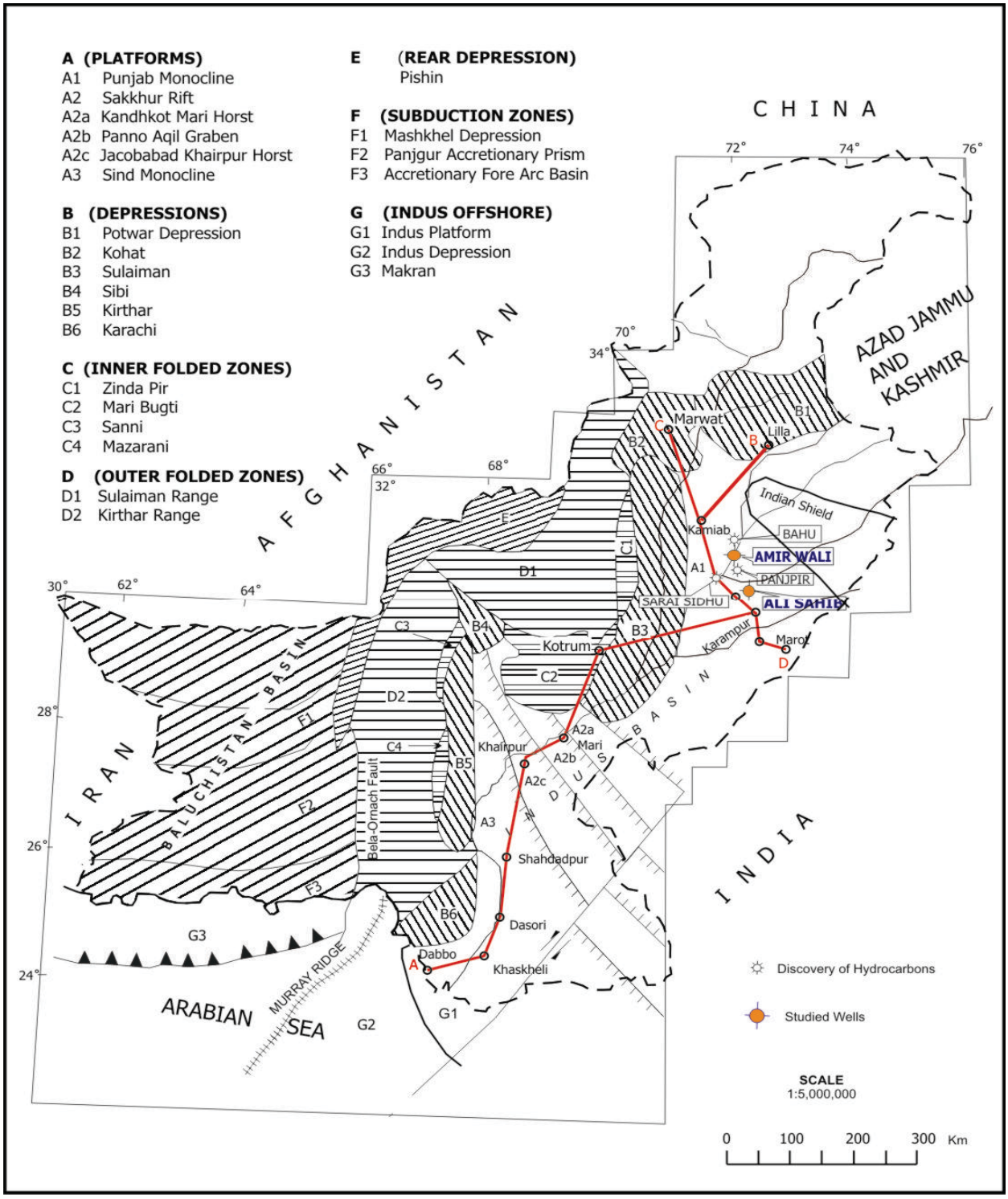

Fig. 1.2: Geological sketch map showing the locations of studied wells (Ali Sahib and Amir Wali drilled by OGDCL in 2005) and of profiles A-B and C-D (modified from Raza *et al.*, 1989).

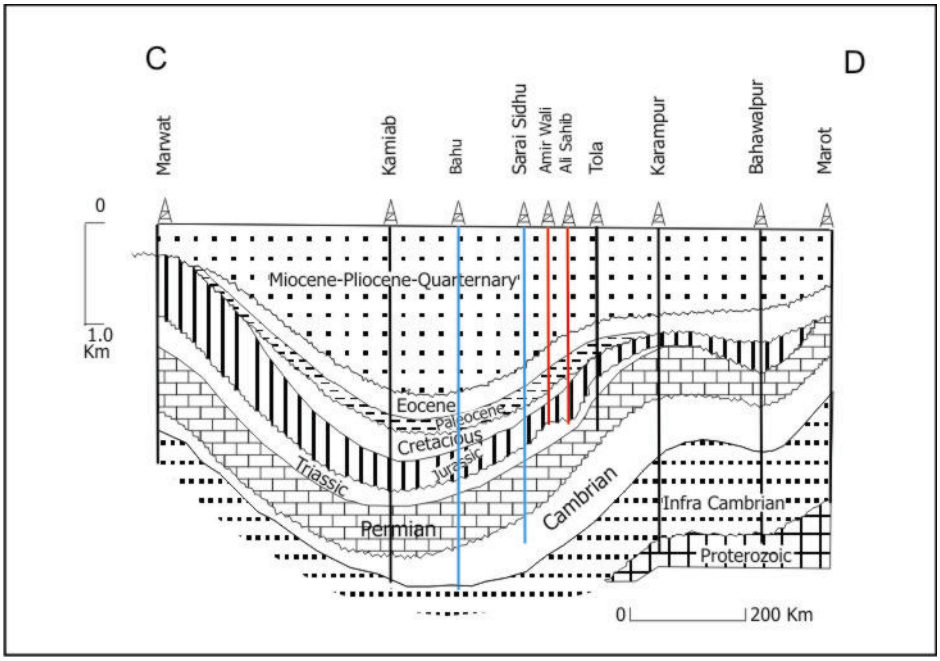

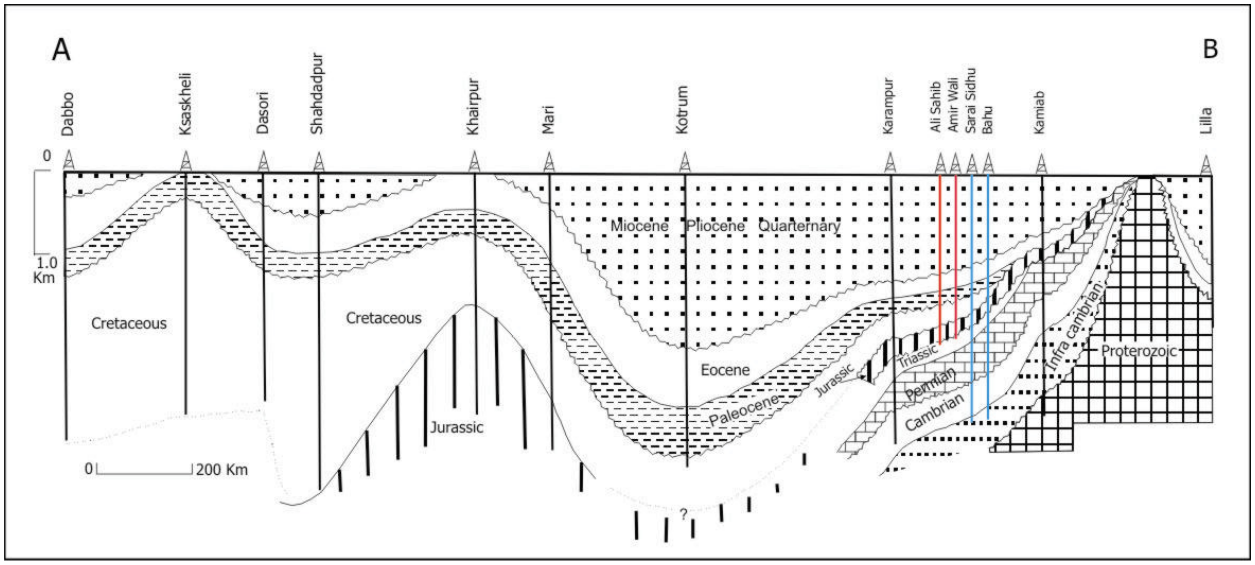

Fig. 1.3: Geological profiles through the Indus Basin and Punjab Platform. Positions of profile line A-B and C-D are shown in Fig. 1.2 (modified from Kazmi & Jan, 1997).

1.4 MOTIVE OF THE PRESENT WORK

The exploration for hydrocarbons in the Punjab Platform (particularly in the Punjab Plain) has been carried out since last 40 years. Despite of growing insights from geophysical investigations and drilling activities, the success ratio of discovery of hydrocarbons in the Punjab Platform in the Indus Basin in Pakistan is still unsatisfactory and is not very much encouraging. Due to lack of systematic studies, numerous wells have been drilled for exploration of hydrocarbons but were abandoned.

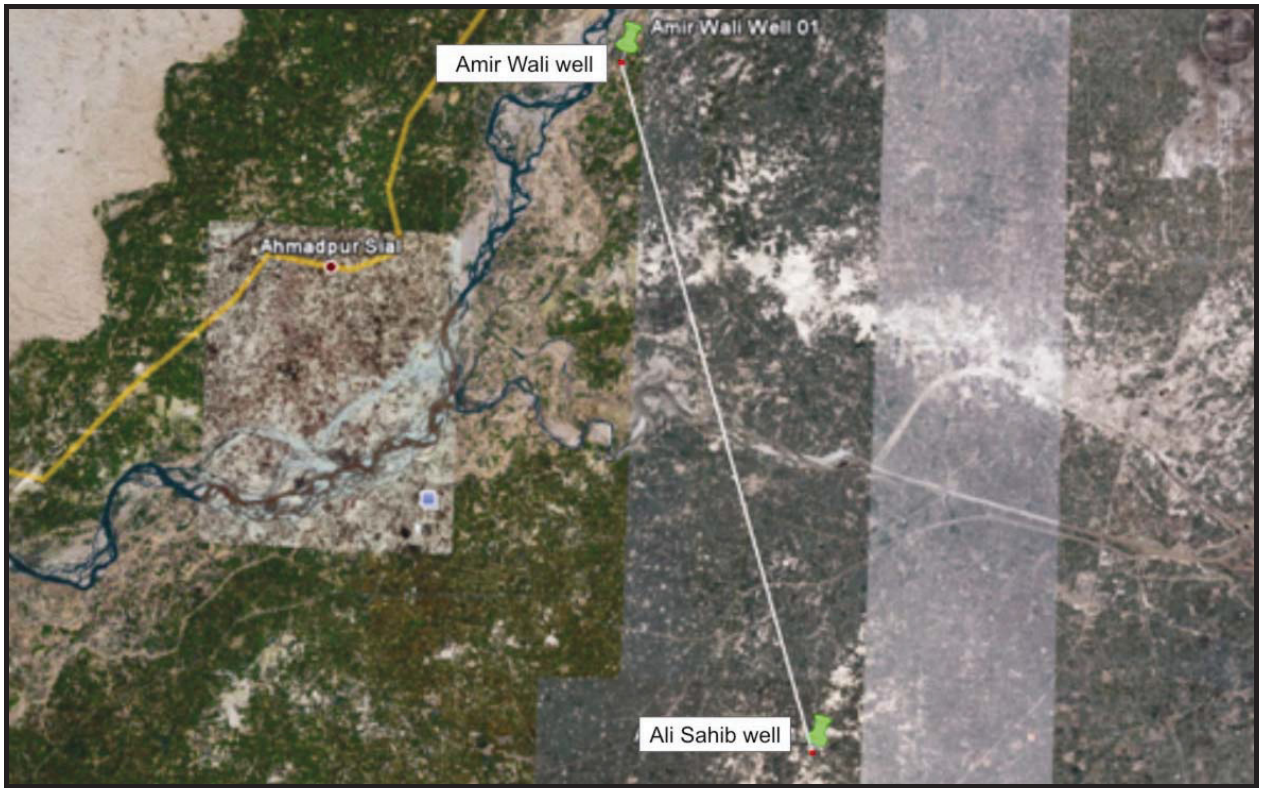

Fig. 1.4: Location map of the Ali Sahib and Amir Wali wells in Punjab province, Pakistan, drilled by OGDCL in 2005 (from Google Earth).

To enhance the success ratio of exploration, a better understanding of the oil-gas system is needed. Until now, only bulk geochemical data (total organic carbon, Rock-Eval pyrolysis) are available for source- and reservoir-rock characterization. However, the interpretation of TOC, hydrogen index (HI) and oxygen index (OI) is insufficient to identify potential hydrocarbon source rocks because of difficulties to distinguish indigenous and migrated hydrocarbons. Though the geophysical logs and general litho-stratigraphy were available, but lacking lithofacies of clastics and microfacies of carbonates are very much relevant in characterization of source and reservoir rocks.

In this study, the interpretation of TOC, maturity parameters in combination with biomarker data, microfacies of carbonates (cores) and lithofacies of clastics (cores) are used to characterize the environment of deposition and the source rock potential of the strata drilled in the Ali Sahib and Amir Wali wells. The aim of the study is to increase our knowledge for further exploration in this area of the Punjab Platform.

1.5 OBJECTIVES

- To demarcate the formation boundaries by studying the lithology of ditch cuttings.
- To prepare general lithological logs of the wells of different lithofacies.
- To determine the maturity level of source rocks.
- To determine the type of porosity (primary or secondary).
- To study diagenesis of source as well as reservoir rocks.
- To study microfacies and to discuss sedimentology and environment of deposition of source and reservoir rocks.
- To understand the plays governing the hydrocarbons in the area.

But before going to above mentioned objectives, results and discussions, it is necessary to have a brief overview on: regional geology (Chapter 2), previous geological work in the Salt Range Region (Chapter 3), geology and stratigraphy of the Punjab Platform (Chapter 4), samples and methodology to the present work (Chapter 5), for better understanding about work accomplished.

2. REGIONAL GEOLOGY AND TECTONIC FRAMEWORK OF PAKISTAN

The Indian Ocean and the Himalayas border the Indo-Pakistan subcontinent which is the product of geodynamic processes of sea floor spreading, continental drift and collisional tectonics. The Indo-Pakistani Plate rifted away from the supercontinent Gondwana approximately 120 Ma. This was followed by extensive seafloor spreading forming the Indian Ocean. Driven by geodynamics forces the Indo-Pakistani Plate travelled ~ 5,000 km northward and collided with the Eurasian Plate. The subduction of the northern margin of the Indo-Pakistani Plate closed the Neotethys and with continued sea floor spreading the Indian Ocean acquired its current extent (Kazmi & Jan, 1997). The collision of the Indo-Pakistan subcontinent and Eurasian Plate lead to the formation of the Himalayas and the adjacent mountain ranges. The geodynamics of Indo-Pakistan subcontinent is briefly reviewed in the following.

2.1 EMERGENCE OF THE HIMALAYAS

The continental drift theory was proposed first by Wegener (1912), who suggested that continental movement may have taken place on a gigantic scale.

According to the theory of plate tectonics, the continents have been joined and separated several times (for details see Birkland & Larson, 1989). Approximately 250 million years ago the proto continent "Pangaea" was existing (Kazmi & Jan, 1997). After rifting, which began in Permian, two separate land masses were formed: The northern block called "Laurasia" (comprising most of present day North America and Eurasia) and the southern block, called "Gondwana" (including most of South America, Africa, Arabia, India, Australia and Antarctica).

During the Middle Cretaceous, the supercontinent continued to break up into different blocks and these blocks drifted into their present positions. The Indo Pakistan subcontinent separated from Gondwana ~ 130 million years ago (Johnson *et al.,* 1976). The precise location of Africa, Antarctica and Australia within Gondwana is still uncertain. Various authors have assigned different locations to continents. Before the introduction of the theory of plate tectonics, reconstructions of Gondwana were based

entirely on land based data and the prevailing geological theories. More recent paleomagnetic data from the ocean floor has enabled more precise reconstruction of the ancient supercontinent (Figs. 2a & 2b).

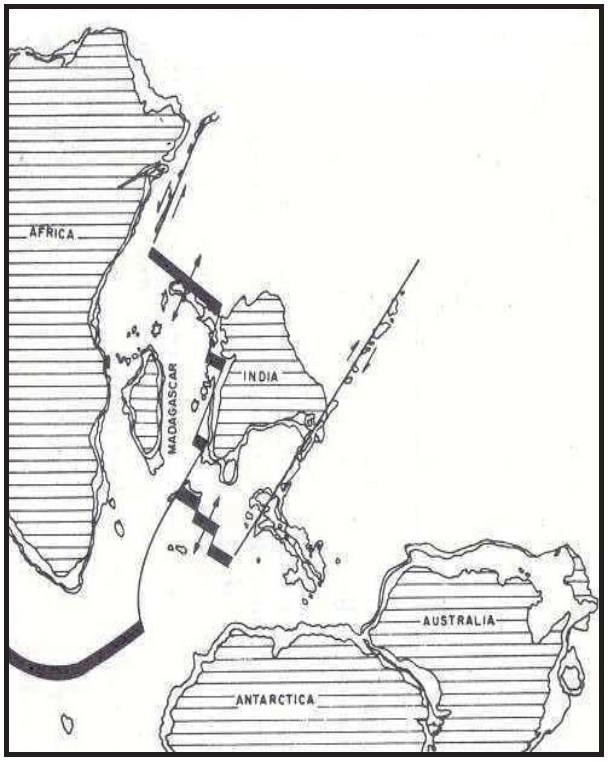

Fig 2a: Position of Indo-Pakistani Plate 75 million years ago. After breaking away from Gondwanalaand, this plate moved rapidly northeastward. New crust was generated along the ridges marked by parallel line and the transform faults east and west of the connected series of ridges enabled unimpeded movement of Indo Pakistani Plate (McKenzie & Sclater, 1976).

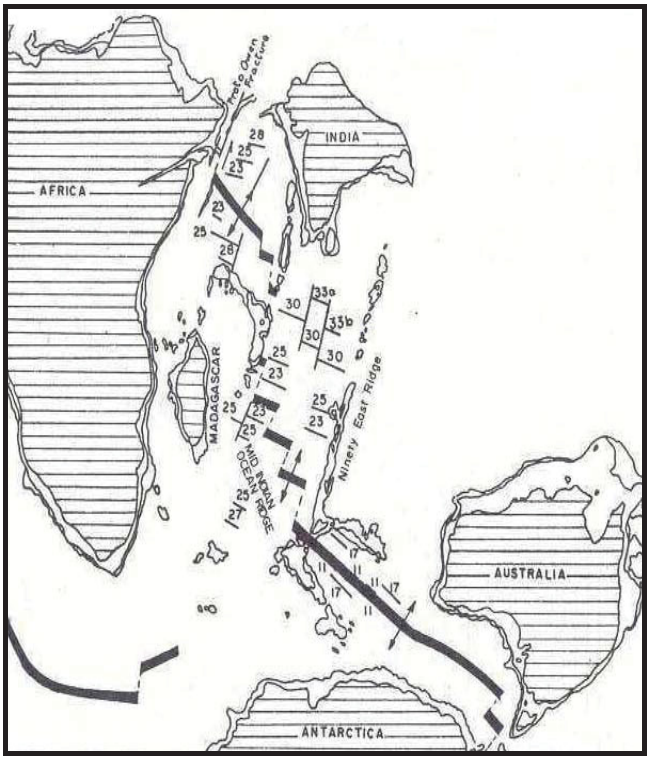

Fig 2b: Position of Indo Pakistani Plate 35 million years ago. By this time the plate had moved 4,000 km northward. At this stage, direction of relative motion among the major Gondwanian plates changed drastic-cally to produce the present day sea floor geometry (McKenzie & Sclater, 1976).

The Indo-Pakistan Plate's predrift position with respect to Australia, Antarctica and Madagascar, has remained problematic as these plates have moved and rotated at varying rates and in different directions since the separation of Indo-Pakistani Plate. Furthermore, the topography of the Indian Ocean and its spreading pattern are complex. Magnetic lineations on the older sections of the ocean are absent (McKenzie, & Sclater, 1976). As a result fixing the position of the Indo-Pakistan Plate requires assumptions to be made concerning the relative positions of Madagascar, the Chagos Trench, the Mauritius Fracture Zone and the rotations of various plates, which are then

intergrated together with bathymetric and geological arguments (McKenzie & Sclater, 1976).

Though older magnetic anomalies are known, their age and relation to the relative Anomaly 33 are not established. Reconstructions of the Indian Ocean and the relative positions of continents for the time period of 80-75 Ma are based on Anomalies 33 and 32 (see Figs. 2a & 2b). It is believed that the Chagos Trench and the Mauritius Fracture Zone were linked and a transform fault extended along Ninety East Ridge (McKenzie, & Sclater, 1976). The ridge south of Sri Lanka (precursor of Mid Indian Oceanic Ridge) spread in such a way that India was driven northward. The Chagos-Mauritius and Ninety East transform faults on either side facilitated the northward movement. New crust was continuously generated along the spreading ridges. Australia and Antarctica remained connected at this time, while Madagascar, Africa, and South America had already separated (Kazmi & Jan, 1997).

It has been estimated that between 130 Ma and 80 Ma the Indo-Pakistani Plate moved northward at a rate of 3 to 5 cm per year (McKenzie & Sclater, 1976). Thereafter its movement accelerated considerably. The ~ 5000 km between the matching set of the Anomalies 21 and 32 shows that from 80 Ma ago. The Indo Pakistani Plate moved at an average rate of about 16 cm/year relative to Australia and Antarctica (Powell, 1979). According to Patriat & Achache (1984) prior to Anomaly 22 (~ 50 Ma.), this rate of movement varied from 15 to 25 cm/year. The movement was facilitated by transformational faulting in the Proto-Oven Fracture Zone and extensive sea floor spreading along Mid Indian Oceanic Ridge. It should also to be noted that the extensive extrusion of Deccan Trap Basalts occurred between 65-60 Ma (Duncan & Pyle, 1988), during the rapid northward drift of Indo Pakistani Plate.

The exact timing of Indian-Eurasian subduction is still unknown. But Patriat & Achache (1984) subduction of Indo-Pakistani Plate under Eurasian Plate began 110 Ma ago (Aptian). At that time, the Indo-Pakistani Plate was moving northward at an average rate of 14.9$\pm$ 4.5 cm/year. The main collision occurred during Late Eocene between 40 and 50 Ma (Powel & Conaghan, 1973). At that time, the rate of relative motion of the

Indo-Pakistani Plate decreased from ~ 10 cm/year to 5 cm/year (Molnar & Tapponnier, 1975).

The Indo-Pakistani Plate had continued its northward migration since that time at a rate of ~ 5 cm/year the resulting ~ 2,000 km of closure of sea between the two plates, thus formed the Himalayas (Kazmi & Jan, 1997).

2.3 TECTONIC ZONES

The geological setting of the regions surrounding Pakistan has two broad geological divisions, the Gondwanian Domain and Tethyan Domain. Pakistan is located at the junction of these two diverse domains. The southeastern sections of Pakistan belong to Gondwanian domain and are sustained by Indo-Pakistan crustal plate (Kazmi & Jan, 1997).

The northernmost and western regions of Pakistan are part of the Tethyan Domain and represent complicated geology and complex crustal structures. On the basis of Plate Tectonics features, geological structures, orogenic history (age and nature of deformation, magmatism and metamorphism) and lithofacies, Pakistan may be divided into the following broad tectonic zones (cf. Fig. 1.2 & Ch. 1).

a) Indus Platform and Foredeep
b) East Baluchistan Fold and Thrust Belt
c) Northwest Himalayas Fold and Thrust Belt
d) Kohistan-Ladakh Magmatic Arc
e) Karakorm Block
f) Kakar Khorasan Flysch Basin and Makran Accretionary Zone
g) Chaghi Magmatic Arc
h) Pakistan Offshore

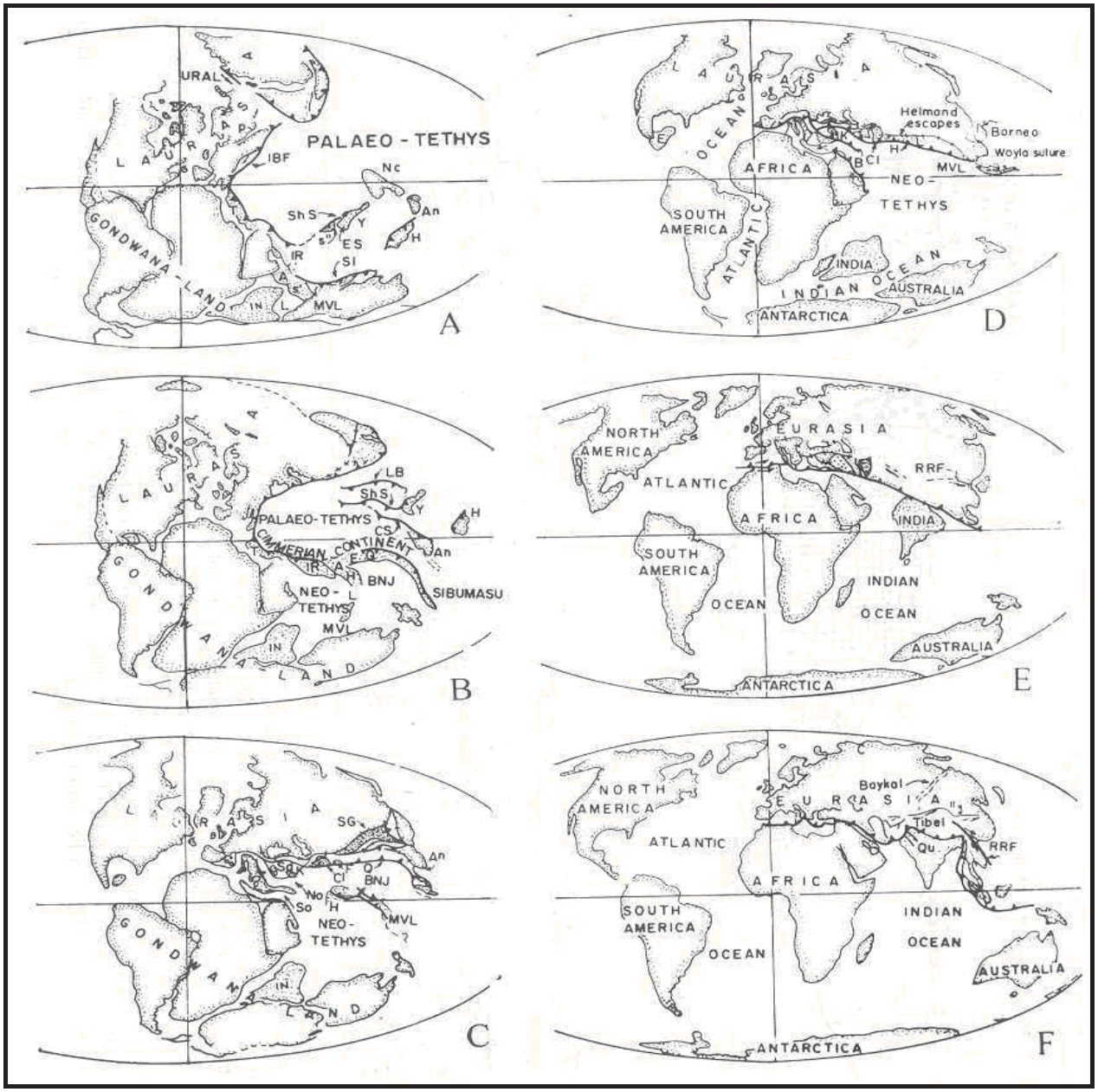

Fig 2.1: Generalized reconstruction of the continents showing evolution of Tethyan Domain (from Sengör *et al.*, 1988). A: Late Permian, B: Early Triassic, C: Late Jurassic, D: Late Cretaceous, E: Middle Eocene, F: Late Miocene.

In the above mentioned tectonic zones, various hydrocarbon discoveries were made only in the Indus Platform and Foredeep. Here a brief discussion is given about the Indus Platform and Foredeep.

2.4 INDUS PLATFORM

The Indus Platform extends over an area of more than 250,000 km^2 in south eastern Pakistan and includes the Indus Plains and Thar-Cholistan Deserts. Gravity and seismic

surveys, supported by limited bore hole data, indicate that in the eastern section, Precambrian rocks form a gentle westward dipping monocline covered by a veneer of Mesozoic to Cenozoic marine to deltaic sediments (Kazmi & Jan, 1997).

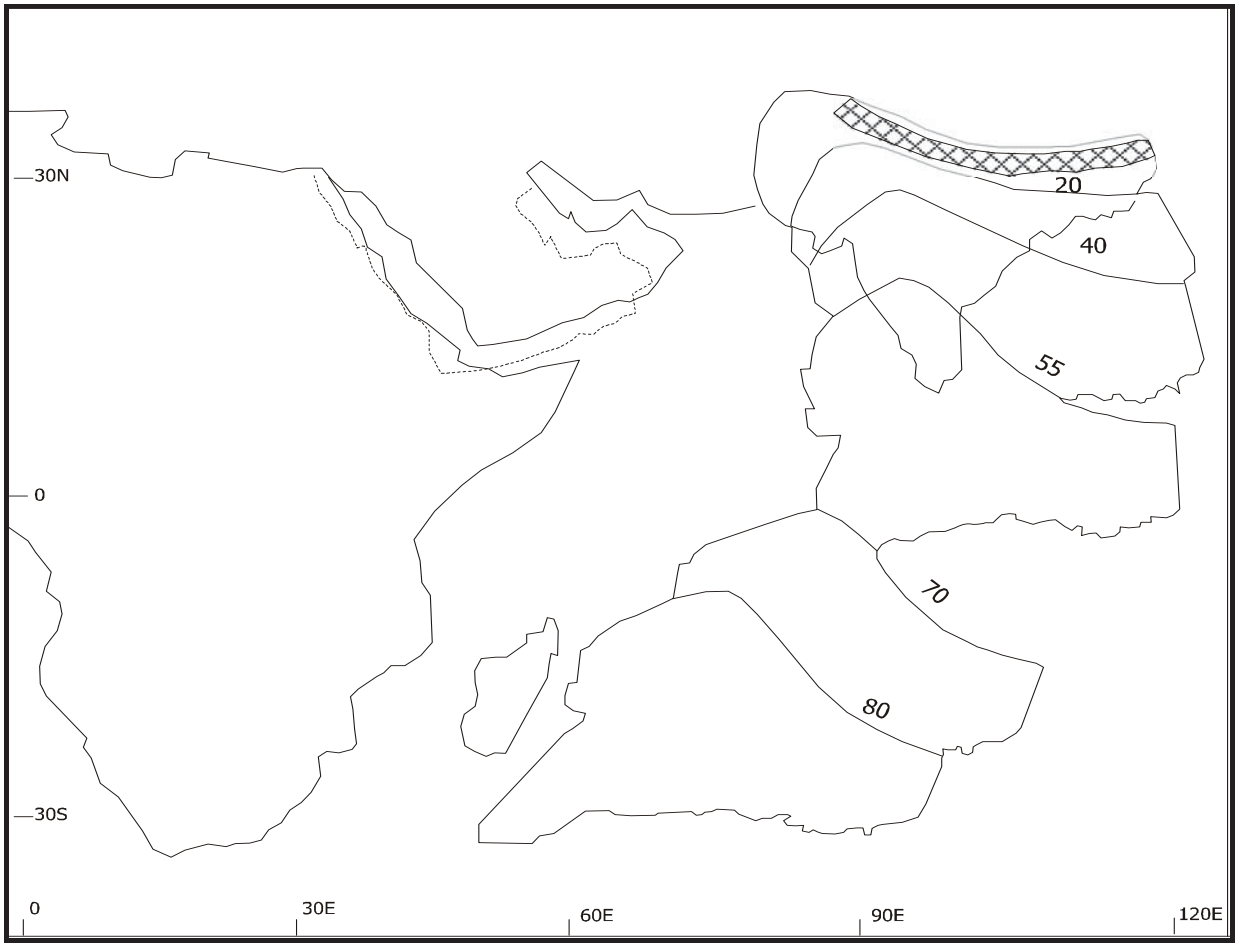

Fig. 2.2: Northward flight of the Indo Pakistani Plate with respect to Africa and Madagascar, since 80 Ma. The stage positions are derived from the relationship between oceanic magnetic anomalies as proposed by La Brecque et al. (1977). The cross hatched strip is the present doubled-up Indo-Pakistani Crust between the Himalayan front and the Indus Ophiolite belt. The dotted line indicates the position of Arabia before the Neogene opening of the Red Sea (modified from Powel, 1979).

The sedimentary cover is relatively thin in the upwarp zones. The downwarps contains a thick sedimentary pile, particularly the foredeeps at the western edge of the platform slope where the sedimentary cover is up to 10,000 m thick (Kazmi & Jan, 1997).

STRUCTURAL ZONES

The Indus Platform and Foredeep comprise following main structural zones (Kazmi & Rana, 1982; Balakrishnan, 1977):

BURRIED RIDGES

a) Sarghodha-Shahpur Ridge

b) Nagar Parkar Ridge

ZONES OF UPWARP

a) Mari-Kandhkot High

b) Jacobabad Khairpur High

c) Thatta Hyderabad High

d) Tharparkar High

ZONES OF DOWNWARP AND PLATFORM SLOPE

a) Southern Punjab Monocline

b) Cholistan Shelf

c) Pannu Aqil Graben

d) Nawabshah Slope

e) Lower Indus Trough

f) Nabisar Slope

FOREDEEPS

a) Sulaiman Foredeep

b) Kirthar Fore Deep

These structural zones are shown in Fig. 4.1. It should be noted that the Jacobabad-Khairpur upwarp divides the Indus Platform into two segments. The lower segment is comprised of the Lower Indus Trough. It is bounded by the Nawabshah and Nabisar Slopes which are in turn flanked by the Thatta-Hyderabad and Tharparkar Highs. The upper segment, in Punjab, is traversed by Sarghodha-Shahpur Ridge, splitting it into northern Punjab Monocline (Khushab-Gujranwala) and southern Punjab Monocline (Mianwali-Bahawalpur) and the Cholistan Shelf. To the west, the Indus Platform sharply deepens to form the Sulaiman and Kirthar Foredeeps.

2.5 BASEMENT ROCKS AND STRUCTURES

Precambrian basement rocks (Kirana Group) crop out as monadnocks in the Sargodha-Shahpur region (in Punjab Province, north of the study area).

These are the exposed summits of the buried Sargodha Shahpur ridge and are largely comprised of metasediments (phyllites, quartzites) and metavolcanics (Fig. 4.4). Davies & Crawford (1971) have dated (Rb/Sr) these rocks 870 $\pm$ 40 Ma.

Geophysical surveys (Balakrishnan, 1977; Farah *et al.,* 1977; Seeber *et al.,* 1980; Malik *et al.,* 1988) and remote sensing studies (Kazmi, 1979; Kazmi & Rana, 1982) indicate that the basement is extensively traversed by NNE to NE and NNW to E-W trending faults. The NE oriented faults conform to the Aravalli-Delhi Trend, whereas the NNW faults are parallel to Jhelum, Kalabagh, Choudhwan, Kingri and Mach strike slip faults (Kazmi & Rana, 1982). Some of the basement faults straddle major structures such as the Sargodha-Shahpur Ridge (Farah *et al.,* 1977) and Kandhkot-Mari and Jacobaabad-Khairpur horsts (Ahmad & Ali, 1991). Other documented and prominent faults are the Cutch and Talhar Faults (Kazmi, 1979; Kazmi & Rana, 1982), Thar Fault (Fasset & Durrani, 1994), and the faults in the Punjab seismic zone (Seeber *et al.,* 1980). The majority of the Late Cretaceous basement faults and rift structures are associated with detachment of the Indo-Pakistani Plate from Gondwana, while the Tertiary faults may be the result of bending of the crustal plate due to collision, and rebound relief tension or compression release. Seismic studies and fault plane solutions indicate that some of these faults are extensional features, while other are strike-slip faults (Seeber *&* Armbruster, 1979).

2.6 SEDIMENTARY COVER

The Indus Platform and Foredeeps are covered by unconsolidated Quaternary deposits with a maximum thickness of 500 m. They are underlain by Siwalik Molasse in northern and western regions of the Indus Platform and in the Foredeep region. South of Sargodha-Shahpur Ridge and extending up to Kandhkot-Mari high, in a roughly triangular area, the Quaternary deposits are underlain by post-Eocene, largely fluvial deposits (the Nari and the Murree Formations). In southern part of the Platform, east of

Indus, the Quaternary deposits are underlain by Paleogene marine and deltaic sedimentary rocks.

The Precambrian and Palaeozoic sequence is restricted to the Punjab region of the Indus Platform. It thins in the Jacobabad-Khairpur region and has not been observed in deep wells of Sindh area. The cover is thinnest in the region of the Sargodha-Shapur Ridge (0-600 m), Jacobabad-Khairpur high (up to 4,000 m), Tharparkar high (10-200 m) and the eastern margin of the Platform. In the Platform slopes and downwarp zones the sedimentary cover is thick while in foredeep zones it attains a thickness of 10,000 m to 15,000 m (Kazmi & Jan, 1997; Raza *et al.*, 1989; 1990).

Structurally the sedimentary cover of the Indus Platform and Foredeep is comprised of several large, gently dipping anticlinal flexures and fault blocks. Oil and Gas reserves have been found in some of these structures. In the Punjab region of the Platform gas reserves have been found in Mesozoic sandstones at Nandpur and Panjpir. In 2006, another gas reserve was discovered in the Bahu Well 01 in Cretaceous (the Lumshiwal Formation) and Jurassic strata (the Samana Suk Formation). The Sarai Sidhu Well reported as oil condensate occurring in the Jurassic Samana Suk Formation (Figs. 1.2 & 1.3). In the Kandkot-Mari horst gas occurs in Eocene carbonate reservoirs.

The Jacobabad-Khairpur horst contains gas in Eocene carbonates and in Jurassic and Triassic sandstones while in the Badin region of Sindh oil and gas has been found in the sandstone of Cretaceous age in structural traps (Malik *et al.,* 1988; Raza, 1989b).

To the north and south of the Indus Platform and Foredeeps, the sedimentary cover has been deformed extensively by the collision of Indo-Pakistani Plate with Eurasian Plate. The deformation forms a broad fold axis with intervening sharp structural flexures. The northern and western margins of this zone are characterised by sutures and obducted masses of ophiolite, while the southern and eastern areas of the zone are comprised of contorted fold and thrust belts (Kazmi & Jan, 1997).

3. PREVIOUS GEOLOGICAL WORK IN THE SALT RANGE REGION

Initial geological research in the Salt Range was based on the stratigraphic sections. Here a brief overview of previous workers and their results.

Wynne (1878)
First person/geologist, who measured the stratigraphic sections in the Salt Range, described the history of Permian and Triassic rocks. He introduced the different names "Purple Sandstone Series" (Khewra Sandstone), "Obolus Beds"´(Kussak Formation), "Pseudomorphic Salt Crystal Zone" ,`Chidru` and `Wargal` Group in 1878-1880.

Middlemiss (1891)
He proposed that the salt marl in the Salt Range Formation was not formed by sedimentary processes. It is instead a secretion of an underlying layer of magma that had intruded beneath the Cambrian Purple Sandstone.

Noetling (1901)
He divided the formations into different groups (Warcha, Dandote, Wirgal and Chidru Groups). He proposed that the Salt Range Formation is much more recent in age. According to him, the overlying strata of the Salt Range Formation are overthrusted.

Holland (1903)
Endorsed the views of F. Noetling about the overthrust of older strata on the "Younger Salt Range Formation (Eocene age)".

Christie (1914)
He proved that the Salt Range Formation was not of igneous origin and was instead a sedimentary rock.

Pascoe (1920)
Reviewed previous reports and concluded that the Salt Range Formation and the Purple Sandstone (Khewra Sandstone) are overlying the Salt Range Formation, were normal sedimentary deposits of Tertiary (Eocene) age. He argued that the position of the Salt Range Formation and the Purple Sandstone below other formations of Cambrian age was due to overthrust.

Gee (1934, 1935, 1945, 1980 and 1989)

Did extensive mapping, measured geological sections and was a major contributor in establishing the stratigraphy of the Salt Range region. In 1934, he suggested that the Salt Range Formation (the Saline Series) and the Kohat Salt (Bahadur Khel Salt) is of Eocene age. But later, he concluded that the Salt Range Formation is a normal sedimentary deposit located in its original position below the Purple Sandstone (Khewra Sandstone). In 1980, Gee proposed a lithostratigraphic subdivision of the region and made four major lithostratigraphic units. He defined different stratigraphic names which are still in use. His other work is mentioned in Ch. 4. Below is a comparison of the names given by him and the approved names by Stratigraphic Committee of Pakistan (SCP).

Present names (SCP)	***Names given by Gee***
Salt Range Formation	Saline Series
Khewra Sandstone	Purple Sandstone
Tobra Formation	Talchir Boulders Beds
Mianwali Formation	Mianwali Series and Ceratite Beds
Kingriali Formation	Kingriali Dolomite
Chichali Formation	Chichali Formation
Hangu Formation	Makarwal Group
Lockhart Limestone	Lockhart Limestone
Nammal Formation	Nammal Formation
Sakesar Limestone	Sakesar Limestone

Sahni (1944)

He reported as first the existence of numerous micro-fossils (plants) from samples taken from the Salt Range Formation at the Khewra and Warcha salt mines. The great majority of which was unidentifiable as to genus and species, being comprised mainly of fragments of angiosperm wood, but there are also gymnosperms tracheids with large round bordered pits, and at least one good, winged, six legged insect with compound eyes. Based on this evidence he claimed that the Salt Range Formation must be of Eocene and not Cambrian age. He found no evidence for faults.

Sokolov & Shah (1966)

These authors presented a comprehensive report about "Major Tectonic features of Pakistan" as a review of previous work. They introduced new terms for some structures. A summary of their work of subdivisions is given below.

- Shield: The Indian Shield occupies eastern regions of Pakistan and consists of Precambrian crystalline rocks. These are exposed in Sargodha and Nagar Parker.
- Slope of Platform: The slope of Indian Shield occupies the Thar region, and parts of the alluvial plains.
- Foredeeps: They showed that some regions such as Potowar Foredeep and lateral uplifts are now stable while Sub-Kirthar and Sub-Sulaiman Foredeeps are still undergoing intensive subsidence.
- Folded Belts: There are two main folded belts in Pakistan, the Northern Himalaya Folded Zone and Southern Baluchistan Folded Zone.
- Median Masses: There are two median masses of Precambrian and Paleozoic consolidation and they are the Karakoram and the Baluchistan median masses. They represent separate blocks of more extensive and hard masses that have undergone crumbling.

Kazmi (1966, 1977, 1984)

Studied the Quaternary deposits of the Indus Plains and correlated them to the Himalayan Quaternary sequence. He named the different Formation of the recent deposits. The most significant of which are the Lahore Formation, Rechna Formation, Chung Formation, Pasrur Gujrat and Khushab Clay and Shekhupura Formation.

Opdyke *et al.* (1982)

They showed with magnetic studies of Siwaliks that the decollement of strata of Salt Range has been rotated in counterclockwise fashion from 10° to 40° and moved to the south. They also suggested that the folds of the strata developed within the last 2 Ma.

Yasin *et al.* (1994, unpublished)

These authors studied the lithology, stratigraphy and paleontology encountered in Fort Abbas Well-01, drilled by Oil and Gas Development Company (Corporation). The Fort Abbas Well was the first in Central Indus Basin near the boundary of Pakistan and India. They observed a different stratigraphy to that of the Salt Range region. The thickness of the stratigraphic units and the lithologies of formations are not in accordance with the Salt Range area. The authors concluded that the hydrocarbons were generated in the Punjab Platform.

Kazmi & Jan (1997)
The authors reviewed/edited various papers on the subject of Geology of Pakistan and published a book "Geology and Tectonic of Pakistan". The book has following chapters: Geomorphic Features, Regional Tectonic Setting and Framework, Stratigraphy, Magmatism, Metamorphism, Noetectonics and Seismicity of Pakistan. The book has some information about mineral deposits and fuel deposits of Pakistan.

Cremo (2001)
The author reviewed discrepancies in the age of the Salt Range Formation. He concluded that the age of the Salt Range Formation is Cambrian or older, but that the age of angiosperms and gymnosperms as well as of human beings also is Cambrian.

Sylvain *et al.* (2002)
They studied predominantly the Eastern Salt Range. Using subsurface data (seismic data and well data), these authors constructed a balanced cross-section, showing a frontal fault bend fold and a set of detachment folds below the Potwar Plateau. They used a software `Thrustpack` and proposed an alternation of periods during which deformation was concentrated on the frontal thrust which occurred between 10 and 5 Ma and was reactivated ~ 1.9 Ma. They studied the relationship between erosional, depositional and deformational histories of the region.

Khan *et al.* (2004)
These authors investigated the Warccha Sandstone of Nilawahan Group (Lower Permian Section) in the Salt Range for potential Uranium deposits. They studied the phosphatic nodules in the Warccha Sandstone and suggested that there would be an occurrence of Uranium in the phosphatic nodules of Warcha Sandstone.

Ahmad *et al.* (2005)
These authors remapped the western Salt Range and noted that the orientation of both large and small scale structures is from NW-SE. They suggested that tectonic transport occurred in a southward direction. They proposed that this was due to lateral movement associated with the Kalabagh Fault.

Ashraf & Gakkhar (2005, unpublished)
The studies were based upon the Ali Sahib Well in District Khanewal in the Central Punjab. They studied the drill cuttings from Eocene to Jurassic. They found the

Dunghan Formation to be of Paleocene age (of South Indus Basin) and that it shows a very close resemblance to the Patala Formation of Paleocene of the Salt Range area. They described 22 major lithofacies from Eocene (1250 m) to Jurassic (to TD. 2050 m). They found nanofossils in Eocene, Upper Paleocene and Lower Cretaceous units.

4. GEOLOGY AND STRATIGRAPHY OF THE PUNJAB PLATFORM

4.1 GEOLOGY OF THE PUNJAB PLATFORM

The Punjab Platform is a part of the Indus Basin and it is a gentle monocline eastward of the Indus Basin (Fig. 4.1). Part of it lies to the north of the Sargodha High (buried ridges) which is a NW-SE trending regional structure feature, while most of it lies to the south. A major section of this platform lies further eastwards across the political border in India, where it is named the Rajasthan Shelf by Verma (1991).

Precambrian basement rocks (Kirana Group) outcrop in the form of monadnocks in the Sargodha-Shahpur region (in Punjab Province, north of the study area). These are the exposed summits of the buried Sargodha-Shahpur Ridge and are largely comprised of metasediments (phyllites, quartzites) and metavolcanics. Some of these rocks have given an isochrone age of 870 $\pm$ 40 Ma (Davies & Crawford, 1971).

As already mentioned (see Ch. 2), the basement of the Punjab Platform is extensively traversed by NNE to NE, NNW to E-W trending faults. Gravity and seismic surveys, supported by limited bore hole data indicate that in the eastern part, Precambrian rocks form a gentle westward dipping monocline, covered by a veneer of Mesozoic to Cenozoic marine to deltaic sediments (Kazmi & Jan, 1997). Glennie (1955), with the help of gravity surveys, found broad zones of upwarp and downwarp in the Indus Platform (Fig. 4.2).

The Punjab Platform contains several tectono-sedimentary cycles starting from the Infra-Cambrian Salt Range Formation followed by the Cambrian clastic-carbonate-evaporite cycle. The Cambrian cycle is followed by Permian tillite-clastic-carbonate cycle after a long hiatus. A thin Mesozoic succession is also present. Then early Tertiary clastics-carbonates exist. Finally the Siwalik Molasses cover this entire succession (Kazmi & Jan, 1997 and Yasin et al., 1994). These tectono-sedimentary cycles are described below.

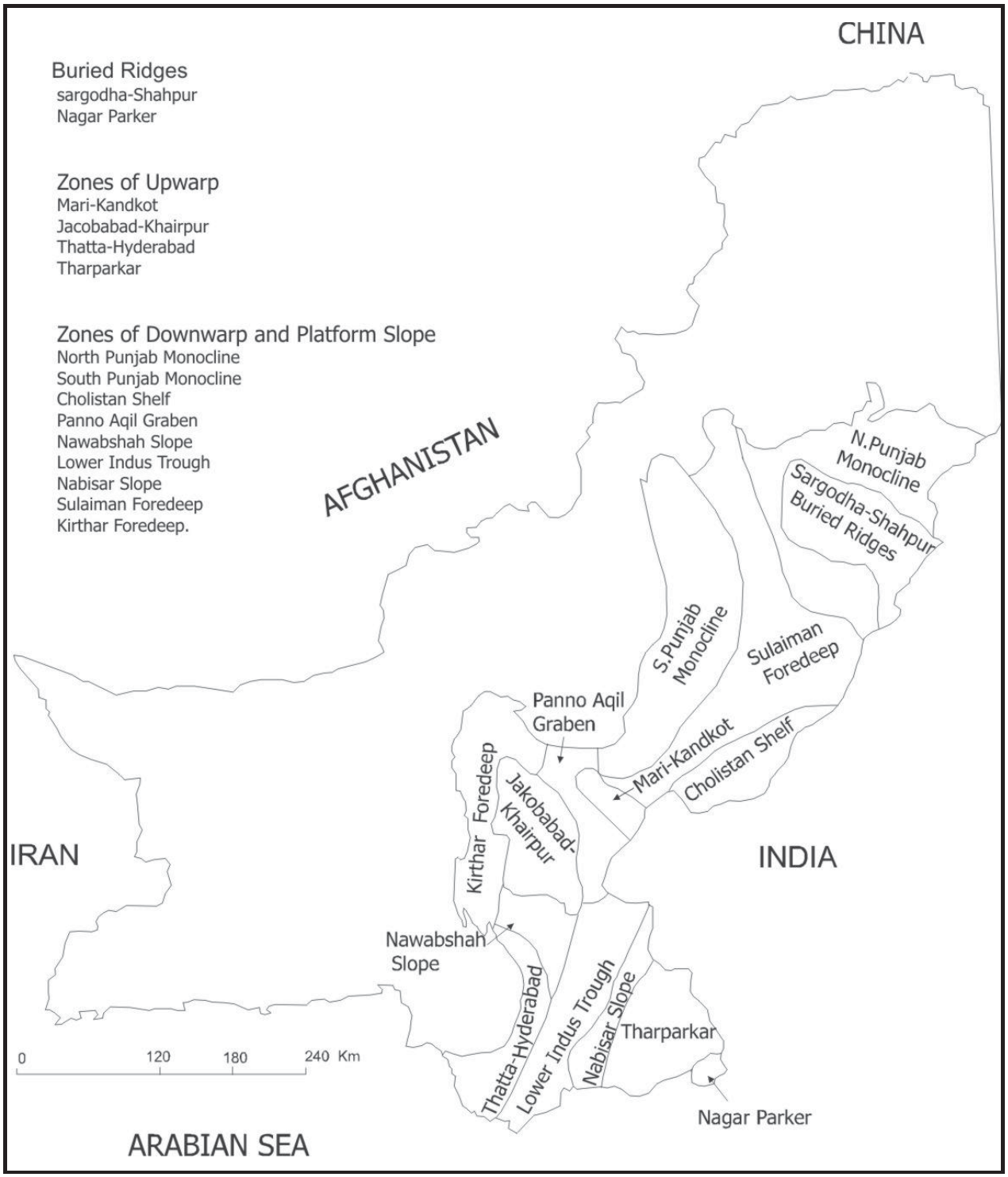

Fig. 4.1: Map showing the tectonic zones of Indus Basin, Pakistan (modified from Kazmi & Jan, 1997).

4.1.2 THE INFRA-CAMBRIAN SALT BASIN CYCLE

The Salt Range Formation is called Infra-Cambrian as it is beneath the Cambrian sediments. On the basis of radiometric dating, Kazmi & Jan (1997) have reported its age as 600 Ma. The nature of the Pre-Cambrian Punjab salt basin is not thoroughly interpreted till now. The Salt Range Formation is present in most parts of the Punjab Platform except over sections of the Sargodha High.

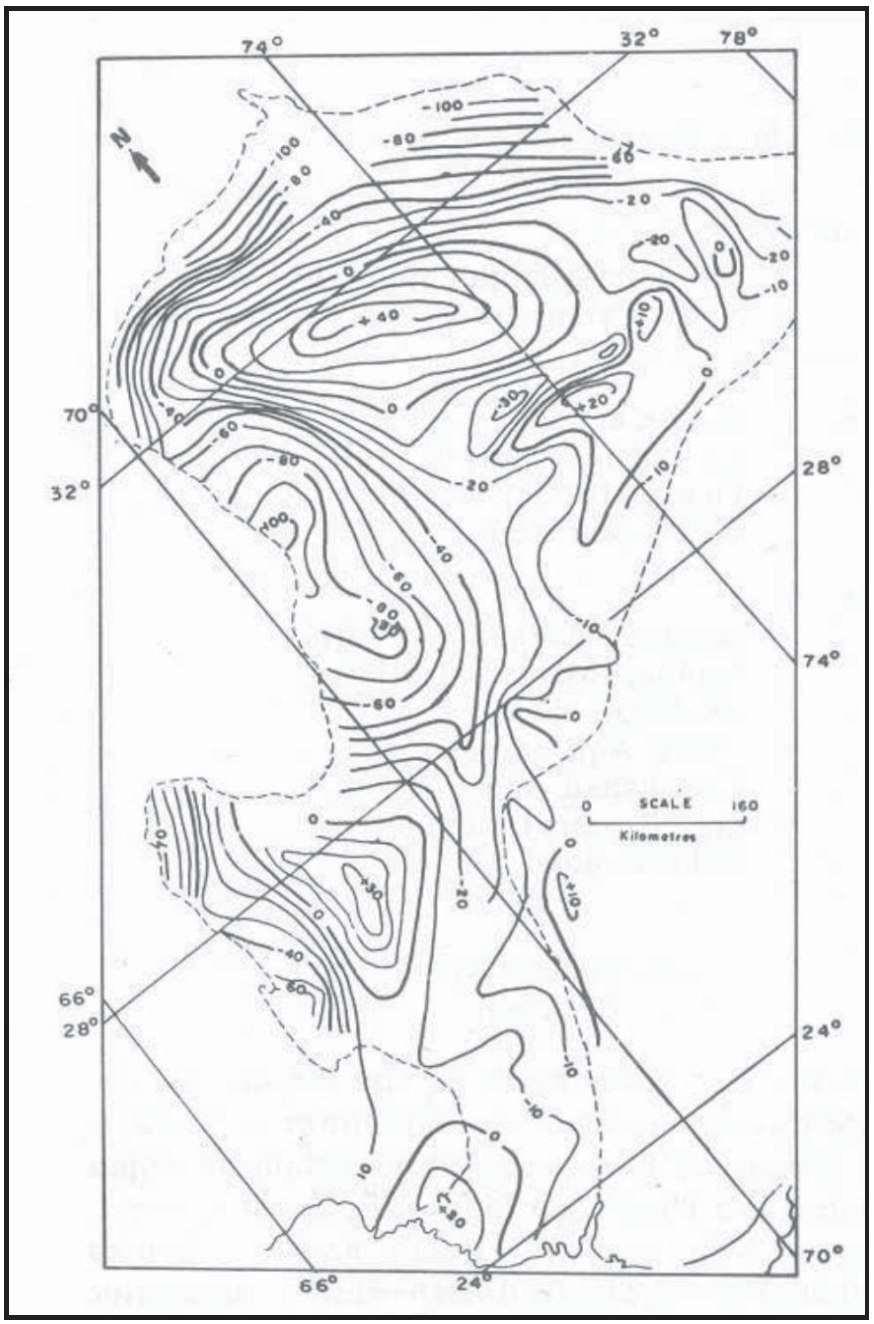

Fig. 4.2: Gravity map of the Indus Plains showing topographical anomalies in milligals (from Glennie, 1955).

Kemal *et al.* (1992), outlines the Pre-Cambrian/Cambrian basin as a NW-SE trending (excluding Potwar Basin) region. Potwar Basin is north of the Sargodha High and it contains a well developed Pre-Cambrian/Cambrian succession. The Pre-Cambrian/ Cambrian sediments of Potowar Basin are truncated to the east over the Hazara-Kashmir Syntaxis that was most likely a protrusion of the Indo-Pakistani Shield and limited the salt basin to the east, which is under discussion. In the Potwar and the Salt Range, the Salt Range Formation consists of red, gypsifereous marl with thick seams of salt in the lower sections, and beds of gypsum, dolomite, greenish clay and oil shales in the upper sections. A thin dioritic, igneous band called Khewra Trap (Jan *et al.,* 1992), exist in the upper sections.

According to the description of Khewra Trap by Jan *et al.* (1992) this magmatic rock consists of minerals which are euhedral, skeletal, spinifex, stellate phenocrysts and they are considered as magnesium rich pyroxenes, completely pseudomorphosed by mineral aggregates similar to talc, the matrix consists of Na-Ca poor K-feldspar (sanidine-orthoclase) with specks of iron oxides. The major and trace elements, suggest the grouping of this rock with ultra potassic continental igneous rocks. The parent magma is thought to have been produced by partial melting of an enriched phlogopite-bearing mantle (Jan *et al.,* 1992).

According to Kemal *et al.* (1992), the thick salt seams in the Salt Range Formation suggest the salt basin was possibly very deep at its full development stage in the Salt Range area. Presence of potassic magmatic rocks suggests intra-plate magmatism, which was possibly associated with a subsiding intracratonic basin, with a restricted connection to the open ocean.

4.1.3 THE CAMBRIAN CYCLE

The Cambrian sediments in the Salt Range area (Fig. 4.6) are classified as Jhelum Group that consists of Khewra Sandstone, Kussak Formation (glauconitic sandstone, shale and dolomite), Jutana Formation (a sandy dolomite) and the Baghanwala Formation (fine grained sandstone and shales containing salt pseudomorphs). The details of lithology and stratigraphy of this group are given in the chapter Stratigraphy

of the Punjab Platform. It consists of one transgressive-regressive cycle with the maximum flooding surface lying in the Kussak Formation. The Baghanwala Formation marks the final regressive phase as it suggests small deltaic and sheet flood deposition in coastal lagoons and sabkhas (Yasin & Janjua, 1994). According to these authors, the base of the Cambrian is Khewra Sandstone, and the boundary between the Salt Range and the Khewra Sandstone is disconformable in the Punjab Platform. They also suggested that there was a mild orogeny before the deposition of the Khewra Sandstone that affected the Salt Range Formation.

4.1.4 THE PERMIAN RIFT BASIN CYCLE

The Cambrian sediments are followed by the Early Permian sediments over the entire Upper Indus Basin. The basin was part of the Gondwana in Late Paleozoic. Gondwana experienced a major glacial episode during that time. It seems that the Punjab Platform remained buried under ice for a considerable period similar to Antarctica today. The ice began to melt in the early Permian as we find first sedimentary activity after Cambrian in the form of glacial deposits of the Tobra Formation. The Permian glaciers carved out deep valleys in the existing Cambrian sediments. We may take the example of the Salt Range and Surghar Ranges, where all Cambrian sediments are present below the Tobra Formation. Towards the west, the Tobra Formation cuts deeper and deeper until all the Cambrian sediments are gone and the Tobra Formation directly lies on the Salt Range Formation (Fig. 4.6), where it contains boulders of salt. Further to the west and south the Cambrian sediments reappear under the Permian sediments. This example suggests the extent of topography carved by the Permian glaciations. The valleys were several hundred meters deep. The Permian valleys carved in the Cambrian sediments were largely filled in the Permian, as there were immense amounts of glacially eroded sediments available to fill them. It is commonly accepted that the breakup of Gondwanaland started as early as the Permian. Verma (1991) has outlined the cratonic areas of India where Permian sediments fill long and narrow, rift-type troughs. These rifts have a NW-SE orientation. Butt *et al.* (1994) found the vitric lava flow or tuff which is 10 to 30 cm thick; and it is made up of brown glass (78%), iron oxide/hydroxide (10%), microcrystalline calcite (5%), xenocrystic feldspar (3%) and quartz (2%). These rocks have been related to the Late Palaeozoic-Early Mesozoic rifting of the Gondwana.

The rifting may have begun during the late stages of glaciation, when large volumes of sediment were being transported. It is also possible that rifting began even earlier and glacial movement may have been controlled by tectonic rifting (Yasin *et al.,* 1994 unpublished).

4.1.5 THE MESOZOIC OPEN SHELF BASIN

The northwestern Indo-Pakistani continent remained as an open shelf during most of the Mesozoic era. The shelf was bordering the Neo-Tethys Ocean. The sediments of this era are broadly similar in Pakistan. So, the Jurassic Chiltan Limestone (Fig. 4.3) in the southern Indus Basin and the Samana Suk Formation (Fig. 4.8) in the northern Indus Basin are lithologically similar. Similarly the Lumshiwal Formation in the north is similar to the Lower Goru Formation in the southern Indus Basin. The Indo-Pakistani continent rapidly drifted northwards during Cretaceous and ultimately collided with the Eurasian Plate and as such this open shelf type sedimentation was terminated (Yasin *et al.,* 1994 unpublished).

4.1.6 THE TERTIARY FORELAND BASIN CYCLE

The Indo-Pakistani continent collided with Eurasia in Late Cretaceous to Early Tertiary. The open shelf style basin was transformed into a foreland basin, which develops in the front and back of the collision orogens. In foreland basins, the subsidence is due to the load of thickening crust in collision zone and the tectonic stresses, which bend the lithosphere on both sides of a collision orogen. The sediment transport direction also changes as new source areas are created due to the rising orogen. The whole basin may consist of many smaller basins and highs due to different rates of relative vertical movements in different areas (Yasin *et al.,* 1994 unpublished).

According to Yasin *et al.* (1994 unpublished) in a developing collisional orogeny, the sedimentary accretionary prism bordering the former trench zone is emplaced tectonically over the colliding continental margin. This sediment mass is reworked and transported backwards onto the craton, from newly created tectonic highs. This sediment mass is most likely represented by the Ranikot, Ghazij, and Patala Formation.

4.1.7 THE TERTIARY/QUATERNARY MOLASSE CYCLE

With continued collision, the sea to the northwest of the Indo-Pakistani shelf kept retreating. In Oligocene, only a small elongated sea remained in southern Pakistan. The continued uplift and huge sediment supply from the rising orogen dried out the remaining sea. Thick non-marine sediments of this cycle covered the earlier deposits in this stage (Yasin *et al.*, 1994 unpublished). This process is still occuring today, as five large rivers are supplying large masses of sediments to the Punjab and Sind basins.

4.1.8 STRATIGRAPHIC NOMENCLATURE IN PUNJAB PLATFORM

The stratigraphy in the Punjab Plains/Platform has been compared to the stratigraphy exposed in the Salt Range area (Figs. 4.5 & 4.8). The stratigraphic nomenclature prevalent in Kohat-Potwar Province is commonly used for Punjab Plains. However, this may not always be valid. The stratigraphy to the south of the Sargodha High (buried ridges) may have significant differences from the Kohat-Potwar stratigraphy. Additionally, further south the stratigraphy becomes more similar to that of Sulaiman Range and of the Lower Indus Basin (Yasin *et al.*, 1994 unpublished).

The locations of the Ali Sahib and Amir Wali Wells are south of Sargodha High (Fig. 1.2), as such the stratigraphy of both the Salt Range (Fig. 4.8) and the Sulaiman Range is used (Fig. 4.3), in particular the Tertiary stratigraphy. A section of the Permian basin is exposed in the Salt Range. The Permian basin also extended into Punjab Plains. As such, the Permian stratigraphy has some similarity in the Punjab Plains and the Salt Range area.

The Mesozoic stratigraphy is broadly similar in both, the Lower Indus and the Upper Indus Basins. However, an exact match in stratigraphy over a wide geographic area should not be expected. As such, the names of formations vary. It should also be noted that in north (in the Salt Range area) rocks are exposed from Pre-Cambrian to Recent, while in south (in Lower Indus Basin), wells have been drilled up to Jurassic rocks. It has been assumed that older formations are present beneath the Jurassic formations. Up to now this assumption is not valid and strong. Precambrian Nagar Parker Granite can be found in Thar Desert, while there is no stratigraphic exposure in Sulaiman Range

older than Triassic. In addition, the Thar Desert has been extensively drilled for coal exploration during the 1990's (some of which I personally logged), there the Tertiary strata directly overlie the Pre-Cambrian Nagar Parker Granite. It could be said that the Mesozoic and Paleozoic strata are missing at least in Thar Desert (in the south eastern part of the Indus Basin).

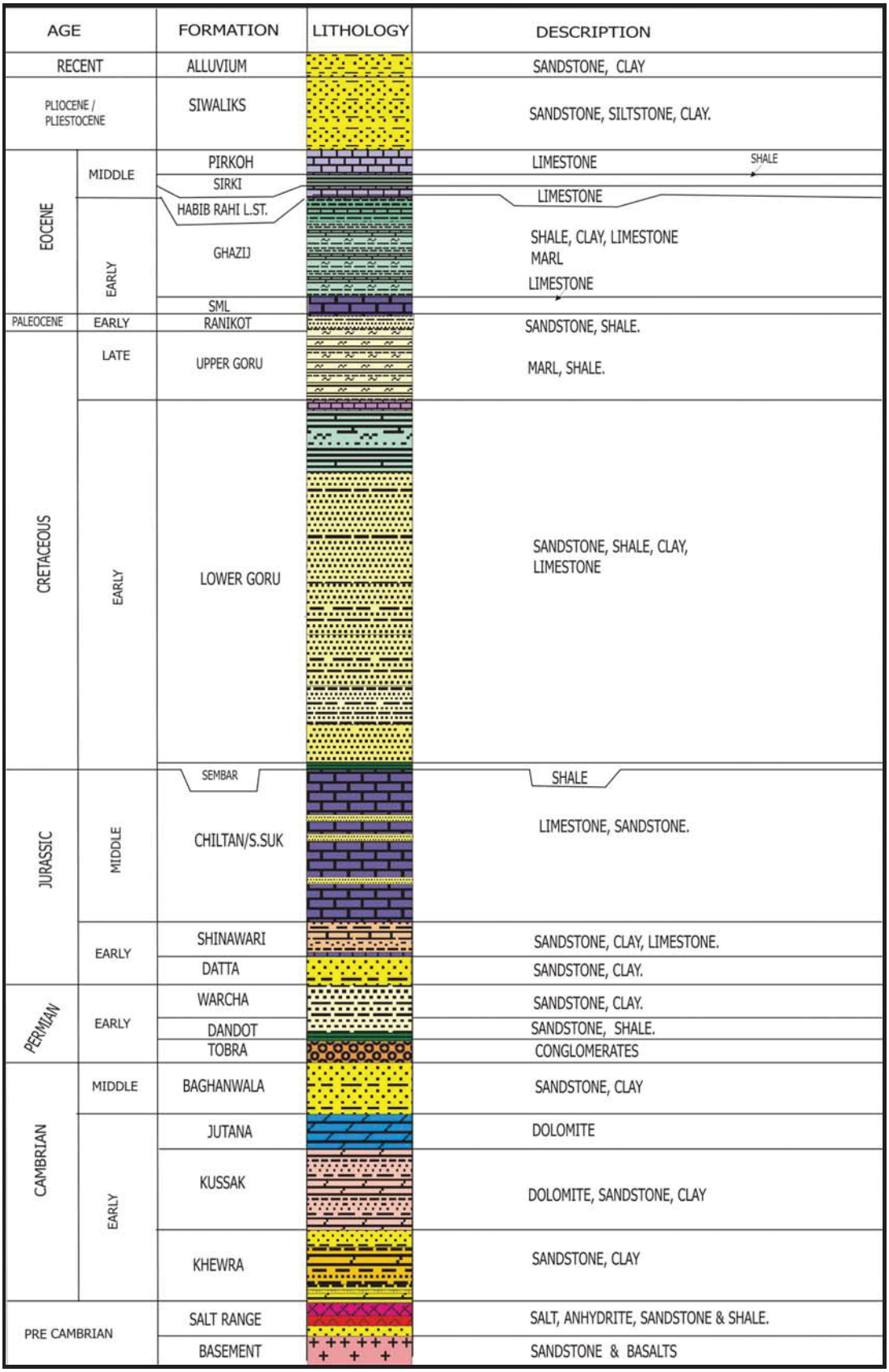

Fig. 4.3: Generalized stratigraphic column of southern part of the study area (stratigraphic boundaries up to Middle Jurassic by drilling data, OGDCL. Below Jurassic, seismic interpretation, OGDCL).

4.2 STRATIGRAPHY OF THE PUNJAB PLATFORM (SALT RANGE AND AD-JOINING AREAS)

In the Punjab Platform the rocks/formations from early Proterozoic to Recent are well exposed in the Salt Range area. The brief description of the formations is given below.

4.2.1 KIRANA GROUP

The unfossiliferous Precambrian metasediments and metavolcanics are exposed near Sargodha and Shah Kot towns. These rocks are inliers in the Punjab Platform and are part of Indo-Pakistani Shield (Fig. 4.4). The Rb/Sr radiometric dating gives an age of 870± 40 Ma. Phyllites, slates, quartzites and sub-ordinates of conglomerates and volcanics are the major lithologies of Kirana Group. The thickness has been stated as more than 2330 m, though its base is not exposed (Kazmi & Jan, 1997 and references therein).

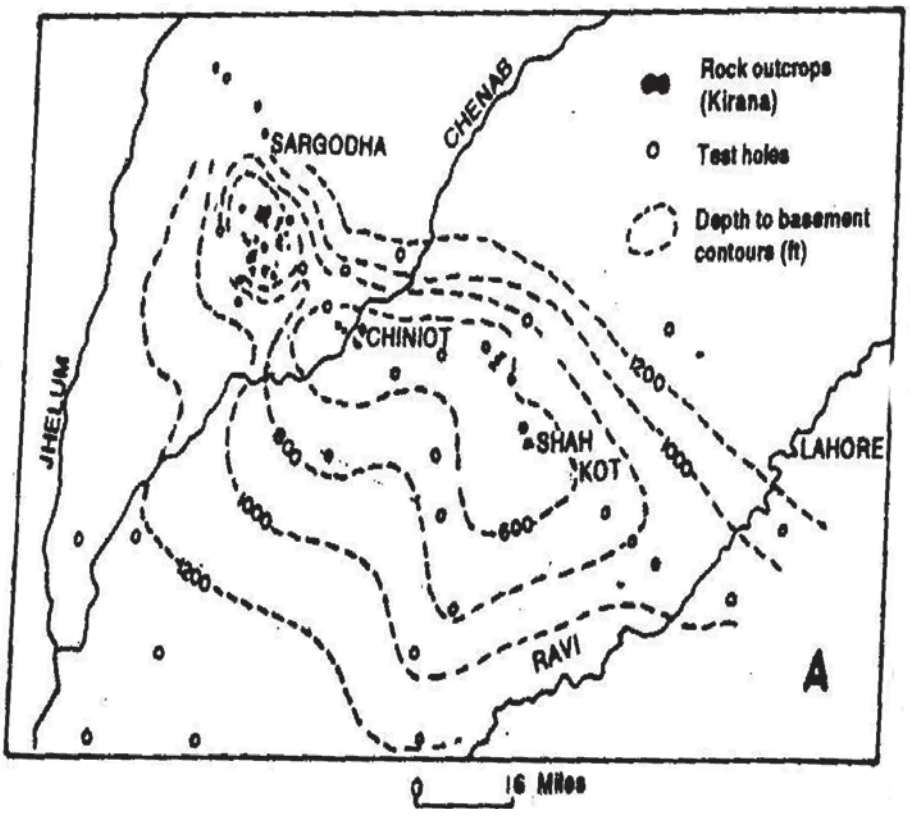

Fig. 4.4: Map showing Pre-Cambrian rock outcrops and depth to the basement in Sargodha Shahpur region (from Kazmi & Rana, 1982).

SALT RANGE FORMATION

In the northwest of the Indo-Pakistani Shield, the sediments of the Salt Range Formation overlie the basement rocks (of Kirana Group). The type locality is Khewra Gorge in the Eastern Salt Range. The Salt Range Formation is widely distributed in Salt Range, between Jogi Tilla in the east and Kalabagh in the northwest (Figs. 4.5, 4.6 & 4.7). It was also found in wells drilled in Kohat-Potwar foredeep in north and in southern Punjab area (in the Fort Abbas Well and in the Bahu Well #01). The lithologies of the Salt Range Formation consist of red, gypsiferous claystone, salt marls, without apparent bedding. It contains thick salt bodies which have been mined for more than 2000 years.

The middle section of the formation is comprised of intercalations of gypsum, dolomite, shale, siltstone, with oil shale layers and a layer of highly altered volcanic rocks known as Khewra Traps. The thickness of Salt the Range Formation is more than 800 m at type locality (base not exposed). In the Kohat-Potwar region, the thickness of the formation may exceed as much as 2000 m locally. This locally increased thickness is assumed to be the result of secondary salt migration and accumulation induced by decollement and southward thrusting of overlying sedimentary rocks. The formation is devoid of age determining fossils. The radiometric dating from the top of the Salt Range Formation has been studied. On the basis of radiometric dating, Kazmi & Jan (1997) reported its age is ~ 600 Ma.

KHEWRA SANDSTONE

The Khewra Sandstone overlies the Salt Range Formation, without an apparent disconformity. The type locality is also the Khewra Gorge. The Khewra Sandstone is widely exposed in the Salt Range and the Khisore Range (Fig. 4.6 and Fig. 4.7). It was also encountered in wells drilled in Kohat-Potwar foredeep in north and in southern and central Punjab area (in the Fort Abbas Well #01 and in the Bahu Well #01).

The Khewra Sandstone is comprised predominately of reddish-brown to purple, thick bedded to massive sandstone with few brown shale intercalations. The sandstone is cross bedded, has large and abundant ripple marks, and mud cracks. The thickness of the Khewra Sandstone is 150 m at the type locality, and 220 m in Fort Abbass Well and

150 m in The Bahu Well #01. Due to the presence of trilobite remains, Schindewolf & Seilacher (1955) assigned a Cambrian age to the formation.

KUSSAK FORMATION

The Kussak Formation disconformably overlies the Khewra Sandstone. At the base of Kussak Formation a widespread thin conglomerates layer exists. The type locality is Kussuk Fort in the Eastern Salt Range (Figs. 4.5 & 4.6). The Kussak Formation is well exposed in the Salt Range, between Jogi Tilla in the east and Chidru Nala in the west. The lithology of the formation consists of grey silty and sandy glauconitic shales, with some sandstone intercalations and in places, black shale's layers. It was also encountered in wells drilled in the Kohat-Potwar foredeep in north and in southern Punjab Plains (in the Fort Abbas Well #01 and in the Bahu Well #01). The thickness of the formation is 75 m at the type locality, and 90 m in the Bahu Well #01. The Kussak Formation contains trilobites and brachiopods. The occurrences of *Neobolus warthi* and *Redlichia noetlingi* (Schindewolf & Seilacher, 1955; Teichert, 1964) indicate an Early Cambrian to Middle Cambrian age.

JUTANA FORMATION

The Jutana Formation overlies the Kussuk Formation conformably. The type locality is Jutana village in the Eastern Salt Range (Fig. 4.5 and Fig. 4.7). It is cliff forming, thick bedded to massive. It is composed of sandy dolomites and dolomitic sandstones with few shale intercalations. The thickness is 75-90 m in the Eastern Salt Range, and 100 m in the Bahu Well #01. The fossil assemblage consists of brachiopods, gastropods and trilobites, among them *Redlichia* and *Pseudotheca noetlingi* and *Pseudotheca subrugosa* (Teichert, 1964) as well as *Cruziana* sp. which indicates an Early Cambrian to Middle Cambrian age (Kazmi & Jan, 1997).

BAGHANWALA FORMATION

The Baghanwala Formation conformably overlies the Jutana Formation. The type locality is near Baghanwala village in the Eastern Salt Range (Fig. 4.5 & Fig. 4.6). The distribution of the Formation is identical with that of the Kussak and Jutana Formations. In the Potwar area, only a few erosional remnants of the Baghanwala Formation have been preserved below the Permian unconformity. It is found in the subsurface of the

Punjab Plains and is comprised mainly of reddish brown shales and platy to flaggy sandstones in which salt pseudomorphs occur abundantly. Ripple marks and mud cracks are also common. The thickness is about 100 m in the type locality, 110 m in the Bahu Well #01 and 365 m in the Fort Abbass Well, but is commonly reduced due to erosion in the other parts of the Salt Range. The formation has only traces of fossils. Due to its contact relationship with the Jutana Formation the age of the Baghanwala is assumed as Middle Cambrian (Kazmi & Jan, 1997).

From the Ordovician to the Carboniferous there is a large unconformity and as such no sediments were reported. Deposition began again in Permian and continued up to the Recent.

The Permian sequence is divided into two major groups. A) Nilawahan Group which consists of mainly clastic sediments. B) Zaluch Group which is comprised of calcareous sediments.

In Nilawahan Group there are four formations, the Tobra Formation, the Dandot Formation, the Warcha Sandstone and the Sardhai Formation.

4.2.2 NILAWAHAN GROUP (CLASTICS)

TOBRA FORMATION

The lower contact of the Tobra Formation is unconformable with other Cambrian formations including the Salt Range Formation (Fig. 4.6). Its type locality is in the village of Tobra in the Eastern Salt Range. The formation is widely distributed throughout the Salt Range and is also encountered in different wells in the Punjab Plains and in Potwar area. The lithology of the formation consists of polymict conglomerates with pebbles and boulders of igneous, metamorphic and sedimentary rocks. Based on the observation of scratched and polished boulders, it is considered as tillite deposits. The thickness of the formation at the type locality is about 20 m, while the thicknesses in the Bahu and Fort Abbass wells are 14 and 20 m, respectively. In Zaluch Nala its thickness approaches to 130 m. In the Western Salt Range, the Tobra Formation developed different facies. Dark grey to black, diamictic mudstone

interspersed with sand sized to boulder size components is dominant. As such this facies is interpreted as fluvioglacial. In the Tobra Formation, Ostracods and fresh water bivalves (Reed, 1936) as well as floral remains, including *Glossopteris* and *Gangomopteris* occur. On the basis of *Striatopodocarpites* and *Protohaploxypinus*, the age of the Tobra Formation has been assigned to the Permian (Kazmi & Jan, 1997).

DANDOT FORMATION

The Dandot Formation has gradational contact with the underlying Tobra Formation. The type locality is Dondot village in the Eastern Salt Range (Fig. 4.5 & Fig. 4.6), but it did not develop in the Western Salt Range. The Dandot Formation consists of dark greenish grey, splintery shale and siltstone with intercalations of sandstone, while in the Central Salt Range, it comprises greenish grey to black, carbonaceous shales with sand flaser alternations. The sandstone is cross bedded. It is 50 m thick in the Salt Range and was drilled 50 m in the Bahu Well #01. The formation contains a rich fauna of brachiopods (*Discina, Martiniopsis,* and *Chonetes*), bivalves (*Eurydesma*), gastropods, preteropods (*Conularia*), bryozoans and ostracods as well as spores (Kazmi & Jan, 1997). As this formation has gradational contact with the Tobra Formation and it contains fauna of age determining quality, it has been assigned to the Early Permian age (Teichert, 1967).

WARCHHA SANDSTONE

The lower contact of the Warchha Sandstone is conformable with the underlying Dandot Formation. The type locality is Warchha Nala in the West, Central Salt Range (Fig. 4.5 & Fig. 4.6). It is widely exposed in the Salt Range and encountered in drilled wells in the Potwar region and below the surface of the Punjab Plains. In the Salt Range, the Warchha Sandstone is generally thick bedded to massive, reddish brown and cross bedded. The sandstone is medium to coarse-grained and arkosic in nature. Dark grey shale is another prominent lithology of Warchha Sandstone. In the Western Salt Range, sandy shale is reddish brown to dark brown in color and contains reddish and white sandstone intercalations. It is 150-165 m thick in the Salt Range area, while it has been encountered 150 m thick in the Bahu Well #01. Though the Warchha Sandstone is devoid of fossils, its contact relationship, the lower with the Dandot

Formation and the upper with the Sardhi Formation (both are fossiliferous) suggest that the Warchha Sandstone is of Early Permian age (Kazmi & Jan, 1997).

SARDHAI FORMATION

The distribution of the Sardhai Formation is similar to the Warchha Sanstone. The type locality is Sardhi (Sohal) Nala in the Eastern Salt Range (Figs. 4.5, 4.6 & 4.7). The formation has a general lithology (in the Eastern and Central Salt Range) of bluish grey, purple and reddish claystone, which becomes dark violet to black in the Western Salt Range. The maximum measured thickness is 60 m in the Western Salt Range and the drilled thickness is 80 m in the Bahu Well # 01. Plant remains and fish scales have been found (Kazmi & Jan, 1997). In the Khisore Range, the claystone contains layers of argillaceous, fossiliferous limestone which have bryozoans and brachiopods (e.g., *Anastomopora* sp.*, Fenestella* sp., *Athyris*, *Spirifer*). On the basis of these fossils, Hussain (1967) assigned its age as Early Permian.

4.2.3 ZALUCH GROUP

It is subdivided into three formations which are differentiated by varying proportions of limestone. The names of the formations are: Amb Formation, Wargal Formation and Chhidru Formation.

AMB FORMATION

The Amb Formation overlies the Sardhai Formation disconformably. The type locality is ~ 5 km southwest of the village of Amb in the Central Western Salt Range (Figs. 4.5, &. 4.6). This formation is also well exposed in Zaluch Nala and Chhidru Nala. It is distributed in the Central Salt Range. The lithology of the formation consists of highly fossiliferous, calcareous sandstone, alternating with sandy limestone. Dark grey to locally black and carbonaceous shale is another feature of the formation. Thin coal beds have also developed near the vicinity of Amb Village. The thickness of the Amb Formation is 80 m in the Salt Range and 50 m in the Bahu Well #01. The Amb Formation contains a large number of fossils including *Glossopteris* and *Gangamopteris* (Balme, 1970). The other rich fauna consists of foraminifera, bryozoans, brachiopods, pelecypods, gastropods, cephalopods, and ostracods (Waagen, 1879, 1889, 1891;

Dunbar, 1933; Reed, 1941; Pascoe, 1959; Teichert, 1966; Kummel & Tiechert, 1970; Pakistan-Japanese Research Group, 1985). On the basis of these fossils, Early Permian age has been assigned to the formation.

WARGAL LIMESTONE

The formation has a good exposure in the Western and Central Salt Range (Figs. 4.5). The prevailing lithology is grey, medium or thick bedded to massive, partly sandy limestone. In places, thin intercalations of dark-grey to black shales are also reported. The thickness of the Wargal Limestone is 180-200 m in the Salt Range, while 50 m in the Bahu Well #01. The Wargal Formation is highly fossiliferous. It is rich in brachiopods, trilobites, pelecypods, gastropods, ammonoids, nautiloids, echinoids, corals, bryozoans, sponges, foraminifera, ostracods, conodonts and fish remains as well as algae and spores (Waagen, 1879-1891; Reed, 1944; Teichert, 1966; Kummel & Teichert 1970; Pakistan-Japanese Research Group 1985). The brachiopods are *Enteletes, Derbyia, Waagenites, Waagenoconcha, Richthofenia, Oldhamina, Linoproductus, Spirigerella, Costifernia, Chonetella, Cleiothyridina, Phricodothyris, Notothyris, Hemiptychina, Terebratuloidea, Kiangsiella, Uncinunellina, and Ditomopyge fatimii.* On the basis of this faunal record, the Wargal Limestone has been assigned as Late Permian (Late Murghabian to early Dzulfian).

CHHIDRU FORMATION

The Chhidru Formation has conformable and gradational contact with the Wargal Limestone. The type locality is Chhidru Nala in the Western Salt Range (Figs. 4.5 & 4.6). It is distributed in the Central and Western Salt Range. The prevailing lithology is dark grey, sandy shale, at the base, overlain by calcareous sandstone, and sandy limestone. At the top of the formation, there is a white sandstone bed which is a characteristic feature of the Chhidru Formation. The maximum thickness is 85 m in the Salt Range while in the Bahu Well #01 it is 25 m thick. Chhidru Formation contains a number of fossils of brachiopods, gastropods, pelecypods, ammonoids, bryozoans, and fusulinids. On the basis of fauna and stratigraphic analysis, it is concluded that the Chhidru Formation is most probably Late Permian of age (Kazmi & Jan, 1997).

MIANWALI FORMATION

Gee (1989) reported that the Mianwali Formation overlies the Chhidru Formation conformably, but Kummel & Teichert (1970) have reported that there is a para-unconformity which is indicated paleontologically and palynologically. The formation is exposed in the Western Salt Range (Figs. 4.5 & 4.6). Kummel & Teichert (1966) divided the formation into three members, Kathwai Member, Mitiwali Member and Narmia Member. The main lithology of the formation is marl, limestone, sandstone, siltstone and dolomite. Fatmi (1977) reported many ammonoid fossils, the most prominent of them are, *Ophiceras, Glyptophiceras, Proptychites, Gyroniotes, Kymatites, Kingites and Ambites.* Brachiopods have been reported by Kummel & Teichert (1966). In 1980, Iqbal & Shah (1980) reported foraminifera, ostrocods, crinoids and conodonts in the Mianwali Formation. The faunal assemblage gives an Early Triassic (Scythian) age.

TREDIAN FORMATION

The Tredian Formation overlies the Mianwali Formation conformably and grades into the overlying Kingriali Formation. It is well exposed in the Salt Range (Figs. 4.5 & 4.6). The prevailing lithology is thin to thick bedded, variegated micaceous sandstone, interbedded with shale in lower sections. There are slump structures and ripple marks. In the upper section, there is massive to thick bedded sandstone which is interbedded with thin dolomite beds. In the Tredian Formation, pollen, spores and wood fragments have been reported. The most significant of them are *Aratrisoporites paenulatus, Calamospora*. Due to its contact relationship and fossil records, a Middle Triassic age has been assigned to the Tredian Formation (Kazmi & Jan, 1997).

KINGRIALI FORMATION

The formation is well exposed in the Salt Range (Figs. 4.5 and Fig. 4.6). It is comprised of thin to thick bedded, grey dolomite and dolomitic limestone and dolomitic shale and marl. The thickness varies from 76 to 106 m. Some brachiopods, bivalves and crinoids have been reported by Fatmi (1977). The lower contact of the Kingriali Formation is gradational with the Mianwali Formation and the upper contact is disconformable with the overlying Jurassic Datta Formation. It has been assigned Late Triassic age (Kazmi & Jan, 1997).

DATTA FORMATION

The Datta Formation overlies the Kingriali Formation unconformably. The prevailing lithologies are coarse to fine-grained, variegated coloured sandstone, shale, siltstone and mud stone. Fine clay, calcareous, dolomitic, carbonaceous and ferruginous beds may also be found in places. Its thickness ranges from 150 m to 400 m. The type section is in the Surghar Range (Figs. 4.7 & 4.8), however, it is also exposed in the Western Salt Range. The thickness in the Bahu Well #01 is 20 m and is 10.5 m in the Fort Abbbas Well. Age diagnostic fossils have not been found as yet, however, it is assigned as Pre-Toarcian (Jurassic) due to its contact relationship (Kazmi & Jan, 1997).

SHINWARI FORMATION

The Shinwari Formation has gradational contact with the underlying Datta Formation. The main lithologies are thin bedded grey limestone, nodular marl, shale and sandstone. Cross bedding and ripple marks are present. It is well exposed in the Samana Range and is not well exposed in the Salt Range. Its thickness varies from 12 m to over 400 m in the Kalachitta and in the Samana Range. This formation includes the following fauna: *Boulieiceras, Terebratula, Spiriferina, Montivaltia, Pholadomya, Zeillaria, Pecten* and *Lima.* It has been assigned Early Jurassic (Toarcian) to Middle Jurassic age (Kazmi & Jan, 1997).

SAMANA SUK FORMATION

The Samana Suk Formation has a transitional lower contact with the Shinwari Formation in Samana Range. It is exposed in the Western Salt Range (Figs. 4.5 & 4.6). The lower contact with the Datta Formation in the Western Salt Range, in places where the Shinwari Formation is lacking, is sharp and slightly disconformable, while the upper contact with the Chichali Formation is disconformable. The thickness ranges from 66 m to 366 m (Kazmi & Jan, 1997). The Samana Suk Formation has also been encountered in different wells. Its thickness is variable i.e., in the Bahu Well #01 it has 100 meters, while in the Ali Sahib and in the Amir Wali wells it is 60 and 100 m, respectively. The Samana Suk Formation consists of medium-grained limestone. Some beds of marl and sandstone are also included in this formation (in drilled data). The limestone is generally well bedded and oolitic and shows dolomitic and arenaceous patches. Dark grey carbonaceous material also occurs. Brachiopods, bivalves, gastropods, ammonites

and crinoids are common fossils. In present study *Bositra shells* have been identified which indicate Middle Jurassic age of this formation as it has been assigned in literature (e.g. Fatmi, 1977).

CHICHALI FORMATION

The Chichali Formation overlies the Samana Suk Formation disconformably. The prevailing lithologies are dark green to black glauconitic shales with subordinate beds of thin sandstone and siltstone. In places, shales show rusty brown, khaki or brownish grey colour. Ferruginous concretions and veins of quartz and calcite are present. Phosphatic nodules are another characteristic feature of the Chichali Formation. Its thickness varies from 12 to 70 m (Kazmi & Jan, 1997). In the Bahu Well #01 it has a thickness of 50 m, in the Amir Wali Well 100 m and in the Ali Sahib Well it is 60 m thick. Ammonites and Belemnites have been found, so Late Jurassic age has been assigned. Earlier, on the basis of Nannofossils, this formation was assigned as Early Cretaceous. In the present study, *Saccocoma* and *Nautiloculina oolithica* (in limestone which was previously considered as the part of the Samana Suk Formation of Middle Jurassic) are found, which indicate a higher Jurassic age.

LUMSHIWAL FORMATION

This formation overlies gradationally and conformably the Chichali Formation (Figs. 4.5 & 4.6). In the Salt Range, the prevailing lithology is grey, thick bedded to massive, current bedded, feldspathic, and ferruginous sandstone. It also contains silty or sandy glauconitic shale at the base. The sandstone of the Lumshiwal Formation is mainly brownish grey, rusty blackish brown on weathered surfaces, and greenish grey to brownish grey on fresh surfaces. The sandstone is medium to coarse-grained and very firm. Its outcrop thickness ranges from 38 to 194 m (Kazmi & Jan, 1997). It has been drilled 110 m in the Bahu Well # 01, 40 m in the Amir Wali and 80 m in the Ali Sahib Well. Ammonites, gastropods, brachiopods, belemnites, echinoids and bivalves have been reported. Based on the fauna, Lower Cretaceous age (Upper Neocomian to Middle Albian) has been assigned (Kazmi & Jan, 1997).

HANGU FORMATION

This formation lies unconformably over various formations of Paleozoic to Mesozoic age (Kazmi & Jan, 1997). The Hangu Formation comprises ferruginous, oolitic and pisolitic laterite, with siltstone and fireclay. The lateritic lithology is reddish brown to reddish black, or reddish grey to greyish on fresh surface and reddish brown, dark grey, and rusty brown on weathered surfaces. The fire clay is pale, white and earthy grey on fresh surface and yellowish brown to rusty brown on weathered surface. It is well exposed in the Western and Central Salt Range and becomes very thin in the Eastern Salt Range (Figs. 4.5 &. 4.6). The Hangu Formation is fine to coarse-grained sandstone and siltstone which grades into fossiliferous shale and calcareous sandstone. The Hangu Formation contains mollusks, corals and foraminifera (Gregory, 1930; Cox, 1930; Davies *&* Pinfold, 1937; Iqbal, 1972; Smout & Haque, 1956). Some of the important foraminifera are: *Miscellania miscella, Lockhartia haimai, L. conditi, Lepidocyclina punjabensis* and *Daviesina longhami.* On the basis of the fauna, the Hangu Formation has been assigned Early Paleocene age.

LOCKHART LIMESTONE

The Lockhart Limestone conformably lies on the Hangu Formation. It is well exposed in the Western and Central Salt Range and becomes thinner to the Eastern Salt Range (Fig. 4.5). This formation consists of predominantly dark grey, fine to medium grained nodular limestone. It is dark grey on fresh surface, while weathered surfaces are dirty grey to dark grey. It has a fair amount of marly and shaly intercalations. Solution weathering and honeycomb weathering may also be seen in some areas. It has variable thickness from 30 m to 240 m. The Lockhart Limestone contains mollusks, corals and foraminifera, echinoids and algae (Cox, 1931; Davies, 1943; Eames, 1952; Haque, 1956; Iqbal, 1969; Latif, 1970). Some of the important fauna are: *Operculina subsalsa, O. juvani, Miscellania miscella, M. stampi, Lockhartia haimai, L. newboldi Lepidocyclina punjabensis, Discocyclina ranikotensis, Alveolina globosa, Assilina dandotica, Nummulites nuttali,* and *Daviesina longhami.* On the basis of the fauna, the Lockhart Limestone has been assigned Paleocene age.

Patala Formation

The Patala Formation lies conformably over the Lockhart Limestone and its type section is Patala Nala in the Western Salt Range (Fig. 4.5). The dominant lithology is shale with subordinate marl, limestone and sandstone. Marcasite nodules are found in the shale. Its thickness ranges from 27 m to 200 m (Kazmi & Jan, 1997). It contains mollusks, ostracods and foraminifera (Cox, 1931; Davies, 1943; Eames, 1952; Haque, 1956; Iqbal, 1969; Latif, 1970). The larger foraminifera include *Lockhartia conditi, Nummulites globosa, Operculina canalifera, O. patalensis, Discocyclina ranikotensis, Assilina dandotica, Daviesina intermedia* and *Kathina nammalensis.* On the basis of the fauna, the Patala Formation has been assigned of Late Paleocene age.

NAMMAL FORMATION

The Nammal Formation overlies the Patala Formation conformably. The type section is in the Nammal Gorge in the Western Salt Range (Figs. 4.5 & 4.6). The prevailing lithology is shale, marl and argillaceous limestone. The lower section is more shaly and marly while the upper section is dominantly limestone. The thickness ranges from 35 m to 130 m. The thickness is in the Bahu Well #01 145 m, in the Amir Wali Well 185 m and in the Ali Sahib Well 175 m. The Nammal Formation contains mollusks and foraminifera (Cox, 1931; Haque, 1956). The important foraminifera are: *Nummulites atacicus, Nummulites subatacicus, Nummulites mamilla, Nummulites lahirii, Nummulites irregularis, Assilina granolosa, Assilina leymeriei, Assilina laminosa, Rotalia trochidiformis, Discocyclina ranikotensis* and *Fasciolites oblonga.* On the basis of the fauna, the Nammal Formation has been assigned Late Paleocene to Eocene age.

SAKESAR LIMESTONE

Sakesar Limestone has gradational contact with the underlying Nammal Formation. The type locality is Sakesar Peak in the Western Salt Range (Figs. 4.5 & 4.6). The dominant lithology is comprised of grey, nodular to massive limestone which is cherty in the upper sections. Near Daudkhel, the Sakesar Limestone laterally grades into massive gypsum. Its thickness varies from 70 m to 300 m in the Salt Range. It has 30 m drilled thickness in the Bahu Well #01, 35 m in the Ali Sahib Well and 25 m in the Amir Wali Well. The formation dominantly contains foraminifera. The important foraminifera species are: *Nummulites atacicus, Nummulites mamilla, Assilina granolosa, Assilina*

leymeriei, Assilina subspinosa, Fasciolites oblonga, Fasciolites globosa, Lockhartia conditi, Lockhartia hunti, Operculina nummulitoides, Orbitiolites complanatus and *Rotalia trochidiformis.* On the basis of the fauna, the Sakesar Limestone has been assigned an Early Eocene age.

CHOR GALI FORMATION

The Chor Gali Formation overlies the Sakesar Limestone. The formation is generally composed of thin to medium bedded marly limestone, argillaceous limestone, marl and subordinate shales. The limestones are rarely massive and generally show flaggy habits due to the increasing marly intercalations. The limestone weathers into creamy light yellow and light grey colors, while the fresh surface colors are light grey. The marl has very light shades of khaki and grey. It is exposed in the Eastern Salt Range (Fig. 4.5). Its thickness ranges from 30 m to 140 m. A rich fossil assemblage including foraminifera (*Assilina, Nummulites*), mollusks and ostracodes has been reported. As such, based on the fauna reported, an Early Eocene age has been assigned (Kazmi & Jan, 1997).

4.2.4 RAWALPINDI GROUP

This group consists of two formations, the Murree Formation and the Kamlial Formation.

MURREE FORMATION

This formation disconformably overlies various Eocene formations. This formation consists of grey and reddish sandstone, red and purple clays and shales with some conglomerates, pebbles and cobbles. The sandstone is medium to coarse-grained and significant cross-bedding can be observed. It represents a thick monotonous fluvial sequence. The thickness ranges from 180 to 600 m in the Salt Range (Fig. 4.5) and more than 3000 m in other areas. The formation is poor in fossils, with only few plant remains, silicified wood, fish remains, frog and mammalian bones recorded. The fauna indicates an Early Miocene age (Kazmi & Jan, 1997).

KAMLIAL FORMATION

The Kamlial Formation overlies the Murree Formation conformably, with a gradational transition; however it also occurs at some localities, directly overlying the Eocene Sakesar Limestone. The prevailing lithology is mainly grey to brick red, medium to coarse-grained sandstone, interbedded with purple shale with subordinate interformational conglomerates. Many mammalian fossils have been reported and Middle to Late Miocene age has been assigned to the Kamlial Formation (Kazmi & Jan, 1997).

4.2.5 SIWALIK GROUP

CHINJI FORMATION

The Chinji Formation has conformable contact with the Kamlial Formation in the Salt Range (Figs. 4.5 & 4.6). The dominant lithology consists of red clays, with subordinate grey to brown, fine to coarse, gritty and soft, cross-bedded sandstone. There are rich vertebrate fauna in the formation. They include turtles, crocodiles, lizards, aquatic birds, water deer, etc. The age of the Chinji Formation has been assigned as Late Miocene (Kazmi & Jan, 1997).

NAGRI FORMATION

The Nagri formation has conformable lower contact with the Chinji Formation. The prevailing lithology is comprised mainly of thick bedded to massive, greenish-grey coloured, medium to coarse-grained, salt and pepper-textured, calcareous sandstone. Reddish to brown sandy clay and conglomerates exist as subordinates. The thickness of the formation ranges from 200 m to 3000 m (Kazmi & Jan, 1997). The formation is rich in vertebrate fossils. The important vertebrate fossils are: *proboscideans, rhinoceratides,* crocodiles*, chelonians and artiodactyls.* Carnivores and primates have been reported. The age of the Nagri Formation has been assigned to the Early Pliocene. (Kazmi & Jan, 1997).

DHOK PATHAN FORMATION

The Dhok Pathan Formation has its gradational lower contact with the Nagri Formation. The prevailing lithology is a thick pile of inter-bedded sandstone and clay. The

sandstone is grey to brown colored and is cross-bedded, medium to coarse-grained and calcareous. The clay of the formation is brown, orange to red in colour. Conglomerates, pebbles and cobbles are present particularly in the upper sections. Its thickness range is 1330 m to 2000 m. There are rich vertebrate fauna in the formation. *Carnivora proboscidea, C. perissodstyla* and *C. artiodactyla* have been reported (Pascoe, 1963). The age of the Dhok Pathan Formation has been assigned as Early to Middle Pliocene.

SOAN FORMATION

The Soan Formation overlies the Dhok Pathan Formation disconformably in the Salt Range (Fig. 4.6). The formation consists of coarse clastic sediments containing massive conglomerates with pebbles, cobbles and boulder beds. Coarse-grained sand/sandstone, siltstone and clay are present as subordinates. Some Vertebrate fossils have been found in the formation. They include *Mastodon sivalensis, Stegodon clifti, Elephas planifron, Sivatherium giganteum, Proamphibos lachrymans, Dichory-phochoerus durandi* and *Sivafelis potens*. A Late Pliocene to Early Pleistocene age has been assigned (Kazmi & Jan, 1997).

LEI CONGLOMERATES

This formation unconformably overlies the Neogene and earlier deposits. This formation consists of rounded to subrounded, pebbles, cobbles and boulders with subordinate medium to coarse sandstone and mudstone. Its thickness ranges from 150 m to 900 m. The Lei Conglomerates have been related to the last major episode of the Himalyan Orogeny. The important vertebrate fossils include: *Elephase hysudricus, Sivatherium giganteum, Dicerohinus platyrhinus, Equua* sp., *Bos* sp. and *Camel* sp. (Pilgrim, 1913; Wadia, 1928; and Pascoe, 1963). The formation has been assigned to Pleistocene age.

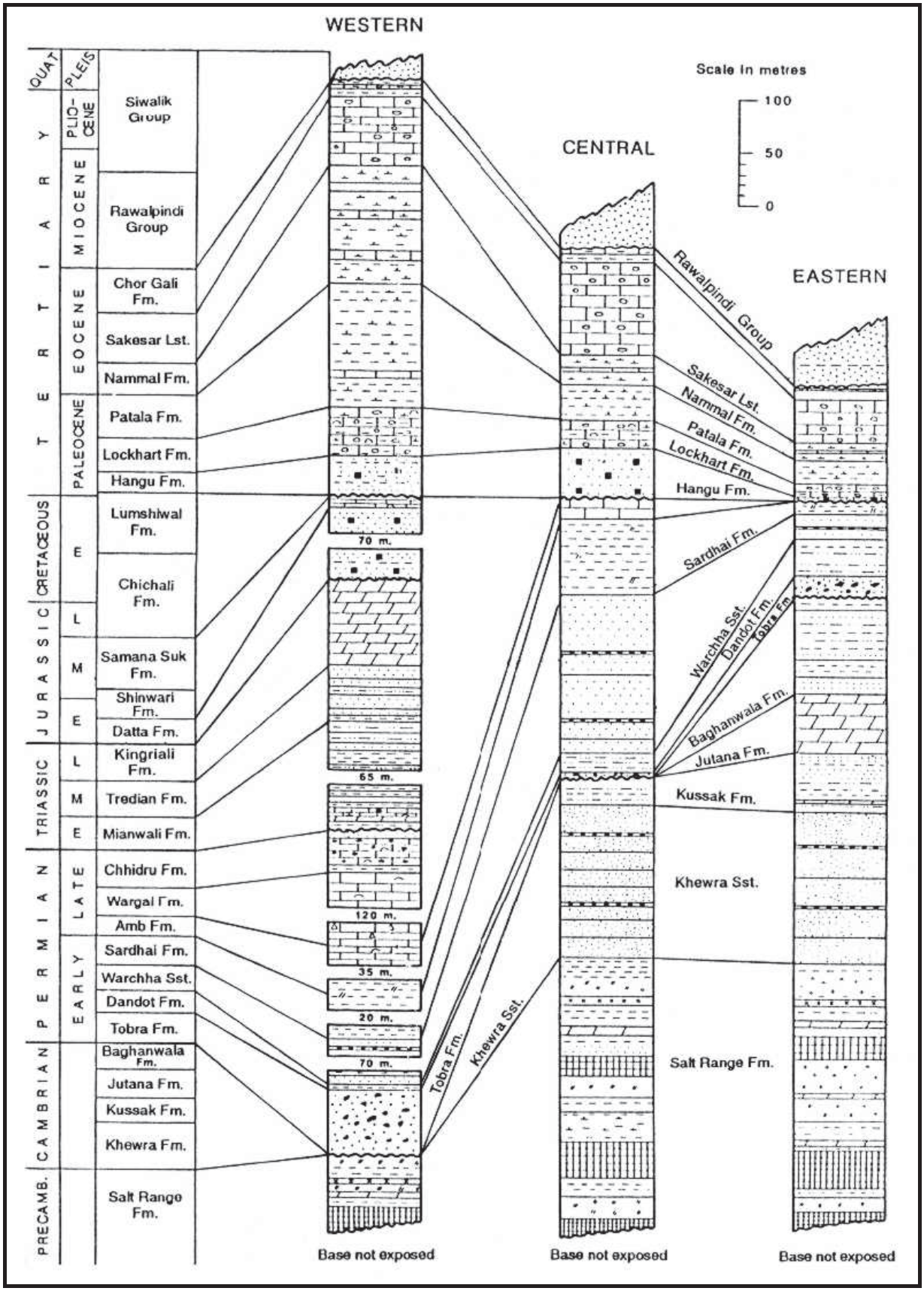

Fig. 4.5: Columnar sections of the sedimentary sequences in the Salt Range (from Fatmi *et al.*, 1984). Vertical: scale in meters; Horizontal: not to scale.

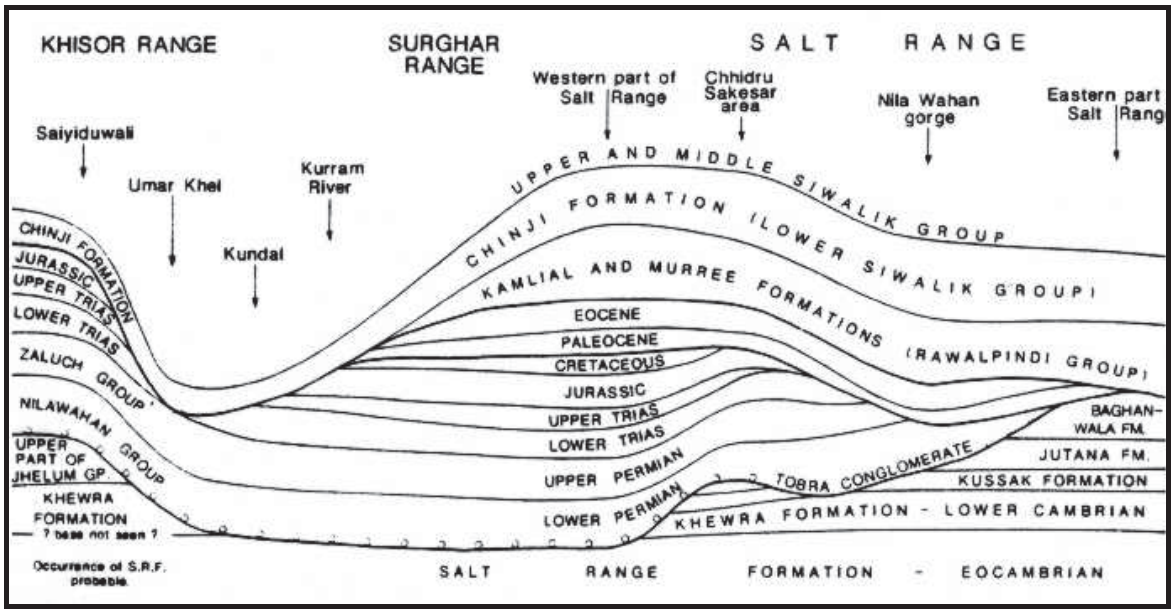

Fig. 4.6: Section showing the stratigraphic sequence of the Salt Range and Trans Indus Ranges (from Gee, 1989)

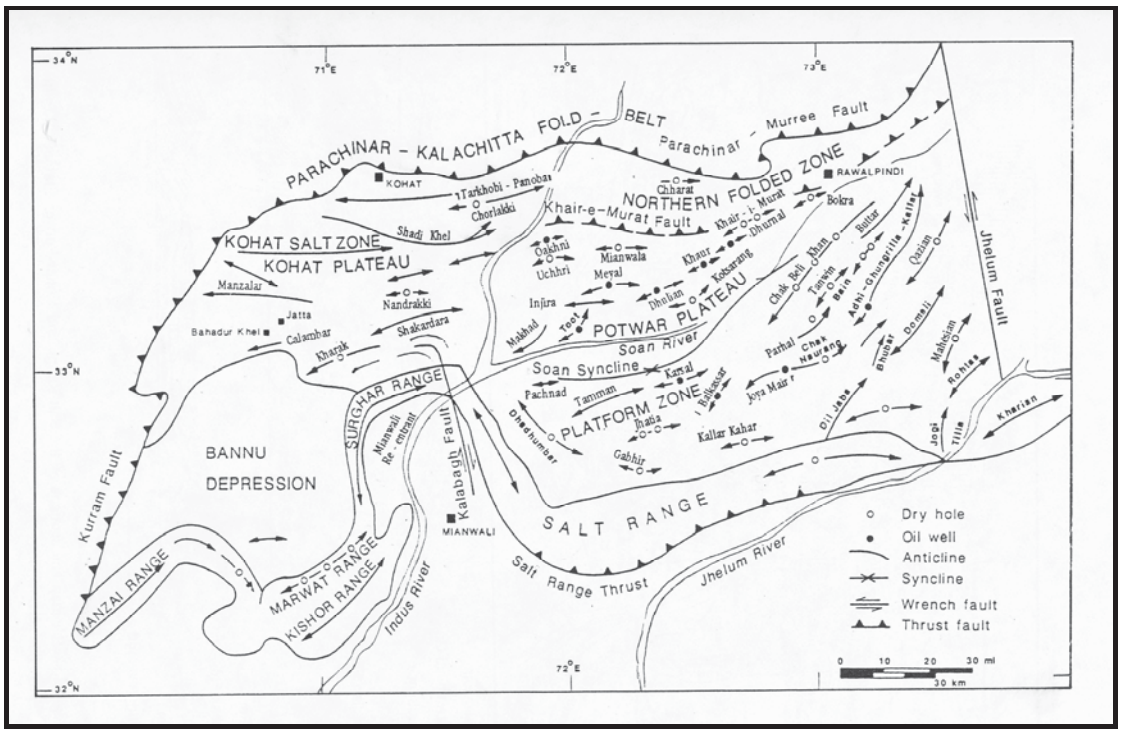

Fig. 4.7: Structural map of the Kohat-Potwar Plateau (from Kazmi & Rana, 1982, Khan *et al.*, 1986).

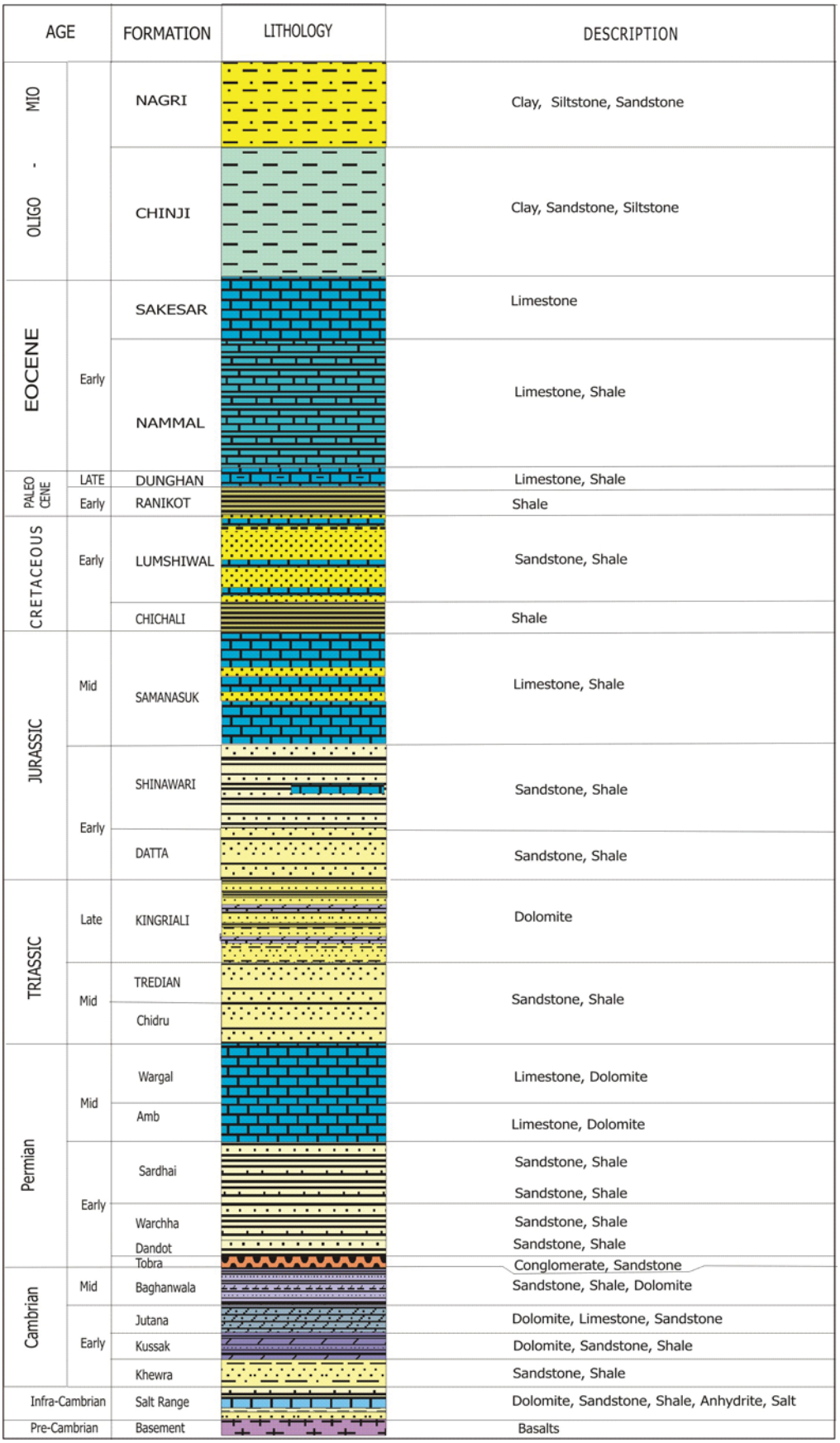

Fig. 4.8: Generalized stratigraphic column of Salt Range Area (data by OGDCL).

5. METHODOLOGY APPLIED TO THE PRESENT WORK

This study is based on the samples from ditch cuttings and cores of the wells Ali Sahib and Amir Wali.

5.1 METHODOLOGY FOR DITCH CUTTING SAMPLES

The samples were transported from the drilling sites to G & R Labs Islamabad, they were washed and cleaned to remove drilling mud and then dried at room temperature. The dried samples were divided into three, for geochemical (cf. Ch. 9, Organic Geochemistry), biostratigraphical and for lithological studies (cf. Ch. 6, Lithology and Stratigraphy of the Wells, Ali Sahib and Amir Wali on the basis of ditch cuttings).

The geochemical analyses include both, ditch cuttings (sample interval 5-10 m) and cores (sample interval 50-70 cm), from both wells. Total organic carbon was determined from more than 300 samples (Table 9.1 & 9.2) after the removal of carbonates by 6*N* hydrochloric acid, using a Leco Carbon-412, Elemental Analyzer. Pyrolysis measurements were performed using a "Rock-Eval 2+" instrument at G & R Labs. (Islamabad, Pakistan). The S1 (free hydrocarbons) and S2 (hydrocarbons liberated through heating of kerogen) peaks (mg HC/g rock) were used to calculate the Hydrogen-Index (HI = S2*100/TOC [mg HC/g TOC]) and the Production-Index (PI = S1/(S1+S2) (Espitalié *et al.*, 1977). The Oxygen Index was calculated from the S3 peak areas (OI = S3*100/TOC [mg CO_2/g TOC]). As an indicator of maturation, the temperature of maximum hydrocarbon generation (T_{max}) was measured.

On the basis of the TOC data, samples from the Ali Sahib and Amir Wali wells were selected for biomarker studies. The sample positions are marked with blue ink in the profiles of the wells (Figs. 5.1 & 5.2). Thirty samples from Paleocene to Jurassic strata of the Amir Wali Well were selected (Fig. 5.3). Ten samples were taken from cores (extension C in sample no.) and twenty were taken from cuttings (extension D). From the Ali Sahib Well, three samples were from cores (Fig. 5.3) and nine samples of cuttings from Cretaceous and Jurassic strata were selected. The drill cutting samples were washed to remove the drilling mud and were subsequently dried at room temperature.

For organic geochemical analyses, representative portions of the selected samples underwent extraction for approximately 1 hour using dichloromethane in a Dionex ASE 200 accelerated solvent extractor at 75°C and 50 bars. After evaporation of the solvent to 0.5 ml total solution in a Zymark TurboVap 500 closed cell concentrator, asphaltenes were precipitated from a hexane-dichloromethane solution (80:1) and separated by centrifuge. The fractions of the hexane-soluble organic matter were separated into NSO compounds, saturated hydrocarbons and aromatic hydrocarbons by medium-pressure liquid chromatography using a Köhnen-Willsch MPLC instrument (Radke *et al.*, 1980).

The saturated and aromatic hydrocarbon fractions were analysed on a gas chromatograph equipped with a 30-m DB-1 fused silica capillary column (i.d. 0.25 mm; 0.25-µm film thickness) and coupled to a Finnigan MAT GCQ ion trap mass spectrometer. The oven temperature was programmed from 70° to 300°C at a rate of 4°C min^{-1} followed by an isothermal period of 15 min. Helium was used as the carrier gas. The sample was injected splitless with an injector temperature of 275°C. The mass spectrometer was operated in the EI (electron impact) mode over a scan range from m/z 50 to m/z 650 (0.7 s total scan time). Data were processed with a Finnigan data system. Identification of individual compounds was achieved on the basis of retention time in the total ion current (TIC) chromatogram and comparison of the mass spectra with published data. Relative percentages and absolute concentrations of different compound groups in the saturated and aromatic hydrocarbon fractions were calculated using peak areas from the gas chromatograms in relation to those of internal standards (deuterated *n*-tetracosane and 1,1´-binaphthyl, respectively). The concentrations were normalised to the total organic carbon content.

Mr. M. Ashraf (at G & R Labs Islamabad, 2005), studied nannofossils in ditch cutting (from Eocene to Jurassic) and completed the biostratigraphy of the Ali Sahib Well (unpublished). The sample interval was 10 m.

General lithological reports (from Eocene to Jurassic) have been carried out by the present author at Geological & Reservoir Laboratories Islamabad in 2005 and 2006 (unpublished cf. Ch. 6) and the general litho-stratigraphy of the wells was established (Figs. 5.1-5.3). The names of the Formations (the Sakesar Limestone, the Nammal

Formation, the Ranikot Formation, the Lumshiwal Formation, the Chichali Formation, the Samana Suk Formation, and the Datta Formation etc.) have been taken from Shah (1977) and from Kazmi & Jan (1997).

5.2 METHODOLOGY FOR CORES SAMPLES

A total of 8 cores (four from each well) were cut up to 9 meters from different potential reservoir and source strata. The recovery ratio of the cores, from friable sandstone was poor and was as low as 2.5 meters (Core III of the Ali Sahib Well). The recovery ratio from limestone was 100 %. The following data relevant to these cores existed, e.g. the core description by well site geologists (length of core recovered, induration, colour, texture, fabric, sedimentary structures, carbonate contents - calcimetry (results of Core I of the Ali Sahib Well and Core I of the Amir Wali Well were not in accordance with the results which were carried out CO_2-volumetrically at University of Leoben), and visual porosity. Natural gamma ray logs (Figs. 5.1 & 5.2) were also available for all cores and used for correlation. All eight cores were divided into lithofacies/microfacies based on core description, lithological logs, petrographical and XRD studies.

X-ray diffractomety (XRD) analyses of all the samples (90 from the cores and 6 from the ditch cuttings) were carried out for semi-quantitative and qualitative composition (in appendix: tables of XRD mineral identification of the Ali Sahib and Amir Wali wells) at the University of Leoben, Austria. Each sample was grounded to powder. All the samples were analyzed by means of X-ray diffractometry in untreated, oriented conditions up to 2° to 65° angle. Some clay rich samples were treated with ethylene glycol (from 2° to 37° 2Θ) to determine the expandable clay minerals. The other XRD measuring conditions were as follows. The diverging and receiving slits were 0.5° and 0.1°, respectively. Sample length parallel to primary beam was 30 mm; goniometer speed was 0.5° 2Θ/min, recode paper speed was 0.5 mm/min; time constant was 1 s; measuring range was 10^3 c/s; Cu-Kα radiation was 50 kV, 20 mA.

From a total of 90 samples collected from the cores, 69 (26 from the Ali Sahib and 43 from the Amir Wali wells) were selected for thin section studies, for microfacies of carbonates and biostratigraphy studies (using the fauna other than nanno fossils, cf. Ch. 7). From the Ali Sahib Well, Core I (1534-1542.16 m, Fig. 5.1) and Core II (1694-

1701 m, Fig. 5.1) have been studied for biostratigraphy and carbonate microfacies analysis. From the Amir Wali Well Core I (1578-1583.38 m), Core III (1760-1769 m) and Core IV (1853-1862 m) were selected (Fig. 5.2). Carbonate thin sections were classified using Dunham (1962) and Flügel (2004). The detail is in Chapter 7, petrography and microfacies analysis of carbonate rocks.

From sandstone samples, blue-dyed, epoxy-impregnated thin sections were made. Point counting for grain size and mineral composition was carried out. All thin sections were examined for sedimentary structures, textures (grain size, sorting and roundness), fabric (grain orientation and packing), pore type, composition and diagenetic features. Grain size statistics (of sandstone see below) were calculated to obtain mean size and sorting (cf. Chapter 8, Petrography and XRD of Clastic Rocks). Sorting was compared to Trask Coefficient of sorting as mentioned by Waples (2002).

From the Ali Sahib Well, Core III (1730.50-1733 m) and Core IV (1886-1893.45 m), Fig. 5.1, have been studied by XRD (for all samples), thin sections (for sandstone samples) and by scanning electron microscope (two samples). From the Amir Wali Well Core II (1615-1621.74 m) was selected (Fig. 5.2) for clastic studies. Five samples from Core II of the Amir Wali Well have been studied with the help of SEM. Six additional samples of ditch cuttings from the Amir Wali Well were also analyzed by XRD to compare with core samples of the Ali Sahib Well (of the Datta Formation). Grain size distribution of sandstones was estimated by point counting (at least 300 grains) on thin sections. Out of total of a 90 samples collected from the cores, 22 samples (14 from Ali Sahib and 8 from Amir Wali well) were selected for studies of clastics (sandstone, claystone and shale). Additional 6 samples from ditch cuttings (claystone) from the Amir Wali Well bring the total number of samples for clastic studies to 28. Nine samples from the Ali Sahib Well consisted of shale/claystone and the remaining 5 samples were sandstone. While the samples from Core II of the Amir Wali Well consisted of claystone and sandstone (cf. Chapter 8).

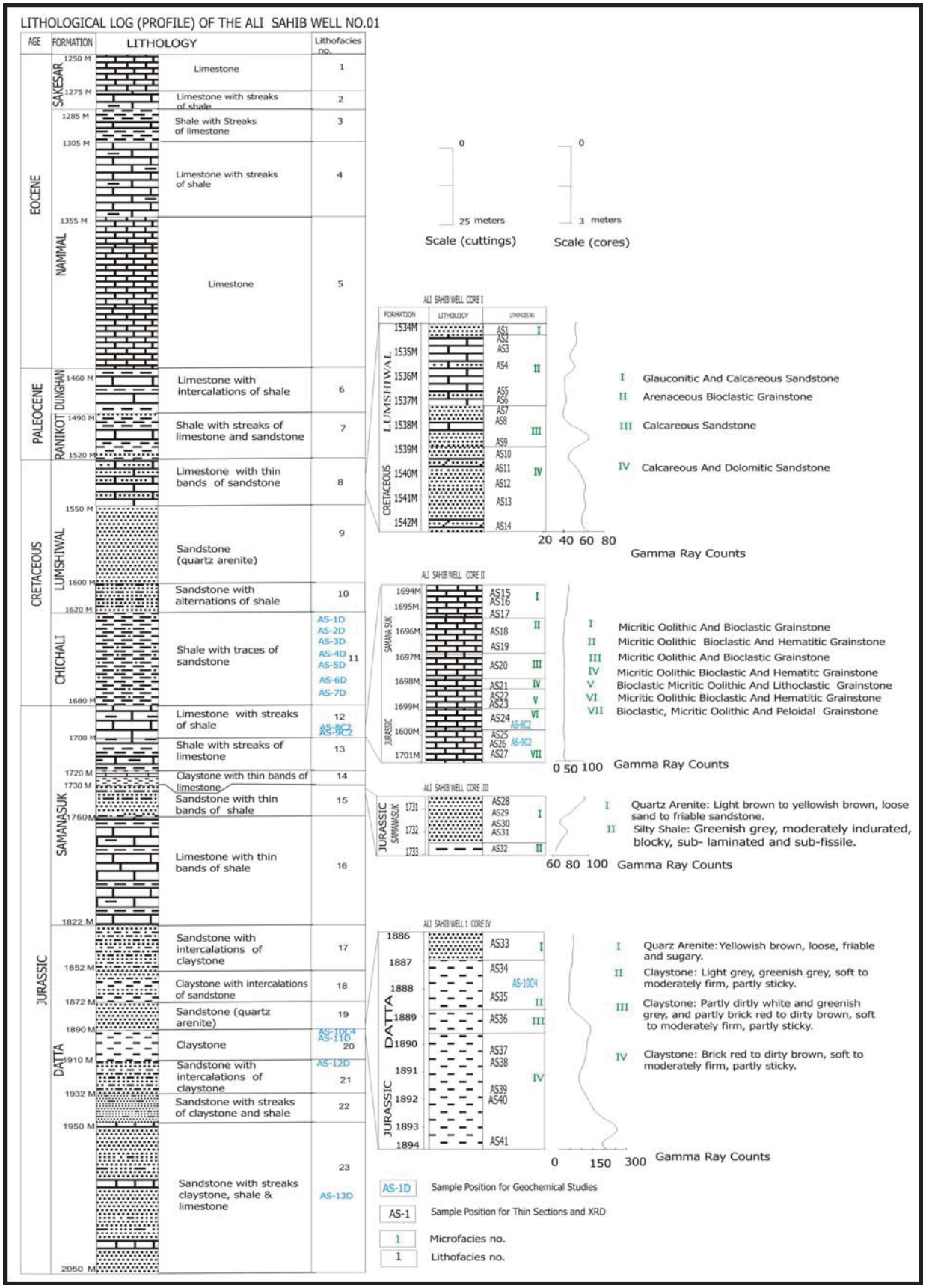

Fig. 5.1: Core and sample positions (depth) in generalized lithological log (profile) of the Ali Sahib Well. Boundary Samanasuk/Chichali, based on ditch cuttings shifted (see Chapter 7).

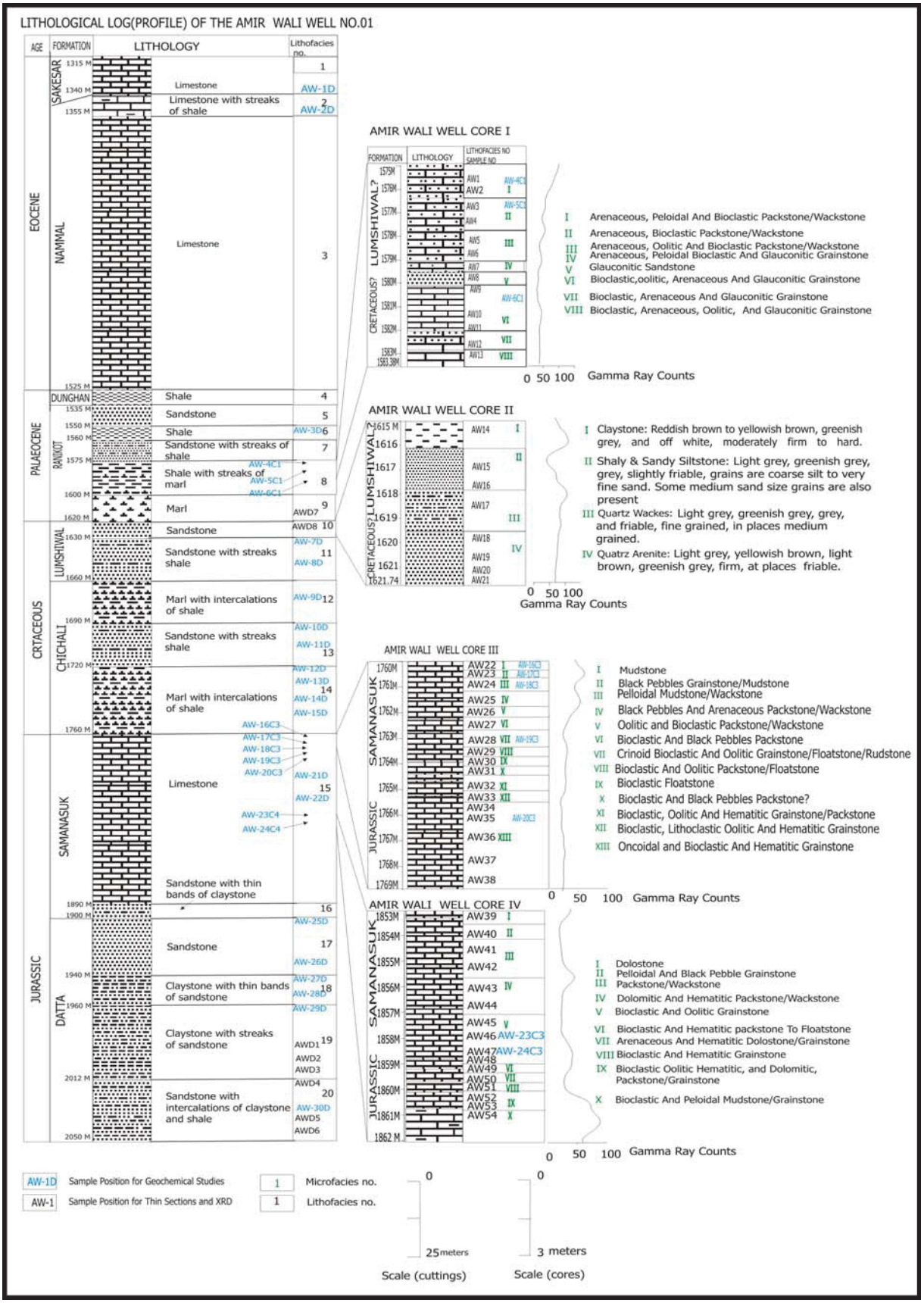

Fig. 5.2: Samples and Core positions (depth) in the lithological log of Amir Wali Well. Boundary Samanasuk/Chichali, based on ditch cuttings shifted (see Chapter 7).

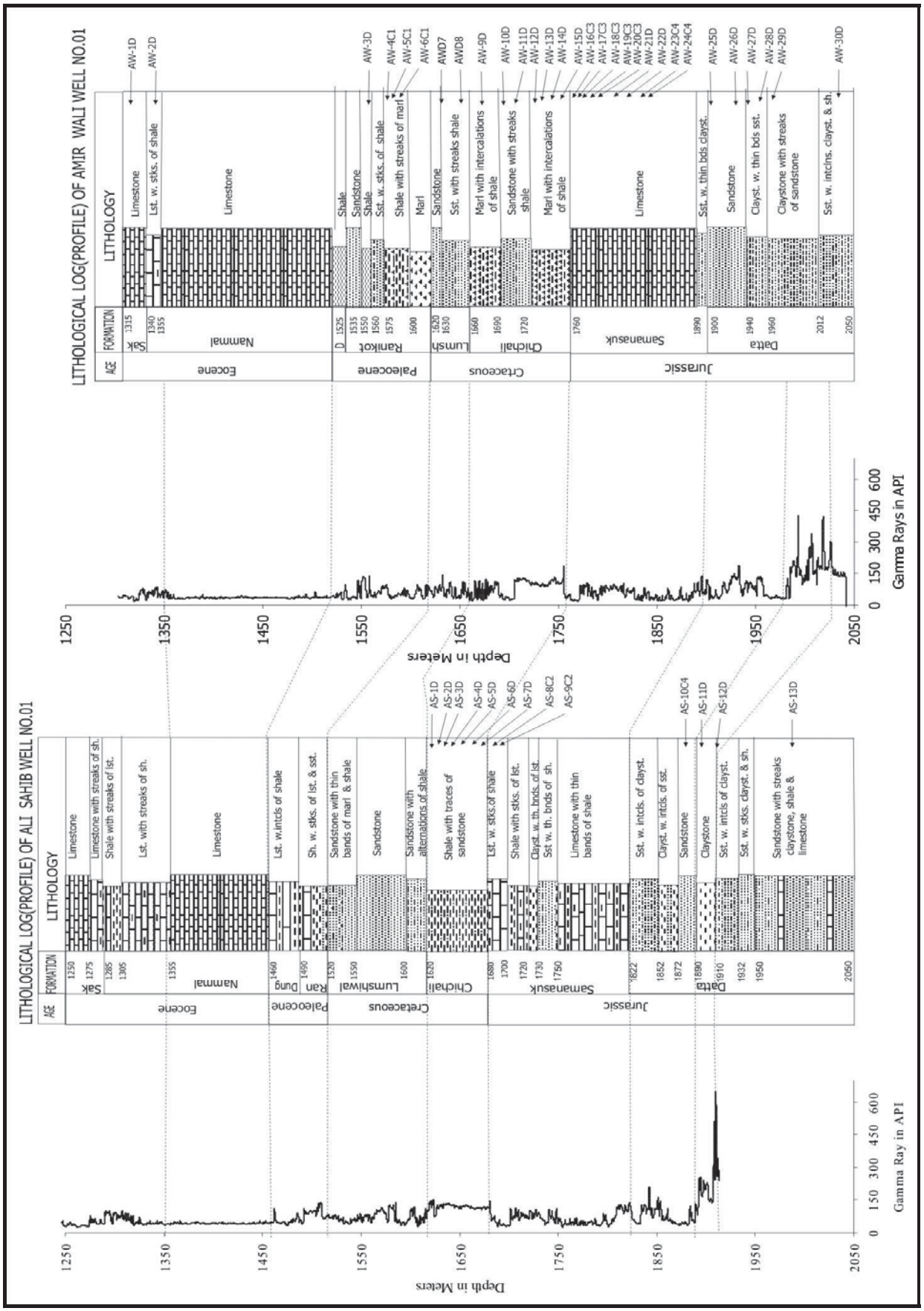

Fig. 5.3: Geochemical sample positions in stratigraphic column and well logs of Ali Sahib and Amir Wali Wells.

In present work, the microfacies were studied to establish the sedimentology, diagenesis and environment of deposition of Punjab Platform. This is a first attempt to understand the sedimentology of Punjab Platform especially in Cretaceous and Jurassic age.

6. LITHOLOGY AND STRATIGRAPHY OF THE ALI SAHIB AND AMIR WALI WELL

6.1 LITHOLOGY & STRATIGRAPHY OF THE ALI SAHIB WELL

Studies of flush cutting from 1250 m of the Sakesar Limestone of Eocene age to target depth (2050 m), which is in the Datta Formation of Jurassic age have been carried out. The Jurassic sequence is the thickest with a thickness of 370 m (up to target depth) and the Paleocene sequence is the thinnest with a thickness of 60 m (Table 6.1). Nannofossil biostratigraphy of the Ali Sahib Well has been carried out by Ashraf (2005).

6.1.1 EOCENE

Sakesar Limestone

1) 1250-1275 m Limestone: White, light grey, dirty white, milky white, medium hard to hard, compact, in places soft and chalky.

2) 1275-1285 m Limestone with Streaks of Shale:
Limestone lithology is same as in 1.
Shale: Light grey to greenish grey, soft, laminated, moderately indurated and calcareous.
Nannofossils: barren

Nammal Formation

3) 1285-1305 m Shale with Streaks of Limestone:
Shale: Medium grey to greenish grey, soft, laminated, moderately indurated and calcareous. Limestone: Light grey and dirty white, medium hard to hard, argillaceous and fossiliferrous.

4) 1305-1355 m Limestone with Streaks of Shale: Lithologies of the sediments are same as above in (3).
Nannofossils: *Sphenolithus radians* (first occurrence indicates the base of NP 11, in early Eocene age)*, Coccolithus pelagicus, Discoaster barbadiensis* and *Coronocyclus nitescens.*

5) 1355-1460 m Limestone: Off white, dirty white, soft to medium hard, chalky, marly, argillaceous, highly fossiliferrous.
Nannofossils: *Sphenolithus radians, Coccolithus pelagicus, Discoaster barbadiensis* and *Coronocyclus nitescens.*

6.1.2 PALEOCENE

Dunghan Formation

6) 1460-1490 m Limestone with intercalation of Shale:
Limestone: White, creamy, light grey, light brown, soft to medium hard, chalky, marly and argillaceous and fossiliferous.
Shale: Greenish grey, pyritic, soft to moderately indurated.
Nannofossils: *Coccolithus pelagicus, Toweius aminens, Toweius pertusus, Discoaster multiradiatus, Prinsius bisulcus* and *Fasciculithus tympaniformis, Sphenolithus anarhopes, Ericogotra* sp*.?*
The last occurrence of *Fasciculithus tympaniformis* and the first occurrence of *Discoaster multiradiatus* define the *NP* 9 in this interval as Late Paleocene.

Ranikot Formation

7) 1490-1520 m Shale with streaks of Limestone and Sandstone:
Shale: Greenish grey, light grey, soft to moderately indurated and slightly calcareous.
Limestone: Light grey, in places dirty white, medium hard, dolomitic.
Sandstone: Transparent to translucent, loose and friable, fine to medium-grained, subangular to subrounded, moderately sorted.
Nannofossils: *Toweius eminens, Toweius pertusus, Sphenolithus anarhopes*
Age: Late Paleocene

6.1.3. CRETACEOUS

Lumshiwal Formation

8) 1520-1550 m Sandstone with thin bands of Marl and Shale:
Sandstone:- Light grey, transparent to translucent, loose and friable, pink and yellowish brown grains are also observed, fine to medium-grained, in places coarse-grained, sub angular to sub rounded, poorly to moderately sorted and cemented.
Marl: Light grey, dirty white, soft, sticky and pasty.
Shale: Greenish grey, light grey, light brown, soft to moderately indurated, slightly calcareous.
Nannofossils: barren

9) 1550-1600 m Quartz Arenite:
Light grey, transparent to translucent, loose and friable, medium hard, quartzose, fine to medium-grained, in places coarse to very coarse-grained, even granule size are present. It is subangular to subrounded, poorly sorted and cemented, calcareous in places.
Nannofossils: barren

10) 1600-1620 m Sandstone with alternation of Shale:
Sandstone: Lithology is the same as above in (4).
Shale: Grey to dark grey, greenish grey, soft to moderately indurated and laminated.
Nannofossils: A number of *Watznaueria barnesae* specimens have been identified.
Age: Cretaceous

Chichali Formation

11) 1620-1680 m Shale with traces of Sandstone:
Shale: Color is yellowish grey; light grey, pyritic, glauconitic and calcareous. Sandstone: Light grey, transparent to translucent, loose and friable, medium hard, quartos (quartzose), fine to medium-grained, in places coarse to very coarse-grained, even granule size are present. It is subangular to subrounded, poorly sorted and cemented, calcareous in places.
Nannofossils: *Watznaueria barnesae, Watznaueria brittanica, Watznaueria biporta, Cyclagelosphaera dflanderei*
Age: Early Cretaceous

6.1.4 JURASSIC

Samana Suk Formation

12) 1680-1700 m Limestone with streaks of Shale:
Limestone: Light grey, medium grey, oolitic, argillaceous, calcite veins were also observed.
Shale: Greenish grey, medium grey, yellowish grey, soft to moderately indurated and calcareous.

13) 1700-1720 m Shale with streaks of Limestone:
Shale: Dirty white, yellowish white, light grey, greenish grey, soft to moderately indurated, calcareous.
Limestone: Light grey, off white, chalky and argillaceous.

14) 1720-1730 m Claystone with thin bands of Limestone:
Claystone: Yellowish brown, dirty white, pasty, sticky and soluble.
Limestone: Light grey to medium grey chalky and argillaceous.

15) 1730-1750 m Sandstone with thin bands of Shale:
Sandstone: Transparent to translucent, loose, friable, fine to medium-grained, subangular to subrounded, sugary, quartzose, moderately sorted.
Shale: Light grey to medium grey, soft to moderately indurated and slightly calcareous.

16) 1750-1822 m Limestone with thin bands of Shale:
Limestone: Light grey, oolitic, argillaceous, the lowest two meters are medium grey.
Shale: Light grey, soft to moderately indurated and slightly calcareous.
Nannofossils: barren

Datta Formation

17) 1822-1852 m Sandstone with intercalation of Claystone:
Sandstone: Transparent to translucent, sugary, quartzose, loose, friable, fine to medium-grained, subangular subrounded and well sorted.
Claystone: Reddish brown, brick red, dusky brown, stiff, soft to moderately

indurated, slightly calcareous.

18) 1852-1872 m Claystone with intercalation of Sandstone: Lithologies are the same as above in 17.

19) 1872-1890 m Sandstone (Quartz Arenite): Transparent to translucent, sugary, light grey and dull white, yellowish brown grains are also observed, quartzose, loose, friable, fine to medium-grained, less than 1% very coarse grained, subangular to subrounded and well sorted.

20) 1890-1910 m Claystone: Brick red, reddish brown, soft and pasty.

21) 1910-1932 m Sandstone with intercalations of Claystone:
Sandstone: Transparent to translucent, sugary, light grey and dull white, yellowish brown grains are also observed, quartzose, loose, friable, fine to medium-grained, ~ 0.5% very coarse grained, subangular to subrounded and well sorted.
Claystone: Brick red, reddish brown, pink, light grey soft and pasty.

22) 1932-1950 m Sandstone with streaks of Claystone and Shale:
Sandstone: Loose, friable, translucent, sugary, light grey and yellowish brown, fine to medium-grained subangular to subrounded, calcareous and well sorted.
Claystone: Brick red, reddish brown, soft and moderately indurated, pasty.
Shale: Medium grey to dark grey, greenish grey and calcareous.

23) 1950-2050 m Sandstone with streaks of Claystone, Shale and Limestone:
Sandstone: Loose, friable, translucent, sugary, light grey and yellowish brown, dirty white, fine to medium-grained, subangular to subrounded, calcareous and moderately well sorted.
Shale: Medium grey, dark grey, greenish grey and dusky brown, splintery and calcareous.
Claystone: Brick red, reddish brown, soft and moderately indurated, silty and pasty.
Limestone: Light grey, olive grey, argillaceous, calcitic veins are also observed.
Nannofossil: The Datta Formation is barren of Nannofossils.

NOTE: The lithological description, as described by the Well Site Geologist, regarding the Shinawari Formation of Jurassic age and the Kingriali Formation of Triassic age, very much resembling to the Datta Formation of Jurassic age. The Datta Formation, which is mainly continental in origin, consists of a variegated lithology i.e., sandstone, shale with irregular distributed calcareous dolomite (Shah, 1977). The writer's personal observations in the field are also supporting Shah's idea. It can be assumed that the Shinawari Formation of Jurassic age and the Kingriali Formation of Triassic age have not been encountered and the drilled strata from 1822-1890 m (the Shinawari Formation) and from 1932-2050 m (the Kingriali Formation) are the lower and upper

sections of the Datta Formation. The well site geologist's descriptions of the Shinawari and Kingriali Formations as being comprised of sandstone and claystone, respectively, are not in agreement with the observations of Shah (1977) and the author's personal observations in the field.

Table 6.1: Lithofacies and their thicknesses of the Ali Sahib Well

AGE	FORMATION	DEPTH [m]	LITHOFACIES	No
EOCENE	SKESSAR	1250-1275	Limestone	1
		1275-1285	Limestone with streaks of shale	2
	NAMMAL	1285-1305	Shale with streaks of limestone	3
		1305-1355	Limestone with streaks of shale	4
		1355-1460	Limestone	5
PALEOCENE	DUNGHAN	1460-1490	Limestone with intercalations of shale	6
	RANIKOT	1490-1520	Shale with streaks of limestone sandstone	7
CRETACEOUS	LUMSHIWAL	1520-1550	Sandstone with thin bands of marl & shale	8
		1550-1600	Quartz Arenite	9
		1600-1620	Sandstone with Alternation of Shale	10
	CHICHALI	1620-1680	Shale with traces of sandstone	11
JURASSIC	SAMANA SUK	1680-1700	Limestone with streaks of shale	12
		1700-1720	Shale with streaks of limestone	13
		1720-1730	Claystone with thin bands of limestone	14
		1730-1750	Sandstone with thin bands of shale	15
		1750-1822	Limestone with thin bands of shale	16
	DATTA	1822-1852	Sandstone with intercalation of claystone	17
		1852-1872	Claystone with intercalation of sandstone	18
		1872-1890	Quartz Arenite	19
		1890-1910	Claystone	20
		1910-1932	Sandstone with intercalation of claystone	21
		1932-1950	Sandstone with streaks of claystone & shale	22
		1950-2050	Sandstone with streaks of claystone, shale & limestone	23

6.2 LITHOLOGY AND STRATIGRAPHY OF AMIR WALI WELL

The studied lithostratigraphic sequence is from the Sakesar Limestone of Eocene age to the Datta Formation of Jurassic age. The Jurassic sequence is the thickest with thickness of 290 m (up to target depth) and the Paleocene sequence is the thinnest with a thickness of 85 m (Table 6.2).

6.2.1 EOCENE

Sakesar Formation

1) 1315-1340 m Limestone: Light grey, dirty white, in places light yellow, medium hard, chalky, in places fossiliferous.

Nammal Formation

2) 1340-1355 m Limestone with streaks of Shale:
   Limestone: Dirty white, light grey, medium hard to hard, soft in places, argillaceous, marly, and highly fossiliferous.
   Shale: grey, dark grey, soft to moderately indurated and calcareous.

3) 1360-1525m Limestone with traces of Marl:
   Limestone: Dirty white, yellowish white, light grey, argillaceous, marly in nature, highly fossilifeous.
   Marl: Traces of marl are whitish grey, soft, pasty and sticky.

6.2.2 PALEOCENE

Dunghan Formation

4) 1525-1535 m Shale: Dark grey black, blocky, soft to moderately indurated.

Ranikot Formation

5) 1535-1550 m Sandstone: Transparent, sugary, subangular, fine to medium-grained, well sorted, and poorly cemented, pyritic.

6) 1550-1560 m Shale: Dark grey to black, blocky, soft to moderately indurated. Nummilites are also observed.

7) 1560-1575 m Sandstone with streaks of Shale and Marl:
   Sandstone: Translucent, very light grey, fine-grained, subangular to subrounded, and well sorted, calcareous, glauconitic and pyritic.
   Shale: medium grey, blocky, soft to moderately indurated.
   Marl: Light grey, medium grey, sticky and pasty.

8) 1575-1600 m Shale with streaks of Marl:
Shale: Medium grey, greenish grey, soft to moderately indurated and calcareous. Marl: Light grey, dirty white, soft, sticky, and pasty.

9) 1600-1610 m Marl: Lithology is the same as above in 5.

10) 1610-1620 m Sandstone with streaks of Shale and Marl:
Sandstone: Translucent, sugary, fine to medium-grained, subangular to sub-rounded, calcareous and glauconitic.
Shale: medium grey, greenish grey, soft to moderately indurated, calcareous.
Marl: Light grey, dirty white, soft, sticky and pasty.

6.2.3 CRETACEOUS

Lumshiwal Formation

11) 1620-1630 m Sandstone: Brick red, reddish brown and light grey, yellowish brown, medium to coarse-grained, even granule sized sediments are found. Grains are subangular to subrounded, moderately sorted, and slightly calcareous.

12) 1630-1660 m Sandstone with streaks of Shale:
Sandstone: Translucent, sugary, medium to coarse-grained, ~0.5% granule sized sediments are visible. Subangular to subrounded.
Shale: Medium grey, greenish grey, soft to moderately indurated.

Chichali Formation

13) 1660-1690 m Marl intercalation with Shale:
Marl: Light grey, dirty white, soft, sticky, and pasty.
Shale: Medium grey, dark grey, greenish grey, soft to moderately indurated, slightly calcareous.

14) 1690-1720 m Sandstone with streaks of Shale:
Sandstone: Translucent, light grey, sugary, loose, friable, medium to coarse-grained even granule size, moderately well sorted.
Shale: Dark grey, soft to moderately indurated, slightly calcareous.

15) 1720-176 m Marl intercalation with Shale:
Marl: Dusky brown, earthy, soft, sticky and pasty.
Shale: Dark grey, greenish grey, soft to moderately indurated, slightly calcareous.

6.2.4 JURASSIC

Samanasuk Formation

16) 1760-1890 m Limestone:
Dirty white, light grey, light brown, medium hard to hard, chalky, argillaceous and fossiliferous. Shale of dark grey color is also observed in places.

17)1890-1900 m Sandstone with thin bands of Claystone:
Sandstone: very light grey, translucent, friable, loose, fine to medium-grained, subangular to subrounded, moderately well sorted and poorly cemented.
Claystone: medium grey, dirty grey, soft to moderately firm, sticky, pasty and soluble.

Datta Formation

18)1910-1940 m Sandstone: Translucent, loose, friable, texture is sugary, fine to medium-grained; ~ 0.5% coarse-grained sediments were also found. The sediments are poorly cemented and moderately sorted.

19) 1940-1960 m Claystone with thin bands of Sandstone:
Claystone: light grey to medium grey, silty, firm and medium hard.
Sandstone: fine-grained, remaining lithology is the same as above in 18.

20) 1960-2012 m Claystone with streaks of Sandstone:
Claystone: Brick red, reddish brown, yellowish brown, light yellow, soft to medium hard.
Sandstone: Translucent, light grey, fine-grained, subangular to subrounded, well cemented and well sorted.

21) 2012-2050m Sandstone with intercalation of Claystone Shale:
Sandstone: Light grey, fine-grained, subangular to subrounded, well cemented and well sorted, pyritic.
Claystone: Off white, reddish brown, moderately firm, sticky, pasty, slightly calcareous.
Shale: light grey to grey, olive grey, laminated, subfissile.

Table 6.2: Lithofacies and their thicknesses of the Amir Wali Well

AGE	FORMATION	DEPTH [m]	LITHOFACIES	No
EOCENE	SAKESAR	1315-1340	Limestone	1
	NAMMAL	1340-1355	Limestone with streaks of shale	2
		1355-1525	Limestone	3
PALEOCENE	DUNGHAN	1525-1535	Shale	4
	RANIKOT	1535-1550	Sandstone	5
		1550-1560	Shale	6
		1560-1575	Sandstone with streaks of shale	7
		1575-1600	Shale with streaks of marl	8
		1600-1610	Marl	9
		1610-1620	Sandstone with streaks of shale and marl	10
CRETACEOUS	LUMSHIWAL	1620-1630	Sandstone	11
		1630-1660	Sandstone with streaks of shale	12
	CHICHALI	1660-1690	Marl intercalation with shale	13
		1690-1720	Sandstone with streaks of shale	14
		1720-1760	Marl intercalation with Shale	15
JURASSIC	SAMANA SUK	1760-1890	Limestone	16
		1890-1900	Sandstone with thin bands of claystone	17
	DATTA	1900-1940	Sandstone	18
		1940-1960	Claystone with thin bands of sandstone	19
		1960-2012	Claystone with streaks of sandstone	20
		2012-2050	Sandstone with intercalation of claystone and shale	21

7. PETROGRAPHY & MICROFACIES OF CARBONATES IN ALI SAHIB & AMIR WALI WELL

7.1 INTRODUCTION

In the present work, carbonate microfacies of the Samana Suk Formation (Middle Jurassic), the Chichali Formation (Late Jurassic) the Lumshiwal Formation (Cretaceous) and the Lumshiwal/Ranikot Formation (Cretaceous/Palaeocene) were studied to establish environment of deposition, sedimentology and diagenesis of the Punjab Platform. The present study is a first attempt to understand the sedimentology of the Punjab Platform especially in the Cretaceous and Jurassic age. Up to now, stratigraphically corresponding sediments were only studied in the Salt Range area and further to the north and to the northwest (Trans Indus ranges, Kalachitta Range etc.) where these formations are exposed (e. g. Shah, 1977; Fatmi, 1977; Qureshi *et al.*, 2005-6; Nizami & Sheikh, 2007).

Ashraf (2005, unpublished) identified different nannofossils species from different formation from the Ali Sahib Well (cf. Ch. 6). He reported that the Sakesar Limestone (Eocene), the Lumshiwal Formation (Cretaceous), the Samana Suk Formation (Jurassic) and the Datta Formation (Jurassic) are all barren of nannofossils.

In the Lumshiwal Formation (Gee, 1945; Fatimi, 1973), *Ammonitoceras* sp*, Ailoceras,* sp. *Douvilleiceras mammilatum, Oxytropidoceras* sp*; Desmoceras* sp; *Cleoniceras* sp*; Branchoceras* sp; and *Lemunoceras* sp. (Fatmi, 1968) have been reported. Its age ranges from Aptian to Albian (Fatmi, 1977) in Kohat area. The Samana Suk Formation has been assigned to Middle Jurassic age (Shah, 1977; Fatmi, 1977; and Nizami & Sheikh, 2007). *Reineckeia ancepto, Chaffatia* sp; *Hubertoceras* sp; *and Kinkeliniceras* sp*;* have been reported in this formation (Kazmi & Jan, 1997). The first attempt to study the Ranikot Group, in the Kirthar area of the Indus Basin, was done by Blanford (1876; 1879) and Vredenburg (1909).

From the analysis of cores, bryozoa, age dating foraminifera and echinodermata were identified, which have never been reported from the Jurassic to Paleocene strata of Pakistan. In this way, these findings are a breakthrough in establishing the

biostratigraphy, especially for the Jurassic strata, which have been declared barren of nannofossils in Pakistan, particularly in the Punjab Platform. The age determining faunas were found in the Samana Suk and Chichali Formation. The Samana Suk Formation (Middle Jurassic, Shah, 1977; Fatmi, 1977) is a significant sedimentary succession. Its thickness varies from 5 m (Nammal Gorge, Salt Range) to 366 m (Sheikh Buddin Hills, Marwat Range). It is also recognizable over a wide area of northern Pakistan (Shah, 1977; Nizami & Sheikh, 2007). Due to the presence of ooids, the depositional environment of the Samana Suk Formation was considered as shallow marine (Shah, 1977) as known from the Surghar Range and Trans Indus Ranges in Pakistan (Nizami & Sheikh, 2007). Fatmi (1977) reported from the top of the Samana Suk Formation the ammonite taxa *Reinneckeia ancepto, Choffatia* sp*., Obtusicostites* sp., *Hubertoceras* sp., *Kinkeliniceras* sp*.* and assigned its age Middle Callovian.

The Chichali Formation (Danilchik, 1961; Gee, 1945) is overlying the Samana Suk Formation and is mainly formed by of glauconitic shale and glauconitic sandstone in all exposed regions (Salt Range, Trans Indus Ranges and in Hazara area). According to Fatmi (1977) the Chichali Formation is mainly Late Jurassic in age. Kazmi & Jan (1997) assigned a Late Oxfordian to Neocomian age to the Chichali Formation. On the basis of nannofossil biostratigraphy (by studying ditch cuttings of the Ali Sahib Well), Ashraf (2005) assigned the age of the Chichali Formation as Early Cretaceous (unpublished report of OGDCL). According to him, the carbonate sequence below the Chichali Formation (which is mainly a clastic sequence) is Jurassic in age, which can be considered as the Samana Suk Formation. There exists up to now no general agreement about the age ranges of these different formations. Mertmann & Ahmad (1994) and Nizami & Sheikh (2007) assigned the Samana Suk Formation to the Middle Jurassic, overlain by the Late Jurassic to Early Cretaceous carbonatic siliciclastic Chichali Formation (Qureshi *et al.*, 2005; Qureshi et al., 2007). Fatmi (1972, 1977), assigned a Late Oxfordian to Early Cretaceous age for the Chichali Formation. In contrast, Köthe (1988) mentioned an Oxfordian to Tithonian age.

According to Mertmann & Ahmad (1994), the base of the Samana Suk Formation should be diachronous (Bathonian to Callovian) and deposition should end in the Callovian. The Chichali Formation starts its deposition in Late Oxfordian after a gap.

All these data came from the Surghar Range and Salt Range in Pakistan further to the north and northwest. This region is highly affected by sea-level fluctuations due to its position in a continent-near facies belt, and therefore, gaps are occurring (Mertmann & Ahmad, 1994) during regressive cycles. Deposition is mainly characterized by shallow-water conditions (e. g; Hallam & Maynard; 1987; Nizami & Sheikh, 2007; Qureshi et al., 2007). Only a transgressive cycle in the Middle Callovian provides exact data to separate the Samana Suk and Chichali Formations. This Samana Suk Formation has been encountered in the Ali Sahib and Amir Wali wells. But its correlation with the shallow-water areas to the north is rather unclear due to the lack of exact data. The investigated wells provide the first data from an environment located in more outer shelf position. Microfacies studies of the Lumshiwal Formation of Cretaceous and the Ranikot Formation of Paleocene age has also been carried out. In these formations, no age determining fossils were found, but microfacies studies give some indication about the environment of deposition.

Biostratrigraphy and microfacies analysis will be very helpful in understanding the sedimentology and environment of deposition of the area, as we need for reconstruction of facies belts. Sedimentological characteristics of carbonates, mixed carbonate-terrigenous and pure terrigenous sediments and their spatial distribution are very important in establishing paleoenvironments, quantitative hydrocarbon reservoir or hydrological modeling studies.

The cores and sample locations in the log profile of bore holes (Ali Sahib and Amir Wali wells) have been described in Figs. 5.1 and 5.2.

7.2 STRATIGRAPHY, MICROFACIES AND AGE DATING

The sediments of Core I of the Lumshiwal Formation in the Ali Sahib Well mainly comprised of siliciclastic mixed with carbonates. The carbonate content is denoted by shell fragments, crinoids, sparite, micrite and dolomite mainly in the layers of the succession. The environment of deposition of these sediments of the Lumshiwal Formation of the Ali Sahib Well can be interpreted as shallow-marine which is in accordance with the environmental interpretation of the Lumshiwal Formation of other authors (e. g. Chaudhry *et al.*, 1997; Qureshi *et al.*, 2005). The presence of glauconite (Fig. 7.1 C & D) and pyrite indicates that the deposition of the sediments occurred in partly reducing conditions. The occurrence of fine quartz grains with coarse quartz grains suggests that intermitted high energy influx was also a characteristic during the deposition of these sediments. Some clastic grains (quartz and tourmaline) are fractured (Fig. 7.1 A). The shells having envelopes of micrite are showing calm to low energy environment. The sea level was almost stable during the deposition of the sediments of Core I of the Ali Sahib Well (Fig. 7.7 B). The depositional setting appears to be subtidal to intertidal in carbonate ramp (Fig. 7.7 A). No age determining fossil was found in Core I of the Ali Sahib Well.

The sediments of Core I of the Ranikot Formation in the Amir Wali Well comprised of siliciclastic mixed with carbonates (Fig. 7.8 D). Quartz is dominant in siliciclastic, while carbonates comprised of bioclasts, ooids, peloids, sparite and micrite. Most of the section consists of shallow water derived material which was transported to the deeper parts. The occasional abundance of quartz can be explained by intermitted floods of high energy from hinterland. Crinoids without encrusting are occurring in micrite matrix (Fig. 7.2 B) indicating that the crinoid has been transported before final deposition in present position. In top of the section (samples AW1 and AW2), shallow-water sediments were found, indicating that the section of Core I of the Ranikot Formation of the Amir Wali Well is shallowing upward (Fig. 7.8 B). A lot of well preserved bryozoa have been observed in Core I of the Amir Wali Well, but its age as well as its species is to be determined (Fig. 7.2 C-F).

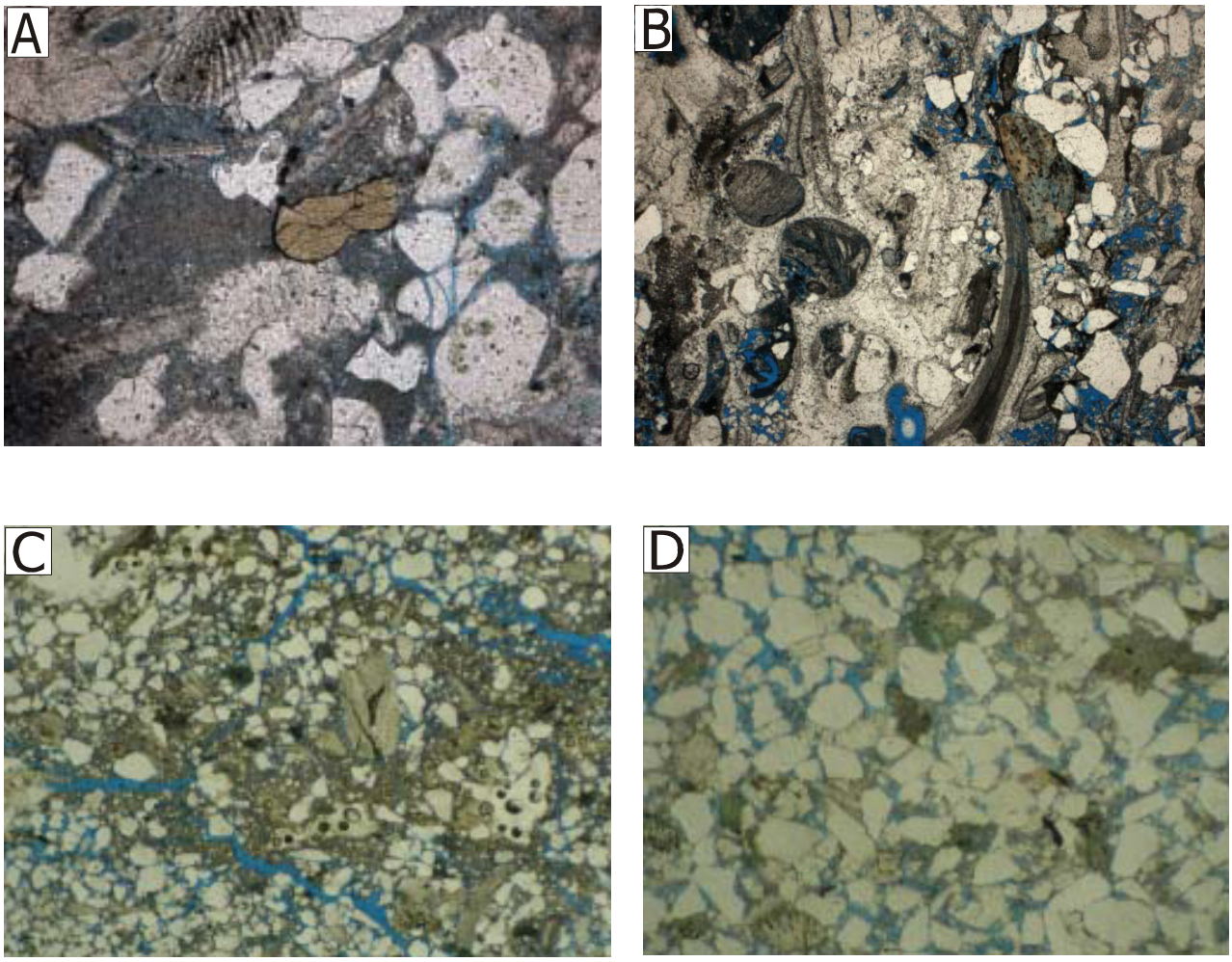

Fig. 7.1: Characteristic microfacies of the Lumshiwal Formation, Core I of the Ali Sahib Well

(A) AS1 (1534.20 C_1): Quartz grains in micrite matrix, one touramaline and one quartz grain is fractured. Bioclasts particularly in the left upper corner can also be seen (width of the photo is 0.70 mm). (B) AS5 (1536.70 C_1): interganular and moldic porosity, shells and other carbonate grains have been bored, one altered tourmaline grain, quartz grains, dominant cement is sparite (width of the photo is about 3 mm). (C) AS10 (1039.10C_1): Quartz grains, dolomitic rhombs, micrite matrix, some glauconite and primary and secondary porosity are obvious. One brachiopod shell and a little glauconite is also present (width of the photo is 1.4 cm). (D) AS11 (1539.65 C_1): Quartz grains having a lot of intergranular porosity, shells and crinoids can also be seen. Glauconite is also present (width of the photo is 0.25 cm).

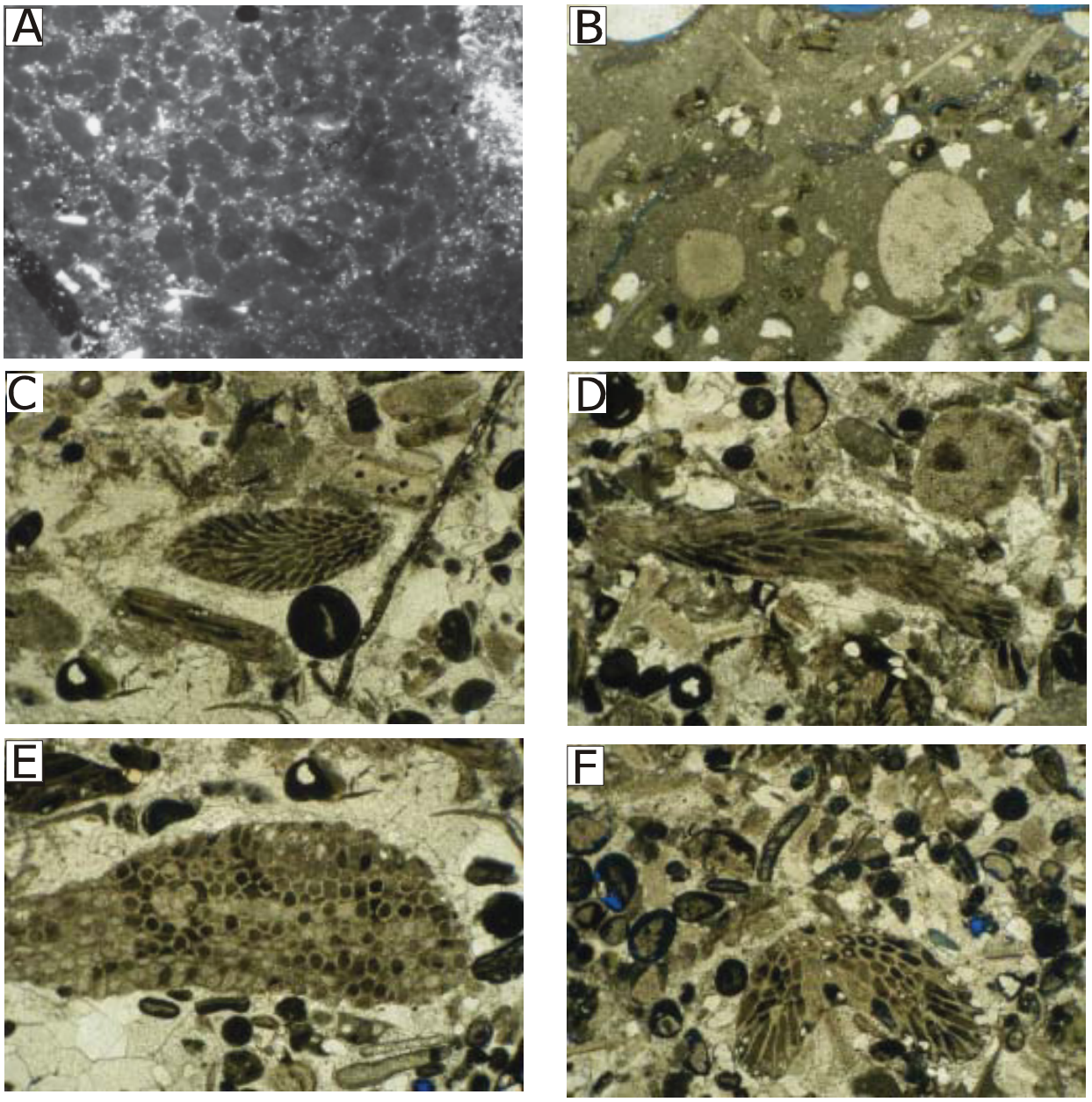

Fig. 7.2: Characteristic microfacies of the Ranikot Formation, Core I of the Amir Wali Well.

(A) AW1 (1575.50C_1): Peloids and microquartz grains (width of photo is 1.4 cm). (B) AW4 (1577.17C_1): Crinoids without micrite rim, quartz and ooids grains in micrite matrix. A fractue in matrix can also be seen (width of photo is 1.4 cm). (C) AW7 (1579.22C_1): Bryozoa partially filled by glauconite, ooids, shells having micritic envelops, and aggregate grains, some crinoids are with micritic rims, a vein is also present which is filled by micrite, the dominant cement is sparite (width of the photo is 0.25 cm). (D) AW7 (1579.22C_1): Well preserved green algae partially filled by glauconite, crinoids and ooids have micritic envelopes. Sparite cement is also obvious (width of the photo is 0. 5 cm). (E) AW7 (1579.22C_1): Well preserved bryozoa with rounded chambers partially filled by glauconite and surrounded by sparite (width of the photo is 0.25 cm). (F) AW11 (1581.54C_1): Ooids, shells having micritic envelopes, well preserved bryozoa, some ooids has begun to dissolve to develop moldic porosity, (width of the photo is 0.5 cm).

The microfacies pattern of Core II of the Ali Sahib Well reflects a complex paleoenvironment. Most dominant are grainstones with shallow-water clasts, including coated grains, bryozoans, shell fragments, brachiopods, micrite ooids and several benthic foraminifera. Of special interest is the occurrence of *Saccocoma* as nucleus (Fig. 7.3b H) in micritic ooids together with rare occurrence of *Nautiloculina oolithica* (Fig.7.3a C & D). *Saccocoma* is found in Oxfordian to Tithonian ages (Flügel, 2004; Aubrecht *et al.,* 2009). It can be interpreted that *Saccocoma* and *Nautiloculina oolithica,* both together indicate an Oxfordian to Tithonian age. The presence of *Saccocoma* in nuclei of ooids and in matrix is an indication of deposition occurred in pelagic environment (Amri *et al.*, 2008). Of special interest is the shedded material from the shallow-water carbonate ramp, together a huge amount of crinoids, beside the micrite ooids (in sense of Jenkyns, 1972), both indicating a deposition in an outer shelf region. During the deposition of the sediments of Core II of the Ali Sahib Well, sea level was might remain stable (Fig 7.9 B), with a lot of tempestites/turbidites currents. This microfacies type corresponds to the microfacies of the Samana Suk Formation as described northwest in the Surghar Range by Mertmann & Ahmad (1994), but is younger in age. The age perfectly corresponds to the age of the Chichali Formation, but lithology and microfacies are completely different.

The section of Core IV of the Amir Wali Well starts with allodapic limestones (Fig. 7.6 A) in a radiolarian rich wackestone and shows a general shallowing upward cycle. The microfacies of the samples of Core IV are characterized by siliciclastic influenced shallow-water carbonates, which consist mainly of grainstones. The grainstones are rich in shells, peloids, small benthic foraminifera and rare oncoids (Fig. 7.6 B & D). Micrite clasts are common, ooids are completely missing. In the upper part of this succession (Core IV), the first *Nautiloculina oolithica* was found (Fig. 7.6 C). This foraminifer is limited to the Bathonian-Tithonian time span. The upper part of the Core IV of the Amir Wali Well follows a deep water succession, which consists of a filament-radiolaria pack-stone. The filaments resemble *Bositra* shells (Figs. 7.5 A-D), characteristic for Middle Jurassic to Oxfordian. *Bositra* Limestones, known widespread in the Middle Jurassic of Tethyan realm, contains several allodapic limestone layers. The components of these mainly shallow-water derived carbonates differ from that in the deeper parts.

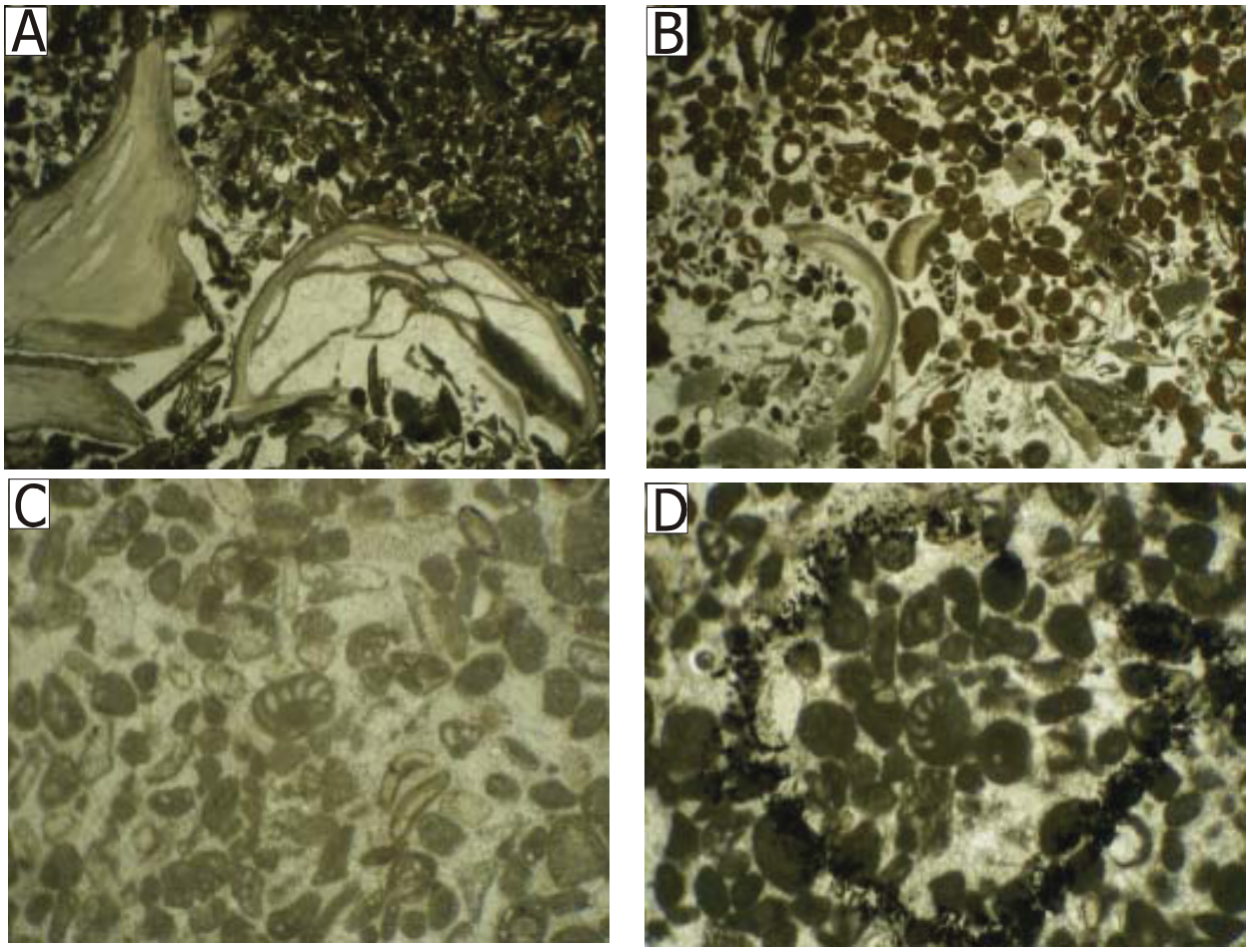

Fig. 7.3a: Characteristic microfacies of the Chichali Formation (Late Callovian to Tithonian?) of the Ali Sahib Well, Core II.

(A) AS23 (1699.00 C_2): Brachiopods shells together with micrite ooids (width of the photo is 1.4 cm). (B) AS21 (1698.21 C_2): Grainstone with micritic ooids, encrusted brachiopods fragments and crinoids (width of the photo 0.25 cm). (C and D) AS22 (1698.40 C_2): Micritic Olliths, bored shells, micritized crinoids and *Nautilucolina oolithica* in centre of the photos, the grains are cemented by sparite (width of the photo is 0.25 cm).

In Core II of the Ali Sahib Well, less shells and peloids are characteristic. Dominant are crinoids, beside micrite ooids in several layers. Small benthic foraminifera, bryozoans, brachiopods fragments are characteristic. Partly micrite ooids are dominating, partly *Saccocoma* occur in the cores of the micrite ooids.

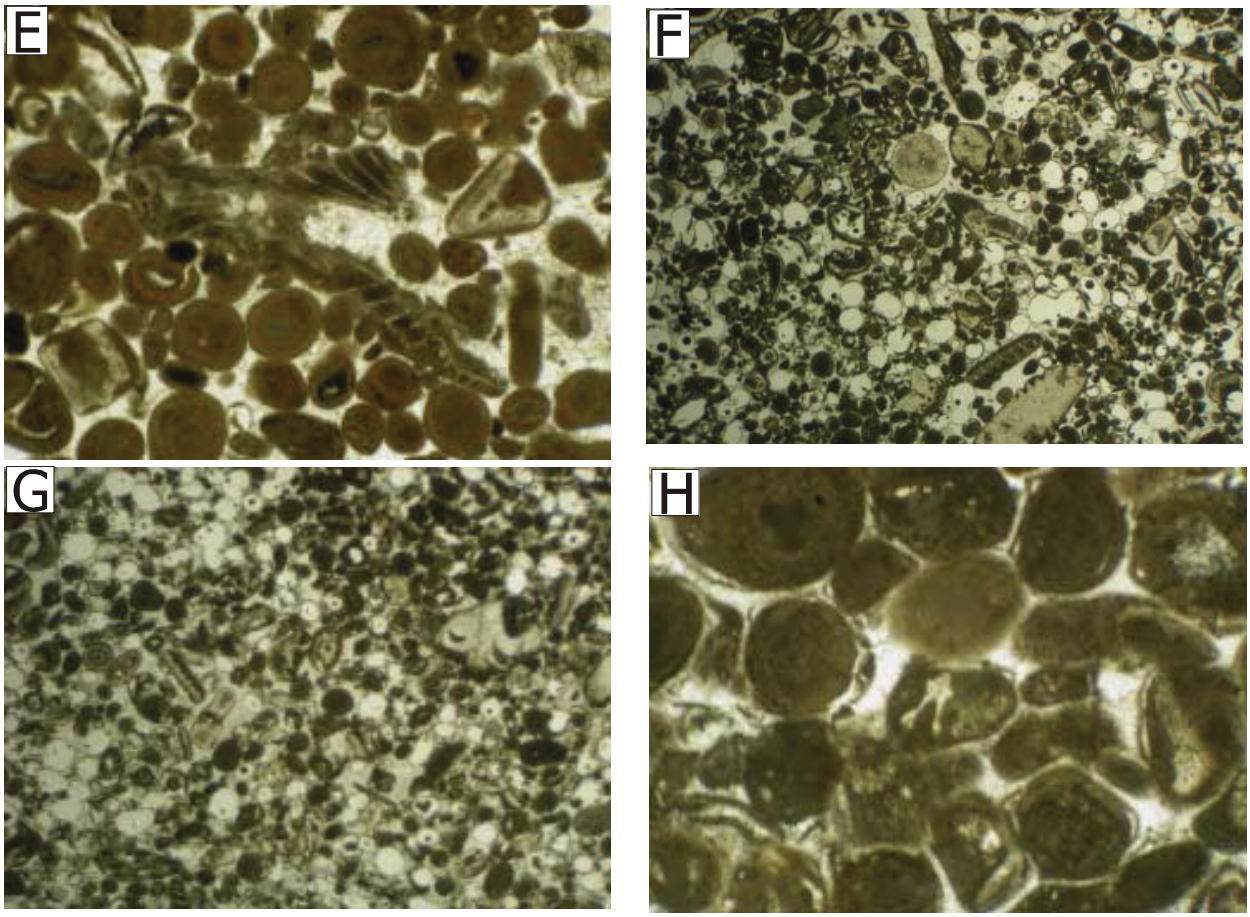

Fig. 7.3b: Characteristic microfacies of the Chichali Formation (Late Callovian to Tithonian?) of the Ali Sahib Well, Core II.

(E) AS21 (1698.21 C_2): Micritic ooliths with bryozoans and encrusted crinoids. Sparite is dominant cement (width of the photo is 1.4 cm). (F and G) AS16 and AS15 (1694.05 C_2, 1694.80 C_2): Micrite ooid facies with small benthic foraminifera, crinoids and recrystallized clasts. Such micrite ooids indicate deeper water environment. Characteristic are also the crinoids without encrusting (width of the photo is 1.4 cm). (H) AS15 (1694.05 C_2): Micritic Ooliths are cemented by sparite cement; a fragment of *Saccocoma* in the nuclei (centre) can also be seen (width of the photo 0.25 cm).

In several samples the occurrence of *Nautiloculina oolithica* proves, beside the occurrence of *Saccocoma*, an Oxfordian to Tithonian age of the succession drilled in Core III as well as in the upper part of Core IV of the Amir Wali Well. Both sections (Core III & Core IV) are characterized by shallowing-upward cycles with radiolarian wackestones at the base representing independent shallowing upward cycles (Figs. 7.10 B & 7.11 B).

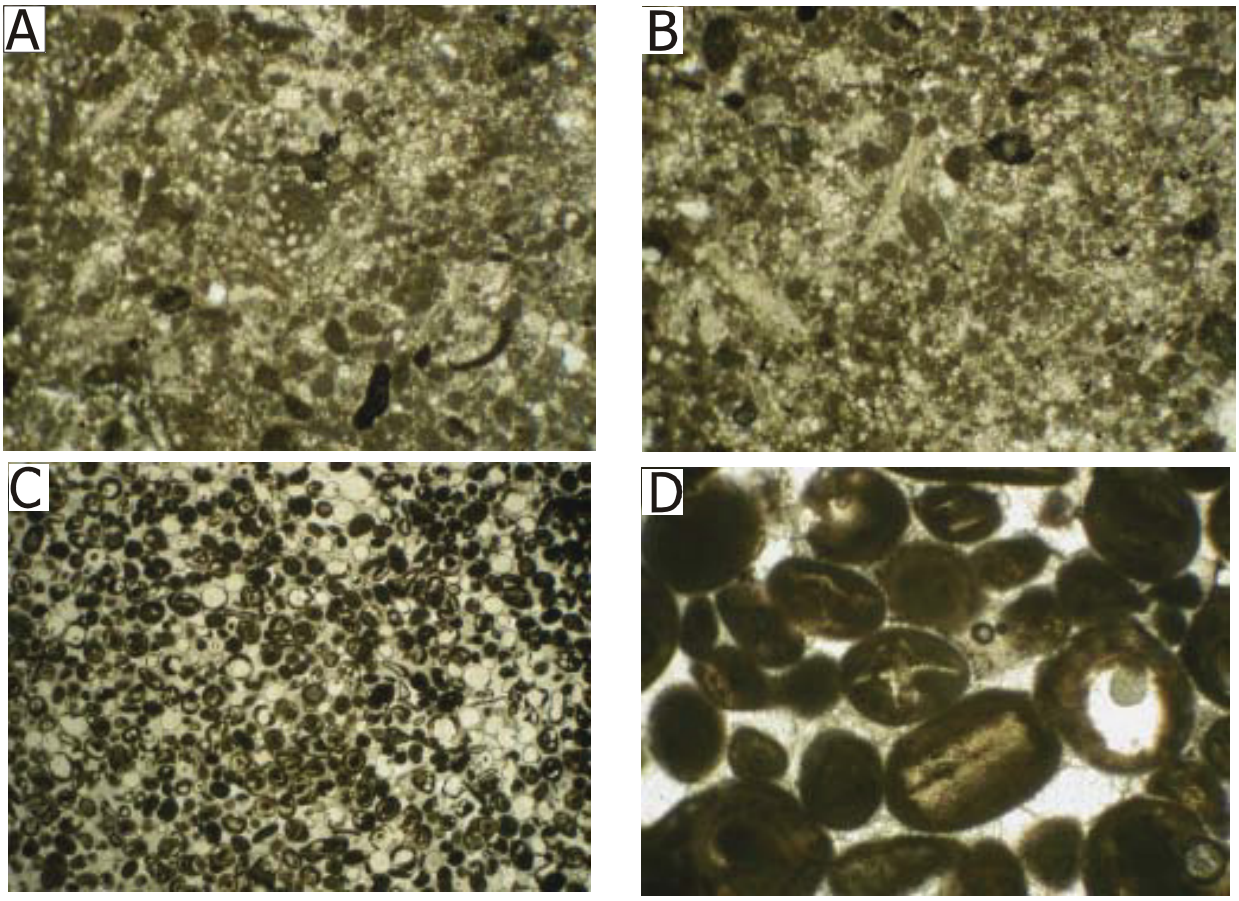

Fig. 7.4a: Characteristic microfacies of the Chichali Formation (Late Callovian to Tithonian?) of the Amir Wali Well Core III & Core IV.

(A) and (B) AW40 (1854.00C_4): peloids/micritic clasts, foraminifera *Nautiloculina oolithica*, some dolomitic/ankerite rhombs (width of the photo is 0.25 cm). (C) AW38 (1768.60C_3): Micrite ooids facies with small benthic foraminifera, ctinoids and recrystallized carbonate clasts. Such micrite ooids indicate deeper water environments (width of the photo is 1.4 cm). (D) AW38 (1768.60 C_3): Well sorted grainstone comprised of ooids/oncoids having a *Saccocoma* (Oxfordian to early Tithonian) in the nuclei, (width of the photo is 1.4 cm).

The microfacies of the lower part of the Core IV is different from the microfacies as known from the Samana Suk Formation. The age range (Bathonian to Callovian) corresponds perfectly to the defined age of the Samana Suk Formation as known from the literature. The upper part of Core IV and Core III of the Amir Wali well, corresponds to the described microfacies of the Samana Suk Formation in the literature, but in age range, it is younger (Late Callovian to Tithonian?).

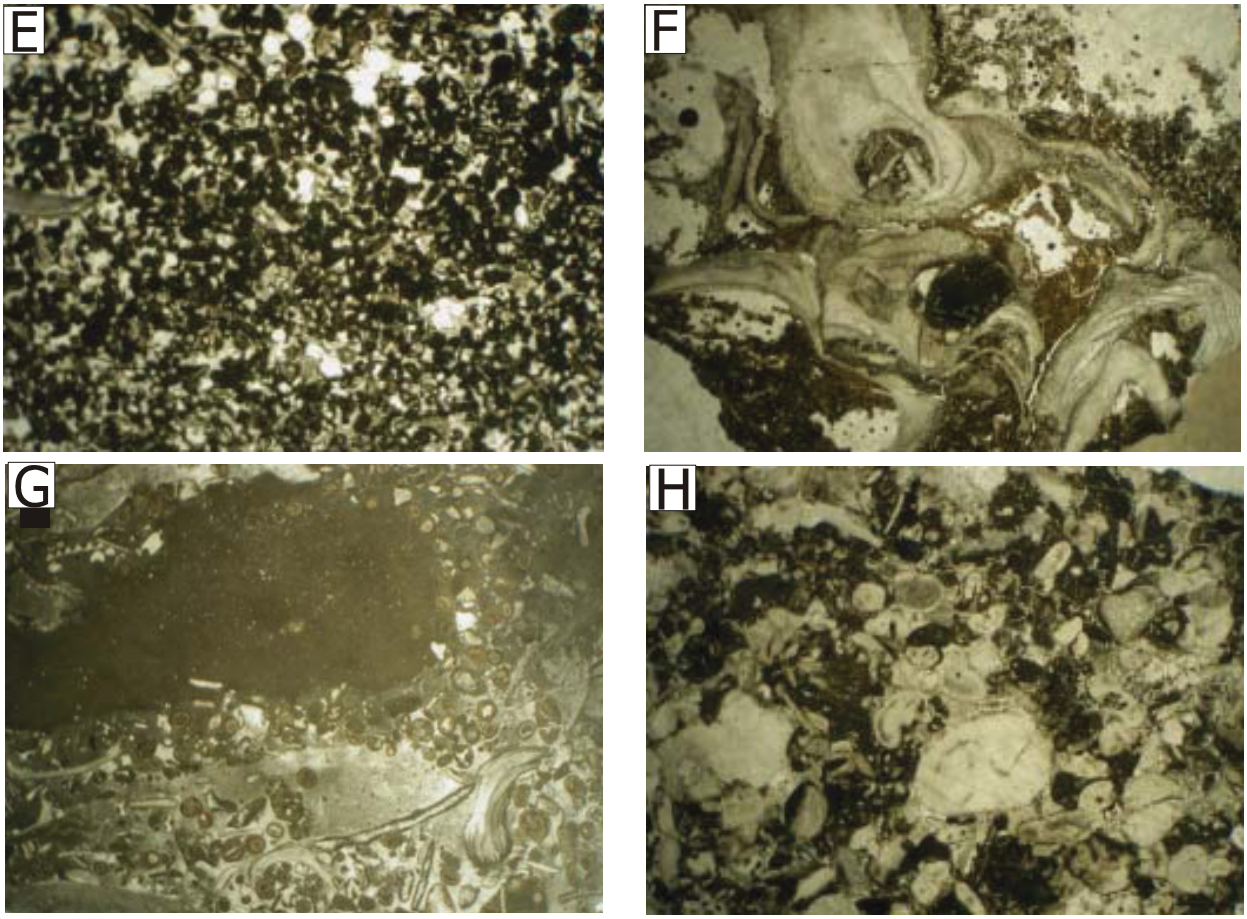

Fig. 7.4b: Characteristic microfacies of the Chichali Formation (Late Callovian to Tithonian?) of the Amir Wali Well Core III & Core IV.

(E) AS36 (1765.70 C_3): Micrite ooids facies similar as in sample AW38, but with some shells and more crinoids, partly without encrusting (width of the photo is 1.4 cm). (F) AW33 (1765.25C_3): Colony of encrusted shells building a bioherm (width of the photo is 1.4 cm). (G) AW29 (1763.45 C_3): Large wackestone clast with radiolarians as plasticlast in a grainstone consists of micrite ooides, encrusted brachiopod shells and crinoids (width of the photo is 1.4 cm). (H) AW28 (1763.30C_3): Poorly sorted crinoidal sand with micrite clasts (width of the photo is 1.4 cm).

Based on this new data of Jurassic sequence (Core II of the Ali Sahib Well and Core III & Core IV of the Amir Wali Well) from the wells, it can be correlated the sedimentary sequences as follows (Fig. 7.12).

A. The lower part of the succession in Core IV of the Amir Wali Well can be correlated with the Samana Suk Formation: Bajocian to Early Callovian. But the microfacies is different. Here in the outer shelf region deposition may start earlier as in northern region in Surghar Range (Mertmann & Ahmad, 1994). The succession evolved in a shallowing-upward manner.

B. The succession drilled in Core III of the Amir Wali Well as well as Core II in the Ali Sahib Well, can be correlated with the lower part of the Chichali Formation (Middle Callovian to Tithonian). But the microfacies correspond to the Samana Suk Formation.

The onset of deposition of shallow-water material is slightly earlier as in the north (Late Oxfordian), due to its paleogeographic position more on the outer shelf area. The *Bositra* Limestone on the base may have an age range from Callovian to Oxfordian, as indicated by the occurrence of of *Nautiloculina oolithica* below and above. Only above this *Bositra* Limestone horizon appear *Saccocoma,* which lasted until the Tithonian.

7.3 DIAGENESIS

The main diagenetic features observed in petrographic studies of Core I and Core II of the Ali Sahib Well and Core I, Core III and Core IV of the Amir Wali Well, are given below.

Glauconite is present in almost all microfacies of Core I of the Ali Sahib Well and in Core I of the Amir Wali Well. Glauconite occurs as partially filled chambers of algae and in other carbonate grains (ooids, bioclasts). Some glauconite is also present. Textural evidence suggests that the glaucnite formed during early diagenesis. The calcite and dolomite cements are present in varying amounts in all five cores. Calcite appears to have been formed during shallow burial. Pyrite as well as hematite also occur. Pyrite occurs as framboids and was formed due to sulphate reducing bacteria. The formation of hematite suggests that it was precipitated due to halmyrolysis (Krauskopf, 1982) as well as due to later diagenetic processes involving circulation of oxygenated waters. Dolomite is also secondary in origin and may have formed due to magnesium rich solutions during diagenesis.

The formation of dolomite has been discussed by various authors. Adams & Rhodes (1960), proposed a seepage reflux model for dolomite association with evaporation. According to them this model favours a high Mg^{2+}/Ca^{2+} ratio and Mg^{2+} rich hypersaline fluids, permeating underlying carbonate sediments. They proposed that the generation of dolomitizing fluids through evaporation of water or tidal flat pore water.

Dolomitization is explained as being formed by hypersaline brines derive from intense evaporation in sabkhas. Dolomite replaces preexisting metastable carbonate sediment. Dolomitizing solution is brine with high Mg/Ca ratio resulting from removal through precipitation of aragonite, gypsum or anhydrite (Ambers & Petzold, 1996).

Flügel (2004) suggested that the dolomite may form in burial process. He proposed that by continuation compactional dewatering of basinal mud rocks and expulsing of Mg^{++} rich fluids from pore water during the transformation of clay minerals (smectite to illite).

Meister *et al.* (2007, 2008), argued that the formation of dolomite may be fixed to certain hot spot of microbial activity, such as the sulphate methane interface (SMI). A maximum alkalinity and minima in dissolved Mg^{+2} and Ca^{+2} concentrations coincident with the SMI indicate that alkalinity production by microbial degradation of organic matter is the driving force for dolomite precipitation. They further described that the temperatures of the formation of dolomite was lower than the present sea water temperatures. According to them, dolomite commonly forms at shallow depths (uppermost 30 m below the sea floor of the sedimentary column) within the sedimentary sequence.

Interpreting the formation of dolomite in these sections, the arguments of Meister *et al* (2007, 2008), and Flügel (2004), can be supported, as there are glauconite as well as pyrite in the sediments, because these two minerals could not form or are difficult to form in hypersaline or in intensive evaporation.

Some intergrainular porosity in Core I of the Ali Sahib Well and in Core I of the Amir Wali Well is still open. Dissolution (secondary) porosity is also a dominant feature in different microfacies of cores of the Ali Sahib and Amir Wali wells, which indicates the sediments were not in equilibrium with the pore water. Some fractures and stylolites have also been observed which indicate that the sediments have gone under stress and compaction.

7.4 CONCLUSIONS

- During the deposition of the sediments of Core I of the Ali Sahib Well, the sea level was more or less stable and deposition occurred in a shallow marine environment.
- The succession of Core I of the Amir Wali Well indicates that sedimentation took place in deeper region as documented by the presence of shallow-marine bryzoa with well preserved crinoids. A shallow upward cycle was found.
- The sediments of the Samana Suk Formation and the Chichali Formation (Core II of the Ali Sahib Well and Core III & IV of the Amir Wali Well) were deposited in an outer, deeper shelf region of a carbonate ramp setting as documented by the occurrence of shallow-marine carbonate clasts and deep water organisms mixed together.
- Fossils dating prove an age of Late Callovian to Early Tithonian for the lower part of the Chichali Formation.
- The lithology of the lower part of the Chichali Formation comprised mainly of carbonates and corresponds to the Samana Suk Formation to the north.
- The occurrence of *Bositra* Limestone on the base of the Samana Suk Formation proves a late Middle Jurassic age, most likely of Callovian age. *Nautiloculina oolithica* below proves a younger age than Bathonian.
- The intercalated *Bositra* Limestone may have an age of Callovian and may be correlated with the Middle Callovian transgression in the Surghar Range.
- The age of the sequence drilled in Core II of the Ali Sahib Well and Core III of the Amir Wali Well is Middle Callovian to Tithonian (of the Chichali Formation), but its microfacies resemble to the Samana Suk Formation of Middle Jurassic.
- The microfacies of the lower section of Core IV of the Amir Wali Well do not resemble with the microfacies of the Samana Suk Formation, but its age is exactly the same as of the Samana Suk Formation (Bathovian to Callovian).
- Due to scarcity of available material of the wells a more precise correlation is impossible. Therefore a lot of questions, especially concerning the correlation of the formations, remains open and need further investigation.

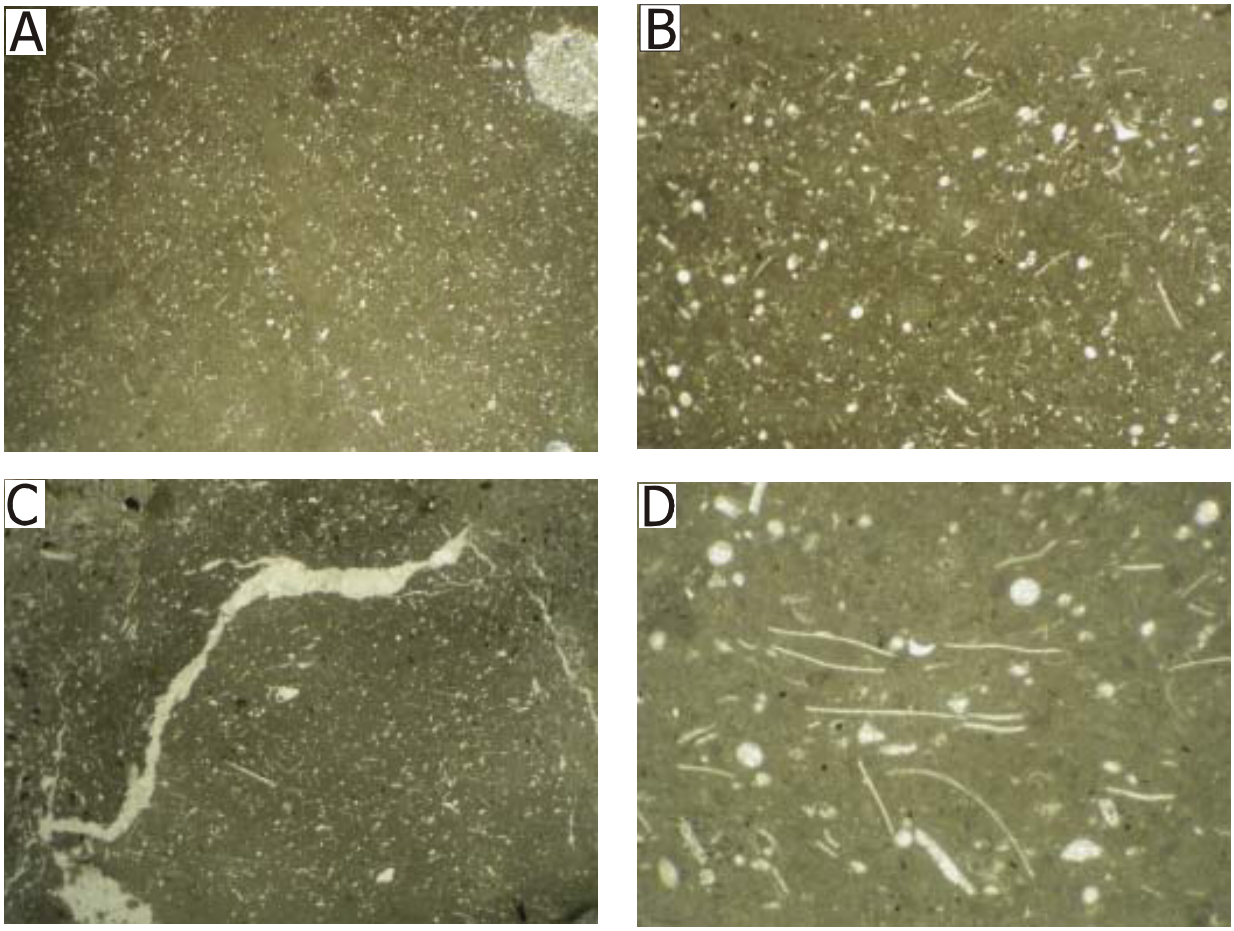

Fig. 7.5: Hemipelagic *Bositra*-Limestone (Callovian) intercalations in the upper part of the Amir Wali Well Core IV.

All figures show a radiolarian and *Bositra*-rich filament limestone as atypical in the Middle Jurassic of the Tethyan realm. (A) AW44 (1856.80C_4): width of the photo is 1.4 cm. (B) enlargement of A (width of the photo is 0.25 cm). (C) AW42 (1855.25 C_4): width of the photo is 1.4 cm. (D) Enlargement of C (width of the photo is 0.25 cm).

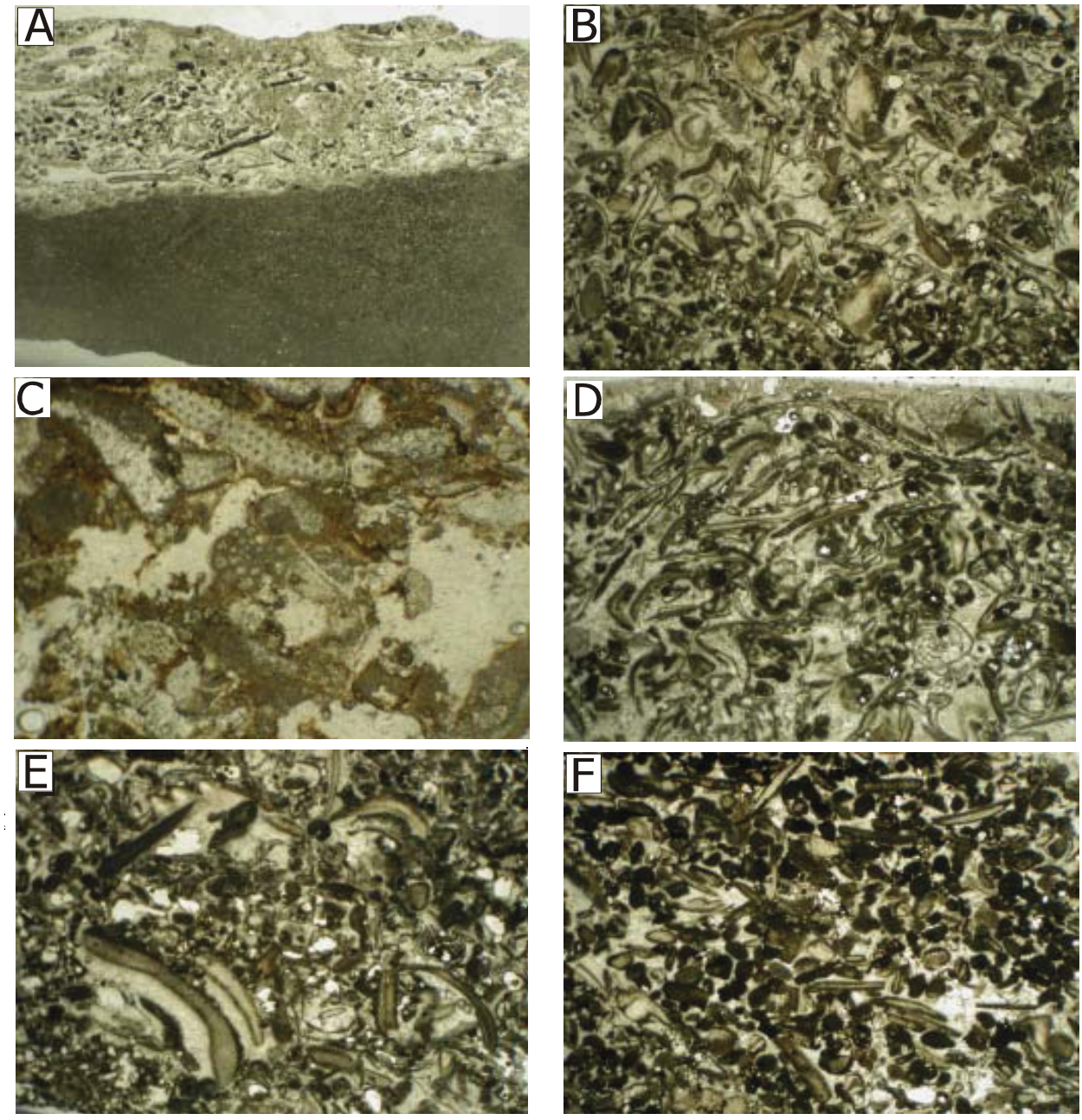

Fig. 7.6: Characteristic microfacies from the Samana Suk Formation (Middle Jurassic) of the Amir Wali Well Core IV (lower part).

(A) AW54 (1861.05C_4): Allodapic limestone on top of a radiolarian wackstone. Radialarians are recrystallized (width of the photo is 1.4 cm). (B) AW51 (1859.55C_4): Grainstone with micrite clasts, shells with micrite envelopes, crinoids remnants and bryozoans.Crinoids, aggregate grains and micritic ooliths are cemented by iron oxides and sparite (width of the photo is 1.4 cm). (C) AW49 (1859.10C_4): *Nautiloculina oolithica* in the central part of the photo (width of the photo is 1.4 cm). (D) AW48 (1858.85C_4): Grainstone enriched in shells together with micrite clasts. All shells with micrite envelope, partly with borings (width of the photo is 1.4 cm). (E) AW47 (1857.90C_4): Beside the shells, crinoids and micrite clasts, some quartz grains can be seen (width of the photo is 1.4 cm). (F) AW45 (1857.40C_4): The same microfacies as in the lower part of the succession is visible in the upper part of the succession. Well sorted grainstones are dominating indicating a still identical depositional environment as well as a similar source area of the carbonate clasts (width of the photo is 1.4 cm).

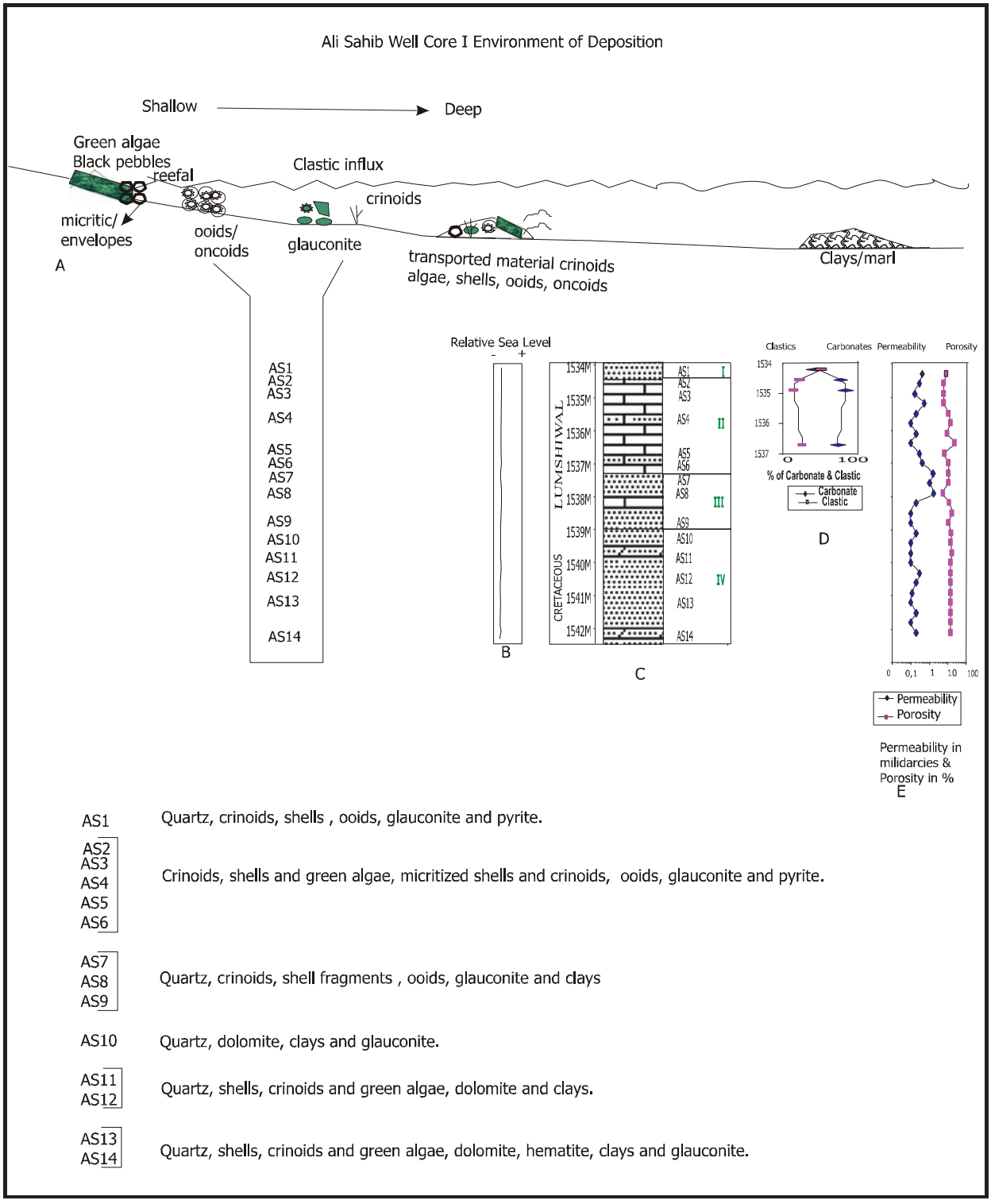

Fig. 7.7: (A) Model of environment of deposition of Core I of the Ali Sahib Well. (B) Relative sea level during the deposition of the sediments. (C) Sample and microfacies position. (D) Carbonate and clastic content. (E) Porosity and permeability variation.

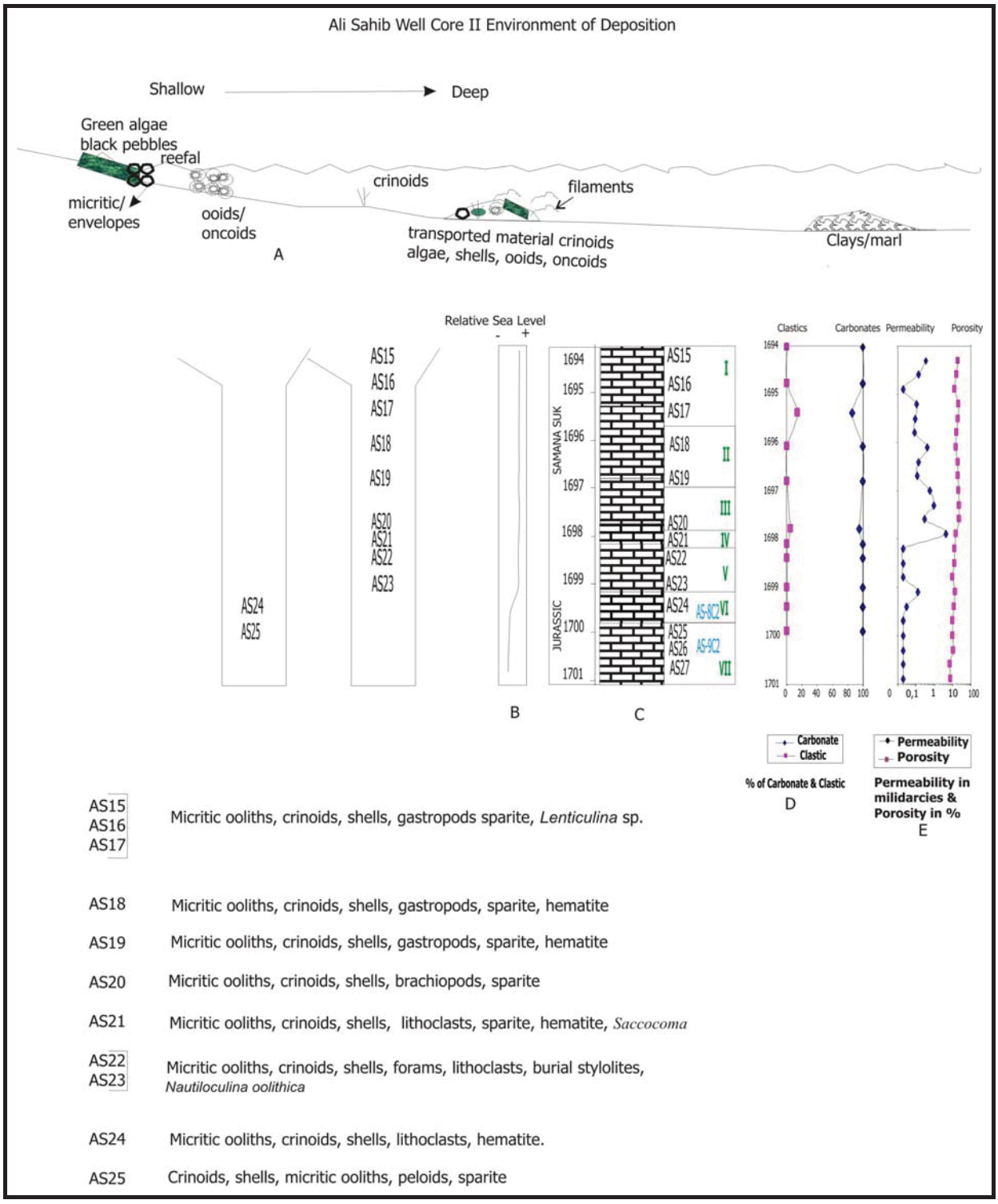

Fig. 7.8: (A) Model of environment of deposition of Core II of the Ali Sahib Well. (B) Relative sea level during the deposition of the sediments. (C) Sample and microfacies position. (D) Carbonate and clastic content. (E) Porosity and permeability variation.

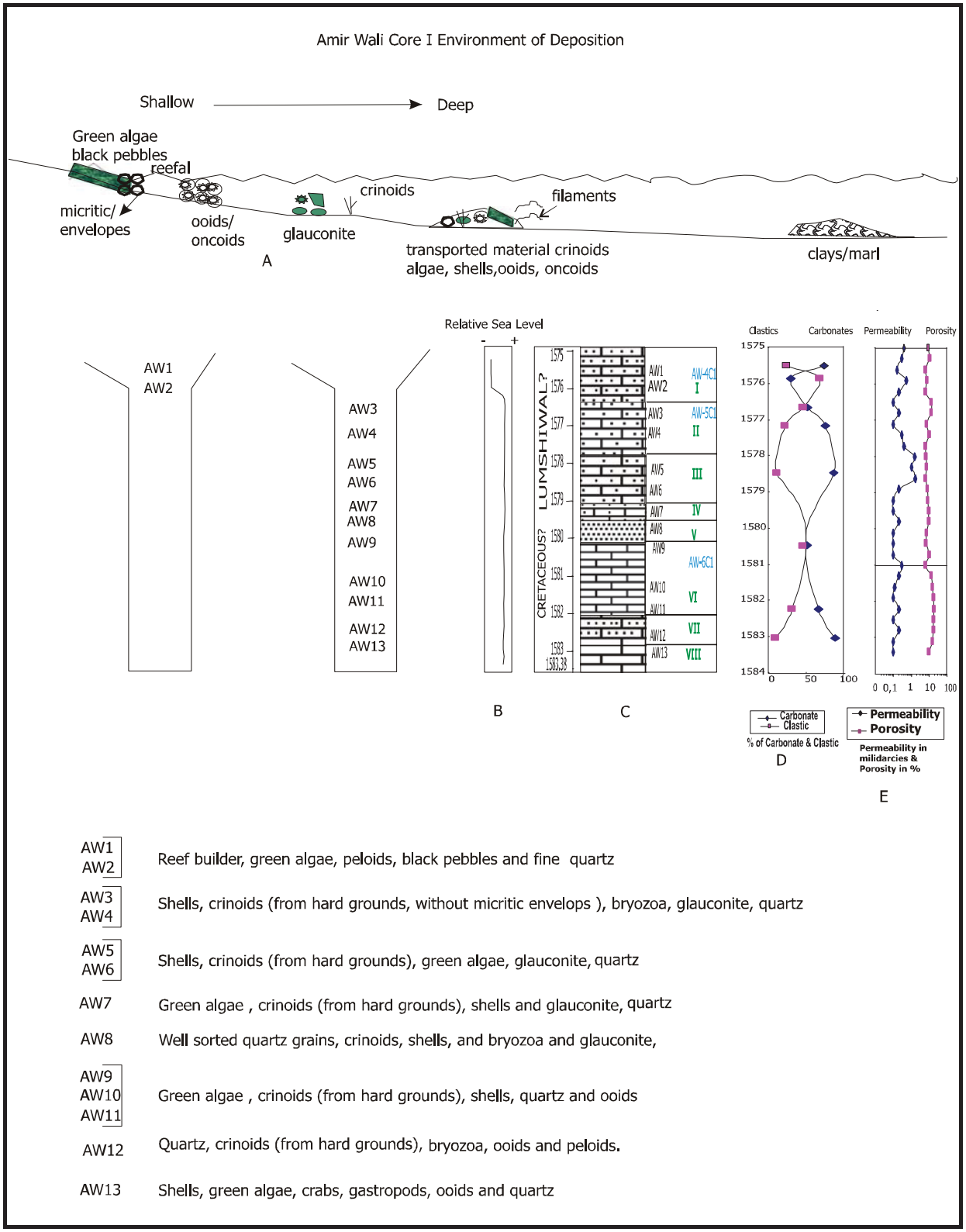

AW1 AW2	Reef builder, green algae, peloids, black pebbles and fine quartz
AW3 AW4	Shells, crinoids (from hard grounds, without micritic envelops), bryozoa, glauconite, quartz
AW5 AW6	Shells, crinoids (from hard grounds), green algae, glauconite, quartz
AW7	Green algae , crinoids (from hard grounds), shells and glauconite, quartz
AW8	Well sorted quartz grains, crinoids, shells, and bryozoa and glauconite,
AW9 AW10 AW11	Green algae , crinoids (from hard grounds), shells, quartz and ooids
AW12	Quartz, crinoids (from hard grounds), bryozoa, ooids and peloids.
AW13	Shells, green algae, crabs, gastropods, ooids and quartz

Fig. 7.9: (A) Model of environment of deposition of Core I of the Amir Walib Well. (B) Relative sea level during the deposition of the sediments. (C) Sample and microfacies position. (D) Carbonate and clastic content. (E) Porosity and permeability variation.

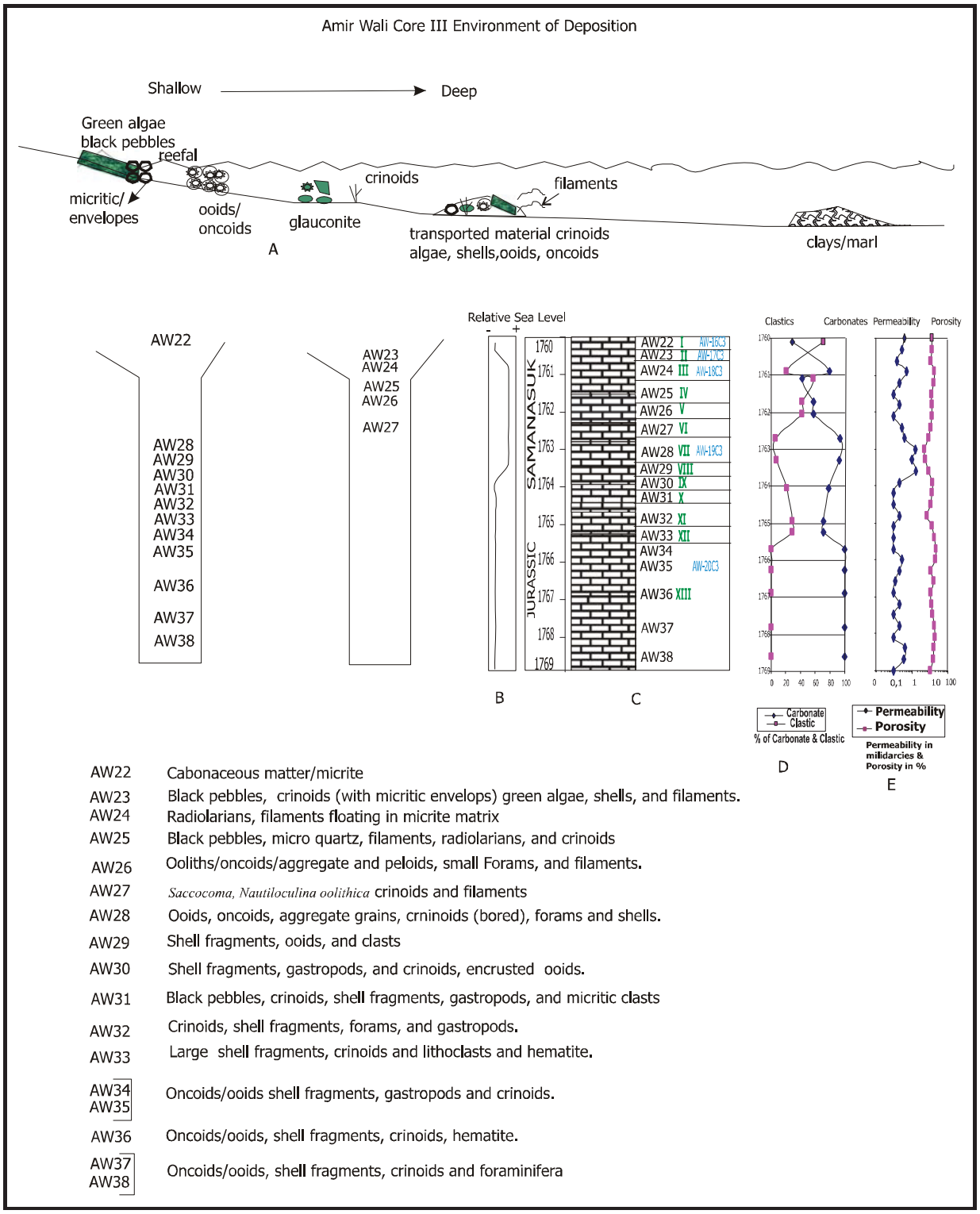

AW22	Cabonaceous matter/micrite
AW23	Black pebbles, crinoids (with micritic envelops) green algae, shells, and filaments.
AW24	Radiolarians, filaments floating in micrite matrix
AW25	Black pebbles, micro quartz, filaments, radiolarians, and crinoids
AW26	Ooliths/oncoids/aggregate and peloids, small Forams, and filaments.
AW27	*Saccocoma, Nautiloculina oolithica* crinoids and filaments
AW28	Ooids, oncoids, aggregate grains, crninoids (bored), forams and shells.
AW29	Shell fragments, ooids, and clasts
AW30	Shell fragments, gastropods, and crinoids, encrusted ooids.
AW31	Black pebbles, crinoids, shell fragments, gastropods, and micritic clasts
AW32	Crinoids, shell fragments, forams, and gastropods.
AW33	Large shell fragments, crinoids and lithoclasts and hematite.
AW34 AW35	Oncoids/ooids shell fragments, gastropods and crinoids.
AW36	Oncoids/ooids, shell fragments, crinoids, hematite.
AW37 AW38	Oncoids/ooids, shell fragments, crinoids and foraminifera

Fig. 7.10: (A) Model of environment of deposition of Core III of the Amir Wali Well. (B) Relative sea level during the deposition of the sediments. (C) Sample and microfacies position. (D) Carbonate and clastic content. (E) Porosity and permeability variation.

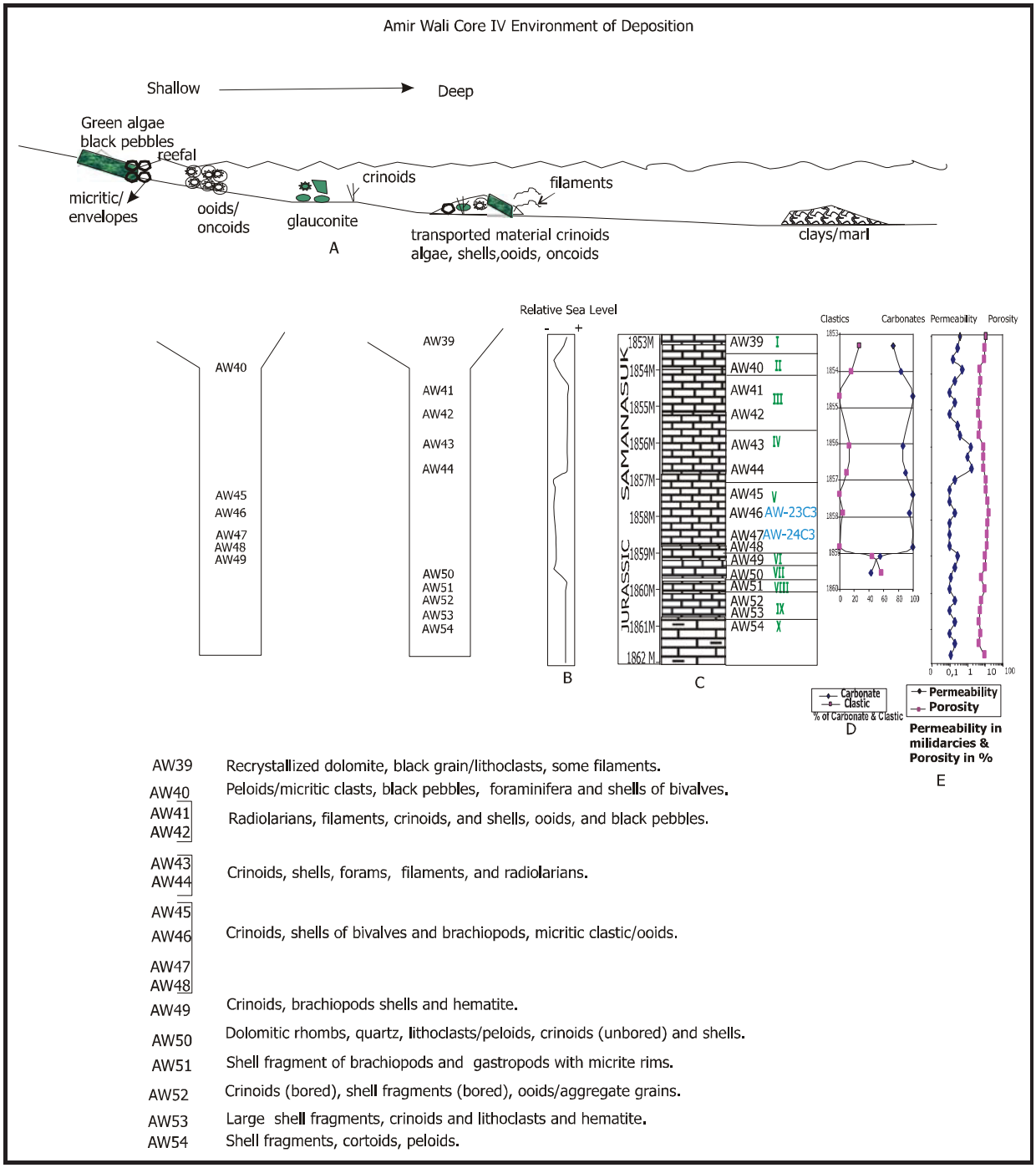

Fig. 7.11: (A) Model of environment of deposition of Core IV of the Amir Wali Well. (B) Relative sea level during the deposition of the sediments. (C) Sample and microfacies position. (D) Carbonate and clastic content. (E) Porosity and permeability variation.

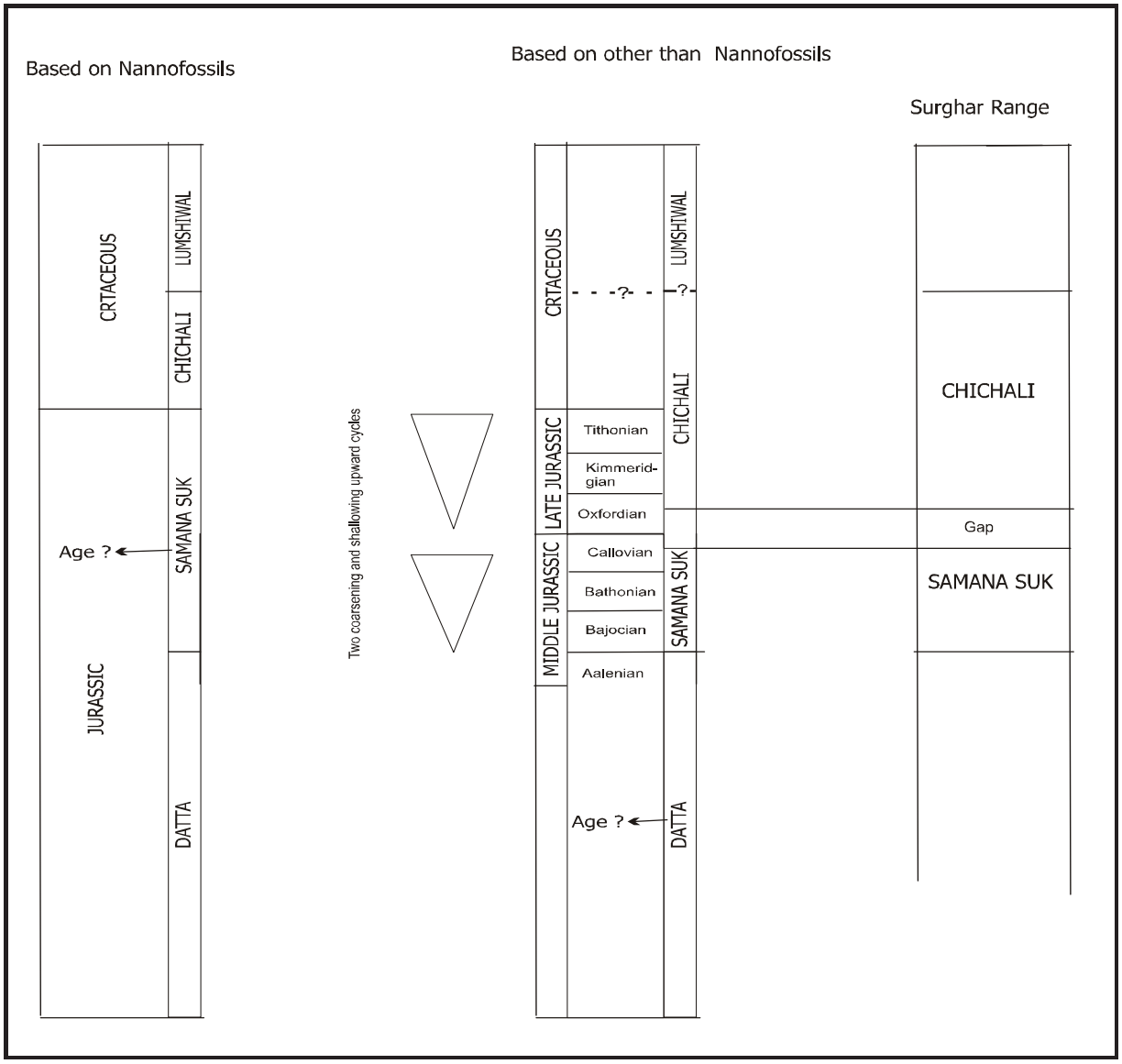

Fig. 7.12: Correlation of the Jurassic drilled sequence (Samana Suk Formation and Chichali Formation) with the Surghar Range northwest of the studied wells (Ali Sahib & Amir Wali).

8. PETROGRAPHY AND XRD ANALYSIS OF CLASTIC ROCKS

8.1 INTRODUCTION

In the present work clastic facies of the Datta Formation (Jurassic), the Samana Suk Formation (Late Jurassic) and the Lumshiwal Formation (Cretaceous) were studied to establish environment of deposition, sedimentology and diagenesis of the these sediments of the Punjab Platform. The present study is a first attempt to understand the sedimentology of the Punjab Platform especially in the Cretaceous and Jurassic age. Up to now, stratigraphically corresponding sediments were only studied in the Salt Range area and further to the north and to the northwest (Trans Indus Ranges, Kalachitta Range etc.), where these formations are exposed. The cores and sample locations in the log profile of bore holes have been described in Figs. 5.1 & 5.2.

The mineral composition determined by point counting of sandstone of the cores is given in the table 8.3a and the mineral composition calculated by ADM software package version 6.22 (Wassermann, Kempten BRD), are given in table 8.3b. When comparing the two tables, significant differences can be seen in the mineral percentages, particularly samples AW17 and AS28. One possible reason is that analysis was carried out with material from different sample lots. The two different methods were used due to the advantages each has with specific rock types, point counting (Table 8.3a) for sandstones and XRD (Table 8.3b) for fine grained siliciclastics. In describing sandstone, Table 8.3a is used, while in claystone/shale/siltstone of the cores, table 8.3b is used, because XRD is the standard method for the analysis of fine grained siliciclastic rocks.

8.2 LITHOFACIES STUDIES IN CORE III OF THE ALI SAHIB WELL

Core III (from 1730.50 to 1733 m) of the Ali Sahib Well has been cut in the Samana Suk Formation of Jurassic age. On the basis of lithology, color and mineral composition, Core III of the Ali Sahib Well has been divided into two lithofacies (cf. Fig 5.1).

Lithofacies I, quartz arenite (AS28, AS29, AS30 and AS31).

Lithofacies II, shaly siltstone (AS32).

Lithofacies I Quartz Arenite (AS28, AS29, AS30 and AS31): The color of the lithofacies is light brown to yellowish brown and transparent. It is loose and friable sandstone (Figs. 8.2a and 8.3a). Quartz grains range from 85 to 95%, opaque minerals from 1 to 2 %, while matrix and cement comprises 5 to 15 % (Table 8.3a). The grains are very fine to fine grained sand, and medium to coarse grained silt, in places medium grained sands also occur. The grains are angular to subangular (some grains subrounded) well sorted to moderately well sorted (Trask Coefficient of sorting ranges from 1.58 to 1.77, Table 8.3). They are poorly cemented, although, some well cemented areas were observed. Siderite is the main cement; however it only occurs in few places (Plate 8.1 E). Some quartz grains show replacement by siderite, the latter showing indications of fracturing (Plate 8.1 E). Clayey matrix is consisting of kaolinite and illite (Plate 8.1 F). Traces of carbonaceous material and pyrite have been identified in the thin section of sample AS31. Clay balls (Plate 8.1 A and 8.3 A) with a lot of quartz grains are also present. Etching of quartz grains can be observed in some clay balls (Plate 8.1 F).

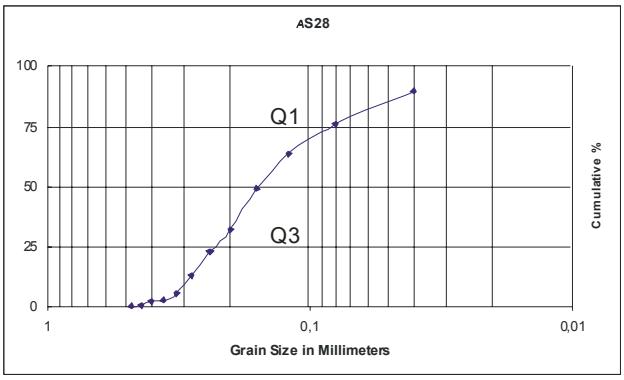

Fig. 8.1a: AS28 (sandstone) Core III of the Ali Sahib Well, grain size distribution, represented by cumulative curve. Trask Coefficient of sorting $(Q_3/Q_1)^{1/2}$ is 1.73.

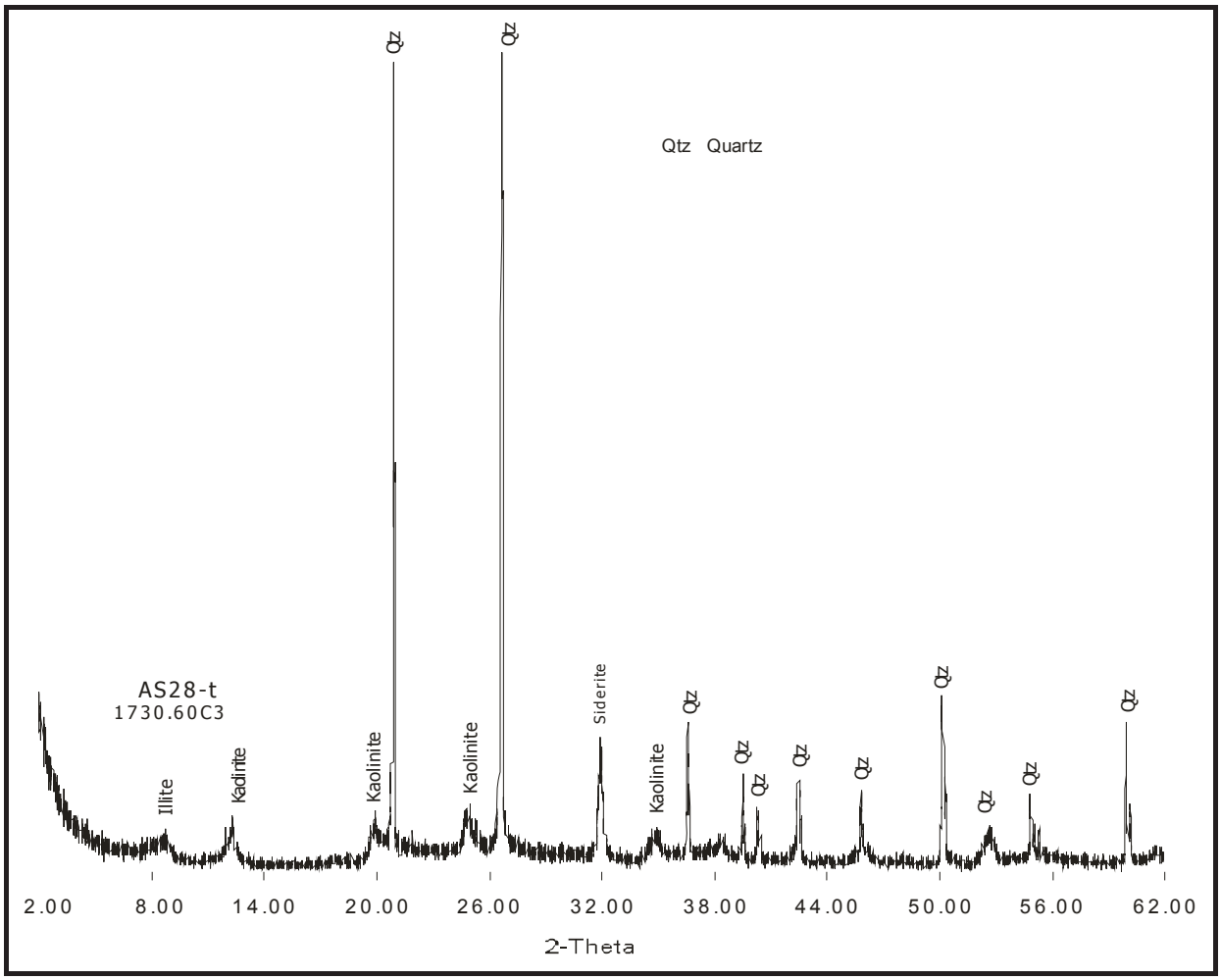

Fig. 8.1b: AS28 (sandstone) Core III of the Ali Sahib Well, X-ray diffractogram (oriented mount, untreated), showing that quartz is dominant, siderite, kaolinite and illite are present.

Fig. 8.2a: AS 29 of Core III of the Ali Sahib Well at 1731.0 m, loose sand to friable sandstone.

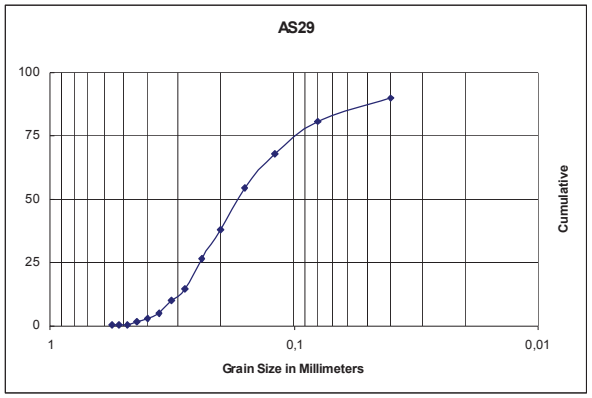

Fig. 8.2b: AS29 Core III of the Ali Sahib Well, grain size distribution, represented by cumulative curve. Trask Coefficient of sorting $(Q_3/Q_1)^{1/2}$ is 1.58.

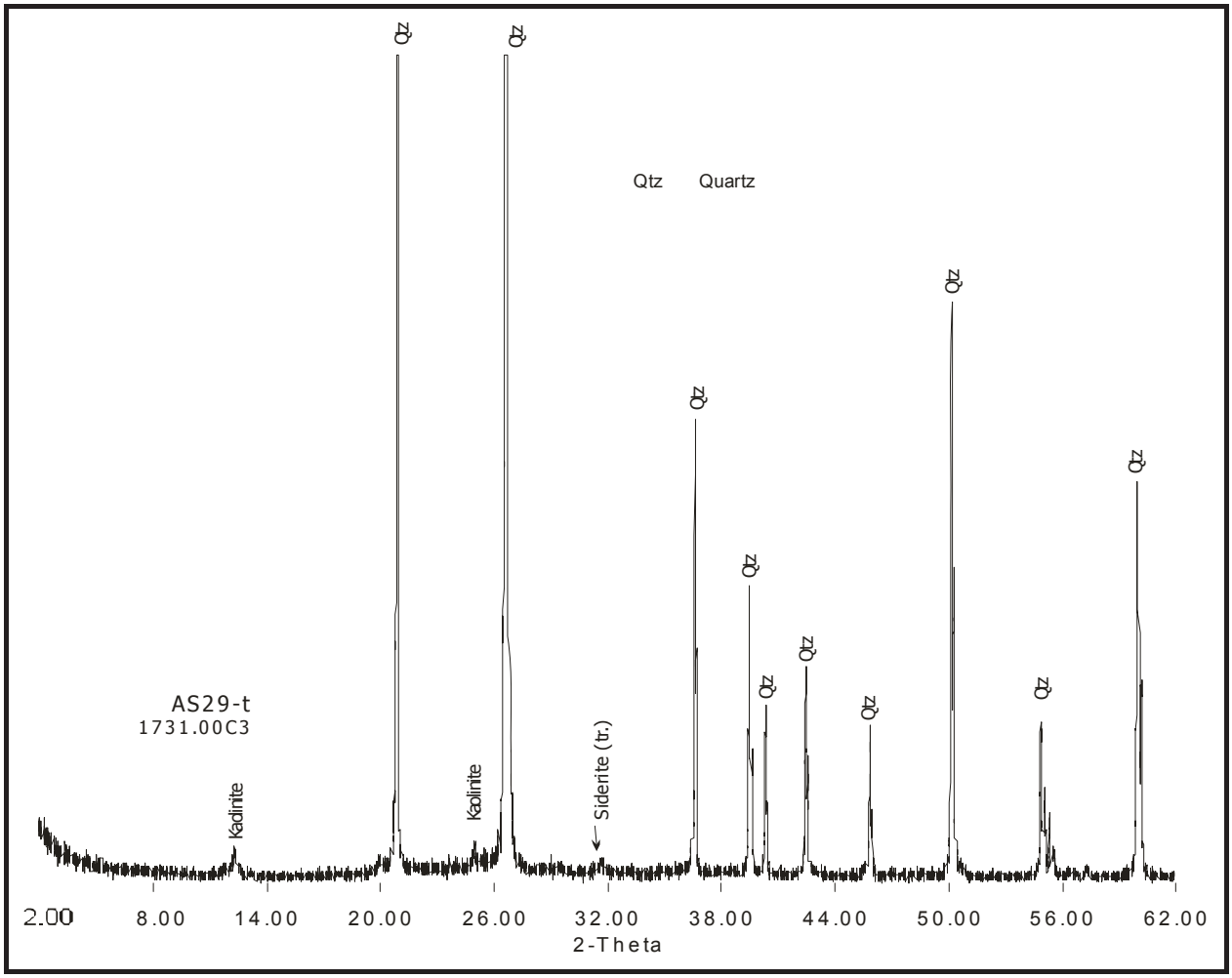

Fig. 8.2c: AS29 (friable sandstone) of Core III of the Ali Sahib Well, X-ray diffractogram (oriented mount, untreated), showing that quartz (major), kaolinite (minor) and traces of siderite are present.

Fig. 8.3a: AS 30 of Core III of the Ali Sahib Well at 1731.60 m, loose sand to friable sandstone.

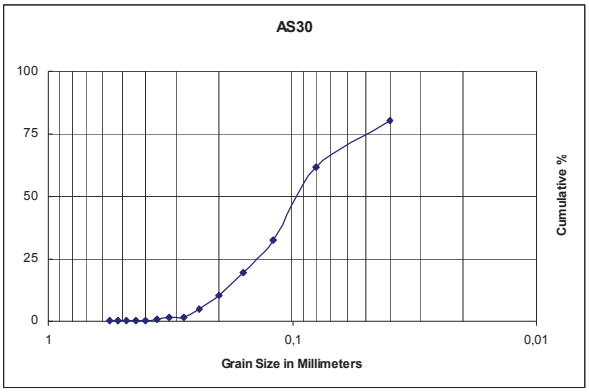

Fig. 8.3b:AS30 of Core III of the Ali Sahib Well, grain size distribution, represented by cumulative curve, Trask Coefficient of sorting $(Q3/Q1)^{1/2}$ is 1.73.

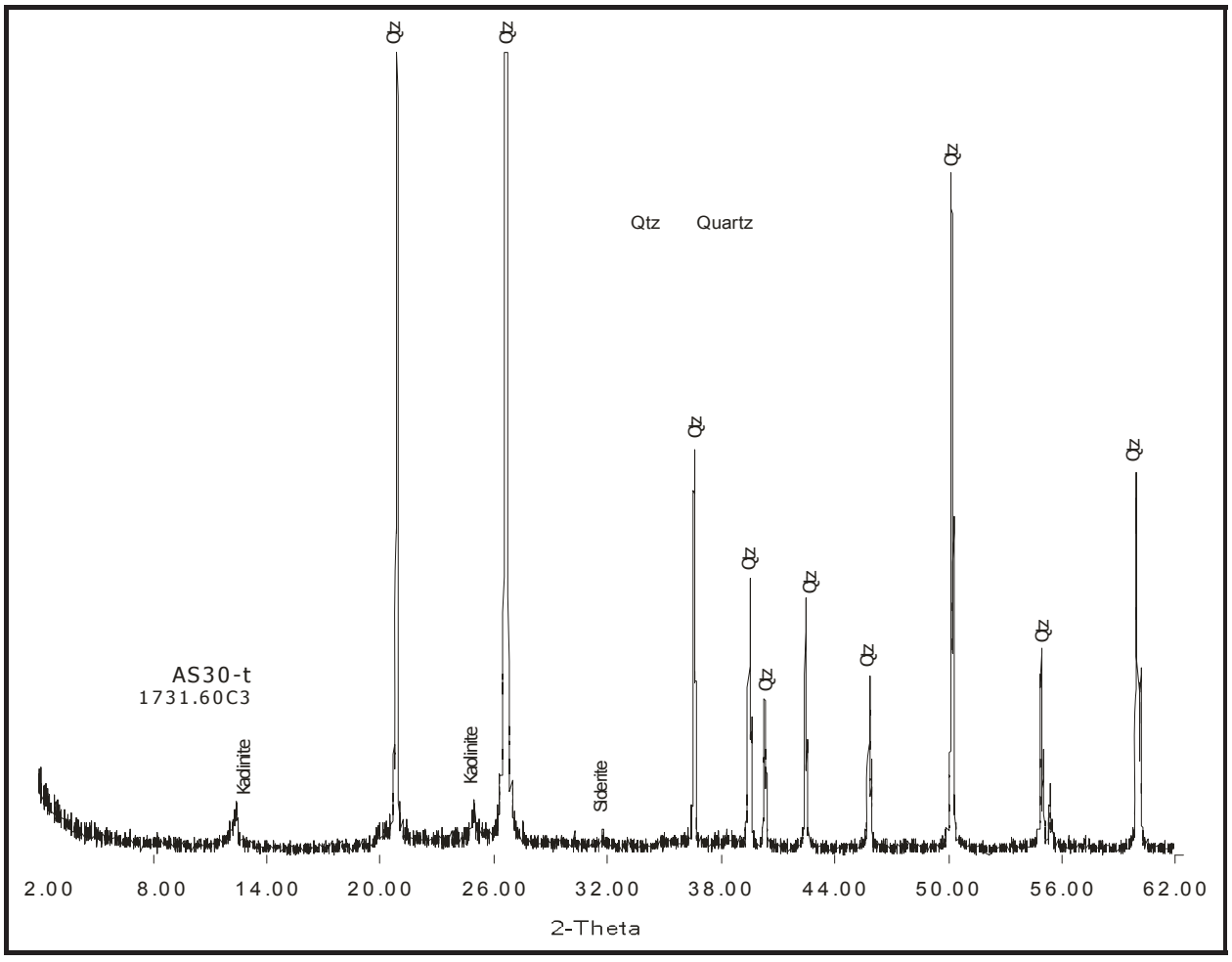

Fig. 8.3c: AS30 (friable sandstone) Core III of the Ali Sahib Well, X-ray diffractogram (oriented mount, untreated), showing that quartz is dominant, kaolinite is minor and siderite is in traces.

Fig. 8.4a: AS31 of Core III of the Ali Sahib Well at 1732.0 m, comparatively cemented sandstone

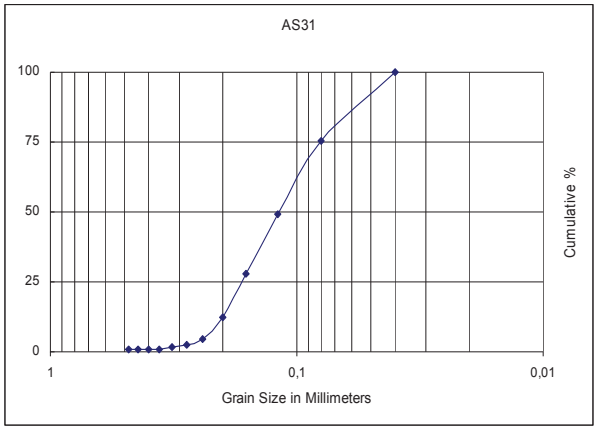

Fig. 8.4b: AS31 of Core III of the Ali Sahib Well, grain size distribution and sorting, represented by cumulati- ve curve. Trask Coefficient of sorting $(Q3/Q1)^{1/2}$ is 1.77.

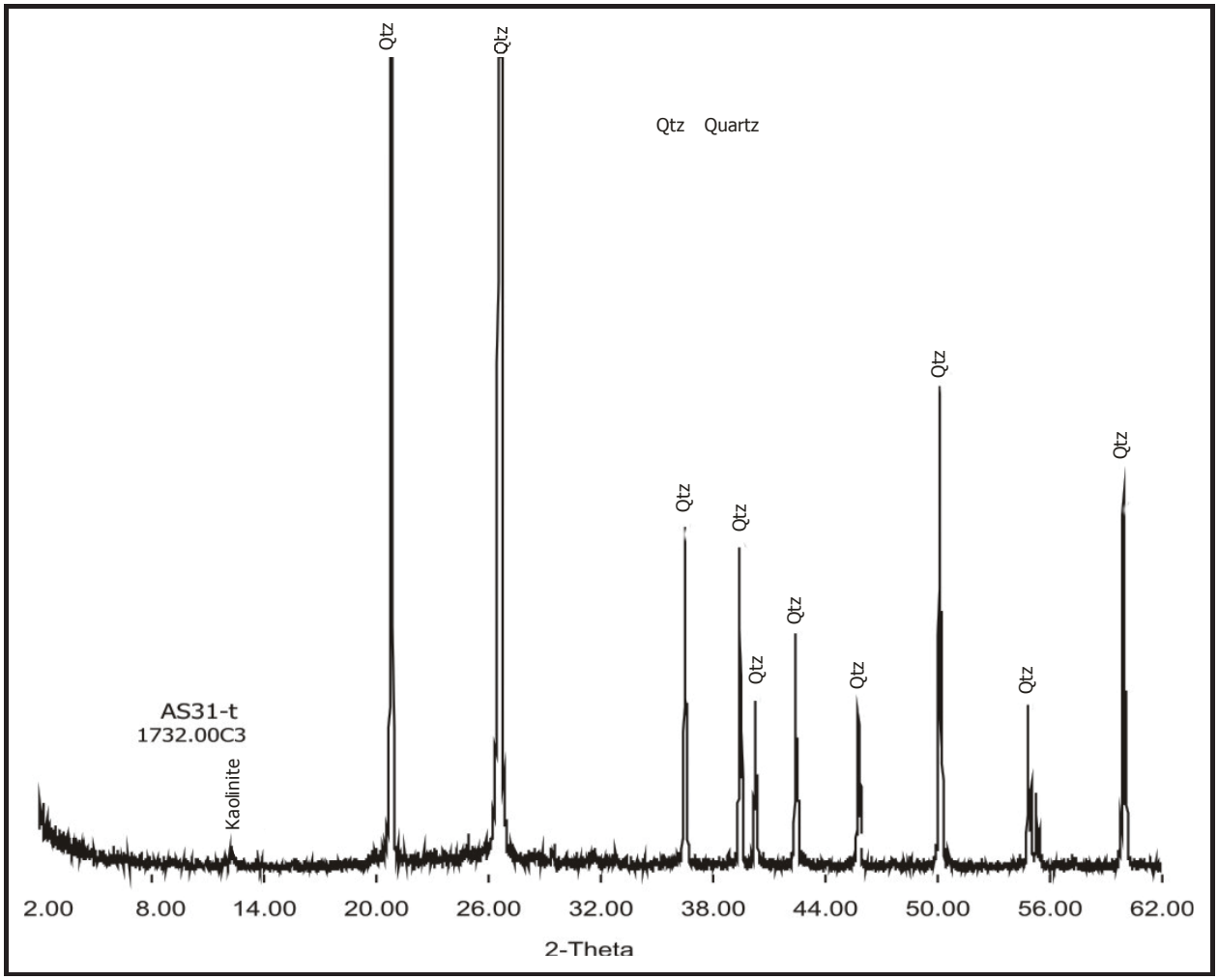

Fig. 8.4c: AS31 (sandstone) of Core III of the Ali Sahib Well, X-ray diffractogram (oriented mount, untreated), showing that quartz is dominant and traces of kaolinite are present.

Lithofacies II Shaly Siltstone (AS32): Greenish grey moderately indurated, blocky, sublaminated and subfissile. The mineralogy, as evidenced by XRD analysis, shows quartz as dominant mineral with subordinate kaolinite (XRD is given in Fig. 8.5). Traces of illite are also indicated in the diffractogram.

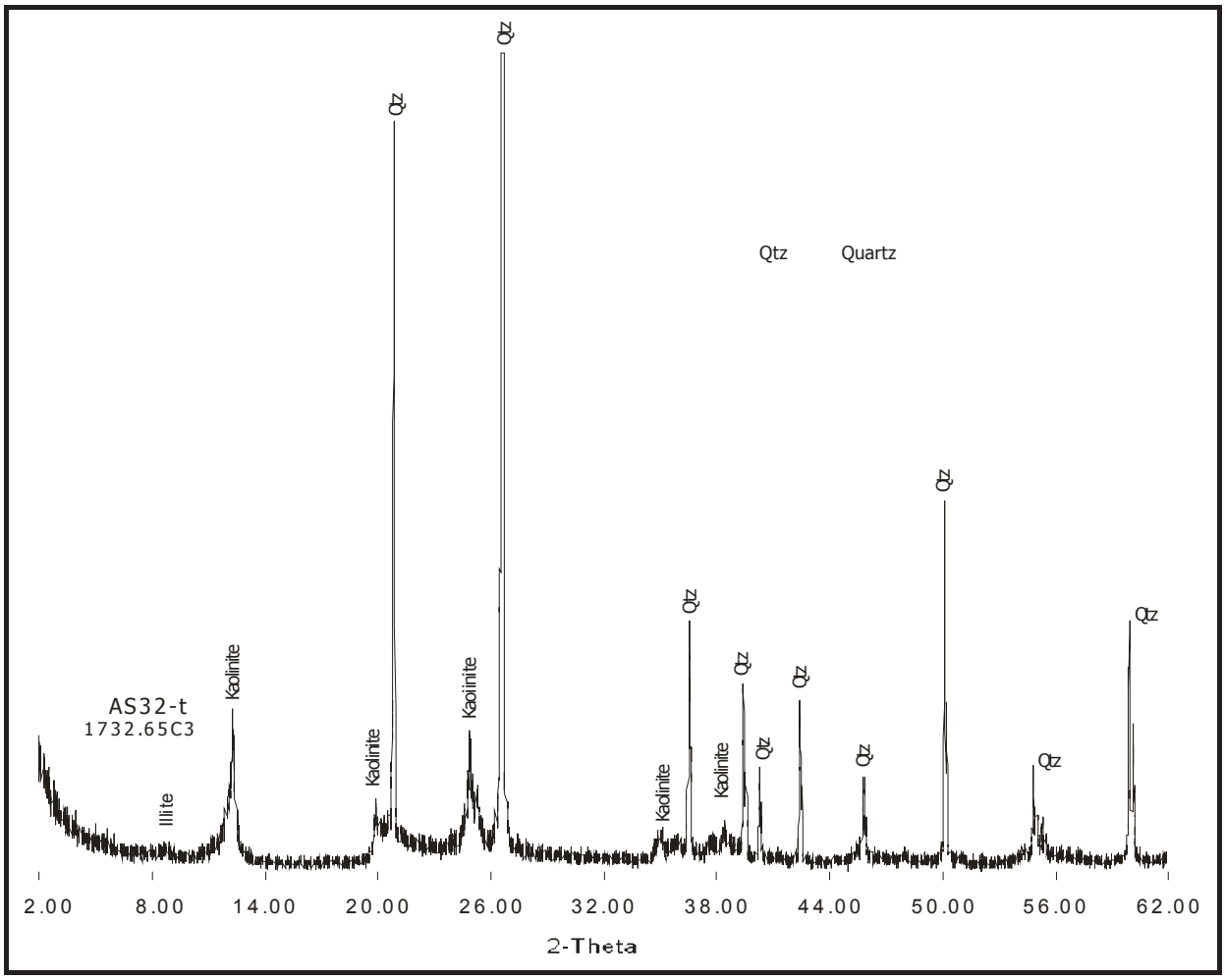

Fig. 8.5: AS32 (shaly siltstone) of Core III of the Ali Sahib Well, X-ray diffractogram (oriented mount, untreated), showing that quartz is dominant and kaolinite present as subordinate. Traces of illite are indicated by very weak reflection at about 10A° (~ 8.8° 2θ).

8.2.1 DIAGENESIS AND ENVIRONMENT OF DEPOSITION OF CORE III OF THE ALI SAHIB WELL

The large number of quartz grains that are loose in all four samples of friable sandstones (samples AS28, AS29, AS30 and AS31), suggests that there were no significant solutions, chemical diagenesis, or precipitation of cements in these samples to ensue lithification. Friability and looseness of the samples also indicates that there

was equilibrium between connate water and the sediments, and there were no further reactions between sediments and the pore fluids. At the base of the lithofacies (sample AS31), some lithification was observed (Fig. 8.4a). It may be assumed that this lithification is due to the minor expulsion of fluids from underlying shale of lithofacies II (sample AS32).

The occurrence of siderite cement in samples AS28 (Plate 8.1E), AS29 and AS30 can be explained in the light of the views of Benito *et al.* (2005) and De la Horra *et al.* (2008). According to these authors the formation of siderite occurs in the reducing organic-rich marsh and swamp environment of flood plains and deltas. Its formation is an early diagenetic phenomenon. Siderite precipitation requires very low pO_2, very high pCO_2, a slightly acid to near neutral pH, and high concentrations of dissolved Fe^{2+} (Siderite is precipitated where the carbonate activity is high and the sulphide activity is low). The latter is rarely attained in marine sediment pore waters because of the abundant dissolved sulphate. Siderite is thus more common in non-marine sediments (Tucker, 1992). In marine environments the bacterial decomposition of organic matter leads to the formation of sulphide, which reacts with the Fe^{2+} ions to form pyrite (Tucker, 1992).

It is concluded that the precipitation of siderite in sediments from samples AS28, AS29 and AS30 had occurred in fluvio-deltaic organic-rich reducing environment. Below these sandstone samples of the Samana Suk Formation (of Jurassic age) of lithofacies I of Core III of the Ali Sahib Well, samples are almost free of siderite (sandstone sample AS31 and a shale sample AS32). This indicates that either, there was no organic material present or that the conditions required for the deposition of siderite were lacking during the deposition of sediments comprising samples AS31 and AS32. The occurrence of a plant remnant in sample AS31 shows that organic material was present, but the other conditions e.g., pH or high concentrations of dissolved Fe^{2+} etc. were not sufficient for the precipitation of siderite. Presence of little pyrite in sample AS31 (observed in thin section) indicates that there were sufficient sulphide ions which reacted with Fe^{2+}. Fracturing in siderite and in some of the quartz grains (Plate 8.1 E) indicates some degree of compaction.

Kaolinite occurs as matrix (Plate 8.1 F) and isolated cement in most of the core samples (from AS28-AS31). There are some clay balls containing a large number of quartz grains (Plate 8.1 A to 8.3 B). In clay balls kaolinite occurs as matrix. Clay balls might be formed by rapid redeposition from sporadic flood deposits.

Occurrence of clay balls, pyrite and some carbonaceous matter (plant), clearly suggests that the environment of deposition was fluvio-deltaic. Very little cementation, no remnants of marine fossils and absence of glauconite are all supporting the idea that deposition occurred in fluvio-deltaic environment. Presence of siderite in sample AS28 to AS30 also further emphasizes that deposition did not occur in a marine environment. The presence of pyrite, siderite and some carbonaceous matter indicates that the environment was some what reducing instead of well oxidized.

It is revealed in photographs (Plates 8.1 to 8.4) of different samples of Core III of the Ali Sahib Well, that the quartz grains are seldom cemented by quartz. The rearrangement of grains would be a cause of porosity reduction. Most of them show point contacts or isolated grains (microphotographs) indicating that porosity reduction by physical compaction is not significant.

To summarize the discussion above, it is suggested that the environment of deposition of Core III was fluvio-deltaic, with reducing conditions. The large quantity of quartz and the angularity of the grains suggest that the provenance consists of preexisting sedimentary quartz-rich rock and quartz grains that underwent only minor transport prior to deposition.

8.3 LITHOFACIES STUDIES IN CORE IV OF THE ALI SAHIB WELL

Core IV (from 1886 to 1893.45 m) of the Ali Sahib Well has been cut from the Datta Formation of Jurassic age. On the basis of lithology, color and mineral composition Core IV of the Ali Sahib Well has been subdivided into IV lithofacies (cf. Fig. 5.1).

Fig. 8.6a: AS33 Core IV of Ali Sahib Well at 1886.40 m, loose sand to friable sandstone.

Fig. 8.6b: AS33 of Core IV of the Ali Sahib Well, grain size distribution represented by cumulative curve. Trask Coefficient of sorting $(Q3/Q1)^{1/2}$ is 1.15.

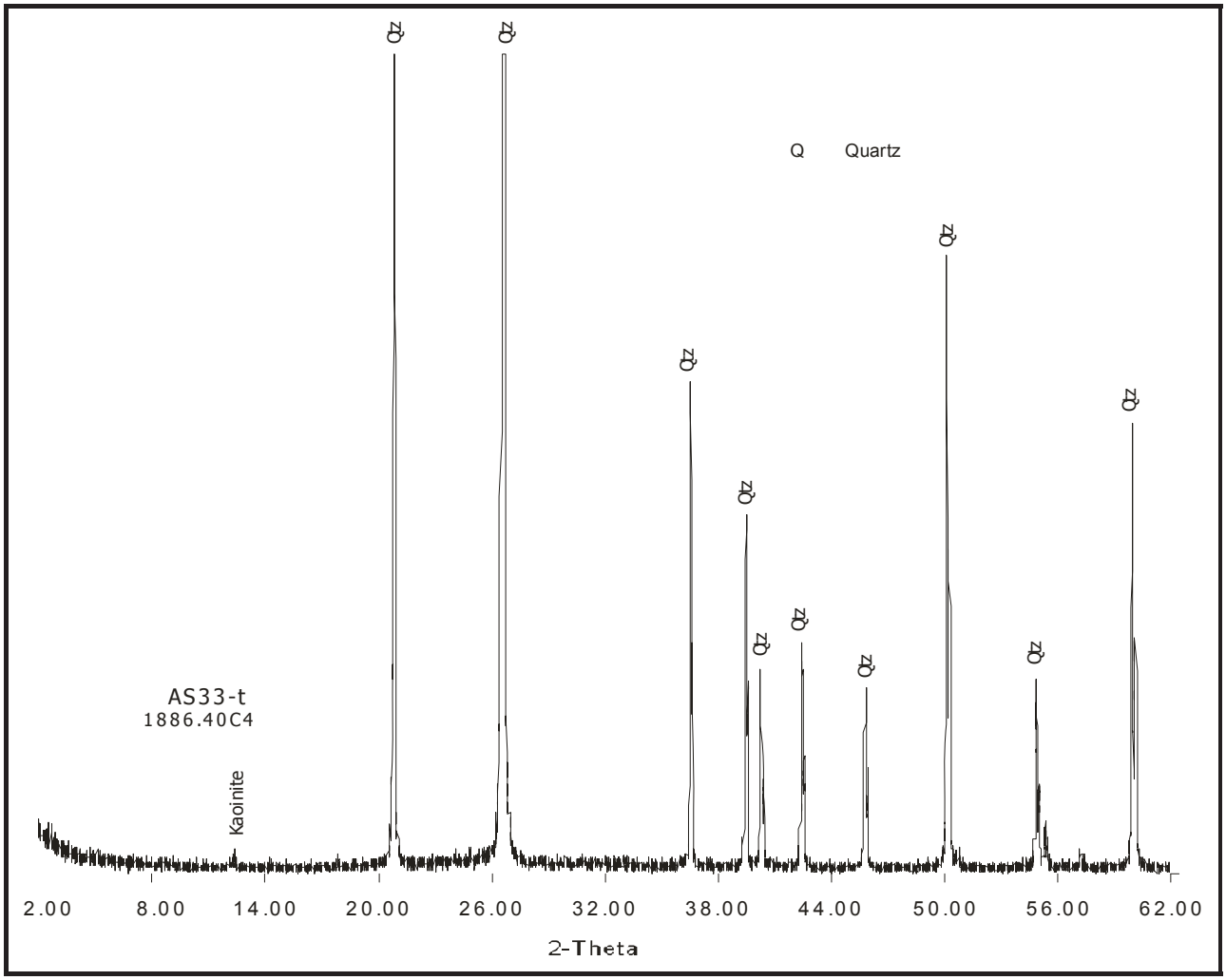

Fig. 8.6c: AS33 (friable sandstone) of Core IV of the Ali Sahib Well, X-ray diffractogram (oriented mount, untreated), showing that quartz is dominant and traces of kaolinite.

Lithofacies I, quartz arenite (AS33).
Lithofacies II, light grey to greenish grey claystone (AS34 and AS35).
Lithofacies III, partly greenish grey and partly brick red claystone (AS36).
Lthofacies IV, brick red to dirty brown claystone (from AS37 to AS41).

Lithofacies I Quartz Arenite (AS33): Yellowish brown, transparent to translucent. It is poorly cemented and friable sandstone. Quartz grains comprise more than 99 % (Table 8.3a). The quartz grains are loose and their appearance is quartzose and sugary (see picture below), more than 95% is medium to coarse-grained sand and less than 5 % fine-grained sand.

Most of the grains are angular to subangular; some subrounded grains were also observed (Plate 8.5). The Trask Coefficient of sorting is 1.15, suggesting very well sorted to well sorted. A few crystals of pyrite (Plate 8.5A & 8.5D) and one grain of tourmaline were observed.

Lithofacies II Claystone (AS34 and AS35): Light grey, greenish grey and yellowish brown, soft to moderately firm, partly sticky and hydrophilic. The mineralogy shown by XRD (Fig. 8.7) proves that kaolinite is dominant. Kaolinite and siderite are more than 90 %. The subordinate mineral is anatase with ~2 % (Table 8.3b). The absence of detectable quantities of quartz is noteworthy. A weak reflection with a d-value of 3.25 Å might indicate the presence of rutile (110 reflection). K-feldspar (microcline), which has a strongest reflection with similar d-value, is less probable, because this kaolinite-rich and quartz-free claystone indicates very intensive chemical weathering conditions.

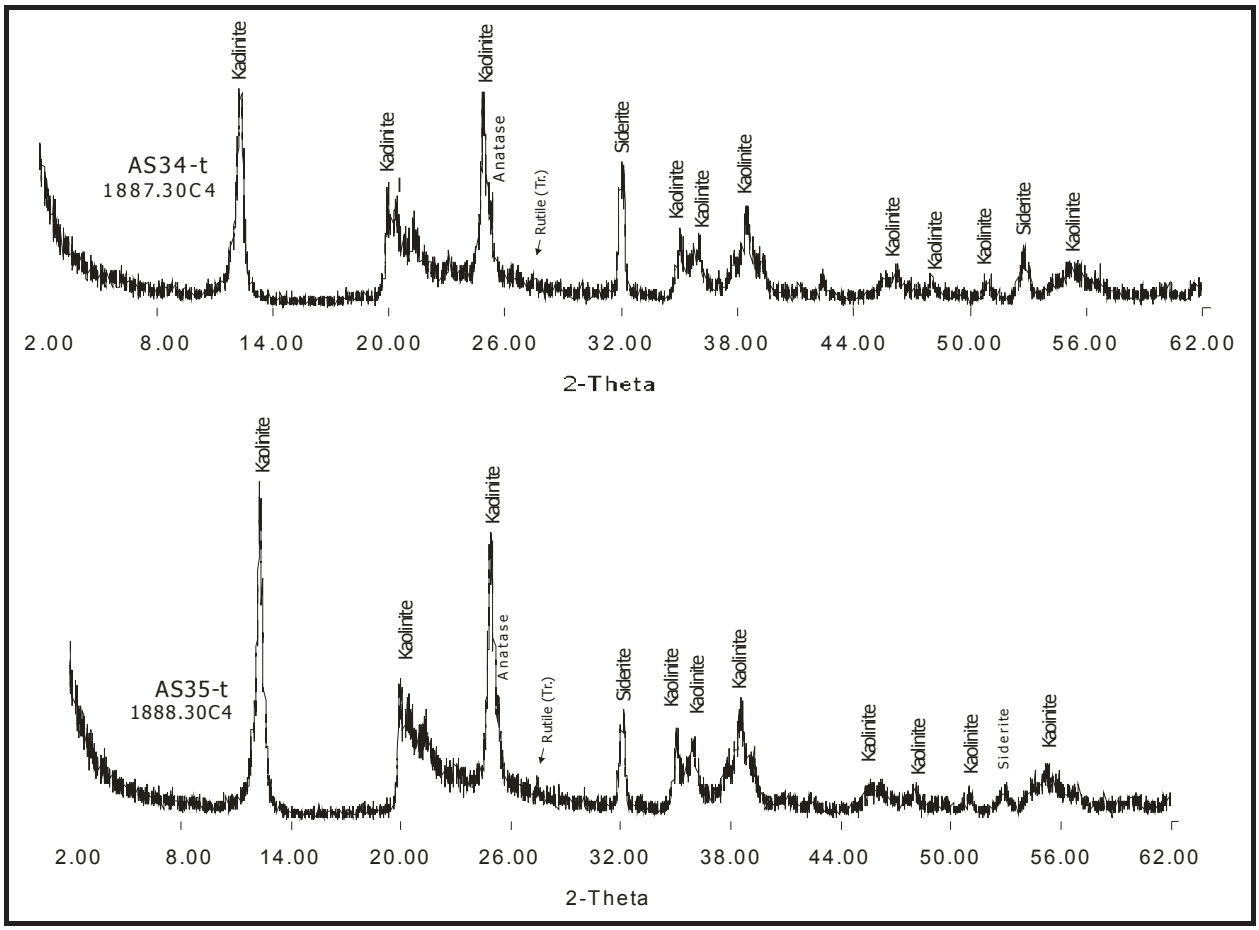

Fig. 8.7: AS34 (above) and AS35 (below) of greenish grey claystone of Core IV of the Ali Sahib Well, X-ray diffractogram (oriented mount, untreated), showing that kaolinite, siderite, anatase (AS35) are present. Quartz does not occur with detectable proportions. Traces of rutile might be present.

Lithofacies III Claystone (AS36): Partly light grey and greenish grey and partly brick red to dirty brown, soft to moderately firm, partly sticky and hydrophilic. The mineralogy is characterized (again) by dominance of kaolinite and the absence of quartz (XRD Fig. 8.8). Traces to minor quantities of siderite, hematite, and muscovite/ illite also occur. A 3.25 Å, reflection indicates traces of rutile (cf. sample AS35).

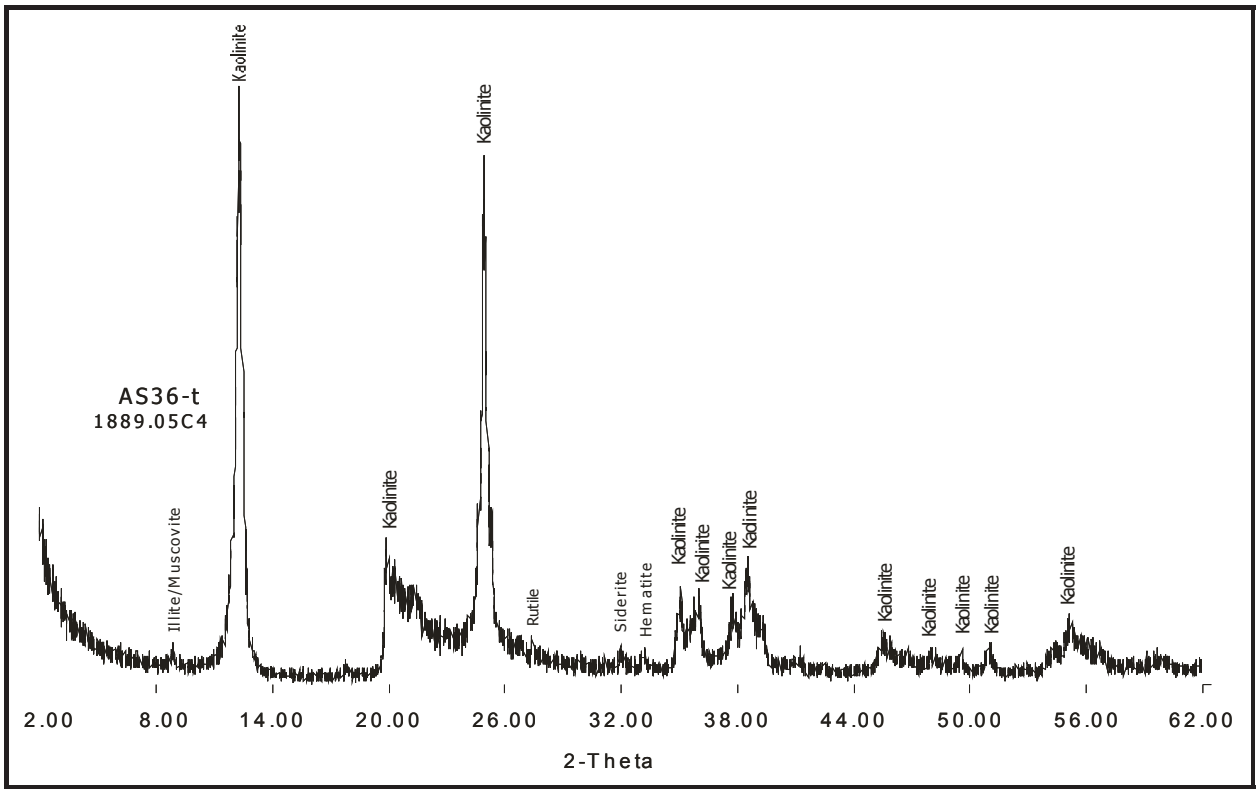

Fig. 8.8: AS36 (partly grey and partly red claystone) Core IV of Ali Sahib Well, X-ray diffractogram (oriented mount, untreated), showing that kaolinite is dominant (greater than 90 %), while illite/muscovite, siderite and hematite are present in minor quantities. Quartz is absent. Traces of rutile might be present.

Lithofacies IV Claystone (AS37, AS38, AS39, AS40, AS41): Brick red to dirty brown, soft to moderately firm, partly sticky and hydrophilic.

The mineralogy shown by XRD (Figs. 8.9 & 8.10 and Tables 8.1 & 8.3b) proves the dominance of kaolinite in all samples. The second dominant mineral is hematite. Traces to minor quantities of muscovite/illite and anatase also occur. Traces of rutile might be present. In sample AS39 traces of oligonite, a Mn-containing siderite, are indicated. A very small quantity of ankerite is present in sample AS38. Together the proportion of kaolinite and Fe minerals (mainly hematite) are greater than 90 % in samples AS37, AS39 and AS41. In samples AS38 and AS40, though kaolinite and Fe minerals (mainly hematite) are dominant, illite also exists in minor quantity.

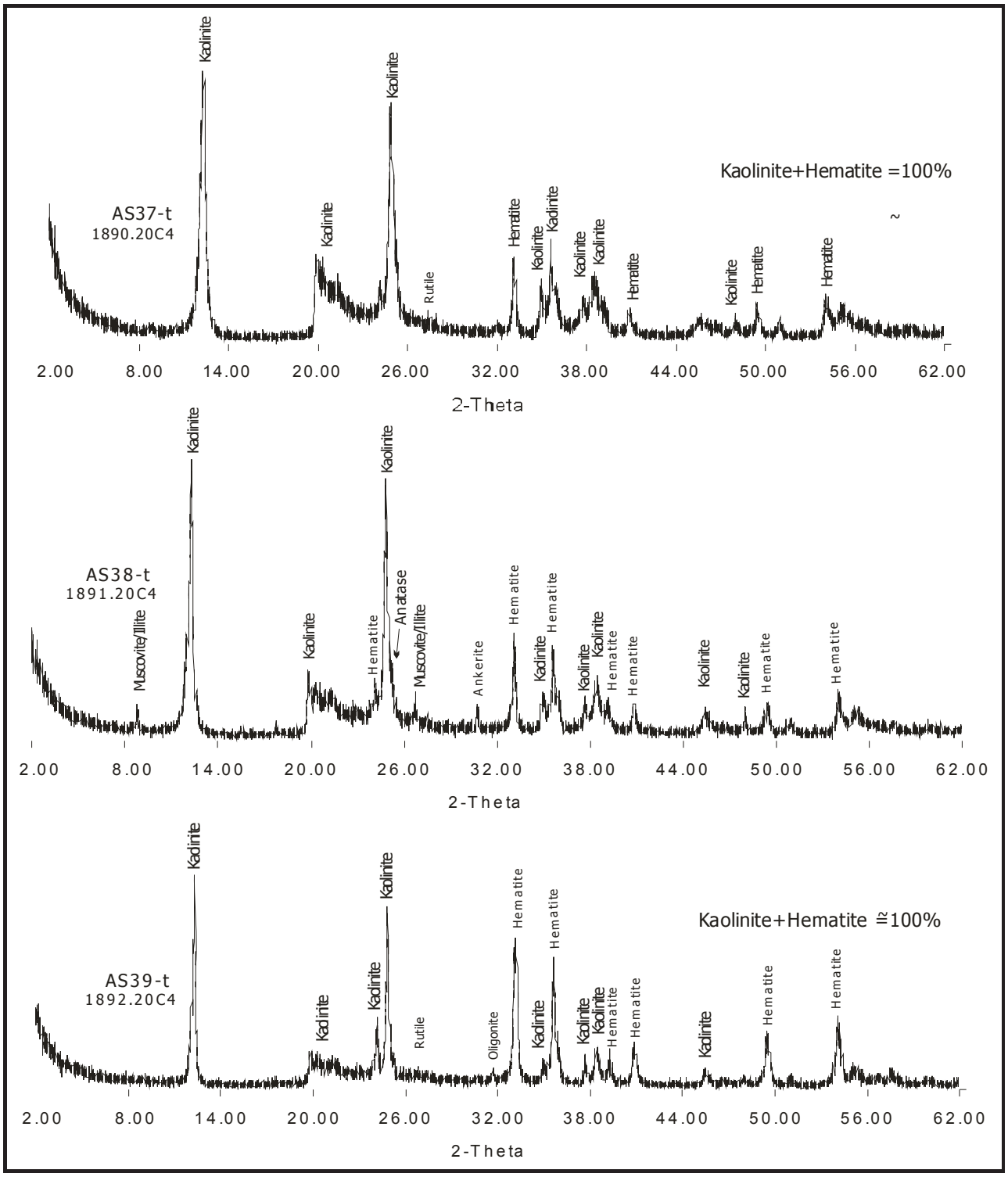

Fig. 8.9: AS37, AS38 and AS 39 (red claystone) of Core IV of the Ali Sahib Well, X-ray diffractograms (oriented mount, untreated), showing that kaolinite and hematite are dominant, minor quantities to traces of anatase, illite, quartz and ankerite in (AS38), are also present. A small reflection with a d-value of 2.82 Å indicates the presence of oligonite, a Mn-containing siderite.

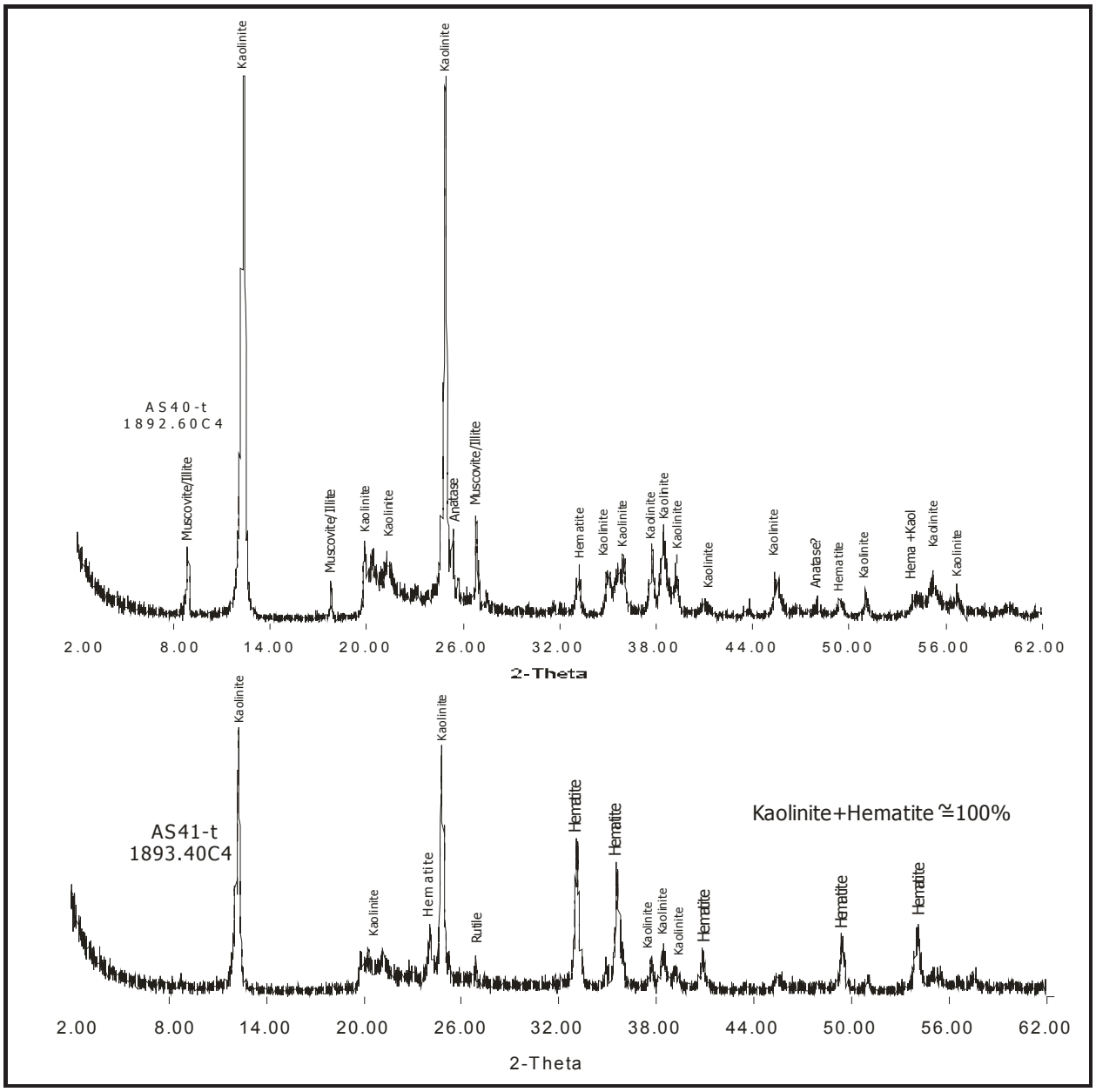

Fig. 8.10: AS40 and AS41 (red claystone) of Core IV of the Ali Sahib Well, X-ray diffractogram (oriented mount, untreated), showing that kaolinite is dominant, hematite and illite/muscovite are present as sub ordinates, while traces of anatase are also present. In AS41, only kaolinite and hematite are present. Quartz is absent in both samples.

8.3.1 DIAGENESIS AND ENVIRONMENT OF DEPOSITION OF CORE IV OF THE ALI SAHIB WELL

The lithology of the Lithofacies I of Core IV (Datta Formation of Jurassic age) of the Ali Sahib Well is comparable to the Lithofacies I of Core III of the Samana Suk Formation of the Late Jurassic of the Ali Sahib Well, both are quartz arenite and are friable

sandstones, and in both, grains are poorly cemented. While the environment of deposition and diagenesis might be similar, a clear evidence of a fluvio-deltaic sedimentary environment is missing in Lithofacies I in Core IV of the Datta Formation. In Lithofacies II (samples (AS34 & AS35), kaolinite, siderite and anatase are present. The conditions of formation for siderite can be assumed to be similar to that described in Core III of the Ali Sahib Well. In Lithofacies II to IV of the Core IV of the Ali Sahib Well, Kaolinite is the dominant mineral (59 to 97 %, Table 8.3b). Other subordinate minerals are siderite, hematite and antase (Table 8.3b). Quartz does not occur with detectable proportions.

In Lithofacies II, kaolinite and siderite are prominent minerals, while in Lithofacies III kaolinite remained prominent, however within the iron minerals there is a transition in siderite to hematite. In Lithofacies IV, kaolinite is the dominant mineral and hematite is subordinate (Figs. 8.8 to 8.10, Tables 8.1a & 8.3b). The distribution of iron minerals in the claystone of Core IV (Datta Formation of Jurassic age) shows changes from the upper section, deposited under reducing conditions, to the lower section, deposited under oxidizing conditions. The transitional conditions are represented in sample AS36, which contains iron minerals, siderite and hematite. Ankerite and illite/muscovite are present in varying amounts in the samples (Figs. 8.9 and 8.10).

Kaolinite is formed in weathering profiles in leached acidic, humid and hot environments (Dunoyer de Segonzac, 1970). The mentioned author also suggested that kaolinite can be formed during diagenesis, as a result of diluted acidic interstitial solutions. According to Bjørlykke (1998), the formation of kaolinite from feldspar and mica in soils and sediments is due to the presence of meteoric water drainage. These conditions occur in zones with a warm and humid climate, particularly under tropical and subtropical conditions. Thus kaolinite is formed due to greater leaching in the presence of high rainfall as reported by (1968). In the light of above discussion about the formation of kaolinite, it can be assumed that the environment of the continental provenance and deposition was warm and humid during the deposition of Lithofacies II to IV of Core IV of the Ali Sahib Well.

Qureshi *et al.*, 2005, carried out the studies of the Lower Jurassic Datta Formation for fire-clays, in Kala Chitta Range, Pakistan (more than 400 km north of the present study area). These authors also found a horizon, the mineralogy of which consists predominantly of kaolinite. Quartz exists in very minor amounts. (However in Lithofacies II to IV of Core IV, from the Datta Formation of the Ali Sahib Well, the quartz and other minerals have been leached in the continental provenance area.) According to these authors, the deposits of the Datta Formation were originated in a provenance area with intensive weathering of alumina-rich rocks. Dorokhin *et al.* (1969), Veletone (1981), studied these types of deposits from different parts of the world and concluded the following summary.

- Presence of rocks with readily soluble mineral whose insoluble residue was rich in alumina.
- A tropical climate with abundant rainfall alternating with dry periods.
- High rock porosity
- A flat or undulating relief.
- Prolonged periods of rest in the continental environment in a given region.

These are ideal conditions for the formation of kaolinite-rich clays. Corresponding conditions for the formation of kaolinite-rich deposits were also reported from Central Europe (e.g. Vortisch & Butz-Braun, 1992). So it can be assumed that weathering of the Pre-Cambrian Sargodha High of Indo-Pakistani Shield (quartzite, andesite, rhyolite, ash, tuff and low grade metamorphic rocks), under tropical seasonal climate conditions produced hematitic, kaolinite-rich clays, laterites and aluminous clays. Reworking was also in progress before final deposition as kaolinite-rich claysstone in Jurassic times.

Hematite was formed by oxidation of ferrous minerals as e.g. biotite, hornblende, or ilmenite (Turner, 1980; Weibel & Friis, 2004; Sheldon, 2005; Parcerisa *et al.*, 2006). In many cases hematite bearing clastic rocks were deposited in continental environments e.g., desert flood plains etc. The hematite develops above the water table and below, if the ground water is oxidizing (Tucker, 1992). Presence of hematite indicates that deposition occurred at the high temperatures of a dry continental environment. The presence of hematite suggests that the environment was rather oxidizing instead of reducing, particularly during the deposition of Lithofacies IV. It is also assumed that

illite/muscovite is essentially clastic, i.e. it was deposited together with kaolinite and there was no or very little diagenetic conversion from kaolinite to illite due to elevated temperature.

It is assumed that ankerite (occurring with minor proportions in sample AS38) is not present in shallow-burial (less than 2 km) diagenesis in limestones and sandstones. Diagenetic ankerite has mostly been interpreted as having formed in association with thermal decarboxylation of organic matter and clay mineral transformations, close to or within the oil window (Boles & Franks, 1979; Kantorowicz, 1985; Macaulay *et al.*, 1993; Hendry *et al.*, 2000). Shallow burial examples are known from mud rocks and associated with coal seams. Irwin *et al.* (1977) proposed that ankerite concretions formed between 34-66 ^{o}C with carbonate supplied from organic matter breakdown via microbial fermentation and thermal decarboxilation. Hendry (2002) suggested that ankerite could form during shallow burial despite an absence of microbial organic matter oxidation reactions to boost carbonate alkalinity.

The occurrence of ankerite in sample AS38 is in agreement with the suggestions of Hendry (2002), with regard to the shallowness of burial during ankerite formation. However, presence of hematite in AS38, (9%, Table 8.3b), indicates an oxidizing environment. The depth of the sample never reached to the oil window (cf. Chapter 9), so thermal decarboxylation of organic matter in neighbouring sediments is unlikely. A possible source of carbonate (CO_2) could be deeper sediments, however due to the absence of ankerite in underlying sediments this is unlikely. Further studies of the stable isotopes of ankerite could indicate the origin of the carbonate ions, i.e. microbial fermentation or thermal decarboxilation.

Compaction is main agent in diagenesis of clay minerals. Through compaction, water is expelled and consequently the thickness of the sediments is reduced up to a factor of ten. At the time of deposition, the muds contain as much as 70-90% water by volume. At approximately 1 km depth, the water content is often reduced to 20-40% by volume (Heling, 1988). Further compaction through water loss requires temperatures approaching 100°C, and this is attained at a burial depth of 2-4 km (Tucker, 1992). At this temperature, clay mineralogy will be changed (reviewed in Singer & Müller, 1983;

and Weaver, 1989). Some workers (Hower *et al.*, 1976; Iman & Shaw, 1985) showed in their studies that initially smectite alters to illite via mixed layer clays of smectite-illite. According to these authors, this reaction is temperature dependant and it occurs at 70-95°C, corresponding to depths of 2-3 km, in areas of average geothermal gradient 30°C/km. At slightly higher temperatures and greater depths, kaolinite is replaced by illite and chlorite. The other important factor in the alteration of clays is the concentration of K^+ in the pore water (Dunoyer de Segonzac, 1970).

After the above discussion, it is concluded, that the samples from this study, which contain dominantly kaolinite, were never buried below 2 km after deposition. All the kaolinite is the result of intensive weathering of eroded preexisting rocks. It is also assumed that the little illite occurring in some samples is clastic, i.e. it was deposited together with kaolinite.

8.4 LITHOFACIES STUDIES IN CORE II OF THE AMIR WALI WELL

Core II (from1615 to 1621.74 m) of the Amir Wali has been cut in the Ranikot/ Lumshiwal Formation of Paleocene/Cretaceous age. On the basis of lithology, color and mineral composition Core II of the Amir Wali Well has been divided into IV lithofacies (cf. Fig 5.2).

Lithofacies I, Claystone (AW 14).

Lithofacies II, Shaly and sandy siltstone (AW15 and AW16).

Lithofacies III, Quartz wackes (AW17).

Lthofacies IV, Quartz arenite (from AW18 to AW21).

Lithofacies I Claystone (AW14): Reddish brown to yellowish brown, greenish grey and off white, moderately firm to hard (Fig. 8.11a). The XRD (Fig. 8.11b, Table 8.1 and 8.3b) of the lithofacies (sample AW14) shows that most of the claystone consists of quartz, kaolinite and illite. Some goethite is also present.

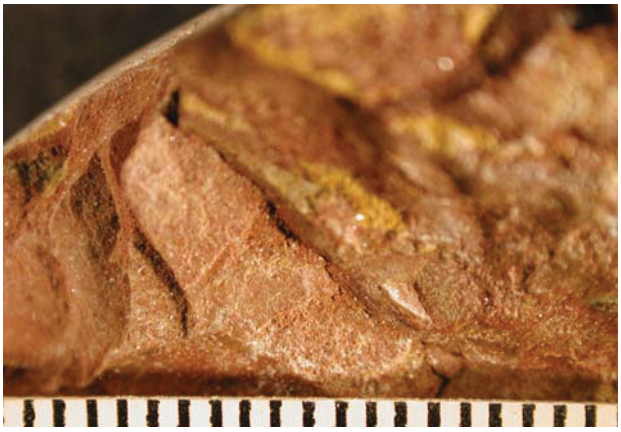

Fig. 8.11a: AW14 of Core II of the Amir Wali Well at 1615.06 m, firm and indurated claystone.

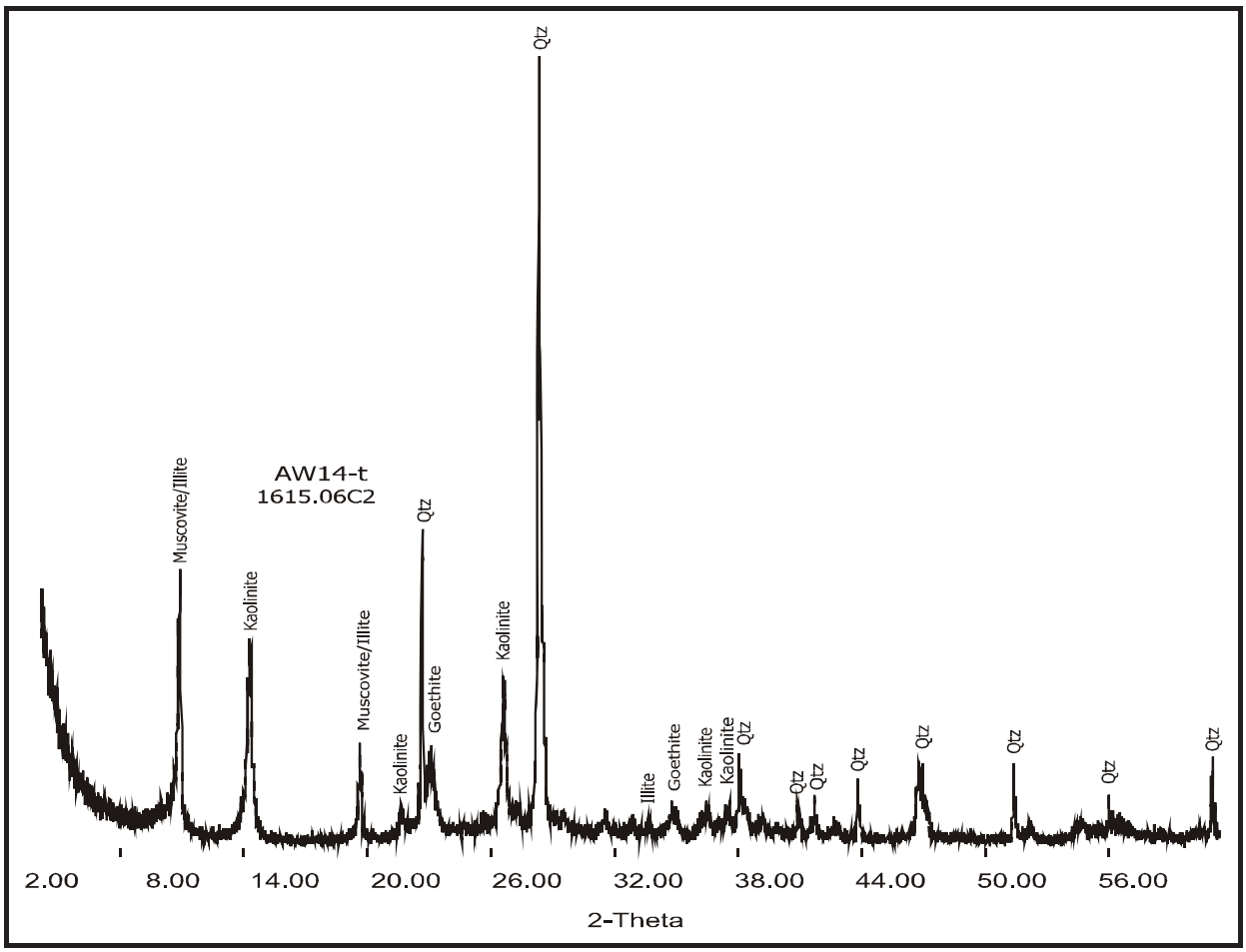

Fig. 8.11b: AW14 (reddish brown claystone), Core II of the Amir Wali Well, X-ray diffractogram (oriented mount, untreated), showing that quartz, muscovite/illite and kaolinite are dominant, while goethite is also present in considerable quantity.

Lithofacies II Shaly & Silty Sandstone (AW15 & AW16): Light grey, greenish grey, grey, moderately firm and hard, grains are coarse silt to very fine sand. Some medium sand size grains are also present, which are subangular to subround. It is fairly cemented and argillaceous. X-ray diffractogram of the lithofacies of sample AW15 shows clastic clay mineralogy with siderite cement. It consists mainly of quartz as the dominant mineral, siderite, kaolinite, illite/muscovite and anatase are present as subordinates. Traces of K-feldspar are also present (cf. Figs. 8.12 & 8.13, Table 8.3b). In sample AW16, only quartz grains with siderite cement occur (Fig. 8.13).

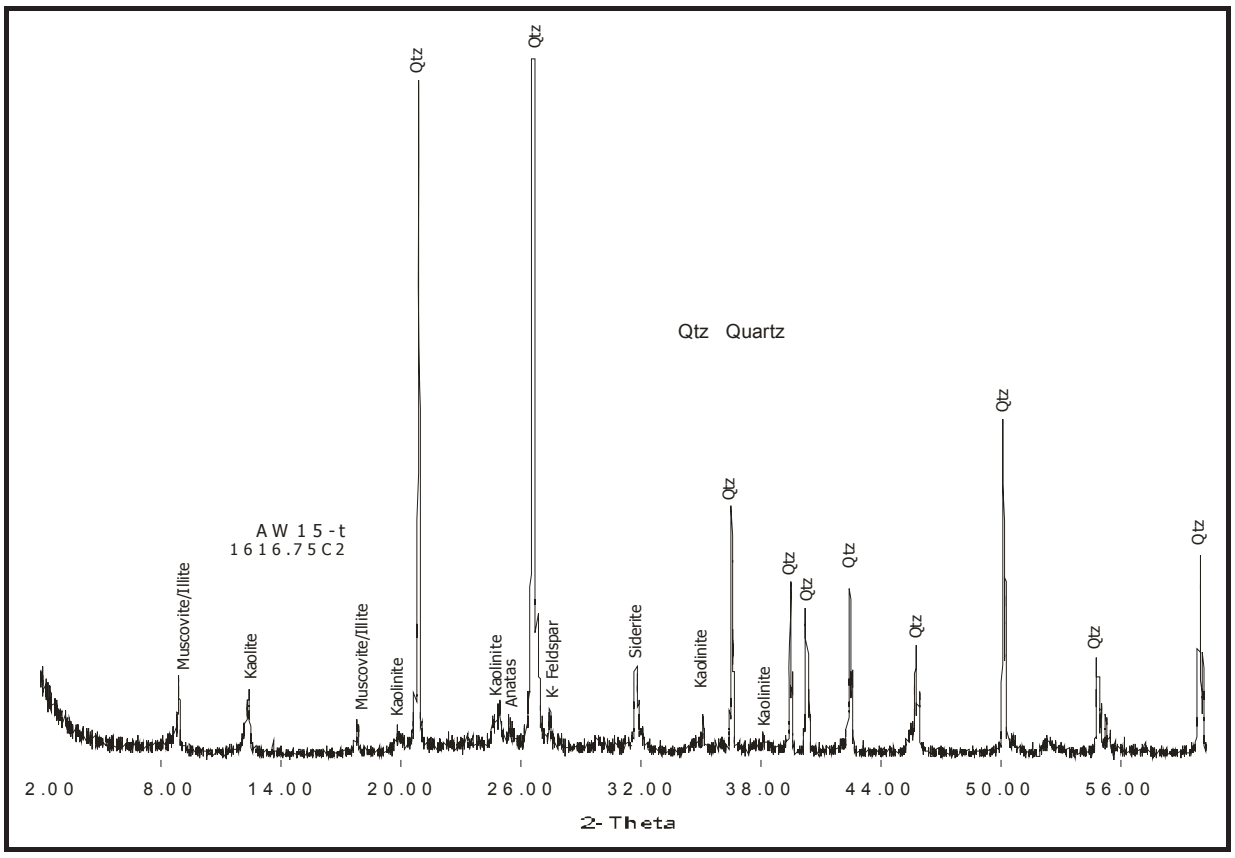

Fig. 8.12: AW15 (shaly sandstone) Core II of the Amir Wali Well, X-ray Diffractogram (oriented mount, untreated), showing that quartz is dominant, kaolinite, muscovite/illite, siderite, K-feldpar and anatase are present as subordinates.

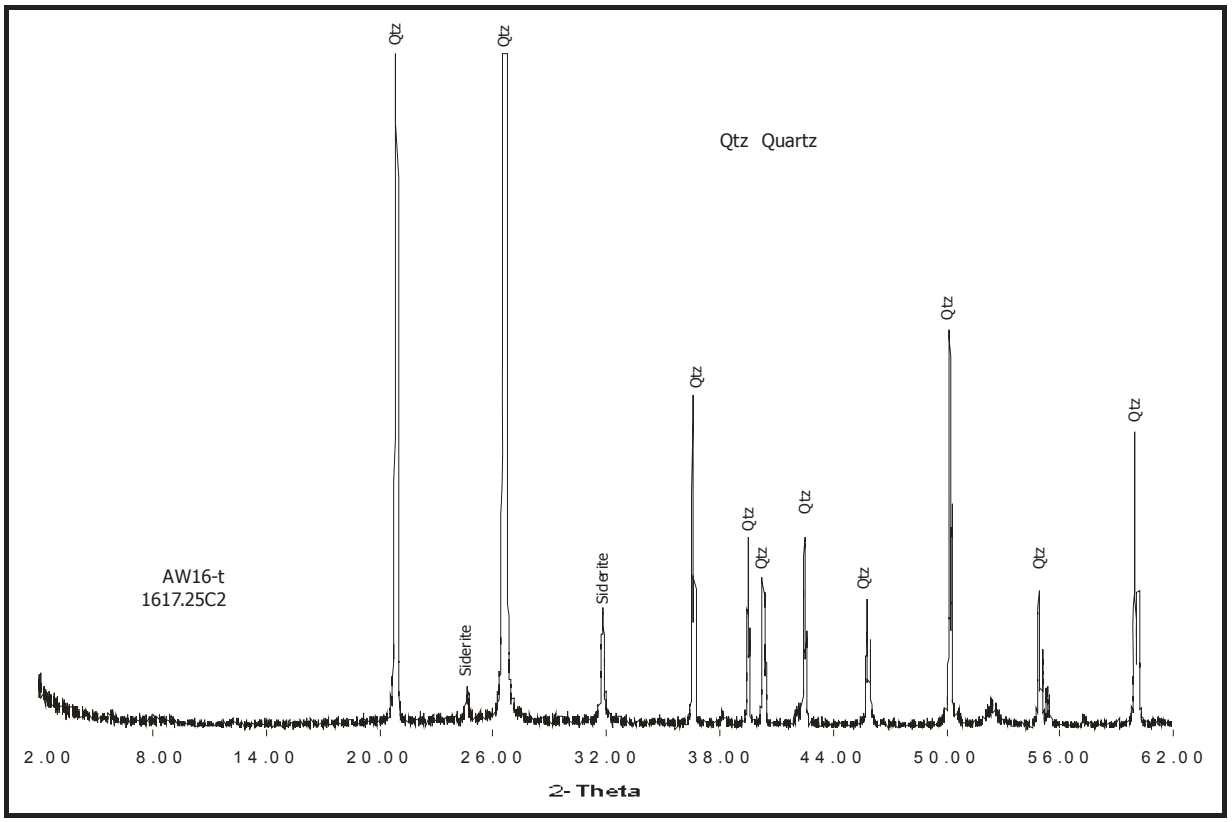

Fig. 8.13: AW16 (silty sandstone) of Core II of the Amir Wali Well, X-ray diffractogram (oriented mount, untreated), showing quartz is dominant while siderite is a subordinate.

Lithofacies III Quartz Wackes (AW17): Light grey, greenish grey, grey, overall sandstone is friable, fine-grained, in places medium-grained, fairly cemented and argillaceous. Quartz grains are angular to subangular, some of them are subrounded. Trask Coefficient of sorting is 1.29, which indicates that quartz grains are well sorted. This lithofacies contains quartz as a dominant mineral (66 %) with kaolinite and illite/muscovite comprising 31 %, opaque minerals are 2 % and feldspars (plagioclase observed in thin section and K-feldspar in XRD) are 1 % (Table 8.3a).

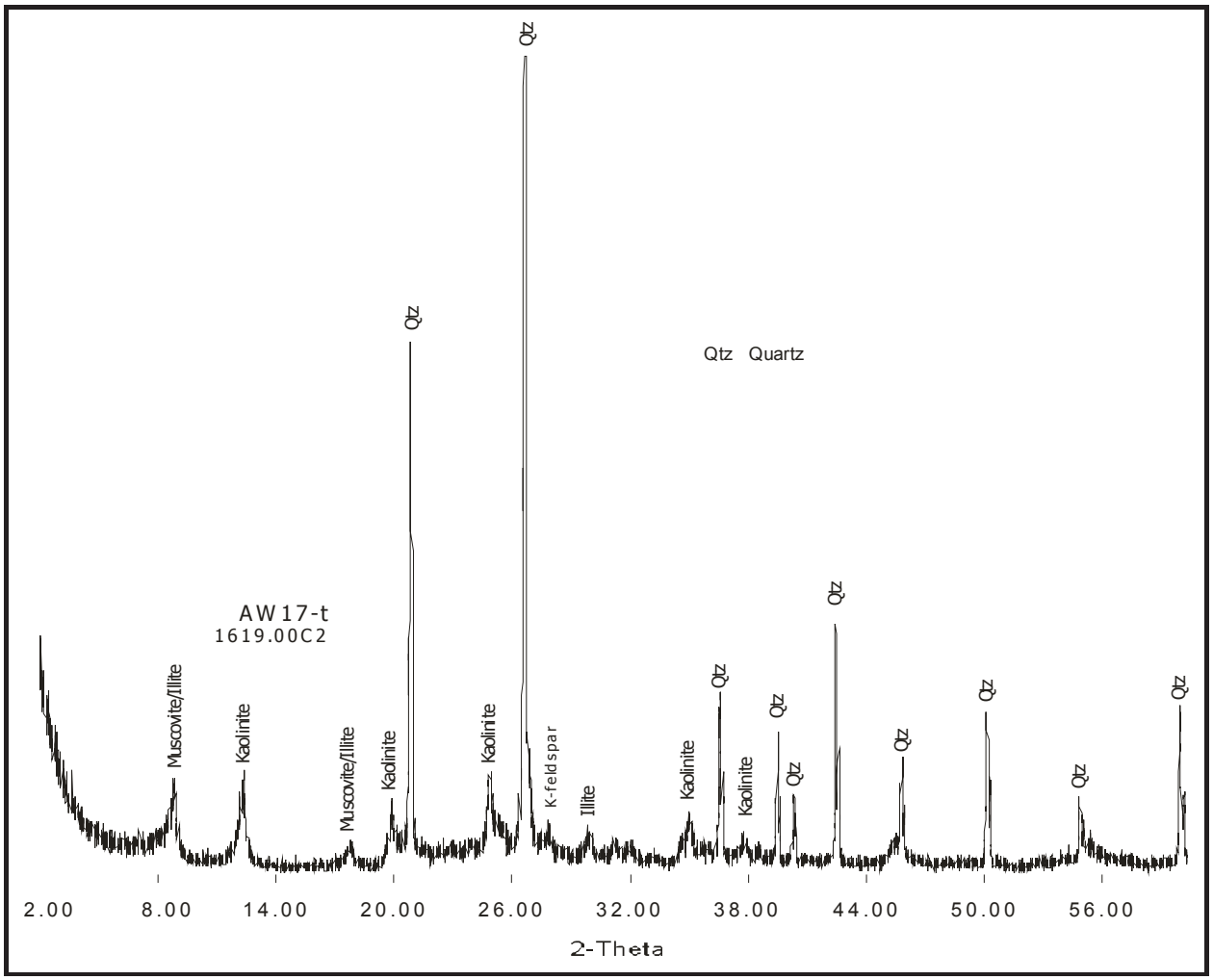

Fig. 8.14a: AW17 (sandstone) Core II of the Amir Wali Well, x-ray diffractogram (oriented mount, untreated), showing that quartz is a dominant, muscovite/illite and kaolinite are present as subordinates, K-feldspar occurs in traces.

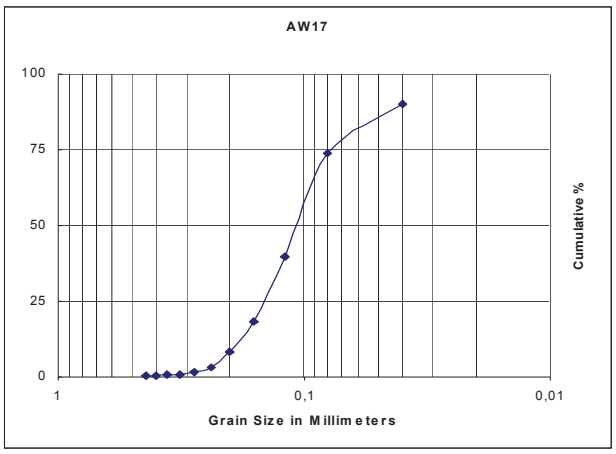

Fig. 8.14b: AW17 of Core II of the Amir Wali Well, size distribution and sorting of grains, represented by cumulative curve. Trask Coefficient of sorting $(Q3/Q1)^{1/2}$ is 1.33.

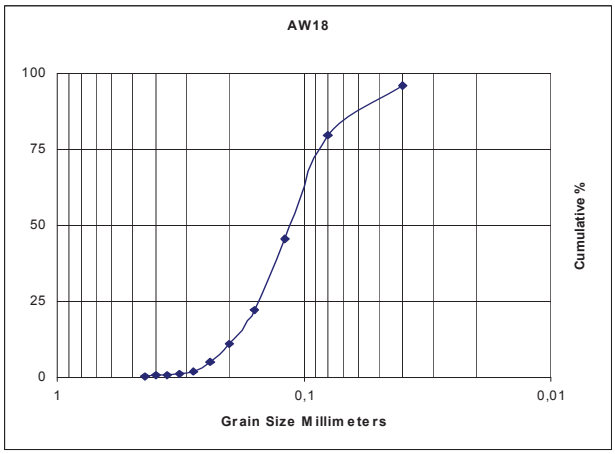

Fig. 8.14c: AW18 of Core II of the Amir Wali Well, size distribution and sorting of grains, represented by cumulative curve. Trask Coefficient of sorting $(Q3/Q1)^{1/2}$ is 1.33.

Lithofacies IV Quartz Arenite (AW18, AW19, AW20 and AW21): Light grey, yellowish brown, greenish grey and light brown, fairly hard and firm. It is friable sandstone. It is fine-grained, in places medium-grained, fairly cemented and argillaceous, at places loose quartz grains also occur. Quartz grains are angular to subangular some of them are subrounded. Trask Coefficient of sorting is 1.33 to 1.75 which indicates that quartz grains are well sorted to moderately well-sorted (Table 8.2). Lithofacies IV (samples AW18, AW19, AW20 and AW21), contains quartz as a dominant mineral (point counting: 83 to 94 %, Table 8.3a) with minor amounts of kaolinite and illite (2 to 12 %), opaque minerals 2 %, and carbonate minerals (2 to 3 %). Of carbonate minerals, only siderite is present which was confirmed by XRD and by SEM (Figs. 8.15c, 8.16c and 8.17c., Plates. 8.7 E, 8.9 E, 8.9 F and 8.10 E). Kaolinite and siderite occur as cements (Plate 8.7 E, 8.9 E, 8.9 F and 8.10 E).

Fig. 8.15a: AW19 of Core II of the Amir Wali Well at 1620.65 m, friable sandstone.

Fig. 8.15b: AW19 of Core II of the Amir Wali Well, size distribution of grains, represented by cumulative curve. Trask Coefficient of sorting $(Q3/Q1)^{1/2}$ is 1.56.

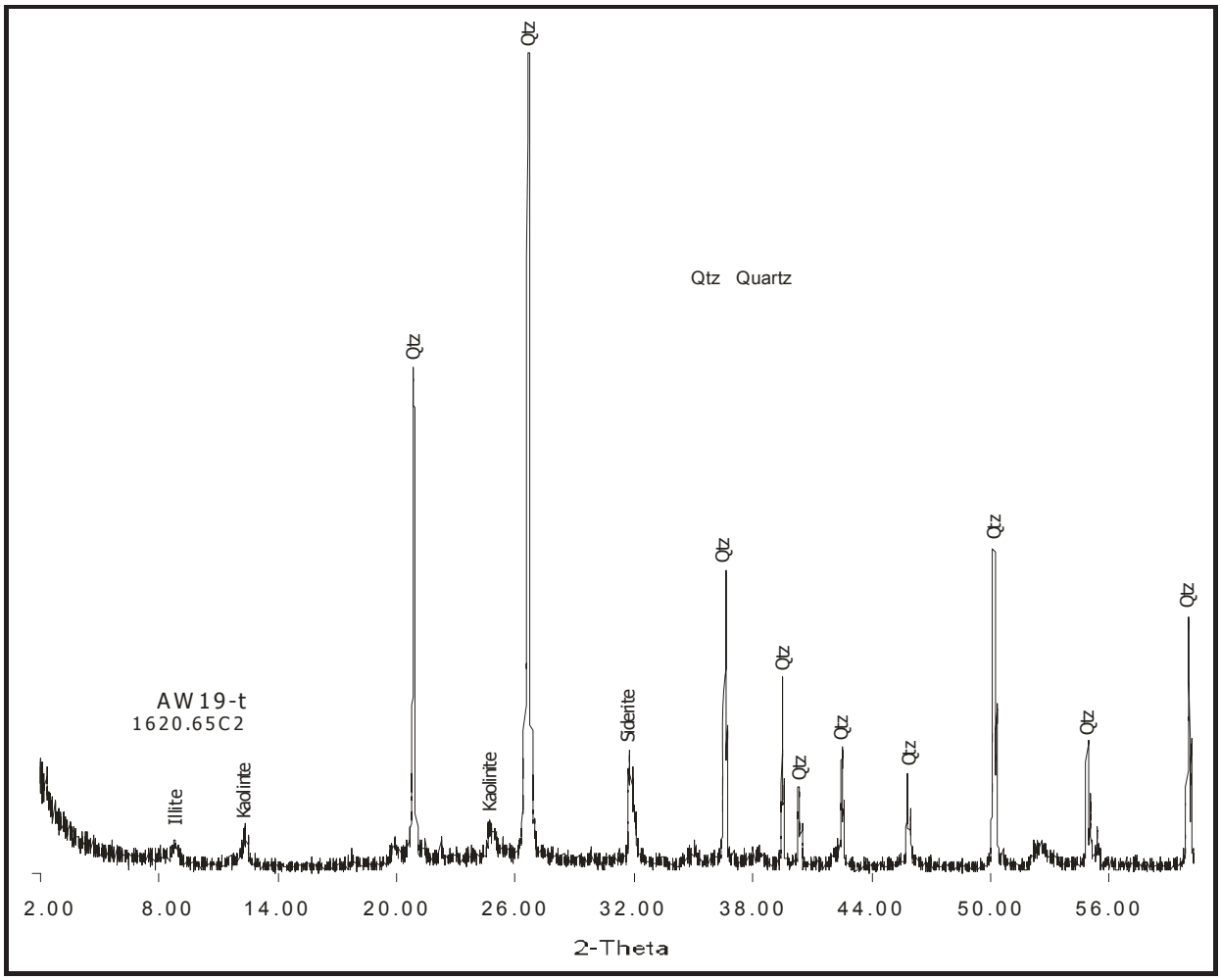

Fig. 8.15c: AW19 (friable sandstone) of Core II of the Amir Wali Well, x-ray diffractogram (oriented mount, untreated), quartz is dominant, siderite, kaolinite and illite are present as subordinates.

Fig. 8.16a: AW20 of Core II of the Amir Wali Well, at 1621.20 m, friable sandstone.

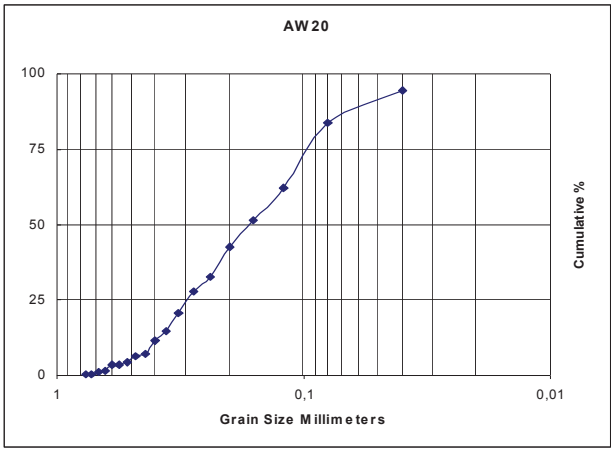

Fig. 8.16b: AW20 Core II of the Amir Wali Well, size distribution and sorting of grains, represented by cumulative curve. Trask Coefficient of sorting $(Q3/Q1)^{1/2}$ is 1.75.

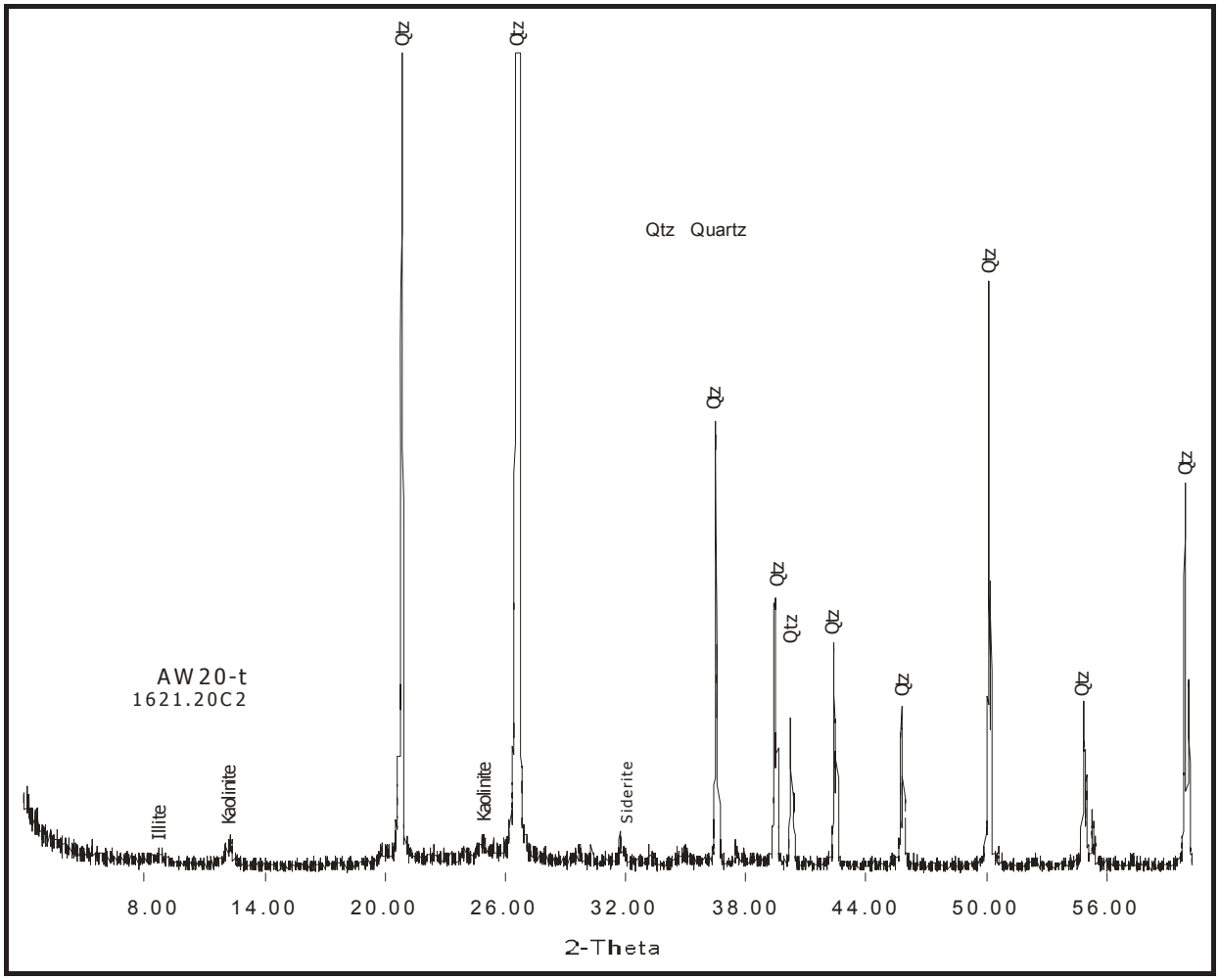

Fig. 8.16c: AW20 (friable sandstone) Core II of the Amir Wali Well, x-ray diffractogram (oriented mount, untreated), quartz is dominant, siderite and kaolinite as minor quantities, traces of illite are present.

Fig. 8.17a: AW21 of Core II of the Amir Wali Well at 1621.65 m friable sandstone.

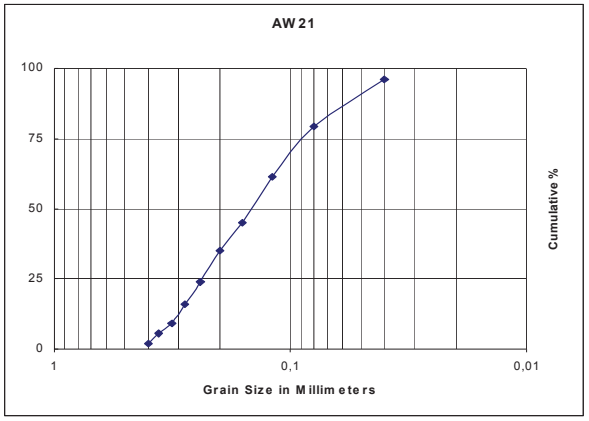

Fig. 8.17b: AW21 Core II of the Amir Wali Well, size distribution and sorting of grains, represented by cumulative curve. Trask Coefficient of sorting $(Q3/Q1)^{1/2}$ is 1.75.

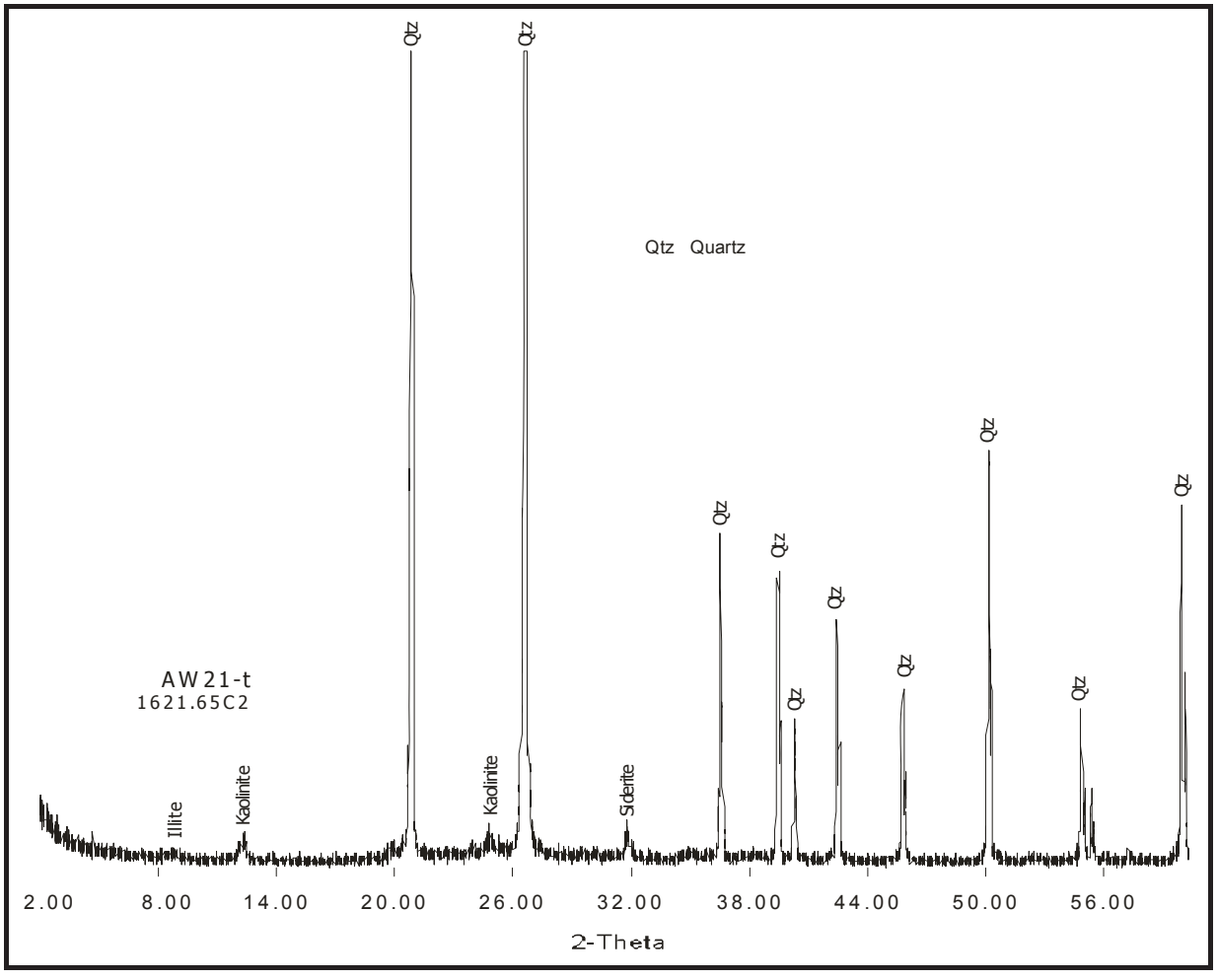

Fig. 8.17c: AW21 (friable sandstone) Core II of the Amir Wali Well, x-ray diffractogram (oriented mount, untreated), showing that quartz is a dominant, kaolinite and siderite are present as subordinates. Traces of illite are weakly indicated.

8.4.1 DIAGENESIS AND ENVIRONMENT OF DEPOSITION OF CORE II OF THE AMIR WALI WELL

Reddish brown color of Lithofacies I (Claystone AW14) is due to the presence of goethite (XRD of AW14). It can be assumed that goethite was formed by the oxidation of preexisting ferrous minerals (e.g. biotite, hornblende or ilmenite), in the continental provenance area, as discussed for instance by Turner (1980), Weibel and Friis (2004), Sheldon (2005) and Parcerisa *et al.*, (2006). The formation of goethite in the sediments is largely controlled by moisture availability during soil formation (Abrajevitch *et. al.,* 2009 and references therein). Detailed studies of soil sequences showed that the goethite and hematite ratio does not depend on the composition of parental rocks, but that it is influenced only by climatic factors (Abrajevitch *et.al.,* 2009 and references therein). According to these authors, high average annual temperatures favour formation of hematite, whereas higher excess of moisture and higher organic carbon promote the formation of goethite. In tropical and subtropical regions where organic carbon content and moisture availability are generally related, the relative abundance of goethite can be used as a indicator of high precipitation, whereas low values indicate drier warmer conditions. Thus goethite formed in oxidized wet conditions (Yi Ge Zhang *et al.,* 2007).

It can be concluded that the formation of goethite in Lithofacies I of Core II of the Amir Wali Well was in tropical to subtropical regions where high precipitation and sufficient organic carbon was present.

In Lithofacies II and IV of Core II of the Amir Wali Well, siderite is present (as cement) in all samples, which is a good indicator of reducing environments and has been described in detail while describing the diagenesis and environment of deposition of Lithofacies I of Core III of the Ali Sahib Well. It can be assumed that similar conditions prevailed during the deposition of siderite in Lithofacies II and IV of Core II of the Lumshiwal Formarion of the Amir Wali Well as were present in Lithofacies I of Core III of the Samana Suk Formation of the Ali Sahib Well. Other minerals (illite and kaolinite) are weathering products from the provenance region.

In Lithofacies III (quartz wackes), kaolinite and illite are present in considerable quantity (XRD software calculation: more than 49%) and siderite is absent. Clays are present as matrix instead of cement. It seems that Lithofacies III of Core II of the Amir Wali Well was deposited as the result of sporadic flooding.

Most of the grains are angular in Lithofacies II to IV, indicating that these sediments did not travel great distances and they were deposited near the region of provenance. Wave actions and other marine influences (glauconite or marine fossils ect.) have not been observed. It is concluded that environment of deposition of Lithofacies of Core II of the Amir Wali Well was a continental fluvial (and/or eolian), swampy area in a tropic to subtropic region.

8.5 SIGNIFICANCE OF DAWSONITE AND BOEHMITE

8.5.1 DAWSONITE ($NaAlCO_3$ $[OH]_2$)

The mineralogy revealed by XRD of sample AWD2 Fig. 8.18 of the Amir Wali Well (ditch cuttings) is worth mentioning. Dawsonite and boehmite occurred along with kaolinite, quartz, hematite and dolomite in sample AWD2 (from the Datta Formation of Jurassic age) of the Amir Wali Well. Dawsonite and boehmite are found for the first time from the Datta Formation.

Several previous occurrences of diagenetic dawsonite have been reported in the literature (e.g. Baker, 1991; Baker *et al.*, 1995; Goldberry & Loughnan, 1977 and Worden, 2006). Occurrences of dawsonite in other environments include low temperature, hydrothermal alteration of feldspathic igneous rocks (Stevenson & Stevenson, 1977 and Taheri *et al.*, 1992) and as a daughter mineral in hydrothermal fluid inclusions (Coveny & Kelly, 1971). Dawsonite is not a ubiquitous diagenetic mineral so it has not been frequently reported. Until now it has been reported from sandstones in several sedimentary basins around the world including in Australia, China, Germany, Middle East, etc. (e.g. Baker, 1991; Du, 1982, Du, 1985; Von Drong, 1985; and Worden, 2006) and now in the Punjab Platform.Goldberry & Loughnan (1977) considered that an external source of sodium and aluminate ions associated with high

pH waters and an excess of CO_2 was needed to produce authigenic dawsonite. Some authors (e.g., Smith & Milton, 1966; Smith *et al.*, 1972, and Smith & Young, 1975), reported non-marine evaporites containing dawsonite, which has been the result from reaction near the sediment-water interface of clays with Na^+ and HCO_3^--rich brines, and with CO_2 of bacterial origin. Baker (1991) envisaged a reaction between bicarbonate-rich waters and detrital feldspars to produce dawsonite. Baker *et al.* (1995) concluded that dawsonite was a result of a large-scale influx of igneous-sourced CO_2 into the sedimentary succession.

Worden (2006) suggested that dawsonite can form in usual conditions. He considered that dawsonite does not require HCO_3^--enriched waters nor is it always associated with extraordinary CO_2 partial pressures. According to him, dawsonite may be a result of deep magmatic sources of CO_2. He also argued that dawsonite cement grew between about 85 and 100 °C.

In the Punjab Platform there was no evidence of hydrothermal or magmatic intrusion in the Datta Formation in the studied wells, as the organic matter (below and above of the sample position AWD2) is immature (cf. Ch. 9). If there would have been a magmatic or thermal intrusion, the organic matter must have been mature or post-mature. It is also noted that the Datta Formation of the Punjab Platform had never reached a temperature of more than 60 °C. The origin of dawsonite in burial diagenesis is not possible. In our case it is suggested, that dawsonite would have formed in feldspar-rich sediments (arkose) having rich quantity of Na in formation water. A second possible method of formation, would involve the presence of clays high quantity of Na^+ and HCO_3^- and a large source CO_2 formed by bacterial activity as proposed by some authors (e.g., Smith & Milton, 1966; Smith et al., 1972, and Smith & Young, 1975).

8.5.2 BOEHMITE (γ-AlO(OH))

Boehmite (AlO(OH)) is formed from the dehydroxylation of gibbsite and is one of the main components of Mediterranean-type bauxite (D'Argenio & Mindszenty, 1995; and Kloprogge *et al.*, 2002). It is largely restricted to subtropical areas (Kloprogge *et al.*, 2002) and has been useful for its paleo-climate significance and as a regional marker of global events (D'Argenio & Mindszenty, 1995).

Gibbsite can transform into boehmite over a temperature range from room temperature (Perić *et al.*, 1996) up to 185°C in a hydrothermal environment (Trolard & Tardy, 1987, and Mehta & Kalsotra, 1991) or at much higher temperature, up to 300 °C (Perić *et al.*, 1996), with the rate of transformation increasing as the temperature increases (Perić *et al.*, 1996).

According to Yuanfeng *et al.* (2009) a terrigenous origin is proposed for the boehmite and quartz in the limestones of Italy. Boehmite was the most important ore mineral in Mediterranean-type bauxites and the product of intensive chemical weathering in a hot climate, deriving from the alteration of aluminosilicates. It provides additional important evidence of a "global greenhouse effect" during the Cretaceous age (Yuanfeng *et. al.*, 2009).

The occurrence of boehmite in the Datta Formation, Amir Wali Well, can be assumed to be of terrigenous origin as there is no evidence of hydrothermal solutions (organic matter is immature, cf. Ch. 9).

A hydrothermal origin for the formation of boehmite in the Datta Formation of the Amir Wali Well is difficult to accept for the reasons described above in the discussion of the formation of dawsonite. It is suggested that first, gibbsite was dehydrated to boehmite in the source area as the result of intense chemical weathering in a hot climate. Later, boehmite, along with other sediments was transported to their present position. The idea of Yuanfeng *et al.* (2009) that boehmite can be formed in terrigenous process is in accordance with the occurrence of boehmite in the Datta Formation in the Amir Wali Well. However, boehmite could also have been formed in the claystone during low temperature diagenesis (< 60 °C) by dehydrooxylation of clastic gibbsite (the latter being a typical product of weathering in a hot and humid climate). A final answer to this

question might be possible by stable isotope analysis after separation or least enrichment of boehmite.

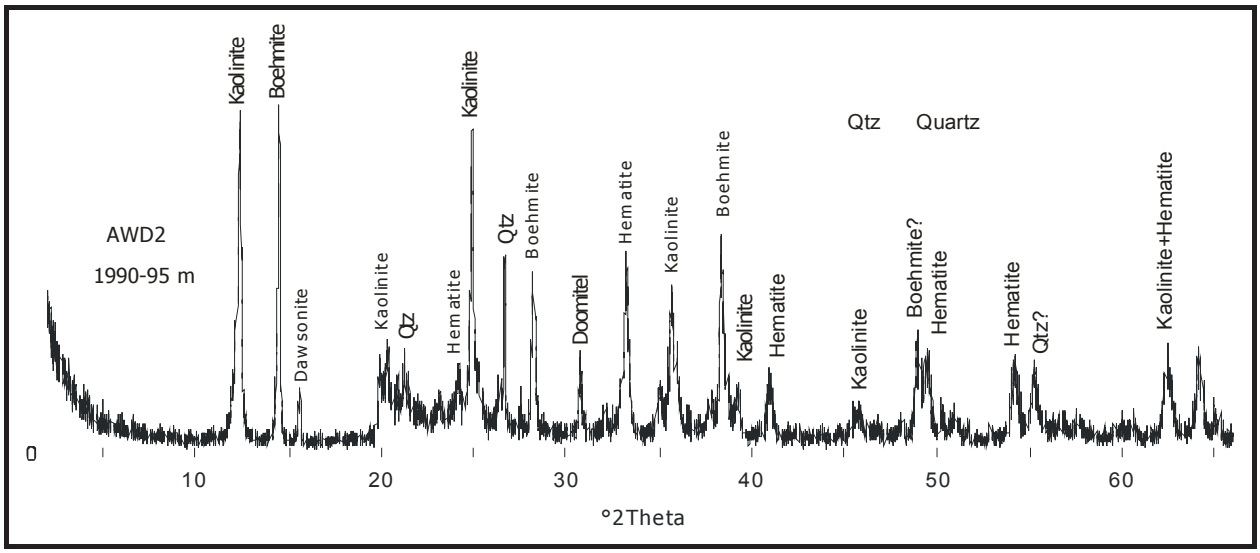

Fig. 8.18: AWD2 (claystone with streaks of sandstone) ditch cuttings of the Amir Wali Well, X-ray diffractogram (oriented mount, untreated), showing that kaolinite and boehmite are dominant, quartz, hematite, dolomite and dawsonite are present as subordinates.

Table 8.1: Minerals Identified by XRD in ditch cuttings in the Amir Wali Well

Sample	Minerals Identified	Lithology	Formation
AWD1	Quartz, Kaolinite, Dolomite and Illite	Claystone	Datta
AWD2	Boehmite, Kaolinite, Quartz, Dolomite, Hematite, Dawsonite,	Claystone	
AWD3	Kaolinite, Quartz, Illite, Calcite, Siderite and Hematite	Claystone	
AWD4	Quartz, Kaolinite, Illite, K-feldspar, Anatase, Calcite, Dolomite and traces of Siderite	Claystone	
AWD5	Quartz, Kaolinite, Illite, K-feldspar, Calcite, Dolomite and traces of Siderite	Sandstone	
AWD6	Quartz, K-feldspar, Kaolinite, Illite, , Anatase, Calcite, Siderite	Sandstone	

Table 8.1a: Minerals Identified by XRD of Core III and Core IV of the Ali Sahib Well and Core II of the Amir Wali Well. Minerals are given in order of decreasing proportion

Sample	Minerals Identified	Lithology	Formation
AW14C2	Quartz, Illite/Muscovite, Kaolinite, Goethite, traces of Calcite	Claystone	Lumshiwal/ Ranikot
AW15 C2	Quartz, Illite/muscovite, Ankerite, Kaolinite, K-feldspar, Anatase	Sandy Siltstone	
AW16 C2	Quartz, Siderite	Sandstone	
AW17 C2	Quartz, Illite/Muscovite, Kaolinite, traces of K-feldspar	Clayey Sanstone	
AW19 C2	Quartz, Siderite, Kaolinite, traces of Illite and K-feldspar	Quartz Arenite	
AW20 C2	Quartz, Siderite, Kaolinite, traces of Ankerite and Illite	Quartz Arenite	
AW21 C2	Quartz, Kaolinite, Siderite, traces of Illite	Quartz Wackes	
AS28C3	Quartz, Siderite, Kaolinite, traces of Illite	Quartz Arenite	Samana Suk
AS29 C3	Quartz and Kaolinite, traces of Siderite		
AS30 C3	Quartz, and traces of Kaolinite, Siderite		
AS31 C3	Quartz, traces of Kaolinite and Calcite		
AS32 C3	Quartz, Kaolinite	Shaly/Siltstone	
AS33 C4	Quartz, traces of Kaolinite	Quartz Arenite	Datta
AS34 C4	Kaolinite, Siderite, Anatase, traces of Rutile	Claystone	
AS35 C4	Kaolinite, Siderite, Anatase, traces of Rutile	Claystone	
AS36 C4	Kaolinite, traces of Siderite, Hematite, Illite/Muscovite and Rutile	Claystone	
AS37 C4	Kaolinite, Hematite, traces of Rutile	Claystone	
AS38 C4	Kaolinite, Hematite, Anatase, traces of Quartz, Ankerite and Illite/Muscovite	Claystone	
AS39 C4	Kaolinite, Hematite, traces of Rutile and Oligonite	Claystone	
AS40 C4	Kaolinite, Illite/Muscovite, Hematite, Anatase	Claystone	
AS41 C4	Kaolinite, Hematite, Rutile	Claystone	

Table 8.2: Trask sorting coefficients (S_o) and calculated depositional porosities for six different verbally defined degrees of sorting

Description	Trask Sorting Coefficient, S_o	Depositional Porosity $Ø_o$, (%)
Very Well Sorted	1.1	41.7
Well Sorted	1.3	38.5
Moderately Well Sorted	1.5	36.2
Moderately Sorted	1.8	33.6
Poorly Sorted	2.35	30.7
Very Poorly Sorted	4.48	26.0

$Ø_o$ calculated as 20.91+22.9/So

Table 8.3: Median, first and third Quartile and Trask coefficient of sorting

	Graphical Estimations					Formation
	Q3	Md = P50	Q1	Median	S_o Trask coefficient of sorting $(Q_3/Q_1)^{1/2}$	
AW17	0.16	0.12	0.09	0.11	1.33	Lumshiwal/ Ranikot
AW18	0.16	0.11	0.09	0.12	1.33	
AW19	0.16	0.11	0.066	0.11	1.56	
AW20	0.3	0.17	0.098	0.18	1.75	
AW21	0.24	0.16	0.09	0.15	1.63	
AS28	0.24	0.18	0.08	0.18	1.73	Samana Suk
AS29	0.25	0.18	0.1	0.18	1.58	
AS30	0.15	0.2	0.05	0.2	1.73	
AS31	0.16	0.1	0.05	0.12	1.77	
AS33	0.62	0.54	0.47	0.53	1.15	Datta

Table 8.3a: Mineralogy of Core III & Core IV of Ali Sahib Well and Core II of Amir Wali Well determined by polarizing microscope

Sample	Minerals Identified						Lithology	Formation
	Qz	Opg	Carb	Felds	Tour	Kao/Ill		
AW17	66	2		1		31	Clayey Sanstone	Lumshiwal/ Ranikot
AW18	84	2	2			12	Quartz Arenite	
AW19	83	2	3			12	Quartz Arenite	
AW20	94	2	2	Tr	Tr	2	Quartz Arenite	
AW21	94	2		Tr		4	Quartz Wackes	
AS28	85	1				14	Quartz Arenite	Samana Suk
AS29	94	2				4	Quartz Wackes	
AS30	96	1				3	Quartz Arenite	
AS31	95	2				3	Quartz Arenite	
AS33	>99	Tr				Tr	Quartz Arenite	Datta

Qz: Quartz; Opg: opaque grains; Car: Carbonates; Felds: Feldspar; Tour: Tourmaline; Kao: Kaolinite; Ill: Illite.

Table 8.3b: Mineralogy of Core III & Core IV of the Ali Sahib Well and Core II of the Amir Wali Well determined by using ADM version 6.22 software for XRD

Sample	Minerals Identified								Formation
	Quartz	Anatase	Hematite	Ankerite	Siderite	Kaolinite	Illite	Rutile	
AW16	95				5				Lumshiwal /Ranikot
AW17	48	1				21	28		
AW19	71				7	11	12		
AW20	92				1	7			
AW21	90				2	8			
AS28	47	1			8	20	23		Samana Suk
AS29	93	7							
AS30	92	8							
AS31	92	8							
AS32	62	5				33			
AS33	93					7			Datta
AS34		2			11	87		Tr	
AS35		3			7	90		Tr	
AS36		1	1		1	97		Tr	
AS37		2	10		3	85		Tr	
AS38	1	7	9	2		69	13	Tr	
AS39		7	23			70		Tr	
AS40		6	5			85	4		
AS41			13			87		Tr	

Tr: Traces

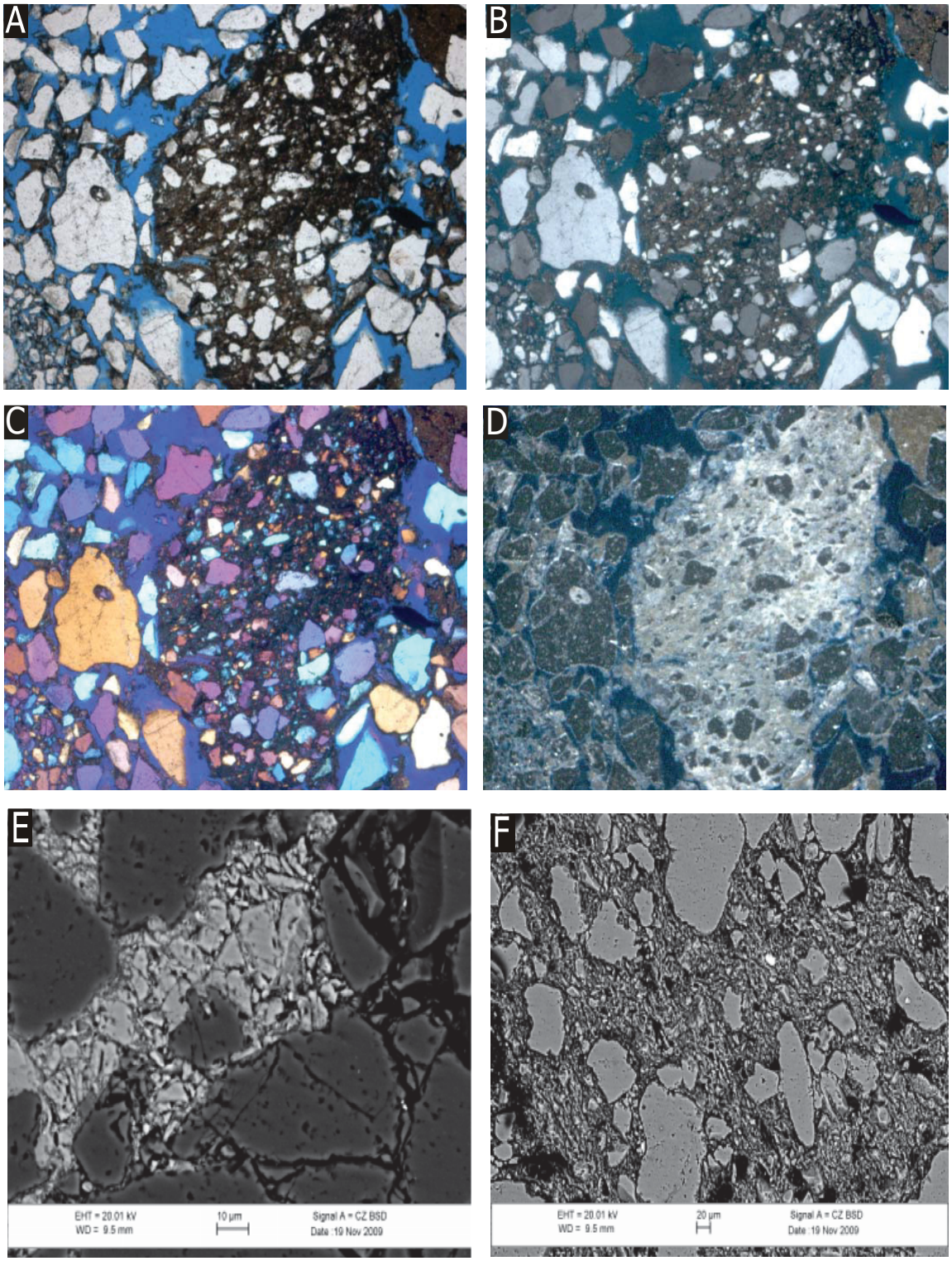

Plate 8.1: (A) AS28, Core III of the Ali Sahib Well: Friable sandstone having clay balls in friable sandstone, quartz grains are angular to subangular (5x PPL). (B) AS28 (5x CN). (C) AS28 (5x QCN). (D) AS28 (5x RL). (E) AS28, Core III of the Ali Sahib Well, fractured siderite cement and quartz grains showing some degree of compaction (SEM back scattered electron image). (F) AS28, Angular to sub-rounded quartz grains in clay matrix. (SEM back scattered electron image). PPL: Plane polarized light; CN: Crossed nicols; QCN; Crossed nicols with additional lambda plate; RL: reflected light. Width of each thin section photograph (A to D) is 2.25 mm.

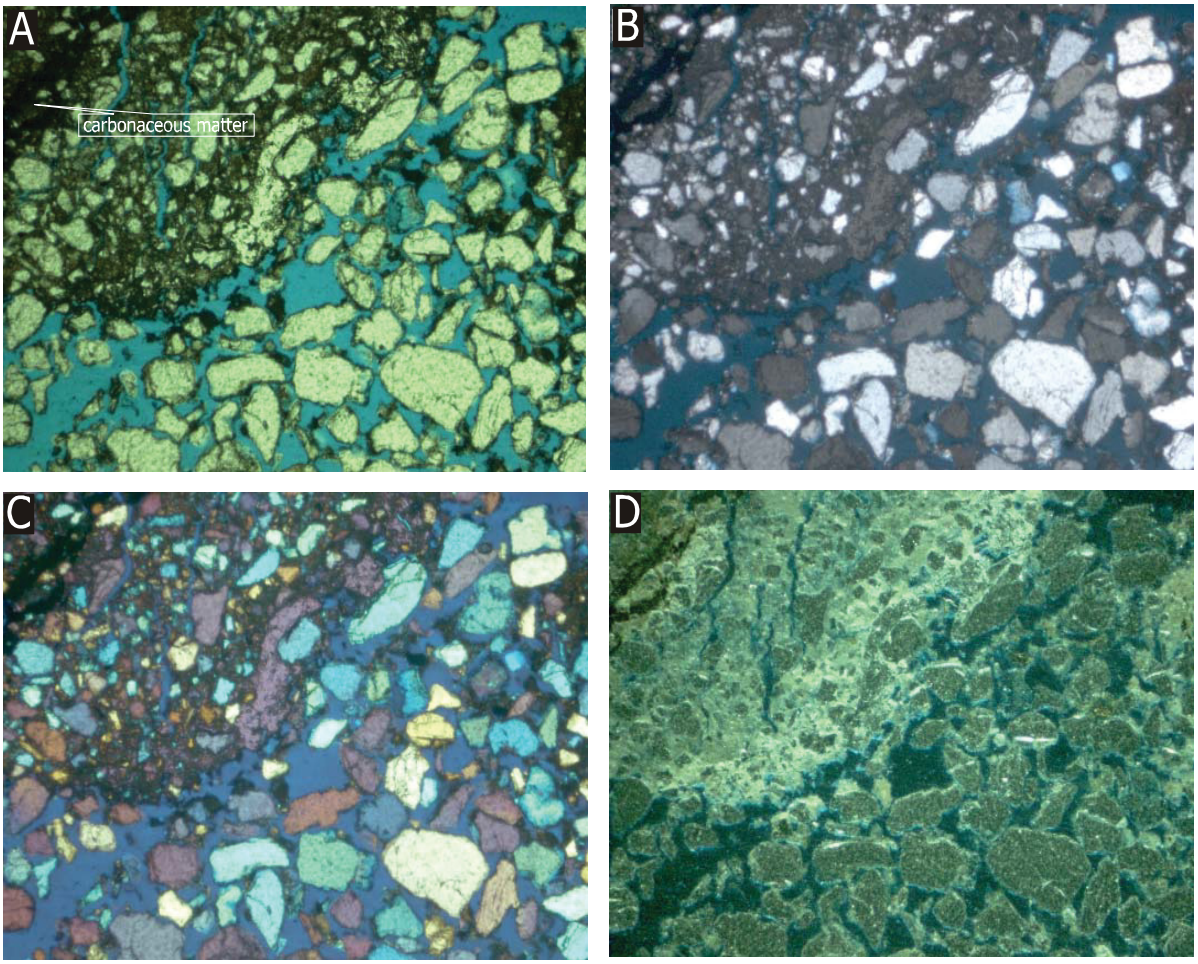

Plate 8.2: (A) AS29 Core III of the Ali Sahib Well: Friable sandstone having clay balls in friable sandstone, quartz grains are angular to subangular (5x PPL). (B) AS29 (5x CN). (C) AS29 (5x QCN). (D) AS29 (5x RL). PPL: Plane polarized light; CN: Crossed nicols; QCN; Crossed nicols with additional lambda plate; RL: reflected light. Width of each thin section photograph (A to D) is 2.25 mm.

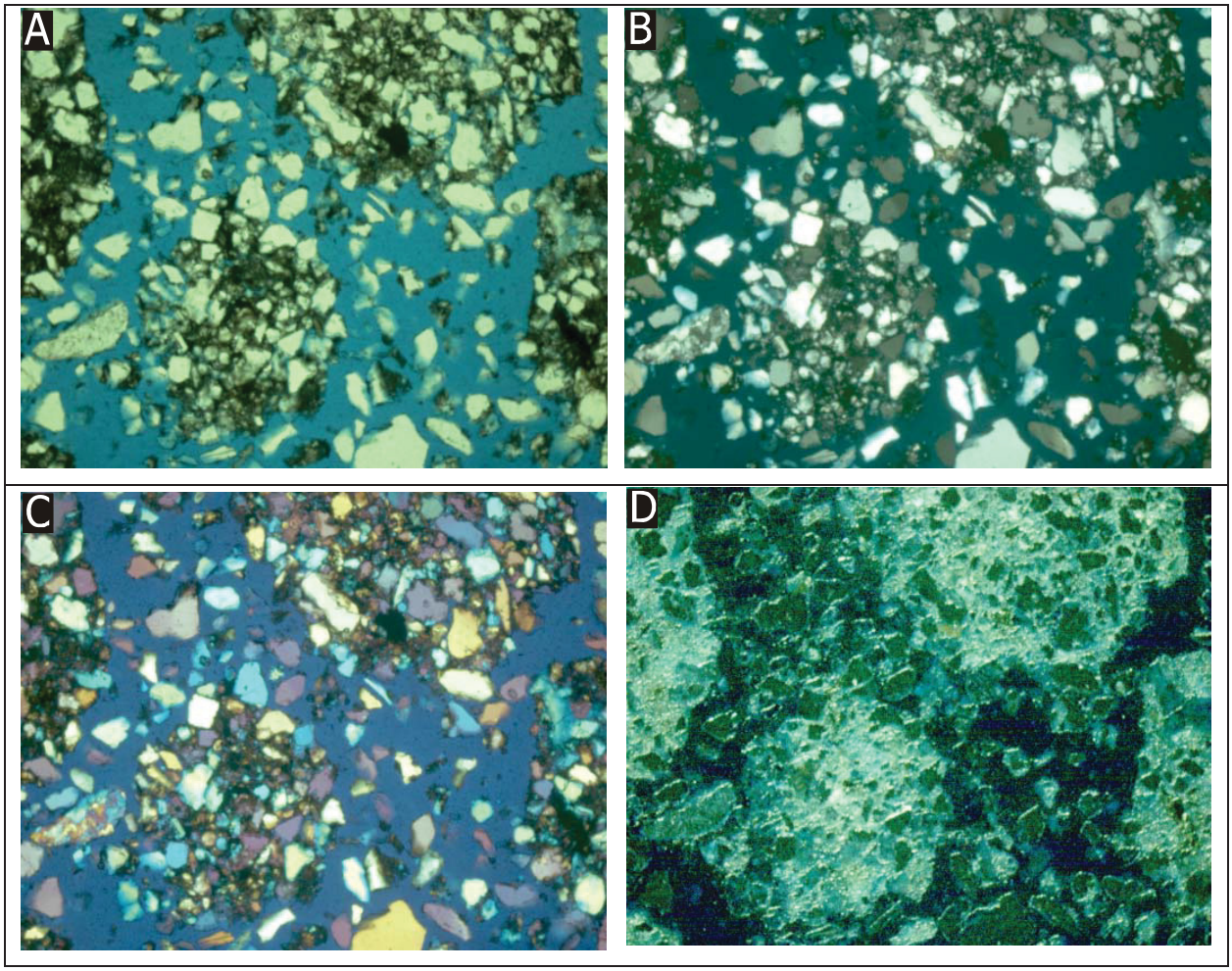

Plate 8.3: (A) AS30 Core III of the Ali Sahib Well: Friable sandstone having clay balls in friable sandstone, quartz grains are angular to subangular (5x PPL). (B) AS30 (5x CN). (C) AS30 (5x QCN). (D) AS30 (5x RL). PPL: Plane polarized light; CN: Crossed nicols; QCN; Crossed nicols with additional lambda plate; RL: reflected light. Width of each thin section photograph (A to D) is 2.25 mm.

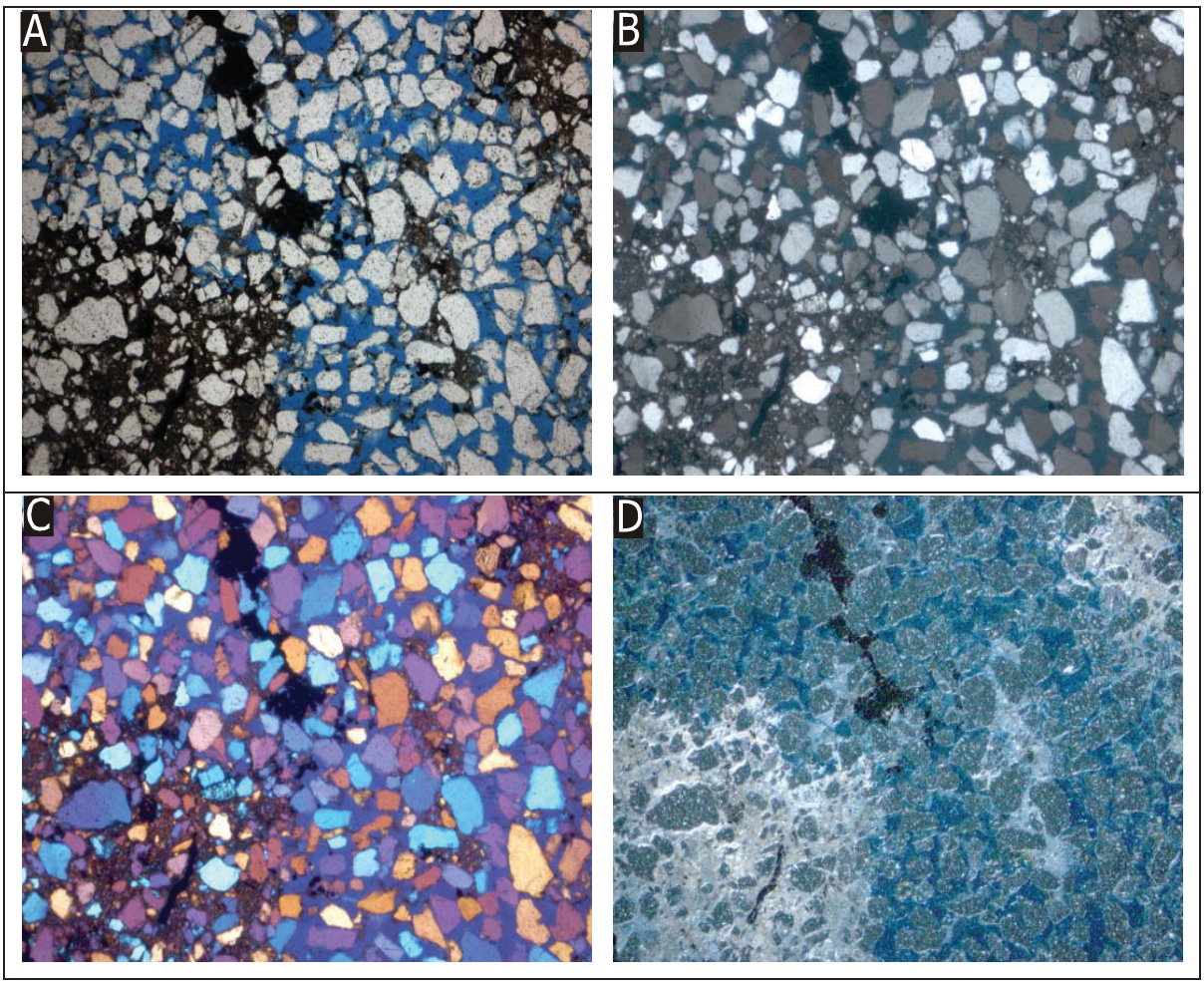

Plate 8.4: (A) AS31 Core III of the Ali Sahib Well: Friable sandstone having clay balls, carbonaceous matter (black) in angular to subangular quartz grains (5x PPL). (B) AS30 (5x CN). (C) AS30 (5x QCN). (D) AS30 (5x RL). PPL: Plane polarized light; CN: Crossed nicols; QCN; Crossed nicols with additional lambda plate; RL: refleted light. Width of each thin section photograph (A to D) is 2.25 mm.

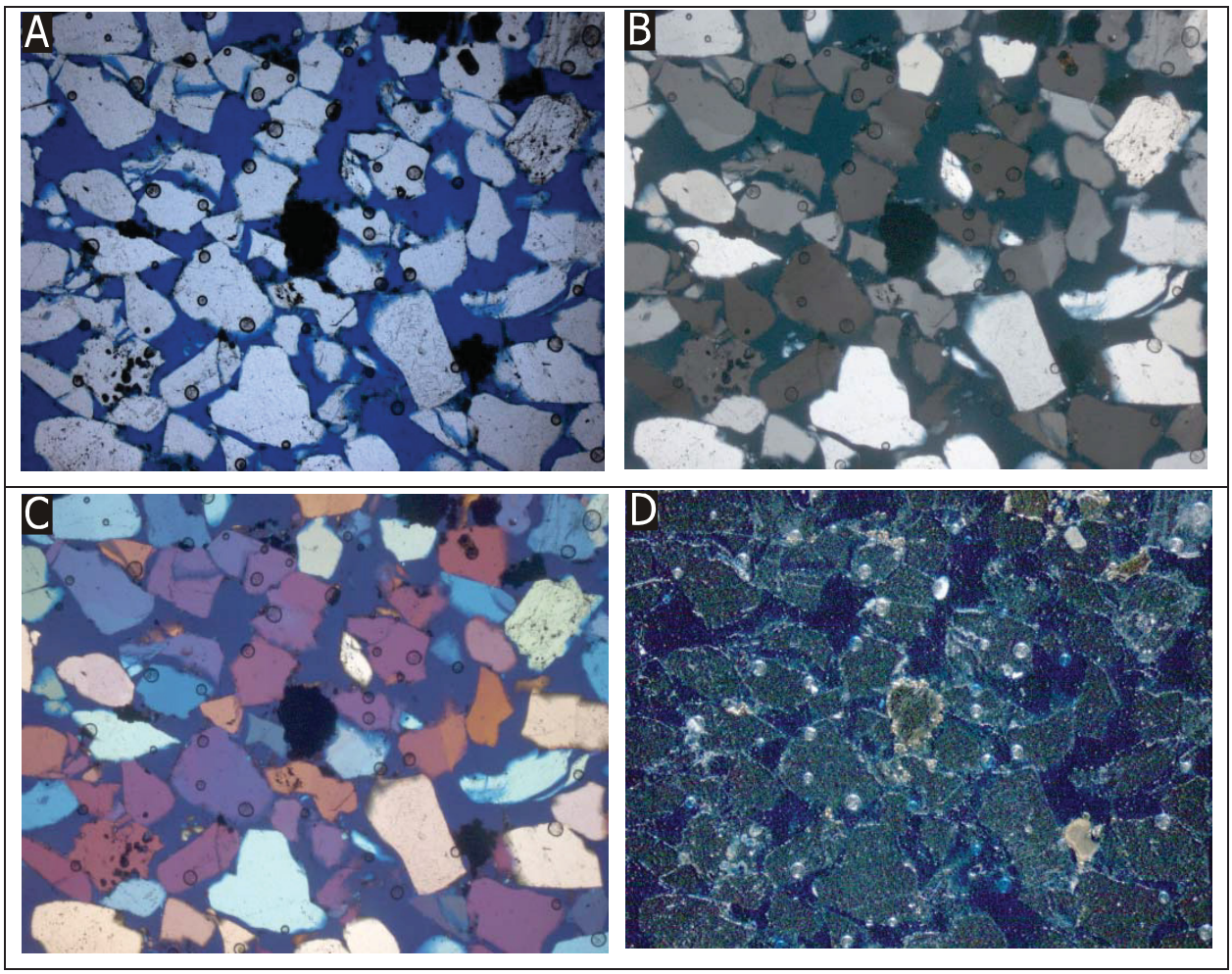

Plate 8.5: AS33 Core IV of the Ali Sahib Well: Friable sandstone having pyrite (black) in angular quartz grains (5x PPL). (B) AS33 (5X CN). (C) AS33 (5x QCN). (D) AS33 (5x RL). PPL: Plane polarized light; CN: Crossed nicols; QCN; Crossed nicols with additional lambda plate; RL: reflected light. Width of each thin section photograph (A to D) is 2.25 mm.

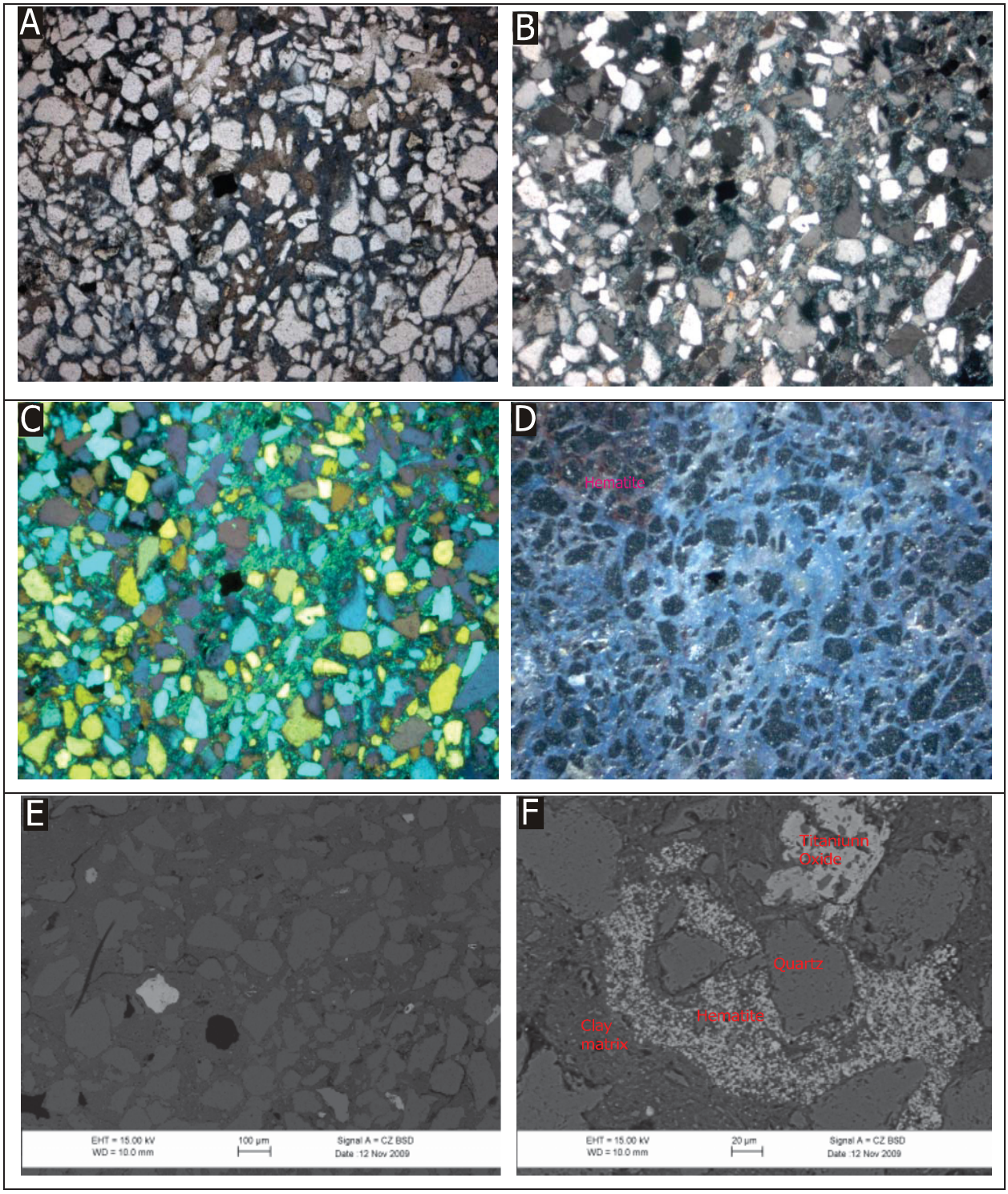

Plate 8.6: AW17 Core II of the Amir Wali Well: Friable sandstone having titanium oxide (black near centre), some carbonate cement in angular to subangular quartz grains (5x PPL). (B) AW17 (5X CN). (C) AW17 (5x QCN). (D) AW17 (5x RL). (E) AW17: Quartz grains in clay matrix, titanium oxide grains (white) are also visible. (SEM back scattered electron image). (E) AW17: Hematite, titanium oxide in clay matrix. Corrosion of quartz can also be seen (SEM back scattered scattered electron image). PPL: Plane polarized light; CN: Crossed nicols; QCN; Crossed nicols with additional lambda plate; RL: reflected light. Width of each thin section photograph (A to D) is 2.25 mm.

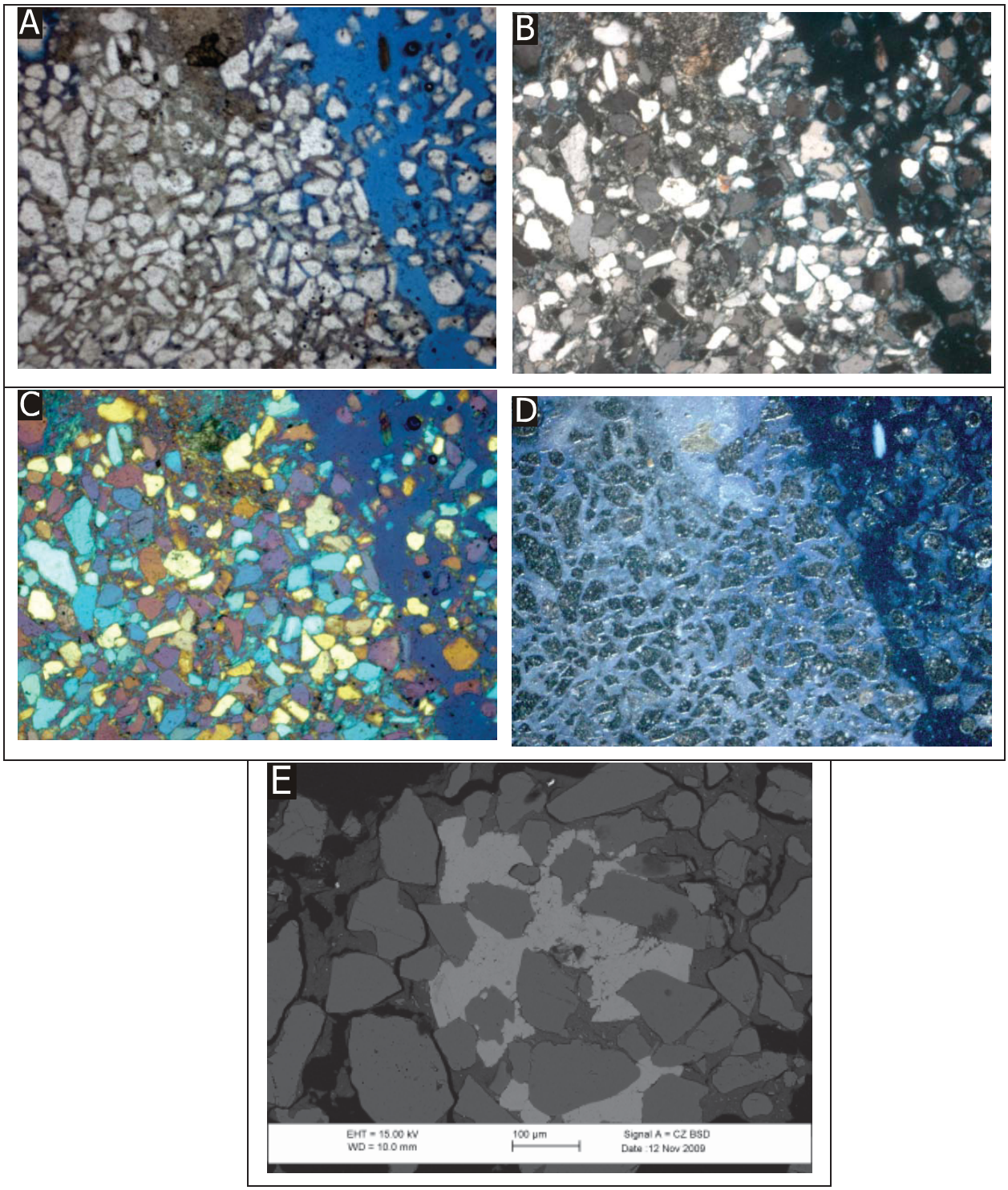

Plate 8.7: AW18 Core II of the Amir Wali Well: Friable sandstone of, angular to subangular quartz grains in clay matrix. Carbonates and clays are also exist as cements (5x PPL). (B) AW18 (5X CN). (C) AW18 (5x QCN). (D) AW18 (5x RL). (E) AW18: Quartz grains cemented by siderite and clay (SEM back scattered electron image). PPL: Plane polarized light; CN: Crossed nicols; QCN; Crossed nicols with additional lambda plate; RL: reflected light. Width of each thin section photograph (A to D) is 2.25 mm.

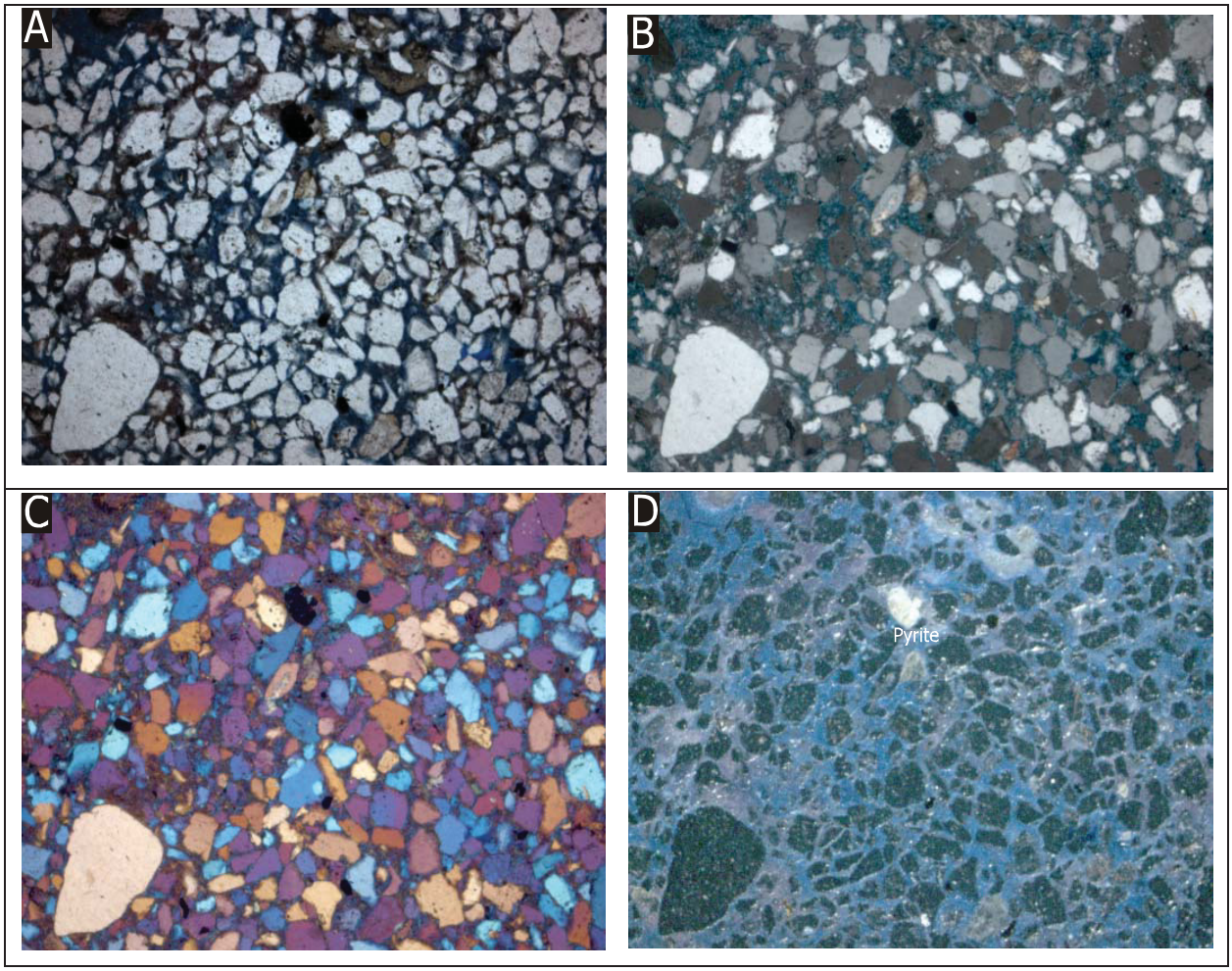

Plate 8.8: AW19 Core II of the Amir Wali Well: Friable sandstone having pyrite (black) in angular to subangular quartz grains (5x PPL). (B) AW19 (5X CN). (C) AW19 (5x QCN). (D) AW19: Pyrite (yellowish white) and hematite staining (red) can be seen (5x RL). PPL: Plane polarized light; CN: Crossed nicols; QCN; Crossed nicols with additional lambda plate; RL: reflected light. Width of each thin section photograph (A to D) is 2.25 mm.

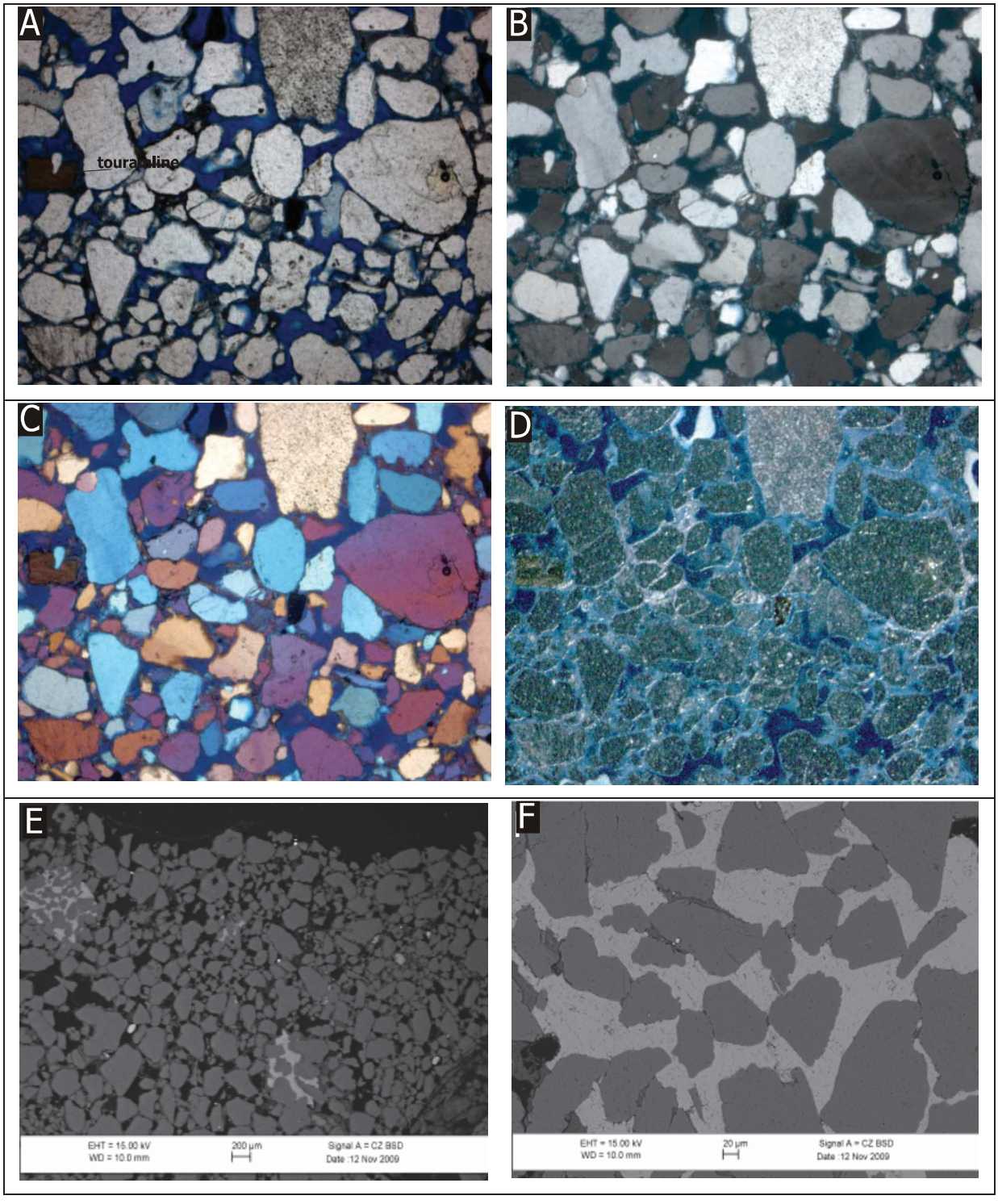

Plate 8.9: AW20 Core II of the Amir Wali Well: Friable sandstone having a touramline grain in angular to subrounded quartz grains (5x PPL). (B) AW20 (5X CN). (C) AW20 (5x QCN). (D) AW20 (5x RL). (E) AW20: Siderite cement occurs at places. (SEM back scattered electron image). (F) AW20: Quartz grains are cemented by siderite. (SEM back scattered electron image). PPL: Plane polarized light; CN: Crossed nicols; QCN; Crossed nicols with additional lambda plate; RL: reflected light. Width of each thin section photograph (A to D) is 2.25 mm.

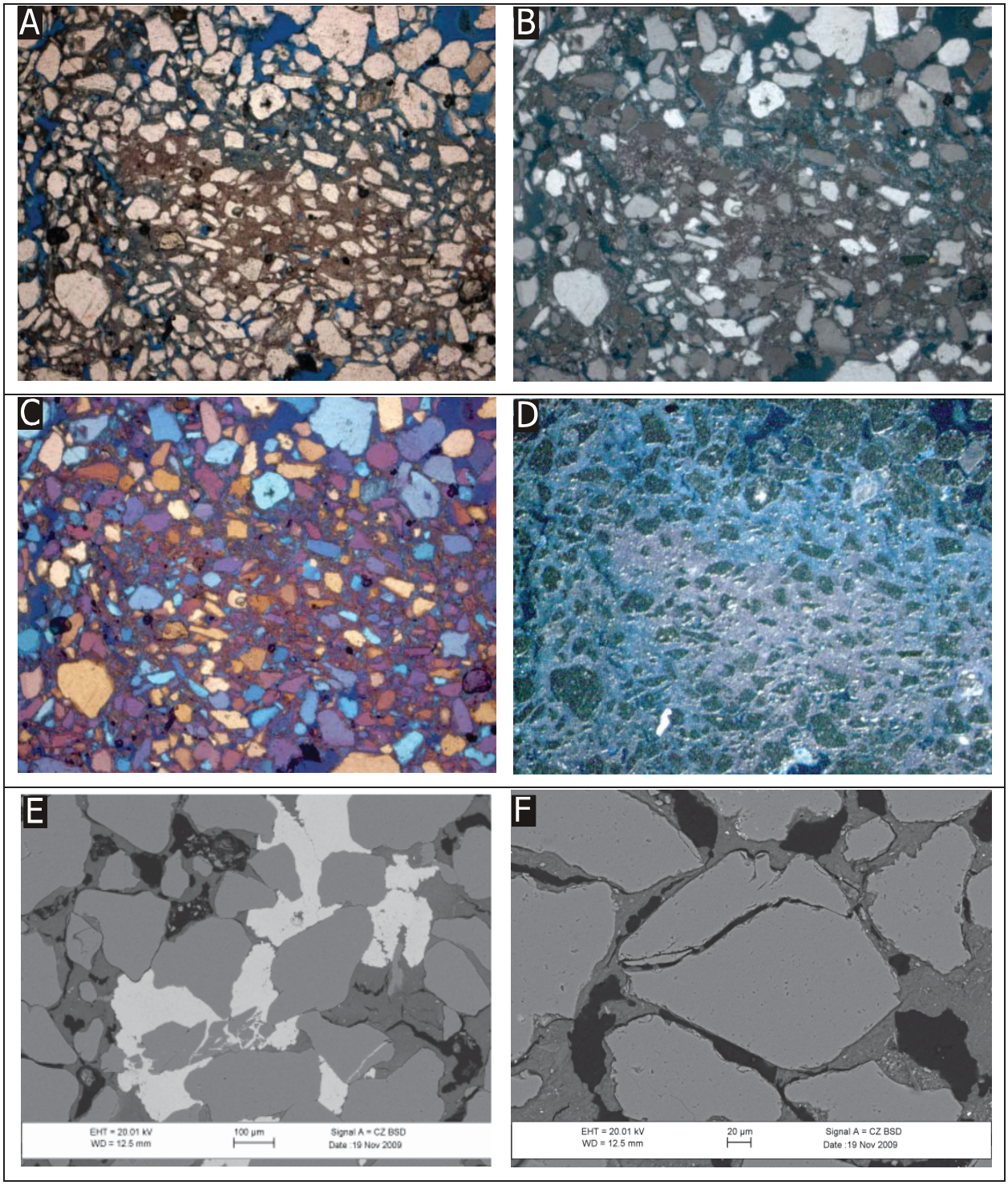

Plate 8.10: AW21 Core II of the Amir Wali Well; Friable sandstone having hematite staining to clay matrix and quartz grains are angular to subrounded (5x PPL). (B) AW21 (5X CN). (C) AW21 (5x QCN). (D) AW21 (5x RL). (E) AW21: Quartz grains are cemented by siderite and kaolinite. (SEM back scattered electron image). (F) AW21: Quartz grain is fractured and surrounded by kaolinite, a little kaolinite can be seen in fracture which indicates kaolinite precipitated after fracturing (SEM back scattered electron image). PPL: Plane polarized light; CN: Crossed nicols; QCN; Crossed nicols with additional lambda plate; RL: reflected light. Width of each thin section photograph (A to D) is 2.25 mm.

9. ORGANIC GEOCHEMISTRY OF THE WELLS

9.1 TOTAL ORGANIC CARBON (TOC) AND ROCK-EVAL ANALYSIS

The samples are characterized by very poor to moderate total organic carbon contents (TOC) in the Ali Sahib Well (between 0.09 and 2.26 wt. %), and comparable TOC values (0.09 to 2.33 wt. %) in the Amir Wali Well (Table 9.1 & 9.2). The sampled formations do not show systematic differences in TOC. Enhanced TOC contents are found in shaly and marly horizons of the Chichali Formation and in the limestones of the Samana Suk Formation.

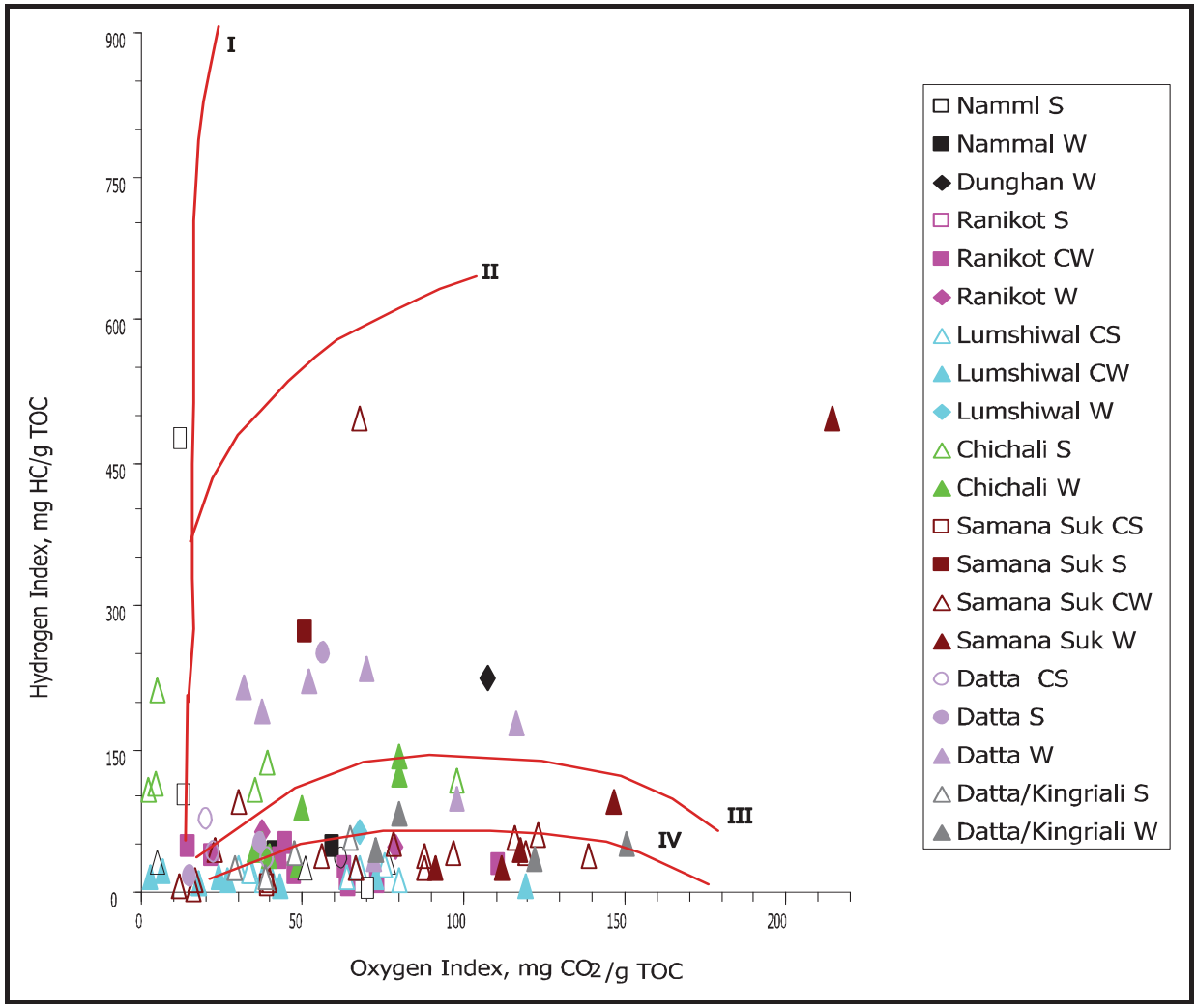

Fig. 9.1A: Hydrogen Index versus Oxygen Index of the Ali Sahib and Amir Wali wells. W: Ditch cuttings of the Amir Wali Well, CW: Core of the Amir Wali Well, S: Ditch cuttings of the Ali Sahib Well, CS: Core of the Ali Sahib Well.

Hydrogen Index (HI) versus Oxygen Index (OI) in Fig. 9.1A or hydrogen Index (HI) versus temperature of maximum pyrolysis yield (T_{max} in Fig. 9.1B), values classifies the organic matter in the selected samples from the Ali Sahib and Amir Wali wells as Type III kerogen with transition to Type II. According to Hunt (1996), it is difficult to discriminate among and to evaluate source rocks with HI values between 100 and 400 mg HC/g TOC. All samples are immature to marginal mature (Fig. 9.1B). The HI values range from 3 to 250 mg HC/g TOC (Table 9.1). Because of relatively low TOC contents, a mineral-matrix effect cannot be excluded. In order to test this assumption, S2 (Hydrocabons cracked from kerogen) is plotted versus TOC in Fig. 9.2 (Langford and Blanc-Valleron, 1990). The equation of the correlation line for the Datta/Kingriali Formations suggests that the "true" HI is 212 mg HC/g TOC. No correlation has been found for the other formations (Fig. 9.2), probably due to variations in S2, caused by differences in kerogen-type beside the mineral matrix effect.

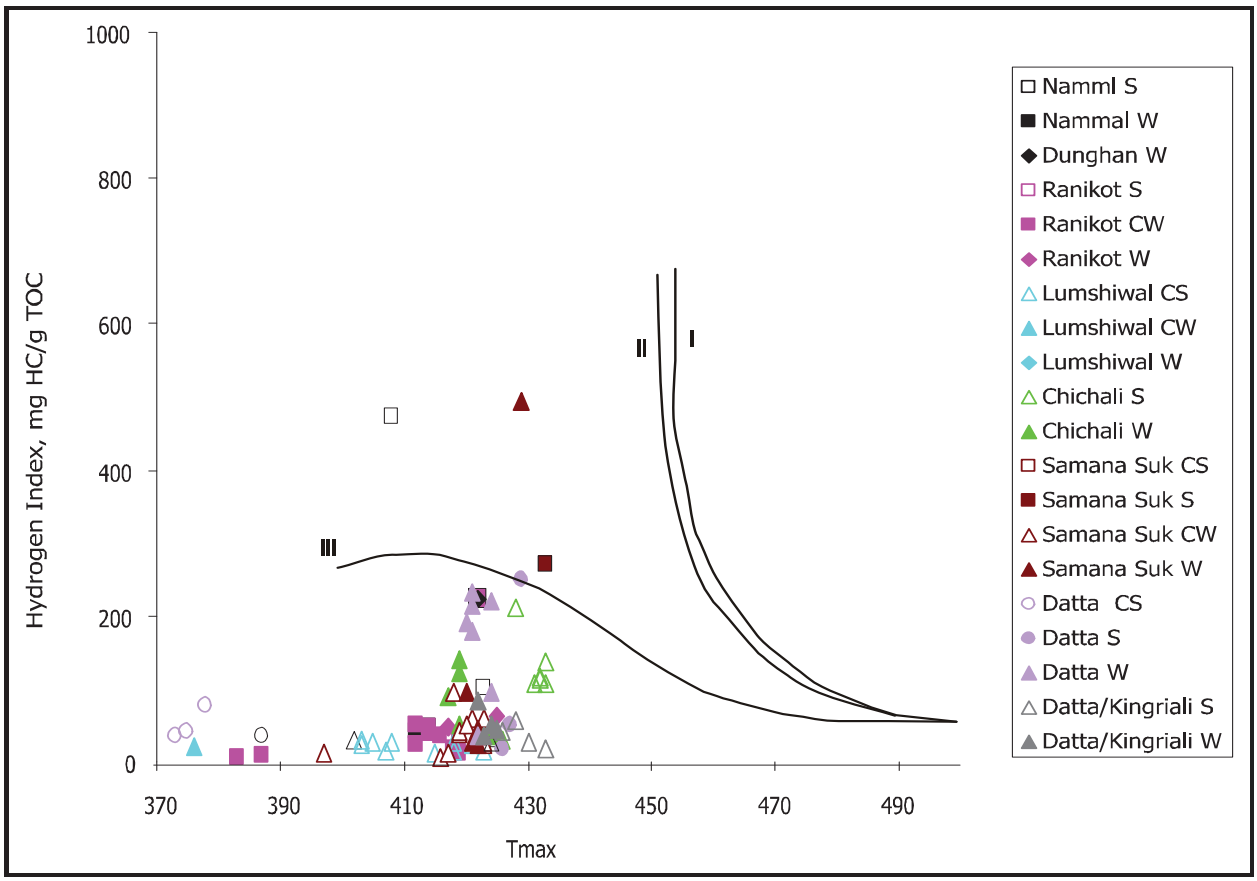

Fig. 9.1B: Hydrogen Index Versus Oxygen Index of the Ali Sahib and Amir Wali wells. W: Ditch cuttings of the Amir Wali Well, C W: Core of the Amir Wali Well, S: Ditch cuttings of the Ali Sahib Well, C S: Core of the Ali Sahib Well.

After correction for the maximum mineral matrix effect in the TOC versus S2 diagram (Fig. 9.2), only few of the samples from the Datta and Chichali Formations reach the geochemical parameters describing a fair generative potential for gas and oil (Peters, 1986). Seven samples including shales, sandstone and marly series of the Chichali Formation (Cretaceous), having TOC values ranging from 1.0 to 1.8 wt. % and HI values ranging from 29 to 212 mg HC/g TOC, are encouraging for a hydrocarbon source rock perspective. The Rock-Eval data of these samples are indicative of a mixture of marine and terrestrial material and are suggested as oil and gas prone. The occurrence of oil condensate in the Sarai Sidhu Well from the Samana Suk Formation raised the idea that this formation can also be considered as a source rock for gas. However, based on the studied samples no source rock potential can be attested to this Formation. Seven samples of the Datta Formation (Jurassic) show comparatively high HI values of 97 to 251 mg HC/g TOC. The OI ranges from 32 to 116 mg CO_2/g TOC (Fig. 9.1A, Table 9.1 & 9.2) which indicates terrestrial influence (Hunt, 1996). The TOC value of the Datta Formation ranges from 0.57 to 1.60 wt. %, indicating a fair hydrocarbon source potential.

Davis et al. (1989) demonstrated that oil fields can form from source rocks lacking high HI values. Distinguishing between type III (potential gas) and type IV (non-generative) kerogen is particularly difficult at low TOC values, because of the mineral matrix effect. He further argued that pyrolysis of low TOC samples (<1.5%) often results in lower HI and higher OI values. Oxygen Index values of samples low in TOC (< 2 wt.%) tend to be higher in high carbonate rocks containing siderite, arguing for a contribution of carbonate to OI (Orr, 1983). In the light of the above discussion, the Chichali Formation and the Datta Formation are considered as potential source rocks for hydrocarbons (oil and gas prone). Higher HI values are observed from the cuttings in comparison to the HI measured in the cores of the same formation. One possibility to explain the higher HI values of cutting samples is the possible contamination by materials from other formations.

Kerogen maturity can be determined by plotting HI versus T_{max} (Hunt, 1996). The petroleum generating range is considered between 430° C to 465° C T_{max}. The T_{max} varies with the type of kerogen as well as maturity, particularly in immature samples. It

has been reported by Peters (1986) that the variation in the T_{max} of immature samples would be up to 20° C due to difference in the type of organic matter. In Fig. 9.1B, it is obvious that a few samples lie in the range of 430° C to 465° C. All the core samples have low T_{max}-values. This is an indication that most of the samples are immature.

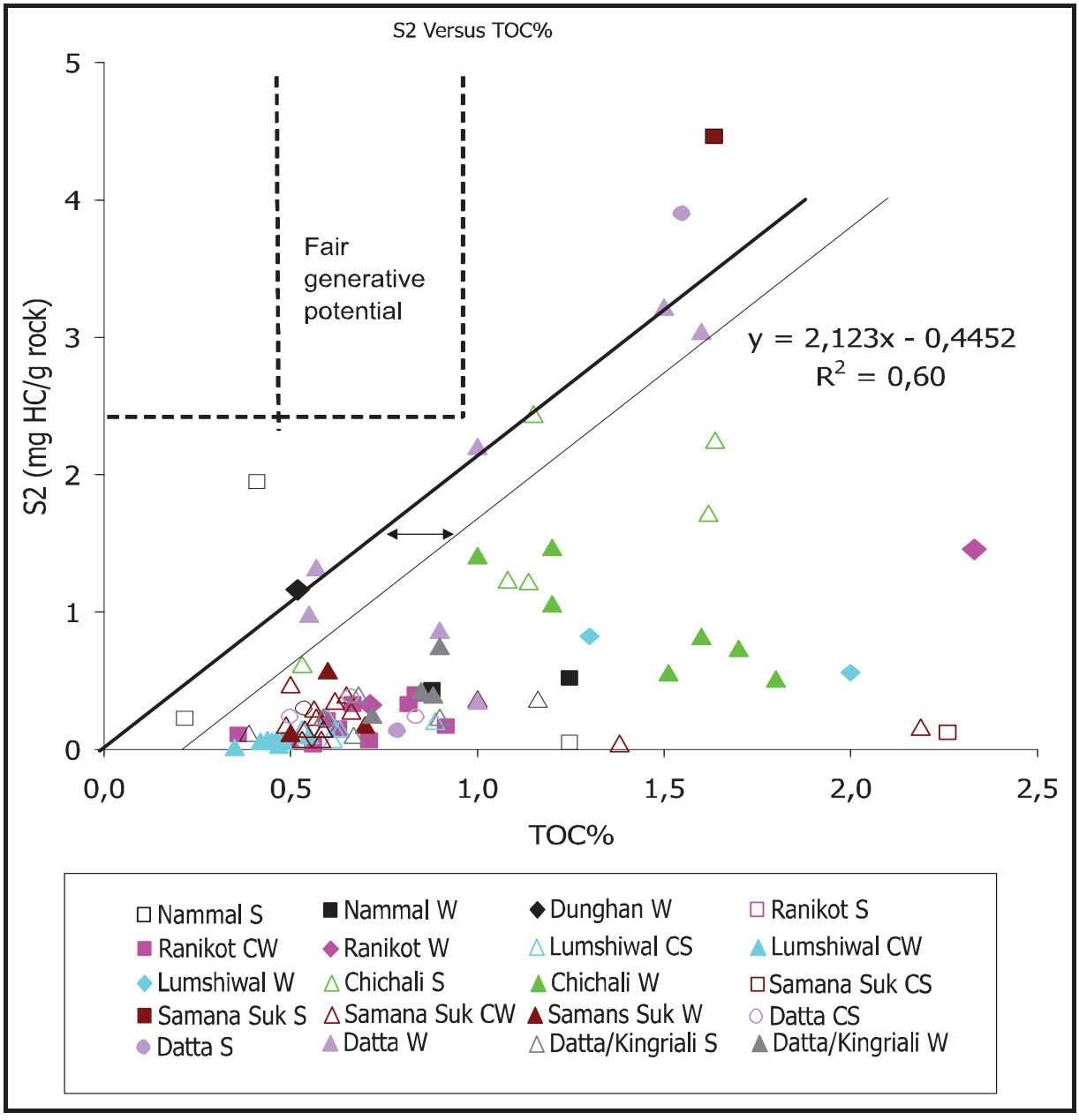

Fig. 9.2: Cross-plot of S_2 (mg HC/g rock) versus TOC. Parameters describing source rock generative potential are outlined (according to Peters, 1986).

The petroleum generating tendency is not good as the kerogen is of type III or IV and the T_{max} (419-433° C) is less than required for the onset of hydrocarbon generation.

A cross plot of TOC versus S1 (free hydrocarbons) was introduced by Hunt (1996) for the distinguishing of indigenous and non indigenous hydrocarbons. From Fig. 9.3, it is obvious that all the organic matter can be considered as indigenous and there is no indication for migrated hydrocarbons in the samples of the Amir Wali and the Ali Sahib wells. However, the Production Index (PI) of several samples exceeds 0.2 (Tab. 2), a value normally observed in mature source rocks or in the presence of migrated hydrocarbons.

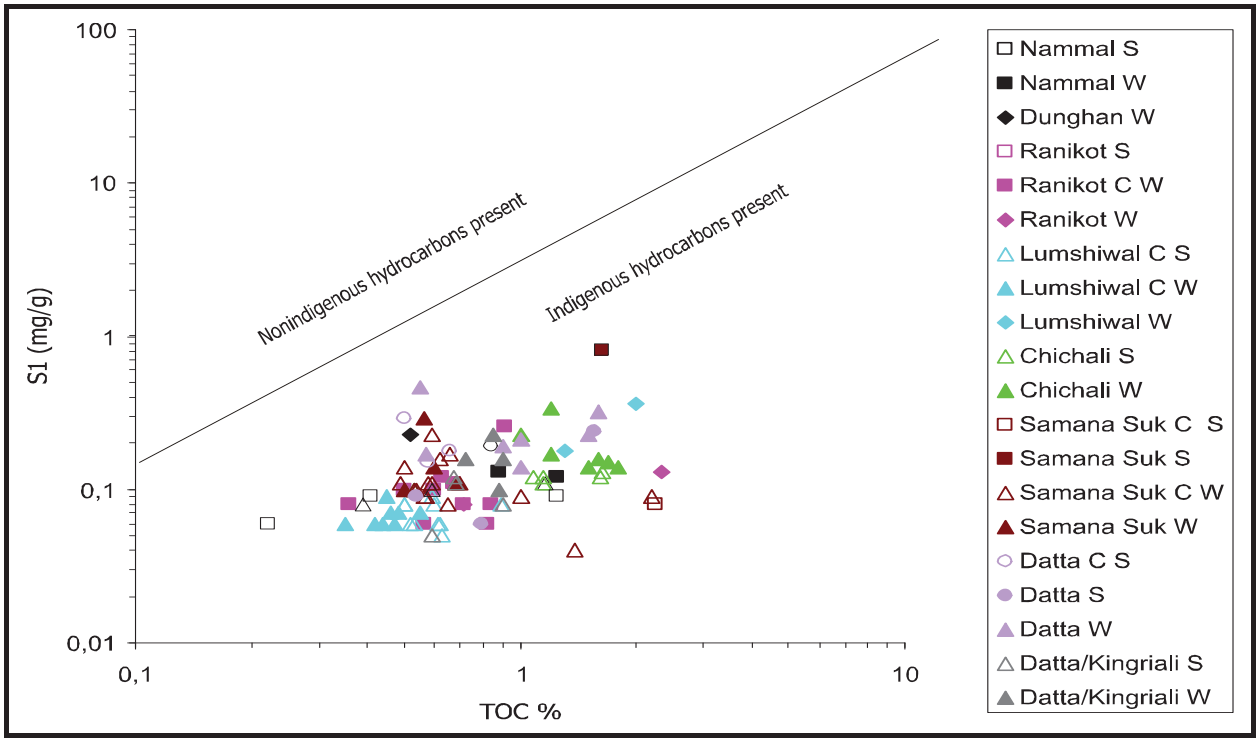

Fig. 9.3: Cross-plot of S_1 (mg free HC/g rock) versus TOC for the distinguishing of indigenous and nonindigenous hydrocarbons (Hunt, 1996). W: Ditch cuttings of the Amir Wali Well, C W: Core of the Amir Wali Well, S: Ditch cuttings of the Ali Sahib Well, C S: Core of the Ali Sahib Well.

9.2 BITUMEN CONTENT AND COMPOSITION

The normalized yields of the extractable organic matter (EOM) from the selected samples of the Ali Sahib Well (12 samples), and from the Amir Wali Well (26 samples) vary from 6 mg/g TOC (0.6 % in the Samana Suk Formation) to 163 mg/g TOC (16.3% in the Datta Formation). In general, the lithology of the samples with high contents of

bitumen extracted is claystone and the lithology of the samples with low contents of extracted bitumen is limestone (Table 9.3).

The bitumen content (EOM yield in % of TOC) of the Nammal Formation of Eocene (two samples) is 1.2 % to 1.8 % of TOC. The Ranikot Formation of Paleocene age (four samples) has the bitumen content from 0.6 % to 1.3 %. From the Lumshiwal Formation of Cretaceous age (two samples), bitumen was 0.9 % to 1.3 % of TOC. Thirteen samples were selected from the Chichali Formation of Cretaceous age. Six shaly samples (from the Ali Sahib Well) show bitumen contents from 0.8 % to 9.0 %, comparable to the normal bitumen content range (5-15 %, Hunt, 1996). While the other seven samples (from the Amir Wali Well), consist of sandtone, shale and marl and have lean to moderate extracted bitumen quantity (0.7 % to 2.9 %). The EOM yields from the rest of the sample set are lean to moderate (0.6 to 3.9 % of TOC). The bitumen content of the Datta Formation (8 samples) is moderate to good (0.6 % to 16.3 % of TOC).

The relative proportions of hydrocarbons of the EOM of the samples are highly variable (between 16 and 94%), and most samples yield relatively high proportions of hydrocarbons (> 25%) taking into account the low maturity (T_{max} < 430°C) of the organic matter (Table 9.3). The saturated hydrocarbon fractions predominate in most samples over the aromatic hydrocarbons. The NSO compounds (polar compounds plus asphaltenes) contribute between 6 and 84 % of the EOM (> 40% in most samples).

9.3 MOLECULAR COMPOSITION OF HYDROCARBONS

9.3.1 n-ALKANES AND ISOPRENOIDS

The *n*-alkane patterns of most of the samples from the Chichali Formation are dominated by short to mid-chain *n*-alkanes (< *n*-C_{25}). The long-chain *n*-alkanes (> *n*-C_{27}) contribute to less than 30 % of the total *n*-alkanes and do not show a marked odd over even predominance, as indicated by values of the Carbon Preference Index (CPI) close to 1.0 (Table 9.4; Fig. 9.6). The CPI was calculated from the concentrations of individual *n*-alkanes using the formula according to Bray & Evans (1961). Some samples show higher CPI values exceeding 1.5, but the long-chain *n*-alkanes in these samples

are of low abundance that may have resulted in erroneous CPI values (Fig. 9.7). Furthermore, these samples are characterized by an even over odd predominance in the C_{15} to C_{31} range. Together with the high relative contents of short-chain *n*-alkanes ($<C_{20}$), which are predominantly found in algae and microorganisms (Cranwell, 1977), an algal/microbial origin is proposed for the organic matter present in the samples (Fig. 9.5). Abundant branched alkanes (iso-, anteiso-, isoprenoidal-) argue for a high contribution of microbial biomass (Cranwell *et al.*, 1987).

The relative proportions of long-chain *n*-alkanes in samples from the Samana Suk and Datta Formations are highly variable (Figs. 9.8 & 9.9) but on average higher as compared to the samples from the Chichali Formation (Figs. 9.6 & 9.7). High proportions of long-chain C_{27}-C_{31} *n*-alkanes relative to the sum of *n*-alkanes are typical for vascular plants, where they occur as the main components of plant waxes (Eglinton & Hamilton, 1967). However, samples with higher amounts of long-chain *n*-alkanes do not show a marked odd over even predominance (Fig. 9.8). Enhanced CPI values are usually found in samples with immature terrestrial organic matter input (Cranwell, 1977). A mixed algal/bacterial and land plant origin is proposed for the organic matter in samples from the Samana Suk and the Datta Formations, as well as in samples from the Lumshiwal Formation (Fig. 9.10). CPI values are considered to have been possibly affected during bacterial reworking and/or maturation (Tissot & Welte, 1984).

Taking into account the low abundance of the acyclic isoprenoids pristane (Pr) and phytane (Ph) in several samples, which resulted in considerable errors in peak integration (standard deviation in the range of $\pm$ 0.2 to 0.3), the Pr/Ph ratios (between 0.5 and 3.5; Table 9.4) must be interpreted with care. According to Didyk *et al.* (1978), Pr/Ph ratios exceeding 3.0 are diagnostic for oxic environments, values between 1.0 and 3.0 indicate dysaerobic conditions during early diagenesis, and values below 1.0 were interpreted as reflecting anaerobic environments. Pristane/phytane ratios are also known to be affected by maturation (Tissot & Welte, 1984) and by differences in the precursors for acyclic isoprenoids (i.e. bacterial origin; Volkman & Maxwell, 1986; ten Haven *et al.*, 1987). An influence of different ranks on pristane/phytane ratios can be ruled out for the sample set. The Pr/Ph values between 1.0 and 3.0 of most samples are interpreted to be consistent with suboxic bottom water conditions and the input of

terrestrial organic matter into the basin. However, an archaeal origin of phytane as well as a contribution of tocopherols to pristane formation (Goossens *et al.*, 1984) cannot be excluded.

Shanmughan (1985), Connon & Cassou (1980), and Talukdar *et al.* (1993) classified the kerogen by cross plotting pristane/*n*-C17 versus phytane/*n*-C18 (Fig, 9.4). The mixed terrestrial marine source of organic matter in different Formations is supported from the cross plot. It is obvious from Fig. 9.4, that the Chichali Formtion and the Lumshiwal Formation (Cretaceous) were deposited in anoxic/reducing marine environment, whereas the Samana Suk and the Datta/Kingriali Formations (Jurassic to Triassic) were deposited in oxic environment. Low Pr/*n*-C_{17} and Ph/*n*-C_{18} ratios are most probably due to the immature character of organic matter, as comparable values have been found in low-rank coal seams (Bechtel *et al.,* 2007).

9.3.2 STEROIDS, TRITERPENOIDS

Only in few samples 5α, 14α, 17α, (H) C_{27} to C_{29} steranes dominating over the 5α, 14β, 17β, (H) steranes are found in low concentrations, insufficient for peak intergration. The C_{27}, C_{28} and C_{29} pseudohomologues are present in variable relative concentrations. The corresponding diasteranes could not be detected. The results are consistent with a mixed algal-terrestrial organic matter source. Algae are the predominant primary producers of C_{27} sterols, while C_{29} sterols are more typically associated with land plants (Volkman, 1986). However, numerous results from recent biomarker studies add to the growing list of micro algae that contain high proportions of 24-ethylcholesterol (Volkman *et al.*, 1999).

Hopanoids are the predominant constituents of the non-aromatic cyclic triterpenoids in all samples. The samples show similar patterns, characterized by the occurrence of 17α, 21β (H)-type hopanes from C_{27} to C_{33}, with C_{28} hopanes absent. The 17β, 21α (H) hopanes from C_{29} to C_{31} are present in low amounts. The predominant hopanoid is the $\alpha\beta$ -C_{30} hopane (Figs. 9.4-9.8). The most probable biological precursors of the hopanes are bacteriohopanepolyols (Ourisson *et al.*, 1979; Rohmer *et al.,* 1992). These compounds have been identified in aerobic bacteria and fungi, as well as in

cryptogames (e.g. ferns, moss) and most recently, sulfate-reducing bacteria (Blumenberg *et al.,* 2006). The ratio of the 22S/ (22S + 22R) isomers of the $17\alpha, 21\beta$ (H) C_{31} hopanes vary between 0.45 and 0.60 (Table 9.4), close to the equilibrium value of 0.6 (Mackenzie *et al.,* 1982). These values argue for a minimum thermal maturity equivalent to vitrinite reflectance values of 0.5% R_r (Mackenzie & Maxwell, 1981), consistent with the measured T_{max} values.

A pentacyclic triterpenoid of the ursane type was found in the non-aromatic hydrocarbon fractions of the samples from the Cretaceous Chichali Formation from the Ali Sahib Well (Fig. 9.7c). The compound was tentatively identified as urs-12.-ene (Philp, 1985). Non-hopanoid triterpenoids containing the structures typical of the oleanane skeleton, the ursane skeleton, or the lupane skeleton are known as biomarkers for angiosperms (Karrer *et al.*, 1977; Sukh Dev, 1989). These compounds are significant constituents of wood, roots, and bark (Karrer *et al.,* 1977).

9.3.3 AROMATIC HYDROCARBONS

In most samples, individual aromatic hydrocarbons are detected in considerable concentrations. The chromatograms are dominated by dimethyl- and trimethyl-naphthalenes, as well as methyl- and dimethyl-biphenyls (Fig. 9.11). Further constituents are phenanthrene, dibenzothiophene and methyl-phenanthrenes. Napthalene, phenanthrene and their methylated analogues derive from a variety of non-specific precursor compounds such as sesquiterpenoids, steroids and triterpenoids (Tissot & Welte, 1984).

The dibenzothiophene (DBT) / phenanthrene ratio (Table 9.4) reflects the amount of free hydrogen sulphide in the environment during organic matter deposition and/or early diagenesis. Information about the depositional environment of the respective source rocks can be provided from crude oil samples using a DBT/phenanthrene versus pristane/phytane diagram (Fig. 9.5; Hughes *et al.,* 1995). All samples fall into the fields characteristic for lacustrine sulphate-poor (Zone 2) or marine shales (Zone 3) as source rocks. As the organic matter has been also extracted from marine limestone and marl, some data points should plot into Zone 1b (Fig. 9.5). This discrepancy may indicate the

presence of free iron in the environment sufficient to bind the H_2S formed during bacterial sulphate reduction. However, the diagram was developed for the characterization of possible source rock lithologies from oil samples, and care must be taken when applying these relationships for classification of extractable organic matter from sediments.

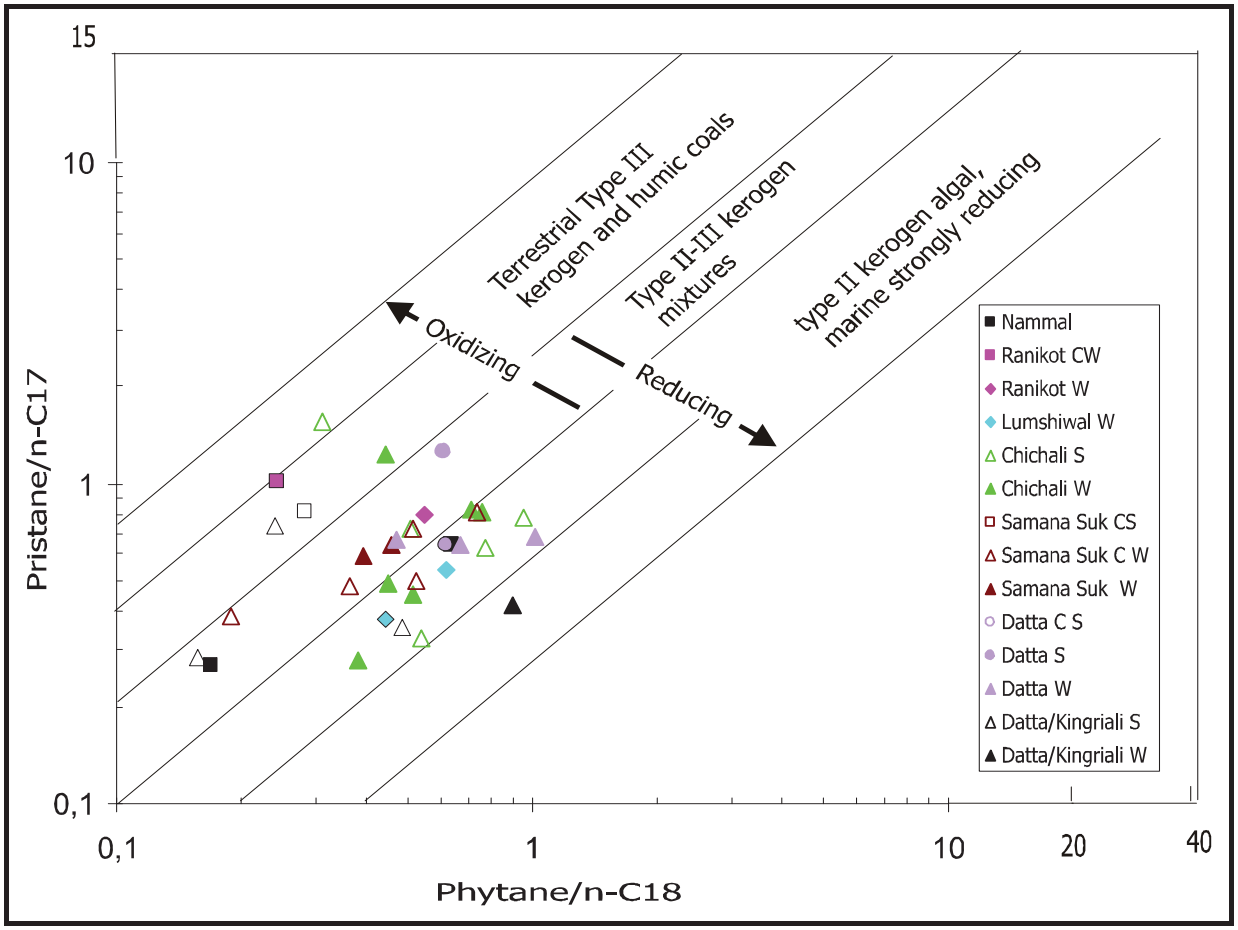

Fig. 9.4: Correlation diagram between pristine/n-17 and phytane/n-18 ratios of the Ali Sahib and Amir Wali wells (Connan & Cassou, 1980). W: Ditch cuttings of the Amir Wali Well, C W: Core of the Amir Wali Well, S: Ditch cuttings of the Ali Sahib Well, C S: Core of the Ali Sahib Well.

A well established maturity proxy used for type III kerogen is the methylphenanthrene index (MPI-1 = 1.5*[((2-MP) + (3-MP))/ ((P) + (1-MP) + (9-MP))]; Radke *et al.*, 1982). For organic matter of low thermal maturity (R_r <1.35%) the equation R_c = 0.6*MPI-1 + 0.4 allows calculation of equivalent vitrinite reflectance (Radke & Welte, 1983). In the samples investigated, the MPI-1 values range between 0.40 and 0.68 (Table 9.4). The average calculated vitrinite reflectance of R_c = 0.73% is higher than the values

estimated from T_{max} and the isomerisation of 17α, 21β (H) C_{31} hopanes (R_r in the range of 0.5 to 0.6%). This discrepancy most probably results from problems in peak area integration due to low intensities of methylphenanthrenes and overlapping peaks.

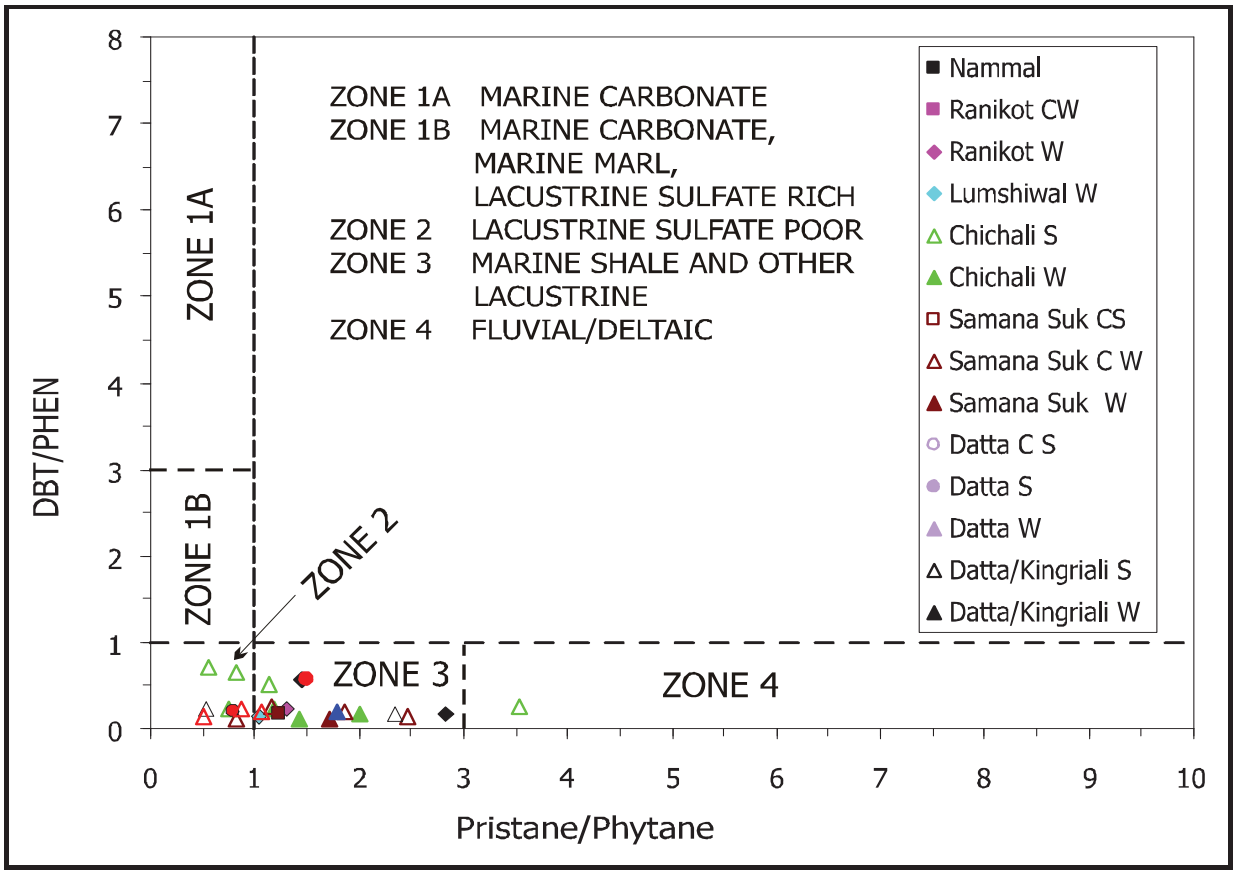

Fig 9.5: Cross-correlation of dibenzothiophene/phenanthrene versus pristine/phytane ratios of samples from the Ali Sahib and Amir Wali wells. Zones characteristic for oil samples from specific source rocks are outlined (according to Hughes *et al.,* 1995). W: Ditch cuttings of the Amir Wali Well, CW: Core of the Amir Wali Well, S: Ditch cuttings of the Ali Sahib Well, CS: Core of the Ali Sahib Well.

9.4 CONDENSATE AND GAS COMPOSITION OF NEIGHBORING WELLS

For the comparison with the molecular composition of hydrocarbons from EOM, the saturated and aromatic hydrocarbon fractions of a condensate sample from the Sarai Sidhu Well (cf. Ch. 1, Fig. 1.2) was included into this study. Beside a hump in the low boiling point range (9-30 min) of the chromatogram, sesquiterpenoids predominate in the saturated hydrocarbon fraction of the condensate (Fig. 9.12a). No *n*-alkanes could be detected. Identified compounds are drimane, homodrimane (Philp, 1985), and re-arranged drimanes (Nytoff *et al.*, 2009). These compounds are most probably derived

from drimenol of microbial origin (Alexander *et al.*, 1983), or reflect a higher plant contribution (Philp, 1994; Nytoff *et al.*, 2009). Additional C_{14}-sesquiterpanes and sesquiterpenes are present, but remaining was unidentified.

Beside a high contribution of unresolvable hydrocarbons in the low boiling point range (Fig. 9.12b), the aromatics consist of dimethyl- and trimethyl-1-alkylbenzenes, as well as trimethyl-dihydro-naphthalenes and the trimethyl- and tetramethyl-tetrahydro-naphthalenes possibly formed through the degradation of pentacyclic precursor molecules (Püttmann & Villar, 1987). The presence of the hump, as well as the absence of n-alkanes in the condensate is interpreted as a result of elevated biodegradation of light hydrocarbons derived from the cracking of petroleum. Sesquiterpenoids are known to be resistent against biodegradation and have been found in biodegraded crude oils (Bendoraitis, 1974).

Natural gas from the Bahu Well was found in Jurassic (Samana Suk) and Cretaceous (Lumshiwal) Formations. The gas composition is different in both lithologies; a higher wetness (C_1/C_2+C_3) is observed in the gas from Jurassic strata. Recently, the close association of dry gas with severely degraded oils has been explained by a common methanogenic biodegradation mechanism in subsurface degraded oil reservoirs (Jones et al., 2008). Wet gas biodegradation results in gases becoming dryer and oils haevier (Larter & di Primio, 2005). In the present case, the condensate may represent the degraded residue of methanogenic biodegradation responsible for the gas accumulations in the study area.

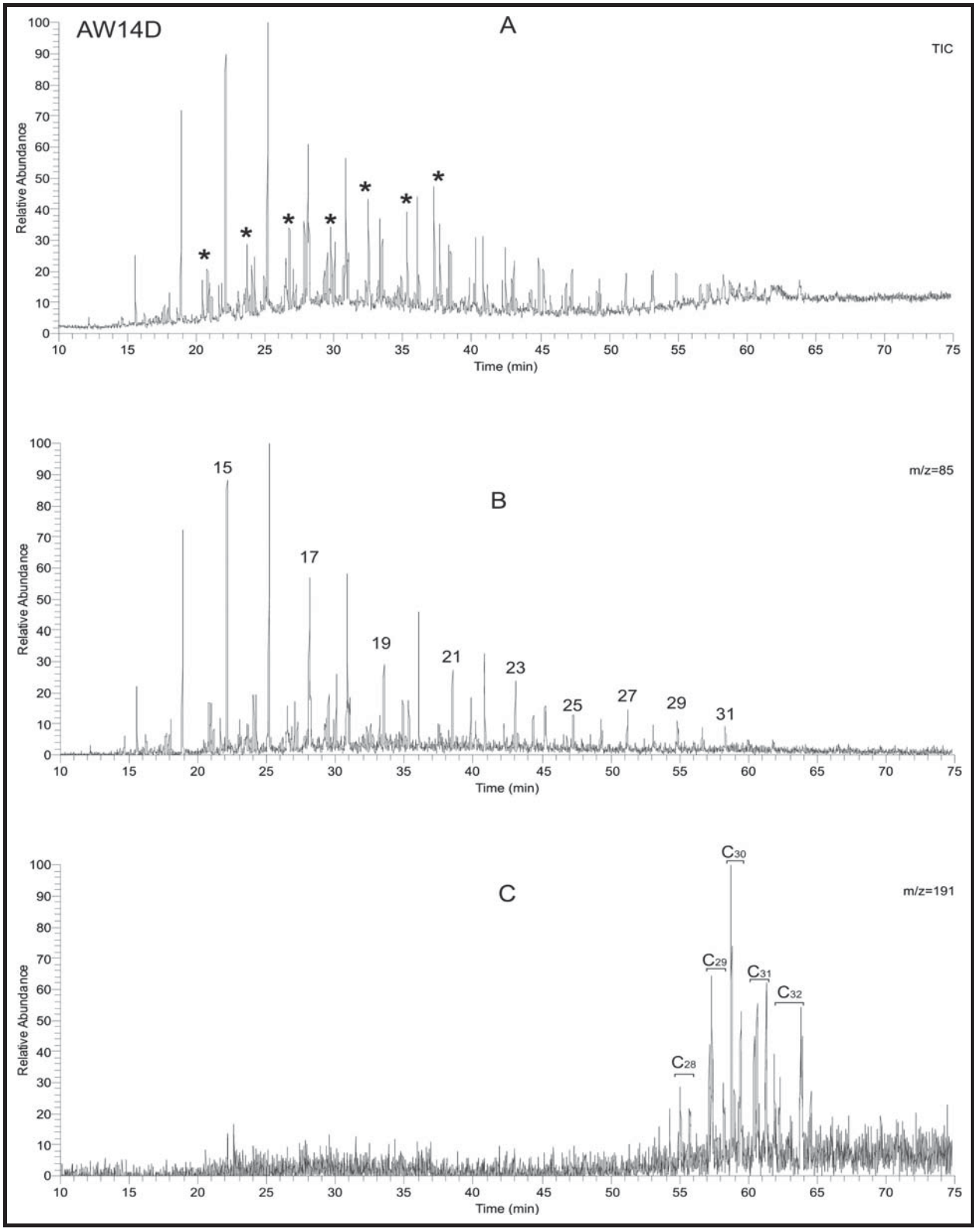

Fig. 9.6: (A) Gas chromatogram (total ion current) of the saturated hydrocarbon fraction of sample AW14D-1 (Cretaceous Chichali Formation). n-alkanes are labeled according to their carbon number; branched alkanes are marked by asterisks. (B) Mass chromatogram of m/z = 85 for n-alkanes. (C) Mass chromatogram m/z = 191 for triterpenoids. Characteristic hopanes are labeled.

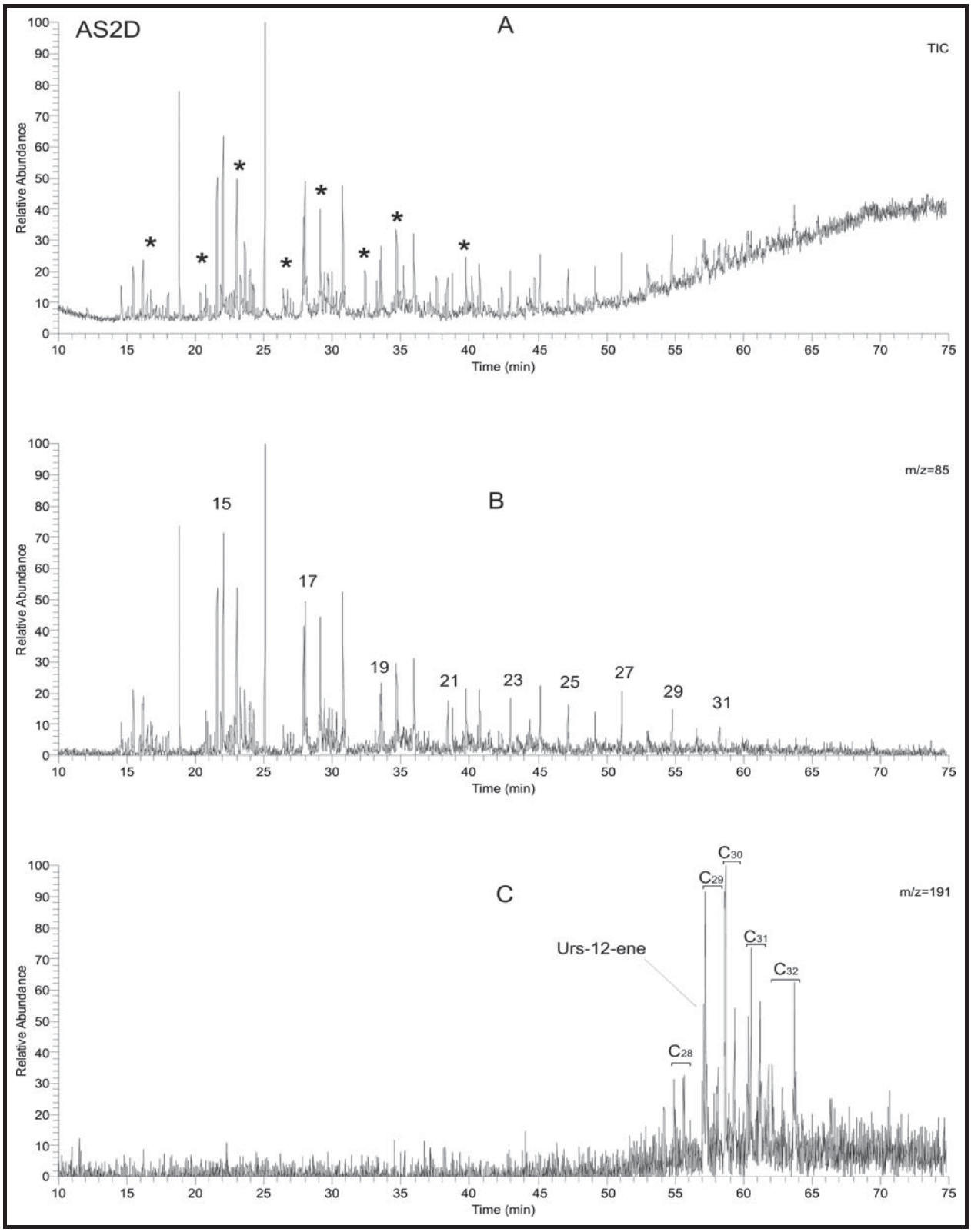

Fig. 9.7 :(A) Gas chromatogram (TIC) of the saturated hydrocarbon fraction of sample AS2D-1 (Cretaceous Chichali Formation). n-alkanes are labelled according to their carbon number; branched alkanes are marked by asterisks. (B) Mass chromatogram (m/z = 85) for n-alkanes. (C) Mass chromatogram (m/z = 191) for triterpenoids. Characteristic hopanes are labelled.

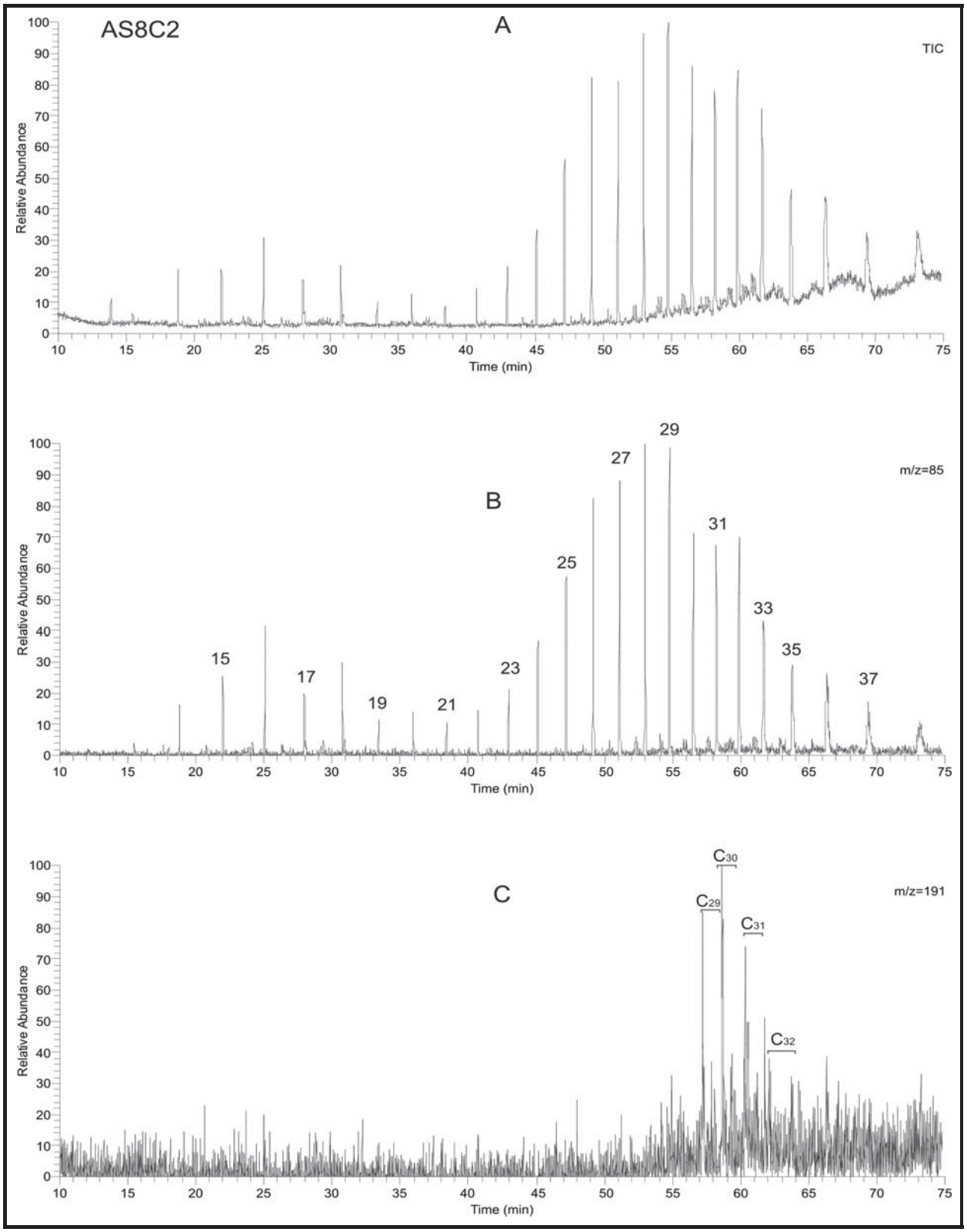

Fig. 9.8: (A) Gas chromatogram (TIC) of the saturated hydrocarbon fraction of sample AS8C-2 (Jurassic Samana Suk Formation.). (B) Mass chromatogram (m/z = 85) for n-alkanes (labelled according to their carbon number). (C) Mass chromatogram (m/z = 191) for triterpenoids.

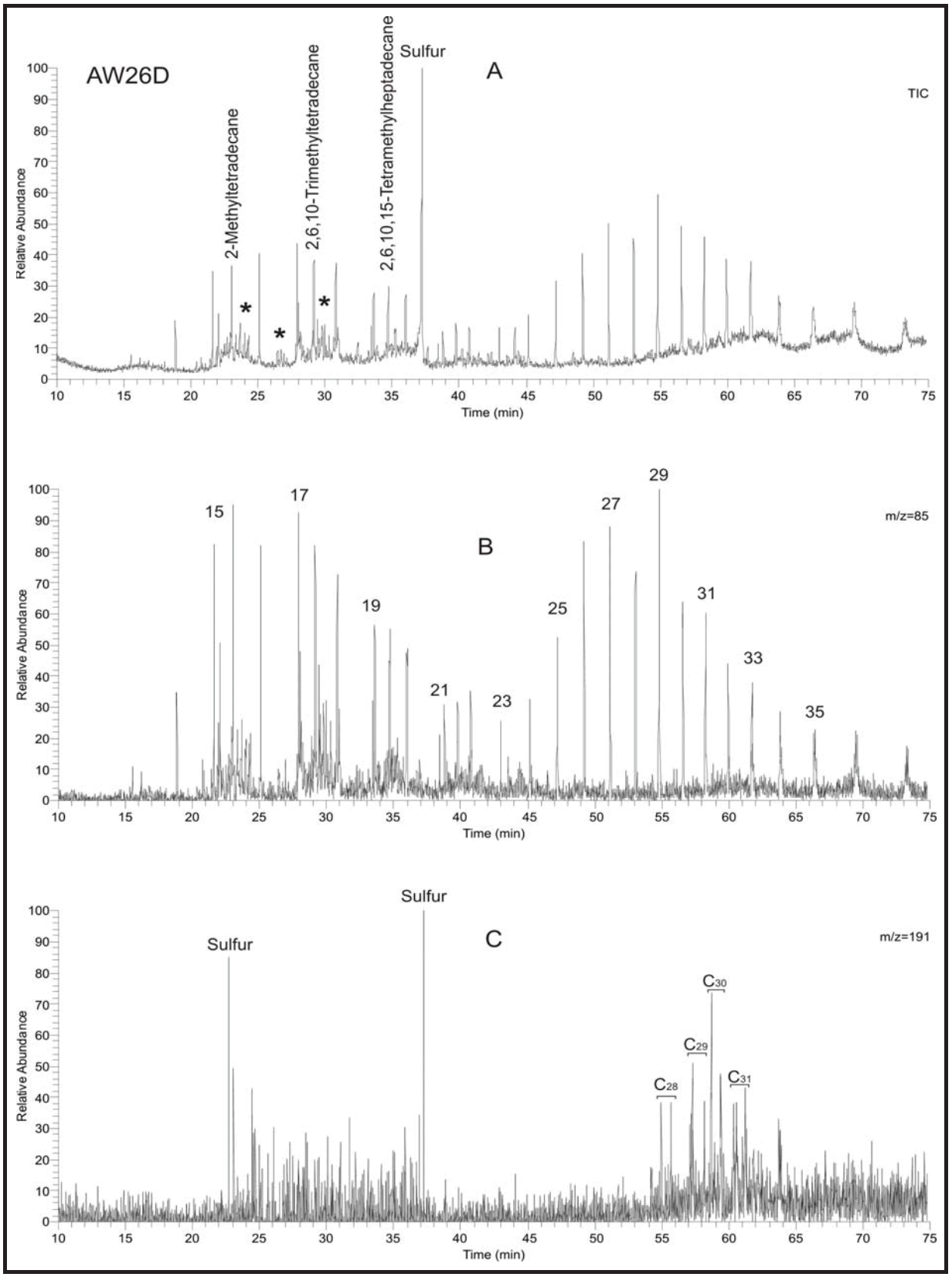

Fig. 9.9: (A) Gas chromatogram (TIC) of the saturated hydrocarbon fraction of sample AW26D-1 (Jurassic Datta Formation.). (B) Mass chromatogram (m/z = 85) for n-alkanes (labelled according to their carbon number). (C) Mass chromatogram (m/z = 191) for triterpenoids.

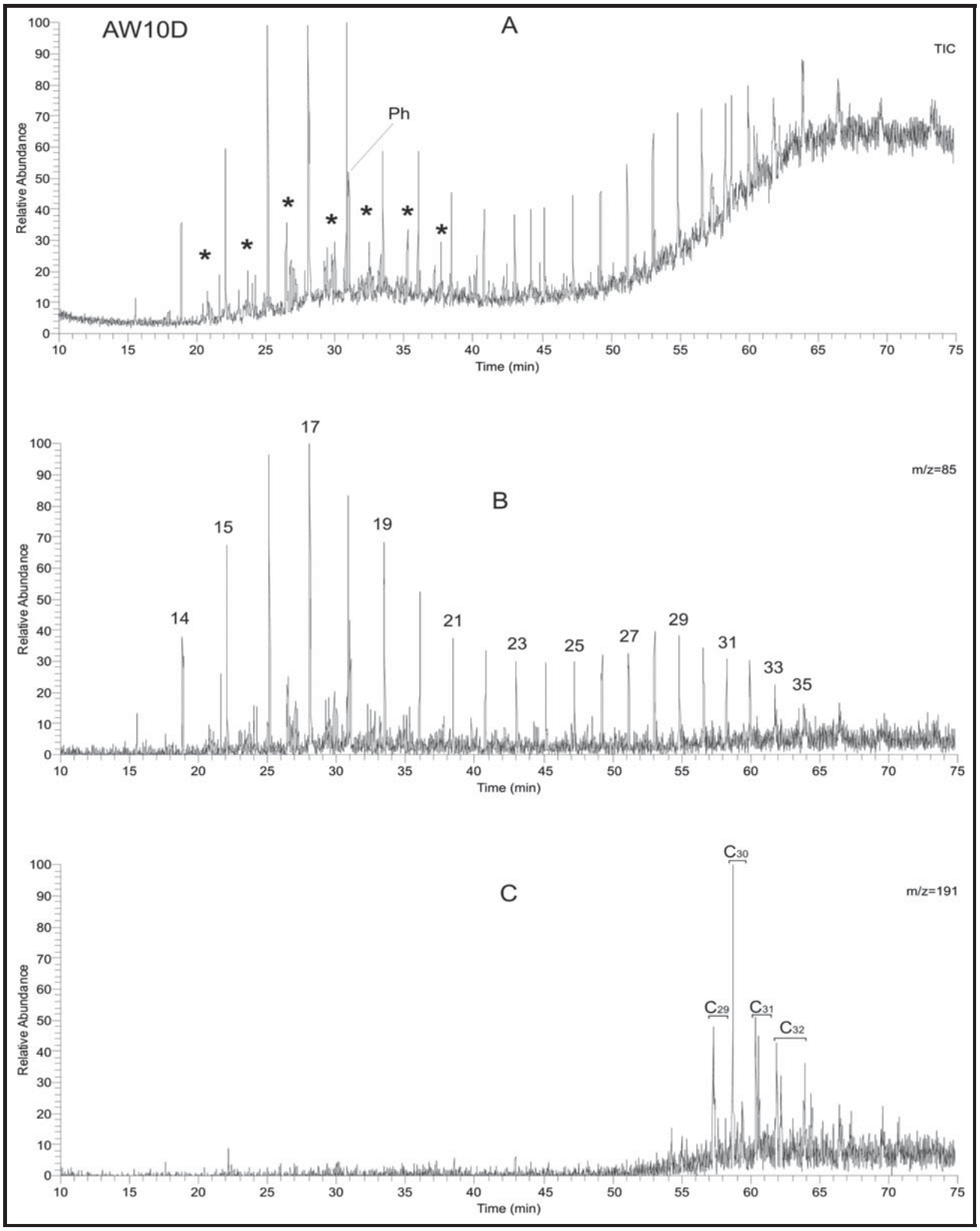

Fig. 9.10: (A) Gas chromatogram (TIC) of the saturated hydrocarbon fraction of sample AW10D-1 (Cretaceous Lumshiwal Formation.). Branched alkanes are marked by asterisks. (B) Mass chromatogram (m/z = 85) for n-alkanes (labelled according to their carbon number). (C) Mass chromatogram (m/z = 191) for triterpenoids.

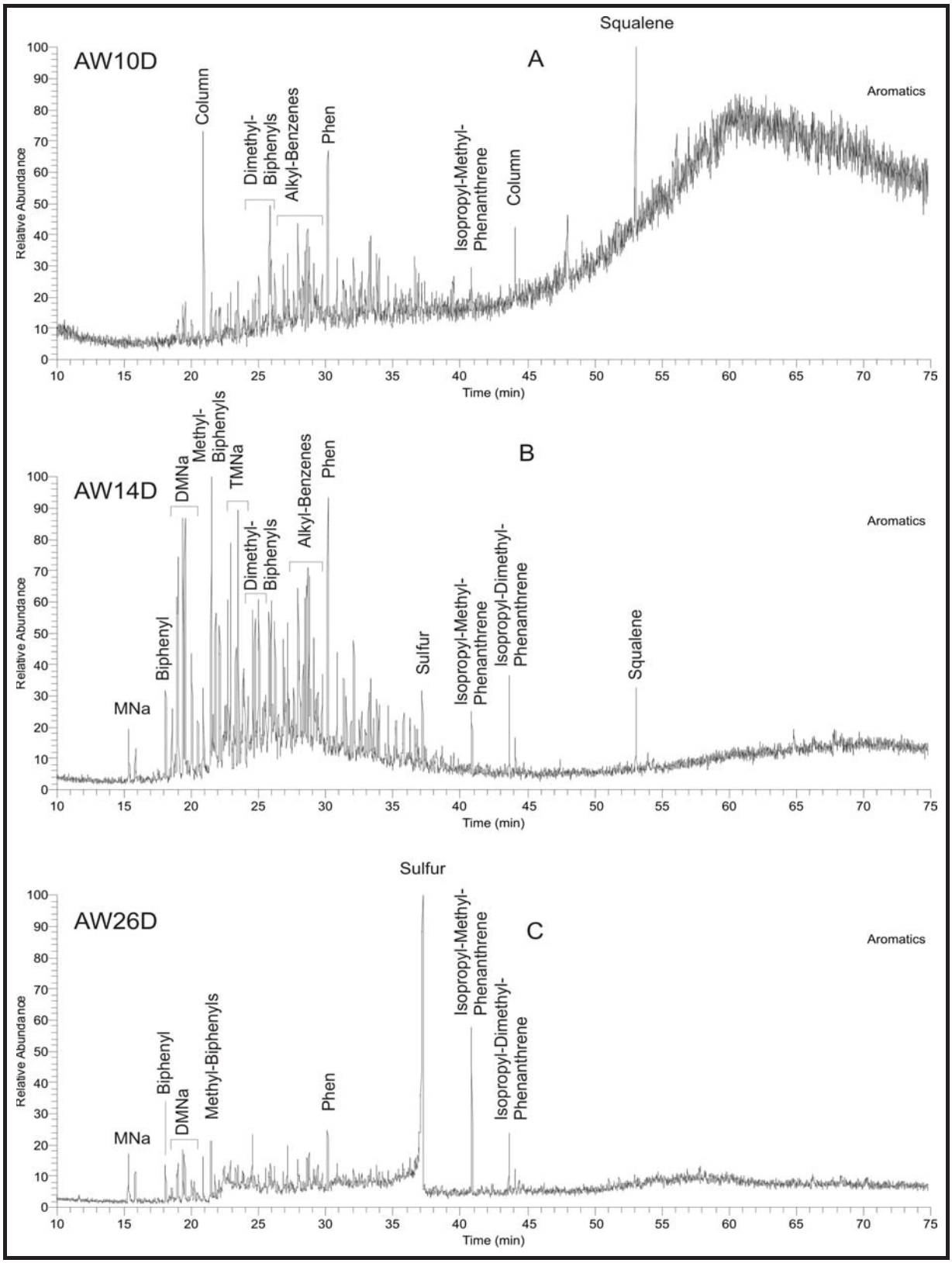

Fig. 9.11: Gas chromatograms (TIC) of the aromatic hydrocarbon fractions of (A) sample AW10D (Cretaceous Lumshiwal Formation.), (B) sample AW14D (Cretaceous Chichali Formation.), and (C) sample AW26D (Jurassic Datta Formation.). MNa = Methyl-Naphthalenes; DMNa = Dimethyl-Naphthalenes; TMNa = Trimethyl-Naphthalenes; Phen = Phenanthrene

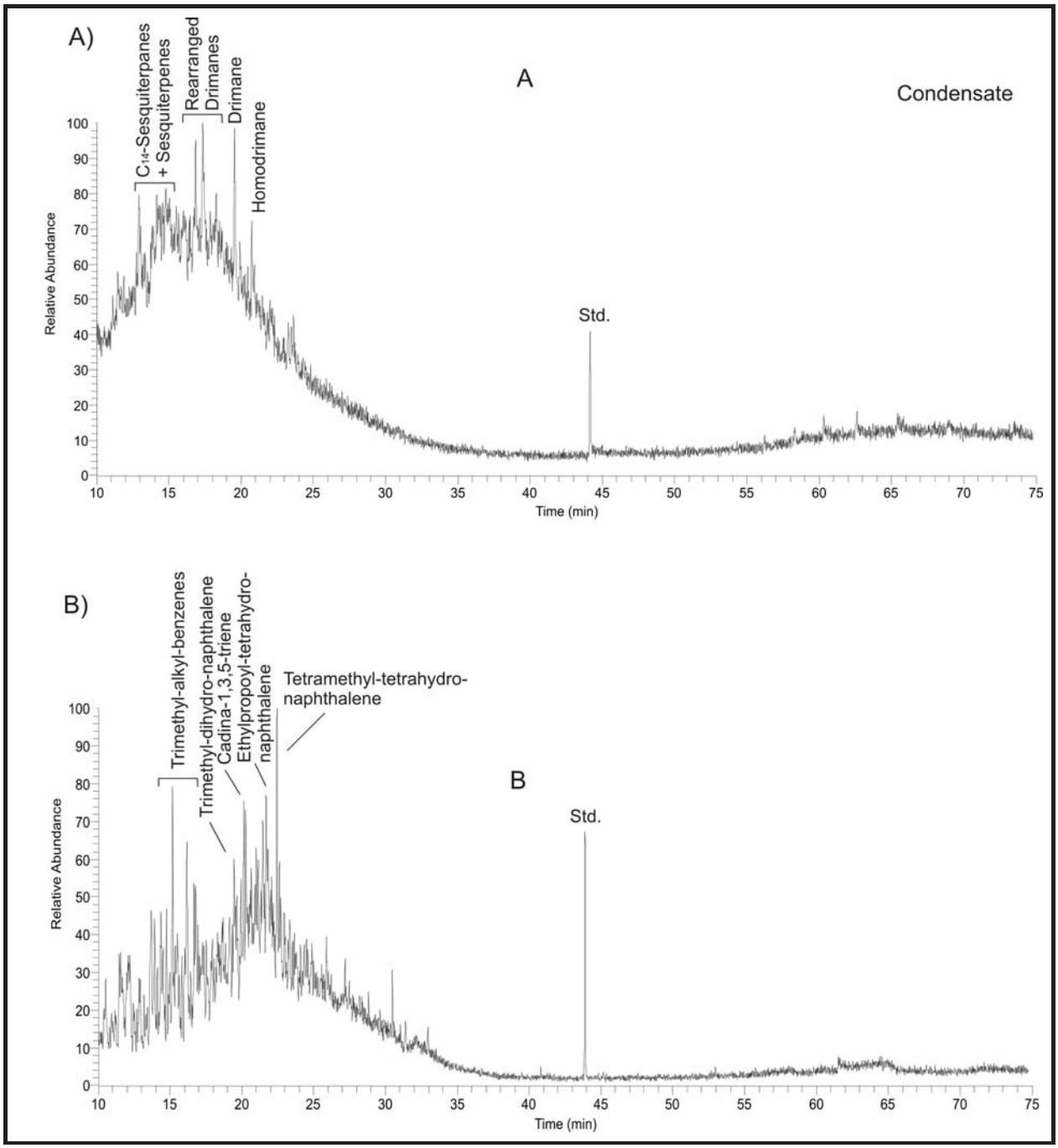

Fig. 9.12: Gas chromatograms (TIC) of (A) the saturated hydrocarbon fraction and (B) the aromatics of the condensate sample from the Sarai Sidhu Well. Identified sesquiterpenoids are labelled.

10. CONCLUSIONS & RECOMMENDATIONS

10.1 CARBONATES

The present work is based on the two wells Ali Sahib and Amir Wali in the Punjab Platform. This work can be subdivided into three parts: (A) Carbonates (B) Clastics (C) Organic Geochemistry.

In carbonates and clastics, core samples were used to study microfacies of carbonates and lithofacies of clastics. In organic geochemistry both ditch cuttings and core samples were used.

The sediments of Core I of the Ali Sahib Well consist of siliciclastics mixed with carbonates. The bored shells, encrusted crinoids and fragments of brachiopods are a characteristic feature of shallow marine carbonate sediments and approximately stable sea level but intermitted energy influx as indicated by the presence of quartz grains. No age determining fossil was found. Glauconite, pyrite and hematite are also present. The formation and age of the sediments can be assumed as it is assigned in the geological drilling order of the company, i.e. the Lumshiwal Formation of Cretaceous age. Cementation took place in early diagenesis and the main cement was calcite. Dolomite appears to be secondary in origin in these sediments.

Core I of the Amir Wali Well comprised also mixed siliciclastic with carbonate sediments. The well preserved bryozoa are a characteristic feature of this core. The age and species of the bryozoa is still in question, but its age can be assumed Paleocene as per geological drilling order of OGDCL. A shallowing upward sequence was found in the sediments of Core I of the Amir Wali Well. The intermitted high energy influx is denoted by the presence of quartz and broken shells. The well preserved bryozoa of shallow marine environment have been transported to deeper micrite matrix environment. The shallow marine environment is denoted by the presence of cortoids, ooids, peloids and black pebbles. Calcite is dominant cement. Glauconite occurs throughout the Core I of the Amir Wali Well.

Saccocoma and *Nautiloculina oolithica* were found in the sediments of Core II of the Ali Sahib Well. These two fossils are very important for biostratigraphy as these two indicate an Oxfordian to Tithonian age. *Saccocoma* indicates that the environment of deposition was deep marine. *Saccocoma* and its fragments were found in the nuclei of ooids which indicate that these ooids were formed in deeper marine environment instead of shallow marine. The age range of these fossils corresponds to the age of the Chichali Formation but the lithology and microfacies resemble to the Samana Suk Formation.

The sediments of Core III and the upper section of Core IV of the Amir Wali Well are correlatable with the sediments and biostratigraphy of the Core II of the Ali Sahib Well. In both places, *Saccocoma* and *Nautiloculina oolithica* were found which indicate an Oxfordian to Tithonian age of these sediments. *Saccocoma* was also found in the nuclei of micritic ooids indicating that the formation of these ooids is not shallow marine.

In the lower section of Core IV of the Amir Wali Well *Bositra* shells were found which are indicative of Middle Jurassic to Oxfordian age. The occurrence of *Bositra* shells is in agreement with the age of the Samana Suk Formation as Middle Jurassic. In these successions (Core III and Core IV of the Amir Wali Well), two shallowing upward sequences were found.

10.2 CLASTICS

Core III and Core IV of the Ali Sahib Well and Core II of the Amir Wali Well are comprised of siliciclastics sediments. In Core III of the Ali Sahib Well, the sediments are loose and friable. At places siderite is found, which can be indicative of reducing organic-rich marsh and swampy environment. Clay balls are another characteristic feature of these sediments. The sediments of Core III of the Ali Sahib Well appear to be deposited in fluvio-deltaic environment. According to the geological drilling order of OGDCL these sediments belonging to the Samana Suk Formation of Middle Jurassic age.

The sediments of Core IV of the Ali Sahib Well are comprised mainly of claystone with a small portion (at top) of quartz arenite. In claystone kaolinite is the dominant mineral.

The other subordinate minerals are siderite, hematite, anatase and illite. The formation of these sediments can be interpreted as the result of intense weathering in humid and hot environment in the provenance area. In geological drilling order of OGDCL, this formation has been included in the Datta Formation of Jurassic age.

In the upper section of Core II of the Amir Wali Well, the sediments are claystone. The presence of goethite can be interpreted as the oxidation of preexisting minerals in excess of moisture availability in the continental provenance area. A large quantity of organic carbon is also a very favourable agent in the formation of goethite. The presence of hematite in these sediments can be interpreted as result of oxidation at high average annual temperatures in the provenance area. In the lower portion of Core II of the Amir Wali Well, the sediments are quartz arenite. The occurrence of ankerite can be interpreted as it was formed in shallow burial. Clay minerals occur as matrix. According to OGDCL drilling order this section of the Amir Wali Well has been attached to cretaceous Lumshiwal Formation.

10.2.1 SIGNIFICANCE OF DAWSONITE AND BOEHMITE

The occurrence of dawsonite and boehmite in ditch cuttings from the Amir Well Well (from the Datta Formation of Jurassic age) can be interpreted of early diagenetic and terrigenous origin. High temperatures, deep diagenetic or hydrothermal origin of these minerals are unlikely because the organic matter below and above of these cuttings are submature to immature. In present case, the arkosic sediments, having a relatively quantity of Na in the formation water have played a main role to dawsonite formation. The clays which are rich in Na^+ and HCO^-_3, together with plenty of CO_2 formed by bacterial activity, can also play a role in the formation of dawsonite. The occurrence of boehmite can be attributed to the dehydration of gibbsite to boehmite due to intense weathering in a hot climate. Then boehmite, along with other sediments, was transported to the present position.

10.3 ORGANIC GEOCHEMISTRY

Rock-Eval pyrolysis data classify the organic matter of selected samples from Jurassic to Eocene strata, drilled in the Ali Sahib and Amir Wali wells (Punjab Platform, Pakistan),

as Type-III kerogen with transition to Type-II. Samples from the Chichali (Cretaceous) and the Datta Formation (Jurassic) reach the parameters describing a fair generative potential for oil and gas. However, all samples are immature to marginal mature, outlining a low petroleum generating tendency. No indications for migrated hydrocarbons are present. The bitumen content of some samples from the Chichali and Datta Formations is moderate to good.

Based on the high relative contents of short-chain *n*-alkanes ($<C_{20}$), an algal/microbial origin is proposed for the organic matter, present in the samples from the Chichali Formation. Abundant branched alkanes (iso-, anteiso-, isoprenoidal-) argue for a high contribution of microbial biomass. A mixed algal/bacterial and land plant origin is proposed for the organic matter in samples from the Lumshiwal, Samana Suk and Datta Formations. Low CPI values of these samples are considered as a result of bacterial reworking. The cross plot of pristane/*n*-C_{17} versus phytane/*n*-C_{18} ratios, suggests an anoxic/reducing marine environment during deposition of the Chichali and the Lumshiwal Formation (Cretaceous), whereas the Samana Suk and Datta/Kingriali Formation (Jurassic to Triassic) were deposited under oxic to dysoxic conditions.

Hopanes, derived from bacteriohopanetetrol found in bacteria and funghi, are the predominant constituents of the non-aromatic cyclic triterpenoids in all samples. The isomerisation of the $17\alpha, 21\beta$ (H) C_{31} hopanes is close to the equilibrium value of 0.6, arguing for a minimum thermal maturity, equivalent to vitrinite reflectance values of 0.5% R_r. The pentacyclic triterpene urs-12-ene, a biomarker for angiosperms, was identified in the Cretaceous Chichali Formation from the Ali Sahib Well.

Based on the DBT/phenanthrene versus pristane/phytane diagram, all samples fall into the fields characteristic for lacustrine sulfate-poor or marine shales, regardless of the origin of the extractable organic matter including marine limestones and marly sequences. Probably, sufficient free iron was present in the environment to bind the H_2S formed during bacterial sulfate reduction. The methylphenanthrene index (MPI-1) ranges between 0.40 and 0.68. The average calculated vitrinite reflectance of R_c = 0.73% from MPI-1 is higher than the values estimated from T_{max} and the isomerisation of $17\alpha, 21\beta$ (H) C_{31} hopanes (R_r in the range of 0.5 to 0.6%).

The presence of a hump in the saturated and aromatic hydrocarbon fractions of a condensate sample from the Sarai Sidhu Well, as well as the absence of *n*-alkanes and the presence of high relative amounts of sesquiterpanes, are interpreted as a result of elevated biodegradation of light hydrocarbons derived from the cracking of petroleum. Sesquiterpenoids are known to be resistent against biodegradation and have been found in biodegraded crude oils. Rearranged drimanes are considered to have been derived from the degradation of pentacyclic triterpenoids found in angiosperms. As urs-12-ene has been identified in the Chichali Formation, a possible origin of the condensate from this Formation is proposed.

Based on the present data, oil and condensate must have been formed deeper in the Punjab Basin, most probably from mature sediments of the Chichali or Datta Formation. The composition of natural gas derived from Jurassic (Samana Suk) and Cretaceous (Lumshiwal) Formations in the Bahu Well reflects a higher wettness (C_1/C_2+C_3) in the Jurassic strata. Based on recent concepts about a common methanogenic biodegradation mechanism in subsurface oil reservoirs, including wet gas biodegradation, the condensate may represent the residue of biodegradation responsible for the gas accumulations in the study area.

10.4 RECOMMENDATIONS

1. Cores from Cretaceous to Jurassic (particularly the Lumshiwal Formation and the Samana Suk Formation) must be gained for investigation, in order to establish the environment of deposition in the Punjab Platform.
2. Biostratigraphy of the Samana Suk Formation and the Chichali Formation may be established by using the *Saccocoma, Nautiloculina oolithica* and other late to Middle Jurassic fauna in the Punjab Platform.
3. Bryozoa found in Core I of the Amir Wali Well need further investigation.
4. Very limited samples and poor core recovery from sandstone horizons from both wells was a hinder to establish lithofacies and diagenesis. Studies of full core recovery would be helpful in establishing characteristics of diagenesis and depositional environment of the Punjab Platform.

5. Biomarker studies of the older Formations would be very important in order to establish the source rock characteristics.
6. Though we can measure the porosity by cutting core plugs and by different logs (at well site), it seems to be equal essential to observe the porosity under microscope.

References

Abrajevitvh, A., Voo Van der, R. & David K. Rea, 2009. Variations in relative abundances of goethite and hematite in Bengal Fan sediments: Climatic vs. diagenetic signals. Marine Geology, 267, pp. 191-206.

Adams, J. E. & Rhodes, M. L., 1960. Dolomitization by seepage refluxion. Amer. Ass. Petrol. Geol. Bull., 44, pp. 1912-1920.

Ahmad, R. & Ali, S. M., 1991. Tectonic and structural development of the eastern part of Kirthar Fold Belt and its hydrocarbon prospects. Pak. J. Hydrocarbon Res., pp. 19-32.

Alexander, R., Kagi, R. & Noble, R., 1983. Identification of the bicyclic sesquiterpenes Drimane and Eudesmane in petroleum. J. C. S. Chem. Comm., pp. 226-228.

Ambers, C. P. & Petzold, D. D., 1996. Geochemical and petrologic evidence of the origin and diagenesis of a Late Mississippian, supratidal dolostone. Carbonates Evaporites, 11, pp. 42-58,

Amri, D. Tanfous, Soussi, M., Bedir, M. & Azaiet, H., 2008. Seismic sequence stratigraphy of the Jurassic of the central Atlas, Tunisia. Journal of African Earth Sciences, 51, pp. 55-88.

Ashraf, M. & Gakkhar, R. A., 2005. Nannofossil biostratigraphy and lithostratigraphy of the Ali Sahib Well #01, District Khanewal, Punjab Province. (G.R. Lab Note No. 444, unpublished data of OGDCL).

Aubrecht, R., Schlögl, J., Krobicki, M., Wierzbowski, H., Matyja, B. A. & Wierzbowski, A., 2009. Middle Jurassic stromatactis mud-mounds in the Pieniny Klippen Belt (Carpathians) - A possible clue to the origin of stromatactis. Sedimentary Geology, 213, pp. 97-112.

Baker, J. C., 1991. Diagenesis and reservoir quality of the Aldebaran sandstone, Denison Trough, east central Queensland, Australia. Sedimentology, 38, pp. 819-838.

Baker, J. C., Bai, G. P., Hamilton, P. J., Golding S. D. & Keene, J. B., 1995. Continental-scale magmatic carbon dioxide seepage recorded by dawsonite in the Bowen-Gunnedah-Sydney basin system, Eastern Australia. Journal of Sedimentary Research, A65, pp. 522-530.

Balakrishnan, T. S., 1977. Role of geophysics in the study of geology and tectonics. Geophysical case histories of India. AEG 1, pp. 9-27.

Balme, B. E., 1970. Palynology of Permian and Triassic strata in the Salt Range and Surghar Range, West Pakistan. In: Kummel, B. & Teichert, C. (eds.) Stratigraphic Boundary Problems: Permian and Triassic of West Pakistan. University of Kansas, Geological Department Spec. Publ., 4, pp. 305-454.

Bechstädt, T. & Dohler-Hirner, B., 1983. Lead-Zinc deposits of Bleiberg-Kreuth. In: Scholle, P. A., Bebout, D. G. & Moore, C. H. (eds.) Carbonate depositional environments. Amer. Ass. Petrol. Geol. Mem., 33, pp. 55-63.

Bechtel, A., Hámor-Vido, M., Sachsenhofer, R. F., Reischenbacher, D., Gratzer, R. & Püttmann, W., 2007. The middle Eocene Márkushegy subbituminous coal (Hungary): Paleoenvironmental implications from petrographical and geochemical studies. Int. J. Coal Geol., 72, pp. 33-52.

Bendoraitis, J. G., 1974. Hydrocarbons of biogenic origin in petroleum aromatic triterpenes and bicyclic sesquiterpenes. In: Tissot, B., Bienner, F. (eds.), Advances in Organic Geochemistry 1973, Editions Technip, Paris, pp. 209-224.

Benito, M. I., de la Horra, R., Barrenchea, J. J., López-Gómez, J., Rodas, M., Alonso-Azcárate, Arche, J. A. & Luque, J., 2005. Late Permian continental sediments in the SE Iberian Ranges, eastern Spain: petrological and mineralogical characteristics and palaeoenvironmental significance. Palaeogeography, Palaeoclimatology, Palaeoecology, pp. 24-39.

Bernet, M., Kapoutsos, D. & Bassett, K., 2007. Diagenesis and provenance of Silurian quartz arenites in south-eastern New York State. Sedimentary Geology, 201, pp. 43-55.

Birkeland, W. Peter & Larson, E. Edwin, 1989. Putnam´s Geology (5th ed). University press, Oxford, 646 pp.

Bjørlykke, K., 1998. Clay mineral diagenesis in sedimentary basins - a key to the prediction of rock properties. Examples from the north Sea Basin. Clay Miner., 33, pp. 15-34.

Blanford, W. T., 1876. On the geology of Sind. Geological Survey of India, Rec., 9(1), pp. 8-22.

Blanford, W. T., 1879. On the geology of Western Sind (second notice). Geological Survey of India, Rec., 17(1), pp. 1-210.

Blumenberg, M., Krüger, M., Nauhaus, K., Talbot, H. M., Oppermann, B. I., Seifert, R., Pape, T. & Michaelis, W., 2006. Biosynthesis of hopanoids by sulfate-reducing bacteria (genus *Desulfovibrio*). Environmental Microbiology, 8, pp. 1220-1227.

Boles, J. R. & Franks S. G., 1979. Clay diagenesis in Wilcox Sandstones of Southwest Texas: implications of smectite diagenesis on sandstone cementation. Journal of Sedimentary Petrology, pp. 55-70.

Bordenave, M. L., Espitalié, J., Leplat, P., Oudin J. L. & Vandenbroucke, M., 1993. Screening techniques for source rock evaluation. In: M.L. Bordenave, (ed.), Applied Petroleum Geochemistry, Editions Technip, Paris, pp. 219-278.

Bray, E. E. & Evans, E. D., 1961. Distribution of n-paraffins as a clue to recognition of source beds. Geochimica et Cosmochimica Acta, 22, pp. 2-15.

Butt, K. A., Islam Z., Chaudhry, M. N. & Khan, J. A., 1994. Discovery of early Permian carbonatite to melinitic/nephlinitic glassy flows in eastern Salt Range, Pakistan. Kashmir J. Geol. 11-12, pp. 105-111

Chaudhry, M. N., Gakkhar, R.A. & Naveed, A., 1997. Facies, microfacies, diagenesis and environment of deposition of Lumshiwal Formation at Thub Top Near Ayubia, District Abbottabad. Pakistan Journal of Hydrocarbon Research, 9, pp. 57-66.

Christie, W. A. K., 1914. Notes on the salt deposits of the Cis-Indus Salt Range. Records of the Geological Survey of India, 44, pp. 241-264.

Connon, J. & Cassou, A. M., 1980. Properties of gases and petroleum liquids derived from terrestrial kerogen at various maturation levels. Geochimica et Cosmochimica Acta, 44, pp. 1-23.

Coveny R. M. & Kelly, W. C., 1971. Dawsonite as a daughter mineral in hydrothermal fluid inclusions. Contributions to Mineralogy and Petrology, 32, pp. 334-342.

Cox, L. R., 1930. The fossil fauna of the Samana Range and some neighboring areas; part 8, the Mollusca of the Hangu Shales, Geological Survey of India. Mem. Paleont. Indica, New Series, 15, pp. 94.

Cox, L. R., 1931. A contribution to the Molluscan fauna of the Laki and basal Kirthar groups of the Indian Eocene. Trans., R., Soc., Edinburgh, 57, 25-92.

Cranwell, P. A., 1977. Organic geochemistry of CamLoch (Sutherland) sediments. Chemical Geology 20, pp. 205-221.

Cranwell, P. A., Eglinton, G. & Robinson, N., 1987. Lipids of aquatic organisms as potential contributors to lacustrine sediments-II. Organic Geochemistry, 11, pp. 513-527.

Cremo, A. M., 2001. Paleobotanical anomalies bearing on the age of the Salt Range Formation of Pakistan. XXI Internationational Congress of History of Science, Mexico.

D'Argenio, B. & Mindszenty, A., 1995. Bauxites and related paleokarst: tectonic and climatic event markers at regional unconformities. Eclogae Geologicae Helveticae, 88, pp. 453-499.

Dandlick, W., 1961. The iron formation of the Surghar and Western Salt Range, Mianwali District, West Pakistan. USGS., Prof., Paper 424-D, pp. 228-231.

Davies, L. M. & Pinfold, E. S., 1937. The Eocene beds of the Punjab Salt Range. Geological Survey of India, Memoir, Paleont., Indica, New Series 24, 1:79p. In: Kazmi, A. H. & Jan, M. Q., 1997. Geology and Tectonics of Pakistan; Graphic Publishers, Karachi, Pakistan, 554 pp.

Davies, L. M., 1943. Tertiary Echinoidea of the Kohat Potwar basin (India), Quart. Jour. Geol. Soc. Lond. 99, 393, 1: 63-77. In: Kazmi, A. H. & Jan, M. Q., 1997. Geology and Tectonics of Pakistan; Graphic Publishers, Karachi, Pakistan, 554 pp.

Davies, R. G., and Crawford, A. R., 1971. Petrography and age of the rocks of Bulland Hill, Kirana Hills, Sargodha District, West Pakistan. Geol., Mag., 108, pp. 235-246.

Davis, H. R., Byers, C. W. & Pratt, L. M., 1989. Depositional mechanisms and organic matter in Mowry shale (Cretaceous), Wyoming. AAPG Bulletin, 73, pp. 1103-1116.

De la Horra, R., Benito, M. I., Lopex-Gomez, J., Arche, A., Barrenecheaa, J. F., & Luque, X., 2008. Palaeoenvironmental significance of Late Permian palaeosols in the South-Eastern Iberian Ranges, Spain. Sedimentology, pp. 1-18.

Didyk, B. R. T., Simoneit, Brassell, S. C., & Eglinton, G., 1978. Organic geochemical indicators of palaeoenvironmental conditions of sedimentation. Nature, 272 1978, pp. 216-222.

Dorokhin, Aruzhinin, Sobolevsky & Gorbunov 1969. Economic mineral deposit. Higher School Bogacheva Publication, House, Moscow, pp. 1-368.

Du, Y., 1982. Secondary dawsonite in Shengli oil field, China. Scientia Geologica Sinica, 10, pp. 434-437.

Du, Y., 1985. Study of diagenesis of a reservoir with a CO_2 gas cap. Oil and Gas Geology, 6, pp. 91-95.

Dunbar, C. O., 1933. Stratigraphic significance of the fusulinids of the Lower Productus Limestone of the Salt Range. Geological Survey of India, Memoir, Palaeotology, Indica 7, 14, 1: 110p. In: Kazmi, A. H. & Jan, M. Q., 1997. Geology and Tectonics of Pakistan; Graphic Publishers, Karachi, Pakistan, 554 pp.

Duncan, R. A. & Pyle, D. G., 1988. Rapid extrusion of Deccan flood basalts at the Cretaceous/Tertiary boundary, Nature, 333, 841-843.

Dunham, R.J., 1962. Classification of carbonate rocks according to depositional texture. AAPG, Mem., 1, pp. 108-121.

Dunoyer de Segonzac, G., 1970. The transformation of clay minerals during diagenesis and low-grade metamorphism: a review. Sedimentology, 15, pp. 281-346.

Eames, F. E., 1952. A contribution to the study of Eocene in Western Pakistan and Western India, Part A. The geology of standard sections in the Western Punjab and Kohat in the Kohat District. Part B. Description of the faunas of certain standard sections and their bearing on the classification and correlation of the Eocene in Western Pakistan and Western India. Quart. Jour. Geol. Soc. London, 107, 2: 159-200, In: Kazmi, A. H. & Jan, M. Q., 1997. Geology and Tectonics of Pakistan; Graphic Publishers, Karachi, Pakistan, 554 pp.

Eglinton, G. & Hamilton, R. J., 1967. Leaf epicuticular waxes. Science, 156, pp. 1322-1335.

A. J., 1968. Chemical weathering in a subtropical igneous terrain, Rio Ameca, Mexico. Journal of Sedimentary Research, 41, pp. 885-984.

Espitalié, J., Laporte, J. L., Madec, M., Marquis, F., Leplat, P., Paulet, J. & Boutefeu, A., 1977. Méthode rapide de caractérisation des roches mères de leur potentiel pétrolier et de leur degré d'évolution. Revue de l'Institut Francais du Pétrole, 32, pp. 23-42.

Farah, A., Mirza, M. A. & Butt, M. H., 1977. Gravity field of the buried shield in the Punjab Plain, Pakistan. Bull., Geol., Amer., 88, pp. 1147-1155.

Fassett, J. E. & Durrani, N. A., 1994. Geology and coal resources of the Thar coal field, Sindh Province, Pakistan. U. S. Geol. Survey, Open File Report, 74, pp. 94-167.

Fatmi, A. N., 1968. the paleontology and stratigraphy of the Mesozoic rocks of Western Kohat, Kalachitta, Hazara, and Trans-Indus Salt Ranges, West Pakistan. PhD thesis, University of Wales, 409 pp.

Fatmi, A. N., 1972. Stratigraphy of Jurassic and Lower Cretaceous rocks and Jurassic ammonites from, northern areas of West Pakistan. Bull., Geol., British Museum Natural History, 20, pp. 299-380.

Fatmi, A. N., 1973. Lithostratigraphic units of the Kohat-Potwar Province, Indus Basin, Pakistan. Geological Survey of Pakistan. Memoir, 10, pp. 80.

Fatmi, A. N., 1977. Mesozoic In: Ibrahim Shah, S. M., (ed.): Stratigraphy of Pakistan, Geological Survey of Pakistan Memoir 12, pp. 29-56.

Fatmi, A. N., Akhtar, M., Alam, G. S., and Hussain, I., 1984. Guide book to geology to Salt Range. First Pakistan Geological Congress, Lahore, Geological Survey of Pakistan, 14 pp.

Feldman, H. R., Brown, M. A. & Archer, A.W., 1993. Benthic assemblages as indicators of sediment stability: evidence from grainstones of the Harrodsburg and Salem Limestones (Mississippian, Indiana). In: Keith, B.D. and Zuppann, C.W. (eds.): Mississippian oolites and modern analogs. AAPG, studies in geology, 35, pp. 115-128.

Flügel, E., 2004. Microfacies of Carbonate Rocks, Analysis, Interpretation and Application. Springer, Heidelberg, Berlin, 976 pp.

Francis, J. E., 1986. The calcareous paleosols of the basal Purbeck Formation (Upper Jurassic), Southern England. In: Wright, V.P. (ed.). Paleosols. Blackwell, Oxford, pp. 112-138.

Frimmel, A., Oschmann W. & Schwark, L., 2004. Chemostratigraphy of the Posidonia Black Shale, SW-Germany, I-Influence of sea level variation on organic facies evolution. Chemical Geology, 206, pp. 199-230.

Gakkhar, R. A., 2006. Lithological and stratigraphical studies of the Amir Wali Well 01, District Jhang, Punjab Province G & R Labs Note 460 (unpublished).

Gee, E. R., 1934. The Saline Series of northwestern India. Current Science, 2, pp. 460-463.

Gee, E. R., 1935. The Saline Series of northwestern India. Current Science, Banglore, Vol. II p 460-463. Saline Series Gee, E. R., 1935a. The Saline Series (Lower Eocene) of northwestern India (abs). Proc. 22nd Indian Sci. Cong., Calcutta, p. 207. Saline Series. In: Kazmi, A. H. & Jan, M. Q., 1997. Geology and Tectonics of Pakistan; Graphic Publishers, Karachi, Pakistan, 554 pp.

Gee, E. R., 1945. The age of the Saline Series of the Punjab and of Kohat. Proceedings of the National Academy of Sciences, India. Section B, 14, pp. 269-310.

Gee, E. R., 1980. Salt Range series geological maps, scale 1:50 000, 6 sheets. Directorate of Overseas Surveys, United Kingdom, for the Government of Pakistan and Pakistan Geological Survey. In: Kazmi, A. H. & Jan, M. Q., 1997. Geology and Tectonics of Pakistan; Graphic Publishers, Karachi, Pakistan 554 pp.

Gee, E. R., 1989. Overview of the geology and structure of the Salt Range, with observations on related areas of northern Pakistan. Special Papers of the Geological Society of America 232, pp. 95-112. In: Kazmi, A. H. & Jan, M. Q., 1997. Geology and Tectonics of Pakistan; Graphic Publishers, Karachi, Pakistan, 554 pp.

Glennie, E. A., 1955. Gravity data and crustal warping in north west Pakistan and adjacent parts of India. Geophysical Journal International, 7, pp. 162-175. Published online: Apr. 2007.

Goldberry, R. & Loughnan, F. C., 1977. Dawsonite, aluminohydrocalcite and nordstrandite and gorceixite in Permian marine strata of the Sydney Basin, Australia. Sedimentology, 24, pp. 565-579.

Goossens, H., de Leeuw, J. W., Schenck P. A. & Brassell, S. C., 1984. Tocopherols as likely precursors of pristane in ancient sediments and crude oils, Nature, 312, pp. 440-442.

Greensmith, J. T. M., 1981. Petrology of the sedimentary rocks (6th ed.). George Allen & Unwin Ltd., London, pp. 240

Gregory, J. W., 1930. The fossil fauna of the Samana Range and some neighboring areas; part 7. The Lower Eocene corals, Geological Survey of India, Mem. Paleont. Indica, New Series 15, pp. 46. In: Kazmi, A. H. & Jan, M. Q., 1997. Geology and Tectonics of Pakistan; Graphic Publishers, Karachi, Pakistan, 554 pp.

Hallam, A. & Maynard, J. B., 1987. The iron ores and associated sediments of the Chichali Formation (Oxfordian to Valanginian) of the Trans Indus Salt Range, Pakistan. Jour., Geol., Soc., London, 144, pp. 107-114.

Harry Satel, 2009, Diagenetic crystallization and oxidation of siderite in red bed (Buntsandstein) sediments from the Central Iberian Chain, Spain. Sedimentary Geology, 213 pp 89-96.

Heling, D., 1988. Ton und Siltsteine. In: Füchtbauer, H., (ed), Sediment und Sedimentgesteine. E. Schweizerbart´sche Verlasbuchhandlung, Stuttgart, pp. 185-231.

Hendry, J. P., Wilkinson, M., Fallick A.E., and Haszeldine, R. S., 2000. Ankerite cementation in deeply buried Jurassic sandstones of the Central North Sea. Journal of Sedimentary Research, 70, pp. 227-239.

Hendry, J. P., 2002, Geochemical trends and palaeohydrological significance of shallow burial calcite and ankerite cements in Middle Jurassic strata on the East Midlands Shelf (onshore UK). Sedimentary Geology, 151, pp. 149-176.

Haque, A. F. M. M., 1956. The smaller foraminifera of the Ranikot and the Laki of the Nammal Gorge, Salt Range. Geological Survey of Pakistan, Mem. Palaeontology, Pakistanica 1, pp. 300. In: Kazmi, A. H. & Jan, M. Q., 1997. Geology and Tectonics of Pakistan; Graphic Publishers, Karachi, Pakistan, 554 pp.

Holland, T. H., 1903. General report on the work carried out by the Geological Survey of India for the Year 1902/03. Calcutta, Geological Survey of India. In: Cremo, A. Michael., 2001. Paleobotanical anomalies bearing on the age of the Salt Range Formation of Pakistan. XXI Internationational Congress of history of Science, Mexico.

Hower, J. Eslinger, E. V., Hower, M. E. & Perry, E. A., 1976. Mechanism of burial metamorphism of argillaceous sediment: 1 Mineralogical and chemical evidence. Bull., Geol., Soc., Amer., 87, pp. 725-737.

Hughes, W. B., Holba, A. G. & Dzou, L. I. P., 1995. The ratios of dibenzothiophene to phenanthrene and pristan to phytan as indicators of depositional enviroment and lithology of petroleum source rocks. Geochim. Cosmochim. Acta 59, pp. 3581-3598.

Hunt, J. M., 1996. Petroleum Geochemistry and Geology (2nd edition). W. H. Freeman & Company, New York, 743 pp.

Husain, B. R., 1967. Saiduwali member, a name for the lower part of the Permian Amb Formation, West Pakistan. University Studies (Karachi), Science & Technology 4, p 88-99. In: Kazmi, A. H. & Jan, M. Q., 1997. Geology and Tectonics of Pakistan; Graphic Publishers, Karachi, Pakistan, pp. 554.

Iman, M. B., and Shaw, H. F., 1985. The diagenesis of Neogene clastic sediments from the Bengal Basin, Bangladesh. J. Sedim. Petrology, 55, pp. 665-671.

Iqbal, M. W. A., 1969. Mega fauna from the Ghazij Formation (lower Eocene) Quetta-Sharigh area, West Pakistan. Geological Survey of Pakistan, Memoir, Palaeontology, Pakistanica 5, 27 p. In: Kazmi, A. H. & Jan, M. Q., 1997. Geology and Tectonics of Pakistan; Graphic Publishers, Karachi, Pakistan, 554 pp.

Iqbal, M. W. A., 1972. Bivalve and gastropods fauna from Jherruk-Lakhra-Bara Nai (Sind), Salt Range (Punjab) and Samana Range (NWFP). Geological Survey of Pakistan, Mem., 9, 104 pp.

Iqbal, M. W. A. & Shah, S. M. I., 1980. A guide to the stratigraphy of Pakistan, Geological Survey of Pakistan, Records, 53, 34 pp.

Islam, Md. R., Rojsatczer Stuart, Ario Risto & Peuraniemi Vesa, 2002. Mineralogical changes during intense weathering of sedimentary rocks in Bangladesh. Journal of Asian Earth Sciences, 20, pp. 889-901.

Irwin, H., Curtis C. & Coleman , M., 1977. Isotopic evidence for source of diagenetic carbonates formed during burial of organic-rich sediments. Nature, 269, pp. 209-213.

Jan, M. Q., Weaver, B. L. & Faruqi, S. H., 1992. Geochemistry of the ultrabasic rocks in the Salt Range, Pakistan (Abstract) GEOSAS I, Islamabad, Pakistan.

Jenkyns, H. C., 1972. Pelagic oolites from the Tethyans Jurassic, Journal of Geology, 80, pp. 21-33.

Johnson, B. D., Powell, C. M. A. & Veevers, J. J., 1976. Spreading history of the eastern Indian Ocean and Greater India's northward flight from Antarctica and Australia. Bull., Geol., Soc., Amer., 87, pp. 1560-1566.

Johnsson, M. J., Stallard, F. & Meade, R. H., 1988. First-cycle quartz arenites in the Orinoco river basin, Venezuela and Colombia. Journal of Geology, 96, pp. 263-277.

Johnsson, M., Stallard R. F. & Lundberg, N., 1991. Controls on composition of fluvial sands from a tropical weathering environment: sands of the Orinoco River drainage basin. Geol. Soci., Amer., Bull., 103, pp. 1622-1647.

Jones, D. M., Head, I. M., Gray, N. D., Adams, J. J., Rowan, A. K., Aitken, C. M., Bennett, B., Huang, H., Brown, A., Bowler, B. F. J., Oldenburg, T., Erdmann, M. & Larter, R., 2008. Crude-oil biodegradation via methanogenesis in subsurface petroleum reservoirs. Nature, 451, pp. 176-181.

Kantorowicz, J. D., 1985. The origin of authigenic ankerite from the Ninian Field, UK North Sea. Nature, 315, pp. 214-216.

Karrer, W., Cherbuliez, E. & Eugster, C. H., 1977. Konstitution und Vorkommen der organischen Pflanzenstoffe, Ergänzungsband I. Birkhäuser, Basel, Stuttgart, 1038 pp.

Kazmi, A. H. & Jan, M. Q. (eds.), 1997. Geology and Tectonics of Pakistan; Graphic Publishers, Karachi, Pakistan, 554 pp.

Kazmi, A. H., 1979. Active fault systems in Pakistan. In: Farah, A. & Dejong, K. A. (eds.), Geodynamics of Pakistan. Geological Survey of Pakistan, Quetta, pp. 285-294.

Kazmi, A. H., & Rana, R. A., 1982. Tectonic map of Pakistan - Scale 1:2,000,000. Geological Survey of Pakistan, Quetta.

Khan, M. A., Ahmad, R., Raza, H. A., & Kemal, A., 1986. Geology of Petroleum in Kohat-Potwar depression, Pakistan. Bull., AAPG, 70 (4), pp. 369-414.

Khan, U., Khattak, N. U., Qureshi, A. A., Akram , M., Khan, H. A. & Nisar, A., 2005. Search for Uranium source in the Warchha Sandstone, Salt Range , Pakistan, using SSNTD technique. Radiation Measurements, 40, pp. 491-495.

Kemal A. H., Blackwill, H. R. & Stoakes, F. A., 1992. Indus Basin hydrocarbon plays. In: Ahmad, G., Kemal, A., A. S., Zaman, H., Humayun, M. (eds.), New Directives and Strategies for Accelerating Petroleum Exploration and Production in Pakistan. Proc. Intern. Petrol. Seminar, Ministry of Petroleum, Islamabad.

Kiessling, W., Flügel, E. & Golonka, J., 2002. From patterns to processes: the future of reef research. In: Kiessling, W., Flügel, E. & Golonka, J. (eds.), Phanerozoic reef patterns. SEPM Spec., Publ., 72, pp. 735-743.

Kloprogge, J. T., Ruan, H. D. & Frost, R. L., 2002. Thermal decomposition of bauxite minerals: infrared emission spectroscopy of gibbsite, boehmite and diaspore. Journal of Materials Science, 37, pp. 1121-1129.

Koken, E. & Noetling, F., 1903. Geologische Mittheilungen aus der Salt Range. No. 1. Das permische Glacial. Centralblatt für Mineralogie, Geologie und Päleontologie, pp. 45-49.

Köthe, A., 1988. Biostratigraphy of the Surghar Range, Salt Range, Sulaiman Range, and the Kohat area, Pakistan, according to Jurassic through Paleogene calcareous nannofossils and Palaegene dinoflagellates, Geologisches Jahrbuch, ser., B, pp. 3-87.

Krauskopf, K. B., 1982. Introduction to geochemistry. McGraw-Hill Book Company, Singapore, 617 pp.

Kummel, B. & Teichert, C., 1966. Relations between the Triassic and Permian formations in the Salt Range and Trans-Indus Ranges, West Pakistan. Neues Jahrbuch Geologie Paläontologie Abhandlungen 125, pp. 297-333. In: Kazmi, A. H. & Jan, M. Q., 1997. Geology and Tectonics of Pakistan; Graphic Publishers, Karachi, Pakistan, 554 pp.

Kummel, B. & Teichert, C., 1970. Stratigraphy and paleontology of the Permian-Triassic boundary beds, Salt Range and Trans-Indus Ranges, West Pakistan. In: Stratigraphic Boundary Problems, Permian and Triassic of West Pakistan, Geological Department University of Kansas Spec., Paper 4, pp. 1-110.

Langford, F. F. & Blanc-Valleron, M. M., 1990. Interpreting Rock-Eval pyrolysis data using graphs of pyrolyzable hydrocarbons vs. total organic carbon. AAPG Bulletin, 74, pp. 799-804.

Larter, S. & di Primio, R., 2005. Effects of biodegradation on oil and gas field PVT properties and the origin of oil rimmed gas accumulations. Org. Geochem., 36, pp. 299-310.

Latif, M. A., 1970. Micropalaeontology of the Canali Limestone, Upper Cretaceous, of Hazara, West Pakistan. Jb. Geol., B. A., 15, pp. 63-66.

Leonard, J. E., Cameron, B., Pilkey, O.H. & Friedman, G. M., 1981. Evaluation of cold-water carbonates as a possible paleoclimatic indicator. Sed., Geol., 28, pp. 1-28.

Lüniger, G. & Schwark, L., 2002. Organofacies and early diagenesis of organic matter from the Oligocene lacustrine Enspel Oil Shale Deposit, Germany. Journal of Sedimentology 148, pp. 275-288.

Mackenzie, A. S. & Maxwell, J. R., 1981. Assessment of thermal maturation in sedimentary rocks by molecular measurements. In: Brooks, J. (ed.), Organic maturation studies and fossil fuel exploration. Academic Press, London, pp. 239-254.

Mackenzie, A. S., Brassell, S. C., Eglinton, G. & Maxwell, J. R., 1982. Chemical fossils: the geological fate of steroids. Science 217, pp. 491-504.

Macaulay, C. I., Haszeldine R. S., & Fallick A. E., 1993. Distribution, chemistry, isotopic composition and origin of diagenetic carbonates: Magnus Sandstone, North Sea. Journal of Sedimentary Petrology, 63, pp. 33-43.

Malik, Z., Kamal, A., Malik, M. A. & Bodenhansen, J. W. A., 1988. Petroleum potential and prospects in Pakistan. In: Raza, H. A. & Sheikh, A. M. (eds.), Petroleum for the Future. Hydrocarbon Development Institute Pakistan, pp. 71-100.

McKenzie, D. P. & Sclater, J. G., 1976. The Evolution of the Indian Ocean. In: Continents Adrift and Continents Aground. Reading form Sci. Amer. Freeman & Company., pp. 139-148. In: Kazmi, A. H. & Jan, M. Q., 1997. Geology and Tectonics of Pakistan; Graphic Publishers, Karachi, Pakistan, 554 pp.

Mehta, S. K. & Kalsotra, A., 1991. Kinetics and hydrothermal transformation of gibbsite. Journal of Thermal Analysis and Calorimetry, 37, pp. 267-275.

Meister, P., Bernasconi, S. M., Vasconcelos C. & Judith, A., 2008. Sea level changes control diagenetic dolomite formation in hemipelagic sediments of the Peru Margin. Marine Geology, 252.

Meister, P., McKenzie, J. A., Vasconcelos, C., Bernasconi, S., Frank, M., Gutjahr, M. & Schrag, D. P., 2007. Dolomite formation in the dynamic deep biosphere, results from the Peru Margin, OPD Leg 201. Sedimentology, 54, pp. 1007-1032.

Mertmann, D. & Ahmad, S., 1994. Shinawari and Samana Suk Formations of the Surghar and Salt Ranges, Pakistan: Facies and depositional environments. Zeitschrift der Deutschen Geologischen Gesellschaft, 145, pp. 305-317.

Middlemiss, C. S., 1880. On the Trans-Indus Extention of the Punjab Salt Range. Geological Survey of India Mem., 17, pp. 163-169.

Middlemiss, C. S., 1891. Notes on the geology of the Salt Range, with a reconsidered theory of the origin and age of the Salt Marl. Records of the Geological Survey of India 24, pp. 19-42. In: Kazmi, A. H. & Jan, M. Q., 1997. Geology and Tectonics of Pakistan; Graphic Publishers, Karachi, Pakistan, 554 pp.

Molnar, P. & Tapponnier, P., 1975. Cenozoic tectonic of Asia: effects of continental collision. Science 189, pp. 419-426. In: Kazmi, A. H. & Jan, M. Q., 1997. Geology and Tectonics of Pakistan; Graphic Publishers, Karachi, Pakistan, 554 pp.

Mordberg, L. E., 1999. Geochemical evolution of a diaspore-crandallite-svanbergite-bearing weathering profile in the Middle Timan, Russia. Journal of Geochemical Exploration, 66, pp. 353-361.

Nizami, A. R. & Sheikh, R. A., 2007. Microfacies analysis and diagenetic settings of the Samana Suk Formation, Chichali Nala Section, Surghar Range, Trans Indus Ranges, Pakistan, Geol., Bull., Punjab University, 42, pp. 37-52.

Noetling, F., 1901. Beiträge zur Geologie der Salt Range, insbesondere der Permichen unde Triasuchea Ablagerungen. Venues Jahrb. Mineral. Beilage, 14: 369-471. In: Kazmi, A. H. & Jan, M. Q., eds., 1997. Geology and Tectonics of Pakistan; Graphic Publishers, Karachi, Pakistan, pp. 554.

Nytoft, H. P., Samuel, O. J., Kildahl-Andersen, G., Johansen, J. E. & Jones, M., 2009. Novel C_{15} sesquiterpanes in Niger Delta oils: Structural identification and potential application as new markers of angiosperm input in light oils. Organic Geochemistry, 40, pp. 595-603.

Odin, G. S. & Matter, A., 1981. De glauconiarum origine. Sedimentology, 28, pp. 611-641.

Ohmoto, H., Watanabe, Y. & Kumazawa, K., 2004. Evidence from massive siderite beds for a CO_2-rich atmosphere before ~1.8 billion years ago. Nature, 429, pp. 395–399.

Omana, L. & Arreola, C. G., 2008. Late Jurassic (Kimmeridgian) larger benthic foraminifera from Santiago Coatepec, SE Puebla, Mexico. Geobios, 41, pp. 799-817.

Opdyke, B. N. & Wilkinson, B. H., 1990. Paleolatitude distribution of Phanerozoic marine ooids and cements. Palaeogeography, Palaeoclimatology, Palaeoecology 78, pp. 135-148, Amsterdam.

Opdyke, N. D., Johnson, N. M., Johnson, G. D., Lindsay, E. H. & Tahirkheli, R. A. K., 1982. Paleomagnetism of the middle Siwalik formations of northern Pakistan and rotation of the Salt Range decollement. Palaeogeography, Palaeoclimatology, Palaeoecology, 37, pp. 1-15.

Orr, W. L., 1983. Comments on pyrolytic hydrocarbons yields, in source-rock evaluation. In: M. Bjoroy et al. (Eds.). Advances in organic geochemistry, 1981, Wiley, Chichester, pp. 775-787.

Ourisson, G., Albrecht, P. & Rohmer, M., 1979. The hopanoids: palaeo-chemistry and biochemistry of a group of natural products. Pure Applied Chemistry, 51, pp. 709-729.

Pakistan-Japanese Research Group, 1985. Permian and Triassic systems in the Salt Range and Surghar Range, Pakistan. In: Nakazawa, K. & Dickins, J. M. (eds.). The Tethy Paleogeography from Paleozoic to Mesozoic, Tokai University Press, pp. 221-312. In: Kazmi, A. H. & Jan, M. Q., 1997. Geology and Tectonics of Pakistan; Graphic Publishers, Karachi, Pakistan, 554 pp.

Parcerisa, D., Gómez-Gras, D. & Travé, A., 2005. A model of early calcite cementation in alluvial fans: Evidence from the Burdigalian sandstones and limestones of the Vallès-Penedès half-graben (NE Spain). Sedimentary Geology, pp. 197-217.

Parcerisa, D., Gomez-Gras, D., Trave, A., Martin-Martin J. D. & Maestro, E., 2006. Fe and Mn in calcites cementing red beds: a record of oxidation-reduction conditions Examples from the Catalan Coastal Ranges (NE Spain). Journal of Geochemical Exploration, 89, pp. 318-321.

Pascoe, E. H., 1920. Petroleum in the Punjab and North West Frontier Province. Memoirs of the Geological Survey of India 40, pp. 330-489. In: Kazmi, A. H. & Jan, M. Q., 1997. Geology and Tectonics of Pakistan; Graphic Publishers, Karachi, Pakistan, 554 pp.

Pascoe, E. H., 1950-1964. A manual of the geology of India and Burma, 1950- Vol.1, p.-483; 1959-Vol.2, p.485-1338; 1964-Vol.3, p. 1345-2130. Govt. of India, Press, Calcutta. In: Kazmi, A. H. & Jan, M. Q., 1997. Geology and Tectonics of Pakistan; Graphic Publishers, Karachi, Pakistan, 554 pp.

Pascoe, E. H., 1959. A Manual of the Geology of India and Burma, Volume II. Calcutta. Geological Survey of India. In: Kazmi, A. H. & Jan, M. Q., 1997. Geology and Tectonics of Pakistan; Graphic Publishers, Karachi, Pakistan, 554 pp.

Patriat, P. & Achache, J., 1984. India-Eurasia collisional chronology and its implications for crustal shortening and driving mechanism of plates. Nature 311, pp. 615-621. In: Kazmi, A. H. & Jan, M. Q., 1997. Geology and Tectonics of Pakistan; Graphic Publishers, Karachi, Pakistan, 554 pp.

Perić, Z., Krstulović, R. & Vućak, M., 1996. Investigation of dehydroxylation of gibbsite into boehmite by DSC analysis. Journal of Thermal Analysis and Calorimetry, 46, pp. 1339-1347.

Peters, K. E., 1986. Guidelines for evaluating petroleum source rock using programmed pyrolysis. AAPG Bulletin, 70, pp. 318-329.

Philp, R. P., 1985. Fossil fuel biomarkers. Applications and spectra. Methods in Geochemistry and Geophysics 23, pp. 1-294.

Philp, R. P., 1994. Geochemical characteristics of oils derived predominantly from terrigenous source materials. Geological Society Special Publication, 77, pp. 71-91.

Pilgrim, G. E., 1913. The correlation of the Siwaliks with mammal horizons of Europe. Geological Survey of India, Rec. 43, pp. 264-326. In: Kazmi, A. H. & Jan, M. Q., 1997. Geology and Tectonics of Pakistan; Graphic Publishers, Karachi, Pakistan, 554 pp.

Powel, C. McA. & Conaghan, P. J., 1973. Plate tectonics and the Himalayas, Earth Planet. Sci. Lett. 20, pp. 1-12. In: Kazmi, A. H. & Jan, M. Q., 1997. Geology and Tectonics of Pakistan; Graphic Publishers, Karachi, Pakistan, 554 pp.

Powell, C. McA., 1979. A speculative tectonic history of Pakistan and surroundings: Some constraints from the Indian Ocean. In: Frarah, A. & Dejong, K. A. (eds.), Geodynamics of Pakistan. Geol. Survey of Pakistan, Quetta, 5-24 pp.

Powell, T. G. & McKirdy, D. M., 1973. Relationship between the ratio of pristane to phytane, crude-oil composition and geological environment in Australia, Nature 243, pp. 37-39.

Püttmann, W. & Villar, H., 1987. Occurrence and geochemical significance of 1, 2, 5, 6-tetramethylnaphthalene. Geochim. Cosmochim. Acta 51, pp. 3023-3929.

Qureshi, M. K. A., Khan, R. M, Ghazi, S. & Butt, A. A., 2005-6. Geology of the Lower Jurassic Datta Formation, Kala Chitta Range, Pakistan. Geol. Bull. Punjab Univ. 40-41, pp. 27-44.

Qureshi, M. K. A., Ghazi, S., Butt, A. A., Ahmad, N., & Khan, R. M., 2007. Microfacies analysis and the environmental pattern of the Chichali Formation, Kalachitta Range, Pakistan, Geological Bulletin University of the Punjab, Lahore, pp. 53-59.

Radke, M. & Welte, D. H., 1983. The Methylphenanthrene Index (MPI): A maturity parameter based on aromatic hydrocarbons. In: Bjoroy, M. (ed.), Advances in Organic Geochemistry. Wiley, Chichester, pp. 504-512.

Radke, M., Welte, D. H. & Willsch, H., 1982. Geochemical study of a well in the Western Canada Basin: relation of the aromatic distribution pattern to maturity of organic matter. Geochimica et Cosmochimica Acta, 46, pp. 1-10.

Radke, M., Willsch, H. & Welte, D.H., 1980. Preparative hydrocarbon group type determination by automated medium pressure liquid chromatography. Analytical Chemistry, 52, pp. 406-411.

Raza, H. A., Ahmad, R., Alam, S. & Ali, S. M., 1989. Petroleum zones of Pakistan. Pak. Jour. Hydrocarbon Research 1, pp. 1-19. In: Kazmi, A. H. & Jan, M. Q., 1997. Geology and Tectonics of Pakistan; Graphic Publishers, Karachi, Pakistan, 554 pp.

Raza, H. A., Ahmad, R., Ali, S. M. & Ahmad, J., 1989. Petroleum prospects: Sulaiman Sub-basin, Pakistan. Pak. Jour. Hydrocarbon Research 1, pp. 21-56. In: Kazmi, A. H. & Jan, M. Q., 1997. Geology and Tectonics of Pakistan; Graphic Publishers, Karachi, Pakistan, 554 pp.

Raza, H. A., Ali, S. M. & Ahmad, R., 1990. Pakistan Offshore an attractive Frontier. Pak. Jour. Hydrocarbon Research 2, pp. 1-42. In: Kazmi, A. H. & Jan, M. Q., 1997. Geology and Tectonics of Pakistan; Graphic Publishers, Karachi, Pakistan, 554 pp.

Reed, F. R. C., 1936. Some fossils from the Erydesma and Conularia beds (Punjabian) of the Salt Range. Geological Survey of India, Mem. Pal., India, 23, pp. 1-36. In:

Kazmi, A. H. & Jan, M. Q., 1997. Geology and Tectonics of Pakistan; Graphic Publishers, Karachi, Pakistan, 554 pp.

Reed, F. R. C., 1941. Non-marine Lamellibranchs etc. from the "Speckled Sandstone" formation (Punjabian) of the Salt Range. Geological Survey of India, Rec., 14, pp. 474-490, In: Kazmi, A. H. & Jan, M. Q., 1997. Geology and Tectonics of Pakistan; Graphic Publishers, Karachi, Pakistan, 554 pp.

Reed, F. R. C., 1944, Brachiopoda and Molluska from the Productus Limestone (Permian) of the Salt Range. Geological Survey of India, Mem. Paleontology, New Series, 23, pp. 1-596. In: Kazmi, A. H. & Jan, M. Q., 1997. Geology and Tectonics of Pakistan; Graphic Publishers, Karachi, Pakistan, 554 pp.

Robison, C. R., Smith, M. A. & Royle, R. A., 1999. Organic facies in Cretaceous and Jurassic hydrocarbon source rocks, Southern Indus basin, Pakistan. International Journal of Coal Geology, 39, pp. 205-225.

Rohmer, M., Bisseret, P. & Neunlist, S., 1992. The hopanoids, prokaryotic triterpenoids and precursors of ubiquitous molecular fossils. In: Moldowan, J. M., Albrecht, P. & Philp, R. P. (eds.), Biological Markers in Sediments and Petroleum. Prentice Hall, Englewood Cliffs, N. J., pp. 1-17.

Rutter, E. H., 1983. Pressure solution in nature, theory and experiment. Journal of the Geological Society London, 140, pp. 725-740.

Sahni, B., 1944. Age of the Saline Series in the Salt Range of the Punjab. Nature, 153, pp. 462-463.

Sajjad A., Irfan, A. & Khan, I.; 2005. Structure and Stratigraphy of the Palaeozoic and Mesozoic Sequences in the vicinity of Zaluch Nala, Western Salt Range, Punjab Pakistan. Pakistan Journal of Hydrocarbon Research, 15, pp. 1-8.

Schindewolf, O. H. & Seilacher, A., 1955. Beiträge zur Kenntnis des Kambriums in der Salt Range (Pakistan). Abh. Akad. Wiss. Lit. Mainz., Math.Nat. Kl., pp. 446.

Seeber, L., & Armbruster, J., 1979. Seismicity of the Hazara arc in northern Pakistan: decollement versus basement faulting. In Frah, A., & Dejong, K. A., (eds.). Geodynamics of Pakistan. Geological Survey of Pakistan, Quetta, pp. 131-142.

Seeber, L., Quettmeyer, R. C. & Armbruster, J. G., 1980. Seismotectonics of Pakistan. A review of results from network data and Implications for the Central Himalaya. Geol. Bull. University of Peshawar, 13, pp. 151-168.

Sengör, A. M. C., Altiner D., Cin A., Ustaomer T. & Hsu K. G., 1988. Origin and assembly of Tethyside orogenic collage at the expense of Gondwanaland. In: Audley Charles, M. G. & Hallam, A. (eds), Gondwana and Tethys. Geol. Soc. Lond., Spec., Publ., 37, pp. 119-81.

Shah, S. M. I. (ed.), 1977. Stratigraphy of Pakistan, Geological Survey of Pakistan, Memoir 12.

Shanmughan, G., 1985. Significance of conifer rain forests and related organic matter in generating commercial quantities of oil, Gippsland Basin, Australia. AAPG Bulletin, 69, pp. 1241-1254.

Sheldon, N. D., 2005. Do red beds indicate paleoclimatic conditions?: A Permian case study. Palaeogeography, Palaeoclimatology, Palaeoecology, 228, pp. 305-319.

Singer, A. & Müller, G., 1983, Diagenesis in argillaceous sediments. In: Larsen G & Chillingar G.V. (eds.), Diagenesis in Sediments and Sedimentary Rocks, pp. 115-212. Elsevier, Amsterdam.

Smith, J. W. & Milton, C., 1966. Dawsonite in the Green River Formation of Colorado. Economic Geology, 61, pp. 1029-1042.

Smith, J. W. & Young, N.B., 1975. Dawsonite: its geochemistry, thermal behaviour and extraction from the Green River Formation oil shale. Colorado School of Mines Quarterly Report, 70, pp. 69-93.

Smith, J. W., Beard, T. N. & Wade, P. M., 1972. Estimating nahcolite and dawsonite content of Colorado oil shale from oil yield assay data. Report of investigation of the US Bureau of Mines, 7689, pp. 1-24.

Smout, A. H. & Haque, A. F. M. M., 1956. A note on the larger foraminifera and ostrocoda of the Ranikot from the Nammal Gorge, Salt Range, West Pakistan. Geological Survey of Pakistan Records 8, pp. 49-60. In: Kazmi, A. H. & Jan, M. Q., 1997. Geology and Tectonics of Pakistan; Graphic Publishers, Karachi, Pakistan, 554 pp.

Sokolove, B. A. & Shah S. H. A., 1966. Major tectonic features of Pakistan. Part-I, Western Province: Sci., Ind., Res., 4: pp. 175-199.

Sukh Dev, 1989. Terpenoids. In: Rowe, J.W. (Ed.), Natural Products of Woody Plants. Vol. 1, Springer, Berlin, pp. 691-807.

Stevenson, J. S. & Stevenson, L. S., 1977. The petrology of dawsonite at the type locality, Montreal. Canadian Mineralogist, 15, pp. 117-120.

Sylvain G., William S., de Lamotte, D. F., Jaswal, T. & François R., 2002. Kinematics of eastern Salt Range and South Potwar Basin (Pakistan): a new scenario. Marine and Petroleum Geology, 19, pp. 1127-1139.

Taheri, A. A., Sturgess, M., Maycock, I., Mitchell, G., Prelat, A., Nurmi, R. & Petricola, M., 1992. Looking for Yemen's hidden treasure, Middle East Well Evaluation Review (Schlumberger) 12, pp. 12-29.

Talukdar, S. C. B., De Toni, Marcano, F., Sweeney, J. & Rangel, A., 1993. Cretaceous source rocks of northern South America. Abstract, AAPG Bulletin, 77, 351.

Teichert, C., 1964. Recent German work on the Cambrian and Saline Series of the Salt Range, West Pakistan. Geological Survey of Pakistan Rec. 11, pp. 1-20. In: Kazmi,

A. H. & Jan, M. Q., 1997. Geology and Tectonics of Pakistan; Graphic Publishers, Karachi, Pakistan, 554 pp.

Teichert, C., 1966. Stratigraphic nomenclature and correlation of the Permian "Productus Limestone" of Salt Range, West Pakistan. Geol. Surv. India, Rec., 15, 1 : 19., In: Kazmi, A. H. & Jan, M. Q., 1997. Geology and Tectonics of Pakistan; Graphic Publishers, Karachi, Pakistan, 554 pp.

Teichert, C., 1967. Nature of Permian glacial record, Salt Range and Khisore Range, West Pakistan. Neues Jahrb. Geol. Pal. Abh. 129, pp. 167-184. In: Kazmi, A. H. & Jan, M. Q., 1997. Geology and Tectonics of Pakistan; Graphic Publishers, Karachi, Pakistan, 554 pp.

ten Haven, H. L., de Leeuw, J. W., Rullkötter J. & Sinninghe Damsté, J. S., 1987. Restricted utility of the pristane/phytane ratio as a palaeoenvironmental indicator, Nature 330, pp. 641-643.

Tissot, B. T. & Welte, D. H., 1984. Petroleum Formation and Occurrences (2nd ed.). Springer Verlag, Berlin, 699 pp.

Trolard , F. & Tardy, Y., 1987. The stabilities of gibbsite, boehmite, aluminous goethites and aluminous hematites in bauxites, ferricretes and laterites as a function of water activity, temperature and particle size. Geochimica et Cosmochimica Acta 51, pp. 945-957.

Tucker, M. E., 1992. Sedimentary petrology, an introduction to the origin of sedimentary rocks (2^{nd} ed.). Blackwell scientific Publications, London.

Turner, P., 1980. Continental red beds. Elsevier, Amsterdam, 562 pp.

Veletone, I., 1981. Bauxite on Peneplained metamorphic and magmatic rocks on setrital sediments and on karst topography, their similarities and contrast of genesis, In: Laterization, Proceed., International seminar, Laterization processes, India, Dec., 11-14, 1979.

Verma, R. K., 1991. Geodynamics of the Indian Peninsula and the Indian Plate Margin. Oxford & IBH, New Delhi, 357 pp.

Volkman, J. K. & Maxwell, J. R., 1986. Acyclic isoprenoids as biological markers. In: Johns, R. B. (ed.). Biological Markers in the Sedimentary Record. Elsevier, Amsterdam, pp. 1-42.

Volkman, J. K., 1986. A review of sterol markers for marine and terrigenous organic matter. Organic Geochemistry, 9, pp. 83-99.

Volkman, J. K., Barrett, S. M. & Blackburn, S. I., 1999. Eustigmatophyte microalgae are potential sources of C_{29} sterols, C_{22}-C_{28} *n*-alcohols and C_{28}-C_{32} *n*-alkyl diols in freshwater environments. Organic Geochemistry, 30, pp. 307-318.

Von Drong, H. J., 1985. Ein vorkommen von dawsonite im Solling, Neues Jahrbuch für Geologie und Paläeontologie Monatshefte, pp. 153-156.

Vortisch, W. & Butz-Braun, R., 1992. A Tertiary weathering profile in volcanic tuffs of the Westerwald. N. Jb., Geol., Paläont., Mh., pp. 701-708.

Vredenburg, E. W., 1909. Molluska of the Ranikot series, introductory note on the stratigraphy of the Ranikot series. Geol., Surv., India, Mem., Palaeont., Indica, New Ser., 3, pp. 5-19.

Waagen, W., 1879. Salt Range fossils, Products limestone group. Geological Survey of India, Memoir, Palaeotology, Indica, Ser. 13, pp. 4-6. In: Kazmi, A. H. & Jan, M. Q., 1997. Geology and Tectonics of Pakistan; Graphic Publishers, Karachi, Pakistan, 554 pp.

Waagen, W., 1889-91. Salt Range fossils: Fossils from the Ceratite formation: Pices-Ammonoidea. Geological Survey of India, Memoir, Palaeotology, India Ser. 13-4, 1 & 2: 324p. In: Kazmi, A. H. & Jan, M. Q., 1997. Geology and Tectonics of Pakistan; Graphic Publishers, Karachi, Pakistan, 554 pp.

Waagen, W, 1882-1885. Salt Range fossils. Productus limestone fossils. Memoir of Geological Survey of India, Palaeontologia Indica, Calcutta, vol. I, part 4 Brachiopoda, pp. 329-770.

Waagen, W., 1895. Salt Range fossils. Fossils from Ceratite Formation. Memoir of Geological Survey of India, Palaeontologia Indica, Calcutta, vol. II, part 1, Pisces-Ammonoidea, 324 pp.

Wadia, D. N., 1928. The geology of the Poonch State (Kashmir) and adjacent portions of the Punjab, Geological Survey of India, Mem. 63, pp. 129-128. In: Kazmi, A. H. & Jan, M. Q., 1997. Geology and Tectonics of Pakistan; Graphic Publishers, Karachi, Pakistan, 554 pp.

Waples D. W., 2002. Evolution of sandstone porosity through time. The modified scherer model: A calculation method applicable to 1-D maturity modeling and perhaps to reservoir prediction. Natural Resources Research, 11, pp. 257-272.

Weaver, C. E., 1989. Clays, Muds and Shales. Elsevier, Amsterdam, 820 pp.

Wegner, A., 1912. "Die Entstehung der Kontinente" Geologische Rundschau, SpringerBerlin/Heidelberg, 3, pp. 276-292.

Weibel, R. & Friis H., 2004. Opaque minerals as keys for distinguishing oxidising and reducing diagenetic conditions in the Lower Triassic Bunter Sandstone, North German Basin. Sedimentary Geology, 169, pp. 129-149.

Worden, R. H., 2006. Dawsonite cement in the Triassic Lam Formation, Shabwa Basin, Yemen: A natural analogue for a potential mineral product of subsurface CO_2 storage for greenhouse gas reduction. Marine and Petroleum Geology, 23, pp. 61-77.

Worden, R. H., Warren, E. A., Smalley, P. C., Primmer T. J. & Oxtoby, N. H., 1995. Evidence for resetting of fluid inclusions temperatures from quartz cement in oilfields: discussion. Marine and Petroleum Geology, 12, pp. 566-570.

Wynne, A. B., 1878. On the Geology of the Salt Range in Punjab. Geological Survey of India, Mem., Paleont. Indica, 242. In: Kazmi, A. H. & Jan, M. Q., 1997. Geology and Tectonics of Pakistan; Graphic Publishers, Karachi, Pakistan, 554 pp.

Wynne, A. B., 1878. On the Geology of the Salt Range in the Punjab. Memoirs of the Geological Survey of India, 14, pp. In: Kazmi, A. H. & Jan, M. Q., 1997. Geology and Tectonics of Pakistan, 554 pp.

Wynne, A. B., 1879. Further Notes on the Geology of the Upper Punjab, Geological Survey of India, Recs., pp. 114-133. In: Kazmi, A. H. & Jan, M. Q., 1997. Geology and Tectonics of Pakistan; Karachi, Pakistan, 554 pp.

Yasin, A. R., Hasan, N., Ashraf, M., Nadeem, A., Sheikh, M. A., and Butt, A. W., 1994. Stratigraphy of the Central Indus Basin, Pakistan. G & R Lab. Note No. 286, (unpublished).

Yasin, A. R. & Janjua, S., 1994. Depositional environments of the Middle Cambrian Baghanwala Formation, Salt Range, Pakistan. Pakistan Journal of Geology, 2.

Yi Ge Zhang, Junfeng Ji, William L. Balsam, Lianwen Liu & Jun Chen, 2007. Highresolution hematite and goethite records from ODP 1143, South China Sea: Co-evolution of monsoonal precipitation and El Niño over the past 600,000 years. Earth and Planetary Science Letters, 264, pp. 136-150.

Yuanfeng, C. , Xiang, L., Xiumian, H., Xiaoming, C. & Yuguan, P., 2009. Paleoclimatic approach to the origin of the coloring of Turonian pelagic limestones from the Vispi Quarry section (Cretaceous, central Italy), Cretaceous Research, 30, pp. 1205-1216.

Appendix

Table A: XRD Mineral Identification in the Ali Sahib Well

Sample	Depth [m]	Minerals Identified
AS1C1	1534.20	Quartz, Calcite and Gypsum?
AS2C1	1534.55	Calcite, Quartz, Gypsum?
AS3C1	1534.90	Calcite and Quartz
AS4C1	1535.65	Calcite and Quartz
AS5C1	1536.70	Calcite and Quartz
AS7C1	1537.30	Quartz, Calcite, Gypsum, Ankerite
AS8C1	1537.80	Quartz, Calcite, Ankerite, Pyrite
AS9C1	1538.65	Quartz, Calcite, Ankerite, Glauconite, Illite, Gypsum?
AS10C1	1539.10	Quartz, Ankerite, Calcite, Hematite, Glauconite
AS11C1	1539.65	Quartz, Ankerite, Calcite, Glauconite, Hematite, Kaolinite, Gypsum?
AS12C1	1540.20	Quartz, Calcite, Ankerite, Glauconite, Pyrite, Kaolinite, Illite K-Feldspar
AS13C1	1541.00	Quartz, Calcite, Ankerite, Hematite
AS14C1	1541.90	Quartz, Calcite, Ankerite, Glauconite, Gypsum?, Kaolinite, Illite, Pyrite
AS15C2	1694.05	Calcite. traces of Quartz
AS16C2	1694.80	Calcite
AS17C2	1695.40	Calcite, Quartz
AS18C2	1696.10	Calcite, Quartz
AS19C2	1696.80	Calcite, Ankerite
AS20C2	1697.80	Calcite
AS21C2	1698.10	Calcite
AS22C2	1698.40	Calcite
AS23C2	1699.00	Calcite
AS24C2	1699.40	Calcite, Quartz, Gypsum?, Ankerite
AS25C2	1699.90	Calcite
AS26C2	1700.00	Quartz, Calcite, Siderite, Kaolinite, Illite/Muscovite
AS27C2	1701.00	Calcite, Quartz
AS28C3	1730.60	Quartz , Siderite, Kaolinite, Illite
AS29C3	1731.00	Quartz , and traces of Siderite, Kaolinite
AS30C3	1731.60	Quartz, Kaolinite, traces of Siderite
AS31C3	1732.00	Quartz, Anatase, and traces of Kaolinite
AS32C3	1732.65	Quartz, Kaolinite and anatase, and traces of illite
AS33C4	1886.40	Quartz and traces of Kaolinite
AS34C4	1887.30	Kaolinite, Siderite, Anatase and traces of Rutile
AS35C4	1888.30	Kaolinite, Siderite, Anatase and traces of Rutile
AS36C4	1889.05	Kaolinite, and traces of Anatase, Illite, Hematite, Siderite, Rutile
AS37C4	1890.20	Kaolinite, Hematite and traces of Rutile
AS38C4	1891.20	Kaolinite, Illite and Muscovite, Hematite, Anatase, Ankerite, traces of Rutile
AS39C4	1892.20	Kaolinite, Hematite, Anatase and traces of Rutile and Oligonite
AS40C4	1892.60	Kaolinite, Hematite, Anatase, Illite/Muscovite
AS41C4	1893.40	Kaolinite, Hematite and Rutile

Table B: XRD Mineral Identification in the Amir Wali Well

Sample	Depth [m]	Minerals Identified
AW1C1	1575.50	Calcite , Quartz and Ankerite
AW2C1	1575.85	Quartz, Ankerite, Calcite, Hematite, Kaolinite, Glauconite and Illite/Muscovite
AW3C1	1576.66	Quartz, Ankerite, Calcite, Hematite, Kaolinite, and Illite/Muscovite
AW4C1	1577.17	Calcite and Quartz
AW6C1	1578.45	Calcite and Quartz
AW8C1	1579.42	Quartz, Calcite, K-Feldspar and traces of Glauconite
AW9C1	1580.05	Calcite and Quartz
AW10C1	1581.03	Calcite and Quartz
AW12C1	1582.22	Calcite and Quartz
AW13C1	1583.01	Calcite, Quartz and Siderite
AW14C2	1615.06	Quartz, Illite/Muscovite, Kaolinite, Goethite and traces of Calcite
AW15C2	1616.75	Quartz, Illite/muscovite, Ankerite, Kaolinite, K-feldspar and Anatase
AW16C2	1617.25	Quartz and Siderite
AW17C2	1619.00	Quartz, Illite/Muscovite, Kaolinite, and traces of K-feldspar
AW19C2	1620.65	Quartz, Siderite and Kaolinite, and traces of Illite and K-feldspar
AW20C2	1621.20	Quartz, Siderite, and Kaolinite, and traces of Ankerite and Illite
AW21C2	1621.65	Quartz, Kaolinite and Siderite, and traces of Illite
AW22C3	1760.10	Quartz, Calcite, Kaolinite, Ankerite, Illite/Muscovite and Pyrite
AW23C3	1760.90	Calcite, Quartz and traces of Kaolinite, Hematite and Gypsum?
AW24C3	1761.10	Calcite, Quartz, Kaolinite, Ankerit and Hematite
AW25C3	1761.70	Calcite, Quartz, Ankerite, Kaolinite, Hematite and Siderite
AW26C3	1762.05	Calcite, Quartz, Ankerite, Kaolinite and Hematite
AW27C3	1762.70	Calcite, Quartz and traces of Ankerite
AW28C3	1763.30	Calcite, Ankerite and traces of Quartz
AW29C3	1763.45	Calcite and Siderite
AW30C3	1764.05	Calcite, Siderite and traces of Quartz, Kaolinite and Gypsum?
AW31C3	1764.45	Calcite, Quartz and traces of Hematite
AW32C3	1764.95	Calcite, Quartz, Siderite, Ankerite, Gypsum? and traces of Hematite and Kaolinite
AW33C3	1765.25	Calcite, Quartz, Siderite, Gypsum? and traces of Kaolinite, Hematite and Pyrite?
AW34C3	1765.70	Calcite and traces of Quartz
AW35C3	1766.25	Calcite
AW36C3	1766.90	Calcite
AW37C3	1767.80	Calcite and Ankerite
AW38C3	1768.60	Calcite and traces of Ankerite
AW39C4	1853.30	Calcite, Ankerite, Quartz, Hematite and traces of Kolinite and Gypsum?
AW40C4	1854.00	Calcite, Quartz, Ankerite and traces of Hematite, Kaolinite, Gypsum? and Glauconite
AW41C4	1854.70	Calcite, Quartz and Ankerite
AW42C4	1855.25	Calcite, Quartz
AW43C4	1856.05	Calcite, Quartz, Ankerite, Gypsum? Hematite and Kaolinite
AW44C4	1856.80	Calcite, and traces of Quartz, Ankerite and Kaolinite
AW45C4	1857.40	Calcite and traces of Quartz, Hematite, Kaolinite and Gypsum?
AW46C4	1857.90	Calcite, Quartz and Siderite
AW47C4	1858.55	Calcite, Quartz and traces of Siderite

AW48C4	1858.55	Calcite and traces of Quartz
AW49C4	1859.10	Quartz, Ankerite, Calcite, Gypsum? Pyrite? And traces of Kaolinite
AW50C4	1859.55	Quartz, Ankerite, Kaolinite, Hematite, Pyrite, Illite/Muscovite and Dolomite?
AW51C4	1859.90	Calcite, Quartz, Ankerite and traces of Gypsum?, Kaolinite and Hematite
AW52C4	1860.35	Calcite, Quartz, Gypsum? and traces of Kaolinite and Hematite
AW53C4	1860.55	Calcite, Ankerite, Pyrite, Quartz and Gypsum?
AW54C4	1861.05	Calcite and traces of Hematite and Quartz

Table 9.1: Bulk organic geochemical data (TOC and pyrolysis) from the Ali Sahib Well

Fm.	Lithology	Depth in Meters	TOC (wt %)	S1 (mg/g)	S2 (mg/g)	S3 (mg/g)	T_{max} (°C)	GP (mg/g)	IP	HI	OI
Sakesar	Limestone	1250 - 55	0,17								
		1260 - 65	0,09								
		1270 - 75	0,12								
		1280 - 85	0,20								
Nammal	Limestone with streaks of shale	1290 - 95	0,29								
		1300 - 5	0,38								
		1310 - 15	0,27								
		1320 - 25	0,40								
		1330 - 35	0,32								
		1340 - 45	0,42								
		1350 - 55	0,38								
	Limestone	1360 - 65	0,37								
		1370 - 75	0,33								
		1380 - 85	0,27								
		1400 - 5	0,31								
		1410 - 15	0,41	0,09	1,94	0,05	408	2,03	0,04	473	12
		1420 - 25	0,42								
		1440 - 45	0,39								
		1460 - 65	0,36								
Dungan	Lst. w/intr Sh.	1480 - 85	0,32								
		1490 - 95	0,18								

Table 9.1: Bulk organic geochemical data (TOC and pyrolysis) from the Ali Sahib Well (continued)

Fm.	Lithology	Depth in Meters	TOC (wt %)	S1 (mg/g)	S2 (mg/g)	S3 (mg/g)	T_{max} (°C)	GP (mg/g)	IP	HI	OI
Ranikot	Sh. w. stks of Lst & Sst.	1500 - 5	0,39								
		1510 - 12	0,22	0,06	0,22	0,03	423	0,28	0,21	100	14
		1520 - 25	0,19								
Lumshiwal	Mly & Shy Sst..	1530 - 32	0,09								
		1534	0,39	0,08	0,12	0,30	402	0,20	0,40	31	77
	Gl. Cal. Sst	1534,56	0,59	0,09	0,15	0,40	405	0,24	0,38	25	68
	Arenaceous Limestone	1535,12	0,50	0,08	0,07	0,40	407	0,15	0,53	14	80
		1535,69	0,45								
		1536,25	0,60	0,08	0,16	0,40	408	0,24	0,33	27	67
		1536,81	0,36								
		1537,37	0,53	0,10	0,15	0,40	403	0,25	0,40	28	75
	Calcareous Sandstone	1537,94	0,42								
		1538,50	0,50	0,08	0,08	0,32	423	0,16	0,50	16	64
		1539,06	0,40								
	Calcareous and dolomitic Sandstone	1539,62	0,25								
		1540,18	0,61	0,06	0,08	0,23	415	0,14	0,43	13	38
		1540,75	0,63	0,05	0,15	0,19	421	0,20	0,25	24	30
		1541,31	0,62	0,06	0,14	0,21	403	0,20	0,30	23	34
		1541,87	0,52	0,06	0,08	0,21	418	0,14	0,43	15	40

Table 9.1: Bulk organic geochemical data (TOC and pyrolysis) from the Ali Sahib Well (continued)

Fm.	Lithology	Depth in Meters	TOC (wt%)	S1 (mg/g)	S2 (mg/g)	S3 (mg/g)	Tmax (°C)	GP (mg/g)	IP	HI	OI
Lumshiwal	Calcareous and dolomitic sandstone	1542,43	0,53	0,06	0,14	0,00	418	0,20	0,30	26	0
		1543,0	0,89	0,08	0,20	0,30	421	0,28	0,29	22	34
		1545 - 50	0,11								
	Quartz Arenite	1570 - 75	0,38								
		1600 - 5	0,30								
	Sst. w/altr. Sh.	1610 - 15	0,25								
Chichali	Shale with traces of sandstone	1620 - 25	1,16	0,11	0,37	0,06	425	0,48	0,23	32	5
		1630 - 35	1,62	0,12	1,72	0,04	431	1,84	0,07	106	2
		1640 - 45	1,15	0,11	2,44	0,06	428	2,55	0,04	212	5
		1650 - 55	1,08	0,12	1,23	0,05	432	1,35	0,09	114	5
		1660 - 65	1,14	0,12	1,22	0,40	433	1,34	0,09	107	35
		1670 - 75	1,64	0,13	2,25	0,64	433	2,38	0,05	137	39
		1680 - 85	0,53	0,10	0,62	0,52	432	0,72	0,14	117	98
Samana Suk	Lst. w/stks. Sh.	1690 - 95	0,33								
	Limestone	1694	0,27								
		1694,62	0,30								
		1695,23	0,29								
		1695,85	0,33								
		1696,46	0,32								
		1697,07	0,38								
		1697,69	0,09								

Table 9.1: Bulk organic geochemical data (TOC and pyrolysis) from the Ali Sahib Well (continued)

Fm.	Lithology	Depth in Meters	TOC (wt%)	S1 (mg/g)	S2 (mg/g)	S3 (mg/g)	Tmax (°C)	GP (mg/g)	IP	HI	OI
Samana Suk	Limestone	1698,31	0,22								
		1698,92	0,20								
		1699,54	0,19								
		1700,15	0,11								
		1700,70	1,25	0,09	0,05	0,88	291	0,14	0,64	4	70
		1701,38	2,26	0,08	0,12	0,88	355	0,20	0,40	5	39
		1702,07	0,39								
	Sh. w/stks. Lst.	1705 - 5	1,64	0,82	4,46	0,84	433	5,28	0,16	272	51
	Sh. w/stks. Lst.	1710 - 15	0,31								
	Claystone with thin bands of limestone	1720 - 25	0,47								
		1730 - 35	0,40								
	Quartz Arenite	1730,5	0,11								
	Sh. with stks of Sst.	1730,75	0,30								
	Sandstone with thin bands of shale	1731	0,18								
		1731,25	0,27								
		1732,5	0,33								
		1740 - 45	0,44								
	Limestone with thin bands of shale	1750 - 55	0,31								
		1760 - 65	0,29								
		1770 - 75	0,48								

Table 9.1: Bulk organic geochemical data (TOC and pyrolysis) from the Ali Sahib Well (continued)

Fm.	Lithology	Depth in Meters	TOC (wt%)	S1 (mg/g)	S2 (mg/g)	S3 (mg/g)	Tmax (°C)	GP (mg/g)	IP	HI	OI
Samana Suk	Limestone with thin bands of shale	1780-82	0,19								
		1790 - 92	0,26								
		1800 - 2	0,40								
		1810 - 12	0,47								
		1820 - 22	0,34								
Datta	Sst. w/intr. of Clst.	1830 - 32	0,30								
	Sst. w/intr. of Clst.	1840 - 42	0,36								
	Sst. w/intr. of Clst.	1850 - 52	0,54	0,09	0,28	0,20	427	0,37	0,24	52	37
	Sst. w/intr. of Clst.	1850 - 52	0,48								
	Quartz Arenite	1886,00	0,38								
	Claystone	1886,57	0,48								
		1887,15	0,33								
		1887,72	0,84	0,19	0,30	0,52	387	0,49	0,39	36	62
		1888,29	0,66	0,18	0,23	0,26	373	0,41	0,44	35	39
		1888,86	0,50	0,29	0,38	0,10	378	0,67	0,43	76	20
		1889,44	0,48								
		1890,01	0,32								
		1890,58	0,58	0,15	0,24	0,13	375	0,39	0,38	41	22
		1891,16	0,45								

Table 9.1: Bulk organic geochemical data (TOC and pyrolysis) from the Ali Sahib Well (continued)

Fm.	Lithology	Depth in Meters	TOC (wt%)	S1 (mg/g)	S2 (mg/g)	S3 (mg/g)	Tmax (°C)	GP (mg/g)	IP	HI	OI
Datta	Claystone	1892,30	0,43								
		1892,87	0,34								
		1893,45	0,47								
		1890 - 92	1,55	0,24	3,89	0,88	429	4,13	0,06	251	57
		1910 - 12	0,79	0,06	0,13	0,12	426	0,19	0,32	16	15
		1930 - 32	0,60								
Datta/Kingriali	Sst. w/stks. Clst & Sh.	1950 - 52	0,44								
	Sandstone with Streaks of claystone, shale and limestone	1960 - 62	0,59	0,10	0,15	0,30	424	0,25	0,40	25	51
		1970 - 72	0,68	0,11	0,39	0,44	428	0,50	0,22	57	65
		1980 - 82	0,67	0,12	0,11	0,26	433	0,23	0,52	16	39
		1990 - 92	0,40								
		2000 - 2	0,90	0,08	0,24	0,26	430	0,32	0,25	27	29
		2010 - 12	0,59	0,05	0,24	0,28	426	0,29	0,17	41	47
		2020 - 22	0,43								
		2030 - 32	0,40								
		2040 - 42	0,39								

TOC: Total organic carbon content; PI: Production Index (S1/ (S1+S2)); HI: Hydrogen index; OI: Oxygen Index; T_{max}: Temperature of maximum pyrolysis yield; S1: mg HC/g rock, free hydrocarbons; S2: mg HC/g rock, Hydrocabons cracked from kerogen; S_3: mg CO_2/g rock. Gl: glauconite; Sst: sandstone; Lst: limestone; Sh: shale; Clstn: claystone; calc: calcareous; dolo: dolomite; Ml: marl; inter: intercalations; stks: streaks; altr: alternations; w: with.

Table 9.2: Bulk organic geochemical data (TOC and pyrolysis) from the Amir Wali Well

Fm.	Lithology	Depth in Meters	TOC (wt%)	S1 (mg/g)	S2 (mg/g)	S3 (mg/g)	Tmax (°C)	GP (mg/g)	IP	HI	OI
Sakr	Limestone	1320 - 25	0,45								
		1330 - 35	0,43								
Nammal	Limestone with streaks of shale	1340 - 45	1,25	0,12	0,51	0,52	412	0,63	0,19	41	42
		1350 - 55	0,88	0,13	0,42	0,52	414	0,55	0,24	48	59
	Limestone	1370 - 75	0,45								
		1390 - 95	0,49								
		1400 - 5	0,42								
		1410 - 15	0,36								
		1420 - 25	0,44								
		1430 - 35	0,36								
		1440 - 45	0,42								
		1450 - 55	0,41								
		1470 - 75	0,47								
		1480 - 85	0,48								
		1490 - 95	0,44								
		1500 - 5	0,49								
		1510 - 15	0,48								
Dunt	Shale	1520 - 25	0,52	0,23	1,16	0,56	422	1,39	0,17	223	108
	Shale/Sandstone	1530 - 35	0,43								
Rani	Sandstone	1540 - 45	0,20								
	Shale	1550 - 55	2,33	0,13	1,45	0,88	425	1,58	0,08	62	38

Table 9.2: Bulk organic geochemical data (TOC and pyrolysis) from the Amir Wali Well (continued)

Fm.	Lithology	Depth in Meters	TOC (wt%)	S1 (mg/g)	S2 (mg/g)	S3 (mg/g)	Tmax (°C)	GP (mg/g)	IP	HI	OI
Ranikot		1560 - 65	0,35								
		1570 - 75	0,71	0,08	0,33	0,56	417	0,41	0,20	46	79
	Arenaceous Limestone	1575	0,60	0,10	0,21	0,26	416	0,31	0,32	35	43
		1575,6425	0,82	0,06	0,32	0,18	414	0,38	0,16	39	22
	Limestone	1576,285	0,84	0,08	0,39	0,12	414	0,47	0,17	46	14
		1576,9275	0,67	0,11	0,33	0,30	412	0,44	0,25	49	45
	Arenaceous Limestone	1577,57	0,63	0,12	0,15	0,40	412	0,27	0,44	24	63
		1578,2125	0,50	0,10	0,06	0,32	419	0,16	0,63	12	64
	Calc. Sandstone	1578,855	0,32								
		1579,4975	0,92	0,26	0,16	0,44	418	0,42	0,62	17	48
	Limestone	1580,14	0,36	0,08	0,10	0,40	419	0,18	0,44	28	111
		1580,7825	0,71	0,08	0,06	0,52	387	0,14	0,57	8	73
		1581,425	0,56	0,06	0,03	0,36	383	0,09	0,67	5	64
	Arenaceous Limestone	1582,0675	0,53								
		1582,71	0,47								
		1583,3525	0,37								
		1583,995	0,35								
	Shale with streaks of marl	1580 - 85	0,48								
		1590 - 92	0,35								
	Marl	1600 - 2	0,25								

Table 9.2: Bulk organic geochemical data (TOC and pyrolysis) from the Amir Wali Well (continued)

Fm.	Lithology	Depth in Meters	TOC (wt%)	S1 (mg/g)	S2 (mg/g)	S3 (mg/g)	Tmax (°C)	GP (mg/g)	IP	HI	OI
Lumshiwal	Sst.w/strk. Sh. & Ml	1610 - 12	0,47								
	Claystone	1615	0,44	0,06	0,07	0,32		0,13	0,46	16	73
		1615,70	0,39								
	Sandstone	1616,38	0,38								
		1617,08	0,48	0,07	0,06	0,13		0,13	0,54	13	27
		1617,77	0,30								
		1618,46	0,32								
	Sandstone w/strk. Sh	1619,15	0,47	0,06	0,03	0,56		0,09	0,67	6	119
	Sandstone	1619,84	0,42	0,06	0,02	0,18		0,08	0,75	5	43
		1620,54	0,38								
		1621,23	0,48								
		1621,92	0,35	0,06	0,06	0,01		0,12	0,50	17	3
		1622,61	0,45	0,09	0,10	0,03	376	0,19	0,47	22	7
		1623,30	0,46	0,07	0,07	0,11		0,14	0,50	15	24
		1624,0	0,55	0,07	0,06	0,10		0,13	0,54	11	18
		1630 - 32	1,30	0,18	0,83	0,88	423	1,01	0,18	64	68
	Sandstone with streaks of shale	1640 - 42	0,52								
		1650 - 52	2,00	0,36	0,56		423	0,92	0,39	28	
		1660 - 62	0,45								

Table 9.2: Bulk organic geochemical data (TOC and pyrolysis) from the Amir Wali Well (continued)

Fm.	Lithology	Depth in Meters	TOC (wt%)	S1 (mg/g)	S2 (mg/g)	S3 (mg/g)	Tmax (°C)	GP (mg/g)	IP	HI	OI
Chichiali	Marl with intercalations of shale	1670 - 72	0,48								
		1680 - 82	1,51	0,14	0,56	0,60	425	0,70	0,20	37	40
		1690 - 92	1,80	0,14	0,52	0,88	426	0,66	0,21	29	49
	Sandstone with streaks of shale	1710 - 12	1,70	0,15	0,73	0,60	423	0,88	0,17	43	35
		1720-22	1,20	0,17	1,06	0,60	417	1,23	0,14	88	50
	Marl with intercalations of shale	1730 - 32	1,00	0,23	1,41	0,80	419	1,64	0,14	141	80
		1740 - 42	1,20	0,34	1,47	0,96	419	1,81	0,19	123	80
		1750 - 52	1,60	0,16	0,83	0,60	419	0,99	0,16	52	38
Samana Suk	Limestone	1760 - 62	0,40								
		1760	0,62	0,16	0,36	0,72	421	0,52	0,31	58	116
		1760,56	0,59	0,23	0,23	0,52	419	0,46	0,50	39	88
		1761,13	0,66	0,17	0,28	0,64	419	0,45	0,38	42	97
		1761,69	0,56	0,09	0,29	0,44	420	0,38	0,24	52	79
		1762,25	0,59	0,11	0,14	0,52	423	0,25	0,44	24	88
		1762,81	0,59								
		1763,38	0,54	0,10	0,14	0,36	423	0,24	0,42	26	67
		1763,9375	0,65	0,08	0,39	0,80	423	0,47	0,17	60	123
		1764,5	0,49	0,11	0,18	0,68	422	0,29	0,38	37	139
		1765,06	1,00	0,09	0,37	0,56	422	0,46	0,20	37	56
		1765,63	0,45								
		1766,19	0,45								

Table 9.2: Bulk organic geochemical data (TOC and pyrolysis) from the Amir Wali Well (continued)

Fm.	Lithology	Depth in Meters	TOC (wt%)	S1 (mg/g)	S2 (mg/g)	S3 (mg/g)	Tmax (°C)	GP (mg/g)	IP	HI	OI
Samana Suk	Limestone	1766,75	0,32								
		1767,31	0,33								
		1767,86	0,45								
		1768,44	0,35								
		1769	0,57	0,09	0,24	0,68	422	0,33	0,27	42	119
		1770 - 72	0,56	0,29	2,77	1,20	429	3,06	0,09	495	214
		1790 - 92	0,68	0,11	0,31	0,80	422	0,42	0,26	46	118
		1800 - 2	0,48								
		1810 - 12	0,44								
		1820 - 22	0,47								
		1830 - 32	0,50	0,10	0,12	0,56	422	0,22	0,45	24	112
		1840 - 42	0,70	0,11	0,18	0,64	421	0,29	0,38	26	91
		1850 - 52	0,60	0,14	0,57	0,88	420	0,71	0,20	95	147
		1853	0,20								
		1853,56	0,09								
		1854,13	0,10								
		1854,69	0,28								
		1855,25	0,18								
		1855,81	0,20								
		1856,38	0,09								

Table 9.2: Bulk organic geochemical data (TOC and pyrolysis) from the Amir Wali Well (continued)

Fm.	Lithology	Depth in Meters	TOC (wt%)	S1 (mg/g)	S2 (mg/g)	S3 (mg/g)	Tmax (°C)	GP (mg/g)	IP	HI	OI
Samana Suk	Limestone	1856,94	0,50	0,14	0,47	0,34	418	0,61	0,23	94	68
		1857,5	2,19	0,09	0,16	0,50	416	0,25	0,36	7	23
		1858,06	0,53	0,10	0,07	0,16	417	0,17	0,59	13	30
		1858,63	1,38	0,04	0,04	0,16		0,08	0,50	3	12
		1859,19	0,32								
	Arenaceous dolostone	1859,75	0,40								
	Limestone	1860,31	0,30								
		1860,88	0,58	0,11	0,07	0,23	397	0,18	0,61	12	40
		1861,44	0,07								
		1862	0,18								
		1870 - 72	0,27								
		1880 - 82	0,20								
		1890 - 92	0,37								
Datta	Sandstone	1900 - 2	1,50	0,23	3,22	0,48	421	3,45	0,07	215	32
		1910 - 12	0,57	0,17	1,33	0,40	421	1,50	0,11	233	70
		1920 - 22	0,41								
		1930 - 32	1,00	0,14	0,35	0,72	422	0,49	0,29	35	72
		1940 - 42	1,60	0,32	3,05	0,60	420	3,37	0,09	191	38

Table 9.2: Bulk organic geochemical data (TOC and pyrolysis) from the Amir Wali Well (continued)

Fm.	Lithology	Depth in Meters	TOC (wt%)	S1 (mg/g)	S2 (mg/g)	S3 (mg/g)	Tmax (°C)	GP (mg/g)	IP	HI	OI
Datta	Claystone with thin bands of sandstone	1950 - 52	0,90	0,19	0,87	0,88	424	1,06	0,18	97	98
		1960 - 62	1,00	0,21	2,20	0,52	424	2,41	0,09	220	52
		1970 - 72	0,46								
		1980 - 82	0,55	0,46	0,98	0,64	421	1,44	0,32	178	116
Datta/Kingriali	Claystone with streaks of sandstone	1990 - 92	0,85	0,23	0,42	1,28	424	0,65	0,35	49	151
		2000 - 2	0,66								
	Sandstone with intercalations of claystone & shale	2010 - 12	0,72	0,16	0,25	0,88	423	0,41	0,39	35	122
		2020 - 22	0,48								
		2030 - 32	0,90	0,16	0,75	0,72	422	0,91	0,18	83	80
		2040 - 42	0,88	0,10	0,39	0,64	425	0,49	0,20	44	73

TOC: Total organic carbon content; PI: Production Index (S1/ (S1+S2)); HI: Hydrogen index; OI: Oxygen Index; T_{max}: Temperature of maximum pyrolysis yield; S1: mg HC/g rock, free hydrocarbons; S2: mg HC/g rock, Hydrocabons cracked from kerogen; S_3: mg CO_2/g rock. Gl: glauconite; Sst: sandstone; Lst: limestone; Sh: shale; Clstn: claystone; calc: calcareous; dolo: dolomite; Ml: marl; inter: intercalations; stks: streaks; altr: alternations; w: with.

Table 9.3: Bulk organic geochemical data of samples (TOC, Aliphatic and Aromatic) from the Ali Sahib and Amir Wali wells

Sample	Formation	TOC[a] (wt.%)	PI[b]	HI[c] (mg HC/ g TOC)	OI[d] (mg CO_2/ g TOC)	T_{max}[e] (° C)	EOM[f] (mg/g TOC)	Sat. HC[g] (%, TOC)	Aro. HC[h] (%, TOC)	NSO (%, TOC)
Ali Sahib Well										
AS1D	Chichali	1.16	0.23	32	5	425	8	49	27	25
AS2D	Chichali	1.62	0.07	106	2	431	9	39	15	47
AS3D	Chichali	1.15	0.04	212	5	428	52	24	14	62
AS4D	Chichali	1.08	0.09	114	5	432	90	26	14	60
AS6D	Chichali	1.14	0.09	107	35	433	44	25	13	63
AS7D	Chichali	1.64	0.05	137	39	433	81	18	10	73
AS8C2	Samana Suk	1.25	0.64	4	70		11	30	6	64
AS9C2	Samana Suk	2.26	0.40	5	39		6	14	16	59
AS10C4	Datta	0.84	0.39	36	62	387	14	48	14	38
AS11D	Datta	1.55	0.06	251	57	429	6	23	19	58
AS12D	Datta	0.79	0.32	16	15	426	163	24	12	64
AS13D	Datta/Kingriali	0.90	0.25	27	29	430	22	35	14	52
AW1D	Nammal	1.25	0.19	41	42	412	12	39	11	50
AW2D	Nammal	0.88	0.24	48	59	414	18	40	10	50
AW3D	Ranikot	2.33	0.08	62	38	425	14	28	10	63
AW4C1	Ranikot	0.82	0.16	39	22	414	14	9	7	84
AW6C1	Ranikot	0.92	0.62	17	48	418	6	29	13	58
AW7D	Lumshiwal	1.30	0.18	64	68	423	9	20	6	74
AW8D	Lumshiwal	2.00	0.39	28		423	13	15	9	76
AW9D	Chichiali	1.51	0.20	37	40	425	14	4	38	58

Table 9.3: Bulk organic geochemical data of samples (TOC, Aliphatic and Aromatic) from the Ali Sahib and Amir Wali wells

Sample	Formation	TOC[a] (wt.%)	PI[b]	HI[c] (mg HC/ g TOC)	OI[d] (mg CO_2/ g TOC)	T_{max}[e] (° C)	EOM[f] (mg/g TOC)	Sat. HC[g] (%, TOC)	Aro. HC[h] (%, TOC)	NSO (%, TOC)
AW10D	Chichiali	1.80	0.21	29	49	426	7	41	28	69
AW11D	Chichiali	1.70	0.17	43	35	423	11	36	14	26
AW12D	Chichiali	1.20	0.14	88	50	417	10	36	8	53
AW13D	Chichiali	1.00	0.14	141	80	419	12	58	16	56
AW14D	Chichiali	1.20	0.19	123	80	419	29	36	9	47
AW15D	Chichiali	1.60	0.16	52	38	419	12	45	11	40
AW16C3	Samana Suk	0.62	0.31	58	116	421	17	44	7	48
AW17C3	Samana Suk	0.59	0.50	39	88	419	23	20	15	64
AW20C3	Samana Suk	1.00	0.20	37	56	422	7	55	13	32
AW21D	Samana Suk	0.68	0.26	46	118	422	39	28	9	63
AW22D	Samana Suk	0.70	0.38	26	91	421	12	63	19	19
AW23C4	Samana Suk	2.19	0.36	7	23	416	26	67	3	30
AW24C4	Samana Suk	1.38	0.50	3	12		14	36	26	38
AW25D	Datta	1.50	0.07	215	32	421	46	39	35	26
AW26D	Datta	1.00	0.29	35	72	422	12	40	54	6
AW27D	Datta	1.60	0.09	191	38	420	28	40	7	53
AW29D	Datta	1.00	0.09	220	52	424	13	2	15	83
AW30D	Datta/Kingriali	0.90	0.18	83	80	422	36	39	22	39

[a]Total organic carbon content; [b]Production Index (S1/(S1+S2)); [c]Hydrogen index; [d]Oxygen Index; [e]Temperature of maximum pyrolysis yield; [f]Extractable organic matter; [g]Saturated hydrocarbon fraction; [h]Aromatic hydrocarbon fraction

Table 9.4: Characteristic biomarker ratios of samples from the Ali Sahib and Amir Wali wells

Sample	*n*-C_{15-19}/ *n*-Alkanes	*n*-C_{21-25}/ *n*-Alkanes	*n*-C_{27-31}/ *n*-Alkanes	CPI[a]	Pr[b] / *n*-C_{17}	Ph[c] / *n*-C_{18}	Pr/Ph	S/(S+R) αβ-C_{31} Hopanes	MPI 1[d]	R_c[e] (%)	DBT[f]/ Phen.[g]
Ali Sahib Well											
AS1D	0.35	0.23	0.28	0.79	0.35	0.48	0.53	0.50	0.44	0.66	0.23
AS2D	0.59	0.18	0.12	1.62	1.54	0.31	3.53	0.50	0.52	0.71	0.27
AS3D	0.33	0.25	0.31	1.40	0.61	0.76	0.74	0.54	0.40	0.64	0.23
AS4D	0.15	0.54	0.17	1.24	0.77	0.94	0.83		0.57	0.74	0.65
AS6D	0.39	0.30	0.20	2.51	0.32	0.54	0.56	0.47	0.55	0.73	0.71
AS7D	0.34	0.29	0.25	1.60	0.71	0.50	1.14	0.50	0.56	0.74	0.52
AS8C2	0.12	0.17	0.59	0.90	0.80	0.28	1.22	0.46	0.61	0.77	0.18
AS9C2	0.12	0.17	0.59	0.90	0.28	0.05	1.57				
AS10C4	0.17	0.24	0.47	0.95	0.28	0.05	1.57	0.50			
AS11D	0.29	0.39	0.21	1.65	0.63	0.61	0.80		0.58	0.75	0.19
AS12D	0.21	0.35	0.31	1.51	1.23	0.60	1.50	0.60	0.68	0.81	0.56
AS13D	0.23	0.39	0.24	0.90	0.72	0.23	2.34	0.56	0.56	0.74	0.17
Amir Wali Well											
AW1D	0.78	0.18	0.04	0.97	0.27	0.17	2.82	0.56	0.69	0.81	0.18
AW2D	0.53	0.33	0.10	1.08	0.63	0.63	1.46	0.57	0.69	0.81	0.56
AW3D	0.49	0.18	0.16	1.05	0.78	0.54	1.32	0.50	0.52	0.71	0.22
AW7D	0.34	0.21	0.22		0.37	0.44	1.03	0.53	0.43	0.66	0.13
AW8D	0.43	0.27	0.21	0.86	0.52	0.62	1.14				
AW10D	0.45	0.20	0.26	0.84	0.82	0.70	1.43	0.59	0.73	0.84	0.12
AW11D	0.35	0.23	0.34	0.81	0.44	0.51	0.81	0.59			

Table 9.4: Characteristic biomarker ratios of samples from the Ali Sahib and Amir Wali wells (continued)

Sample	*n*-C_{15-19}/ *n*-Alkanes	*n*-C_{21-25}/ *n*-Alkanes	*n*-C_{27-31}/ *n*-Alkanes	CPI[a]	Pr[b] / *n*-C_{17}	Ph[c] / *n*-C_{18}	Pr/Ph	S/(S+R) αβ-C_{31} Hopanes	MPI 1[d]	R_c[e] (%)	DBT[f]/ Phen.[g]
AW12D	0.53	0.22	0.15	0.92	0.79	0.74	1.69	0.49			
AW13D	0.43	0.27	0.19	0.97	0.28	0.37	0.46				
AW14D	0.57	0.24	0.08	0.97	0.47	0.44	1.20	0.50	0.52	0.71	0.23
AW15D	0.59	0.17	0.12	1.11	1.21	0.43	2.02	0.47	0.47	0.68	0.18
AW16C3	0.27	0.25	0.32	1.13	0.28	0.15	1.86	0.45	0.53	0.72	0.20
AW17C3	0.39	0.23	0.26	1.19	0.38	0.18	2.48	0.49	0.51	0.70	0.15
AW19C3	0.20	0.34	0.32	1.08	0.80	0.72	1.17				0.27
AW20C3	0.25	0.37	0.24	0.97	0.71	0.51	1.16	0.46			
AW21D	0.53	0.20	0.16	0.79	0.58	0.39	1.73		0.52	0.71	0.10
AW22D	0.32	0.19	0.38	0.97	0.63	0.45	1.53	0.49			
AW23C4	0.47	0.37	0.03	1.03	0.47	0.36	1.10	0.51			
AW24C4	0.40	0.42	0.02	1.91	0.48	0.52	0.83	0.47	0.76	0.86	0.13
AW26D	0.27	0.16	0.43	0.99	0.63	0.66	0.87	0.56	0.48	0.69	0.22
AW27D	0.36	0.18	0.36	1.74	0.66	0.47	1.06	0.52			0.20
AW28D	0.59	0.14	0.14	1.24	0.66	1.00	0.51	0.58	0.57	0.74	0.15
AW30D	0.39	0.26	0.21		0.89	0.40	1.79	0.53	0.65	0.79	0.21

[a]Carbon preference index (according to Bray and Evans, 1961); [b]Pristane; [c]Phytane; [d]Methylphenanthrene Index (according to Radke et al., 1982); [e]Calculated vitrinite reflectance equivalence from MPI 1 (Radke and Welte, 1983); [f]Dibenzothiophene; [g]Phenanth